Endosomal Docking of mTOR Modulates mTORC1 Activity

Inauguraldissertation

zur

Erlangung der Würde eines Doktors der Philosophie

vorgelegt der

Philosophisch-Naturwissenschaftlichen Fakultät

der Universität Basel

von

Anna Melone

aus Möhlin AG

Basel, 2014

Genehmigt von der Philosophisch-Naturwissenschaftlichen Fakultät

auf Antrag von

Prof. Dr. Matthias P. Wymann

Prof. Dr. Christoph Moroni

Basel, den 24. April 2012

Prof. Dr. Martin Spiess, Dekan

TABLE OF CONTENTS

1 Summary

The mammalian target of rapamycin (mTOR) is an atypical serine/threonine kinase, evolutionary conserved from yeast to human, which forms two functional distinct and independently regulated multiprotein complexes, dubbed mTORC1 and mTORC2. mTORC1 contains mTOR, raptor, mLST8, PRAS40 and DEPTOR, and is sensitive to the immunosuppressive and anti-cancer drug rapamycin. mTORC1 regulates translation via phosphorylation of S6K1 and 4E-BP1, two well-characterized effector proteins. mTORC2 consists of mTOR, rictor, mLST8, mSIN1, protor and DEPTOR, and is rapamycin-insensitive. It regulates the organization of the actin cytoskeleton and is involved in cell survival.

Both mTORC1 and mTORC2 are stimulated by growth factors, but only mTORC1 is controlled as well by cellular energy status and nutrients such as amino acids. How cells sense amino acid sufficiency to control protein synthesis and eventually cell growth is largely unknown. Amino acid deprivation results in rapid dephosphorylation of S6K1 and 4E-BP1, while amino acid stimulation leads to the rapid mTORC1-mediated phosphorylation of these molecules. Moreover, amino acid stimulation triggers the re-localization of mTORC1 to late endosomes/lysosomes, where Rheb is supposed to be localized and thereby allowing Rheb to directly interact with and activate mTORC1. Additionally, vacuolar protein sorting 34 (Vps34), the sole class III phosphatidylinositol 3-kinase (PI3K), and its phospholipid product phosphatidylinositol 3-phosphate [PtdIns(3)P] have also been implicated in mTORC1 activation. However, concerns exist in connecting Vps34 with mTORC1 regulation. Therefore, we have decided to investigated in more depth the role of Vps34 and PtdIns(3)P in the amino acid pathway to mTORC1. Ectopic expression of either wild type or kinase-dead human Vps34 (hVps34) did not change mTORC1 activity. Deletion of hVps34 by RNAi did not result in a complete decrease of mTORC1 activation, indicating that another PI3K might generate PtIns(3)P. Depletion of the class II PI3K isoforms PI3K-C2α and PI3K-C2β, which have been demonstrated to generate PtdIns(3)P as well, leads to an isoform specific regulation of mTORC1 activity. PI3K-C2α deletion increased, while PI3K-C2β knockdown only partially reduced mTORC1 activity. However, by directly affecting cellular PtdIns(3)P availability either by sequestering PtdIns(3)P with a tandem FYVE domain (Fab1/YOTB/Vac1/EEA1; named after the first four proteins in which it was identified) or by acute treatment with exogenous PtdIns(3)P, mTORC1 activity almost

completely decreased or strongly increased, respectively. These results confirm the requirement of PtdIns(3)P in the mTORC1 pathway.

Consistent with the requirement of PtdIns(3)P in endosomal homeostasis, we reasoned that PtdIns(3,5)P_2, which is generated by PIKfyve using PtdIns(3)P as substrate and required for early to late endosome trafficking, might as well be implicated in the amino acid-dependent pathway to mTORC1. Pharmacologic inhibition of PIKfyve strongly decreased mTORC1-mediated phosphorylation of S6K1 without affecting the catalytic activity of mTOR and PtdIns(3)P generation, and abrogated the translocation of mTOR to late endosomes indicating that the inhibiting effect on mTORC1, induced through the inhibition of PIKfyve, is probably due to a defect in endosomal membrane transport to late endosomes.

We are the first to show that PtdIns(3,5)P_2, generated by PIKfyve, is involved in mTORC1 activation and moreover, demonstrating that an unperturbed endosomal transport is required for late endosomal re-localization of mTORC1 induced by amino acids.

However, the above described result cannot be generalized for different cell lines. While in HEK293 cells PIKfyve inhibition strongly blocked mTORC1 activity, in A375 cells, an aggressive melanoma cell line, the inhibition was less pronounced. This can be explained that A375 cells have a constitutive active MAPK pathway due to B-Raf V600E mutation, which impinges on mTORC1 activity. Therefore, this indicates that cancer cells with mutated MAPK or PI3K-Akt/PKB pathway cannot be treated solely with the PIKfyve inhibitor but need additional treatments.

2 Introduction

The target of rapamycin (TOR) story began with the isolation of the bacterium *Streptomyces hygroscopicus* from a soil sample collected in Easter Island (Rapa Nui in the native language), that produces a macrolide called rapamycin after Rapa Nui, the location of its discovery (Vezina et al., 1975). Besides having anti-fungal properties, rapamycin possesses immunosuppressive and anti-proliferative properties. Moreover, in a yeast genetic screen rapamycin treatment led to the identification of two independent genes that, when mutated, conferred resistance to rapamycin. These two genes were named *target of rapamycin 1* and *2* (*TOR1* and *TOR2*) (Heitman et al., 1991). Importantly, follow up studies on TOR functions revealed TOR being fundamental in cell growth and cell proliferation. Rapamycin treatment or inactivation of both *TOR* genes in yeast resulted in a severe decrease in translation initiation and an arrest in the early G1 phase of the cell cycle (Barbet et al., 1996; Kunz et al., 1993). Moreover, inhibition of TOR functions in yeast phenocopied the physiological changes characteristic of nutrient starved cells that arrest the cell cycle in G1 due to loss of translation and enter into G0 (Barbet et al., 1996). The role of TOR in nutrient response has also been found in higher eukaryotes. Genetic studies in *Drosophila melanogaster* revealed that loss of *dTOR* and amino acid withdrawal cause similar phenotypes including reduction in cell size and proliferative defects leading to G1 arrest (Oldham et al., 2000; Zhang et al., 2000). In mammalian cells, amino acid insufficiency and inhibition of mammalian TOR (mTOR; also known as FRAP, RAFT1 and RAPT) function by rapamycin selectively induce dephosphorylation of the two best-characterized mTOR substrates p70 ribosomal S6 kinase (S6K1) and eukaryotic initiation factor 4E-binding protein 1 (4E-BP1, also known as PHAS1) (Burnett et al., 1998; Hara et al., 1998; Iiboshi et al., 1999) and rapamycin treatment reduces cell size (Fingar et al., 2002). In metazoan, TOR responds to a plethora of signals such as growth factors, nutrients, energy and stress. Nonetheless, in mammals nutrients in form of amino acids seem to be the most critical signal for mTOR activation, inasmuch as in the absence of amino acids mTOR can not be effectively activated by growth factors (Hara et al., 1998).

2.1 Molecular composition of mTOR complexes

2.1.1 The TOR protein

TOR is a large protein of approximately 280 kDa and was originally identified in 1991 in *Saccharomyces cerevisiae* (Heitman et al., 1991) and since then homologues have been found in other eukaryotes including fungi, plants, worms, flies and mammals (Jacinto and Hall, 2003) indicating that TOR is conserved in all eukaryotes. Yeast contains two *TOR* genes, *TOR1* and *TOR2*, while higher eukaryotes contain only one *TOR* gene (Wullschleger et al., 2006). TOR is the founding member of the phosphatidylinositol 3-kinase-related protein kinase (PIKK) family (Kunz et al., 1993; Schmelzle and Hall, 2000; Wullschleger et al., 2006). All PIKK members, including TOR, ATM (ataxia-telangiectasia mutated), ATR (ATM and Rad3 related), DNA-PK (DNA-dependent protein kinase), SMG-1 (suppressor of morphogenesis in genitalia-1) and TRRAP (transformation/transcription domain associated protein), contain a conserved C-terminal region with strong homology to the catalytic domain of phosphatidylinositol 3-kinases (PI3Ks) (Abraham, 2004). Despite this homology to lipid kinases, TOR and the other PIKK members are Ser/Thr protein kinases, except TRRAP that has no catalytic activity (Abraham, 2004). The N-terminus of TOR contains 20 tandem repeats of 37-43 amino acids termed HEAT repeats (huntingtin, elongation factor 3, a subunit of protein phosphatase 2A and TOR1) (Andrade and Bork, 1995) and each HEAT motif forms a pair of antiparallel α-helices (Groves et al., 1999). The HEAT repeats in TOR mediate protein-protein interaction (Kim et al., 2002) and membrane localization (Drenan et al., 2004; Kunz et al., 2000; Liu and Zheng, 2007; Sabatini et al., 1999). Next to the HEAT repeats is the FAT (FRAP, ATM and TRRAP) domain followed by the FRB (FKBP12-rapamyicin binding) domain, the catalytic and the FATC (FAT C-terminus) domain (Fig. 1). The FAT domain is present in all PIKK members and is found in combination with FATC domain that is located at the very C-terminus of TOR. Both domains are believed to function in protein-protein interactions (Jacinto and Hall, 2003) and FATC to be essential for protein kinase activity (Abraham, 2004). The FRB domain is the FKBP12-rapamycin binding site that upon binding of FKB12-rapamycin complex inhibits TOR function (Schmelzle and Hall, 2000). Consistent with the many protein-protein interaction domains in TOR, TOR forms a multiprotein complex.

Initial studies in *Saccharomyces cerevisiae* revealed that TOR1 and TOR2 act as nutrient sensors and control cell size and proliferation (Barbet et al., 1996). In *Drosophila melanogaster* and *Caenorhabditis elegans* inactivation of the TOR homologue caused developmental arrests that resembled the developmental arrest of starved larvae (Long et al., 2002; Oldham et al., 2000; Zhang et al., 2000). In mice, TOR is also needed for development, inasmuch as homozygous mTOR deletion resulted in embryonic lethality due to defect in cell proliferation and cell growth (Gangloff et al., 2004; Murakami et al., 2004).

2.1.2 Components of mammalian TOR complex 1 and 2

TOR forms two functionally distinct and independently regulated complexes, TOR complex 1 (TORC1) and TOR complex 2 (TORC2) (Table1 summarizes the components of the single complex and their functions). Both complexes are sensitive to growth factors but only TORC1 is rapamycin and nutrient-sensitive, while TORC2 is rapamycin and nutrient-insensitive (Loewith et al., 2002; Wullschleger et al., 2006). Many of the TOR complex 1 and 2 components are highly conserved from yeast to mammals (Loewith et al., 2002) (Table 1). Mammalian TORC1 (mTORC1) (Fig. 1) contains mTOR, raptor (regulatory-associated protein of mTOR; homologue of the yeast KOG1) (Hara et al., 2002; Kim et al., 2002; Loewith et al., 2002), mLST8 (mammalian lethal with sec thirteen, also known as GβL) (Kim et al., 2003), PRAS40 (proline-rich Akt substrate of 40 kDa) (Fonseca et al., 2007; Sancak et al., 2007; Thedieck et al., 2007) and DEPTOR (DEP domain-containing mTOR-interacting protein) (Peterson et al., 2009).

mTORC2 (Fig. 1) also contains mTOR, mLST8 and DEPTOR but no raptor and PRAS40. Instead, mTORC2 contains rictor (rapamycin-insensitive companion of mTOR; the yeast AVO3 homologue) (Sarbassov et al., 2004), mSIN1 (mammalian stress-activated map kinase-interacting protein 1; the yeast AVO1 homologue) (Frias et al., 2006; Jacinto et al., 2006; Yang et al., 2006) and Protor (protein observed with rictor) (Pearce et al., 2007).

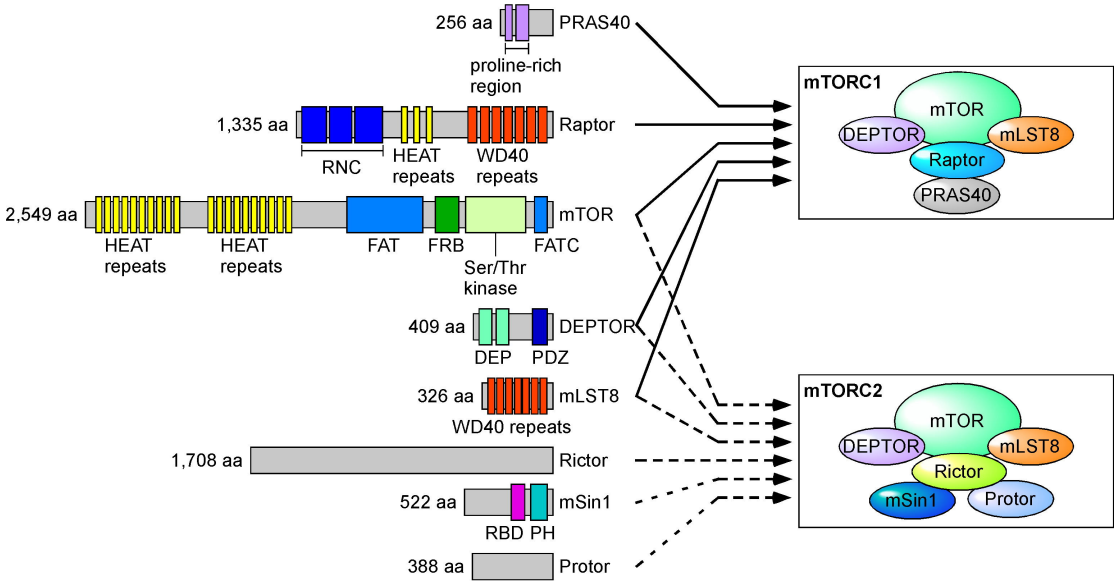

Fig. 1: Components of mammalian TORC1 and TORC2 and their domain organizations. Mammalian target of rapamycin (mTOR) complex 1 (mTORC1) and mTORC2 are multi-protein complexes with shared and unique components. Both complexes contain mTOR, mammalian lethal with sec thirteen 8 (mLST8) and DEP domain-containing mTOR-interacting protein (DEPTOR). Specific to mTORC1 are regulatory-associated protein of mTOR (raptor) and proline-rich Akt substrate of 40 kDa (PRAS40). Unique to mTORC2 are rapamycin-insensitive companion of mTOR (rictor), mammalian stress-activated map kinase-interacting protein 1 (mSin1) and protein observed with rictor (protor).
The N-terminus of mTOR contains two large blocks of HEAT repeats, which mediate protein-protein interactions. Following the HEAT repeats are the FAT domain, the FRB domain (the binding site of FKBP12-rapamycin complex) that is only accessible by FKBP12-rapamycin in mTORC1, the Ser/Thr kinase domain and the C-terminal FATC domain. PRAS40 contains proline-rich regions at the N-terminus. Raptor contains many protein-binding domains consisting with its function as a scaffolding protein. Next to the raptor-N-terminal conserved (RNC) domain are three HEAT repeats followed by seven WD40 repeats at the C-terminus. DEPTOR consists of two DEP domains at the N-terminus and a PDZ domain at the C-terminus. The structure of mLST8 consists almost entirely of seven WD40 repeats. Rictor and Protor do not have any recognizable functional domains. mSin1 contains a Ras binding domain (RBD) and pleckstrin homology (PH) domain that probably interacts with phospholipids.
HEAT: huntingtin, elongation factor 3, a subunit of protein phosphatase 2A and TOR1; FAT: FRAP, ATM and TRRAP; FRB: FKBP12-rapamycin binding; DEP, disheveled, egl-10, pleckstrin; PDZ: postsynaptic density 95, discs large, zonula occludens-1. (Figure modified from Zoncu et al. (Zoncu et al., 2011a))

Table 1: Mammalian TORC components and functions and their orthologues in yeast

Mammals	yeast	Function
mTOR	TOR1, TOR2	Ser/Thr protein kinase of mTORC1 and mTORC2
Raptor	KOG1	Defining component of mTORC1; mTOR scaffold protein that brings substrates to the mTOR kinase
mLST8 (GβL)	LST8	Component of mTORC1 and mTORC2; stabilizes mTOR complexes and is required for mTOR kinase activity, scaffold protein
PRAS40		Component of mTORC1; raptor-binding protein; negatively regulates mTORC1 kinase activity
DEPTOR		Component of mTORC1 and mTORC2; negatively regulates mTORC1 and mTORC2 activation
Rictor	AVO3	Defining component of mTORC2; required for complex stability and mTORC2 activity
mSin1	AVO1	Component of mTORC2; required for complex assembly and stability; important for mTORC2 activity and intracellular membrane localization
	AVO2	Component of yeast TORC2; non-essential protein; no mammalian homologue found
Protor		Component of mTORC2; rictor-binding protein

2.1.3 Molecular functions of the individual mTOR-associated proteins

Raptor is highly conserved among all eukaryotes and all raptor homologues have at their N-termini a unique domain named RNC (raptor-N-terminal conserved) divided into 3 blocks. RNC is followed by three HEAT repeats and seven WD40 repeats near the C-terminus (Hara et al., 2002; Kim et al., 2002) (Fig. 1). The association between Raptor and mTOR requires the HEAT repeats of mTOR and multiple sites on raptor (Kim et al., 2002). Raptor is a mTOR scaffold protein that interacts with the known mTORC1 substrates (4E-BP1 and S6K1) by binding to their TOS (TOR signaling) motifs and thus presenting S6K1 and 4E-BP1 to the mTORC1 kinase for phosphorylation (Hara et al., 2002; Nojima et al., 2003; Schalm and Blenis, 2002). Raptor plays a positive role in maintaining an active mTORC1 pathway, as deletion of raptor expression negatively affects the activation of mTORC1 downstream effectors, cell size and embryonic development (Guertin et al., 2006; Hara et al., 2002; Kim et al., 2002; Polak et al., 2008). Moreover, the interaction between raptor and mTOR is sensitive to nutrient availability. In nutrient deprived conditions, raptor-mTOR association is stable and strong, whereas in nutrient-rich conditions it is

unstable. A strong association of raptor with mTOR results in the inhibition of the mTOR catalytic activity (Kim et al., 2002).

mLST8 (also named GβL) is a component of both mTOR complexes (Kim et al., 2003; Sarbassov et al., 2004), consists of seven WD40 repeats and, like mTOR and raptor, is conserved through all eukaryotes (Kim et al., 2003) (Fig. 1). mLST8 binds strongly to the catalytic domain of mTOR in both complexes and is necessary for the catalytic activity of mTOR and stability of both complexes (Kim et al., 2003; Wullschleger et al., 2005). Consisting to its essential role for both TOR complexes, homologous deletion of mLST8 results in embryonic lethality (Guertin et al., 2006).

PRAS40 is a proline-rich protein having proline-rich regions at the N-terminus, otherwise lacking known domains (Kovacina et al., 2003) (Fig. 1) and it seems to be conserved only in higher eukaryotes (Oshiro et al., 2007; Vander Haar et al., 2007). It associates with raptor through its TOS motif and is thus mTORC1 specific (Fonseca et al., 2007; Oshiro et al., 2007; Wang et al., 2007). The primary function of PRAS40 is to inhibit mTORC1 signaling to its physiological substrates S6K1 and 4E-BP1. The inhibitory effect on mTORC1 signaling is relieved through phosphorylation of PRAS40 by mTORC1 and Akt/PKB (product of the retrovirus AKT8/Protein Kinase B) (Fonseca et al., 2007; Oshiro et al., 2007; Sancak et al., 2007; Vander Haar et al., 2007; Wang et al., 2008a).

DEPTOR is an mTOR-interacting protein found in both mTOR complexes and negatively regulates mTORC1 and mTORC2 activities (Peterson et al., 2009). It is only found in vertebrates and contains at its N-terminus two DEP (disheveled, egl-10, pleckstrin) domains and a PDZ (postsynaptic density 95, discs large, zonula occludens-1) domain at the C-terminus (Peterson et al., 2009) (Fig. 1). The interaction between mTOR and DEPTOR involves the FAT domain of mTOR and the PDZ domain of DEPTOR (Peterson et al., 2009). Interestingly, DEPTOR is an unstable protein and is rapidly degraded following stimulation with growth factors (Peterson et al., 2009).

Rictor does not contain any functional domains and is not well conserved among eukaryotes (Fig. 1); however, rictor homologues share common domain architectures (Sarbassov et al., 2004). Rictor is the defining component of mTORC2 (Jacinto et al., 2004; Sarbassov et al., 2004) and essential for both mTORC2 complex formation and its biological function (Sarbassov et al., 2005; Yang et al., 2006). Rictor deletion

in mice has been demonstrated to be embryonic lethal underscoring its essential role in mTORC2 function (Guertin et al., 2006).

mSin1 is an essential component of mTORC2 (Frias et al., 2006; Jacinto et al., 2006; Yang et al., 2006) and contains a Raf-like Ras binding domain (RBD) followed by a pleckstrin homology (PH) domain at the C-terminus (Schroder et al., 2007) (Fig. 1). The PH domain of mSin1 has been demonstrated to bind to phosphoinositides and to localize to both the plasma membrane and to a large cytoplasmic structure (Schroder et al., 2007). Therefore, mSin1 might guide mTORC2 to the plasma membrane. Indeed, in yeast Avo1, the mSin1 homologue, has been shown to be necessary to target TORC2 to the plasma membrane (Berchtold and Walther, 2009). mSin1 forms a tight complex with rictor and is also involved in the interaction with mTOR. Together with rictor, mSin1 is required for integrity, complex formation and for the kinase activity of mTORC2 (Frias et al., 2006; Yang et al., 2006). mSin1 interacts with Akt/PKB suggesting that mSin1 might serve as a scaffold to present Akt/PKB to mTORC2 (Jacinto et al., 2006). One interesting aspect of Sin1 is that in human, in contrast to other species, five different Sin1 isoforms exists that are generated by alternative splicing (Schroder et al., 2004) but only three of them (isoform 1, 2 and 5) assemble separately into mTORC2 thereby generating three distinct complexes (Frias et al., 2006). All three different mTORC2s phosphorylate the hydrophobic motif Ser473 of Akt/PKB in vitro, but only two complexes containing hSin1.1 and hSin1.2 isoforms are regulated by insulin (Frias et al., 2006). This indicates that in human the three distinct mTORC2s may respond to different signals.

Protor does not possess any recognizable functional domains (Fig. 1) and no homologues have been found in lower eukaryotes, including yeast and *Drosophila* (Pearce et al., 2007). Protor binds specifically to rictor and is thus a component of mTORC2. Alike DEPTOR, it is not involved in assembly and integrity of mTORC2 (Pearce et al., 2007).

2.2 Downstream targets of the mTOR complexes

Consistent with the distinct subunits composition of mTORC1 and mTORC2 and the fact that only mTORC1 is rapamycin sensitive, substrate specificity is also determined by the TOR complex. The best known substrates of mTORC1 are eukaryotic translation initiation factor 4E (eIF4E)-binding protein (4E-BP1) and the

p70 ribosomal protein S6 kinase (S6K1) (Burnett et al., 1998). Phosphorylation of 4E-BP1 and S6K1 by mTORC1 requires the recruitment of both substrates to mTORC1 through raptor followed by the phosphorylation by the mTOR kinase (Hara et al., 2002; Nojima et al., 2003; Schalm and Blenis, 2002). Consequently, by phosphorylation activated S6K1 and inactivated 4E-BP1 regulate mRNA translation initiation and progression. Hypophosphorylated 4E-BP1 is bound to eIF4E (eukaryotic initiation factor 4E), but when hyperphosphorylated (on Thr37, Thr46, Ser65 and Thr70) 4E-BP1 dissociates from eIF4E and allows eIF4E to be incorporated into the eIF4F complex. eIF4F complex is recruited via eIF4E to the 5'-cap of mRNA permitting the translational machinery to be assembled and translation to be initiated (Gingras et al., 2001). CAP-containing mRNAs encode for proteins important for cell proliferation, such as c-Myc and cyclin-D1 (Sonenberg and Gingras, 1998). Activation of S6K1 by Thr389 phosphorylation by mTORC1 leads to the translation of a different subset of mRNAs containing a terminal oligopolypyrimidine (TOP) track at the 5'-end. These types of mRNA encode for proteins of the translational machinery, such as ribosomes and elongation factors (Jefferies et al., 1997; Wullschleger et al., 2006).

Another physiological substrate of mTORC1 is PRAS40 (Fonseca et al., 2007; Oshiro et al., 2007; Wang et al., 2007). PRAS40 exerts a negative effect on mTORC1 downstream substrates probably by competing with 4E-BP1 and S6K1 for binding to raptor (Oshiro et al., 2007; Wang et al., 2007). PRAS40 is phosphorylated on Ser183 and Ser221 by mTORC1 in a rapamycin-dependent manner (Oshiro et al., 2007; Wang et al., 2008a) and alike other mTORC1 substrates, PRAS40 phosphorylation is positively influenced by Rheb (Ras homologue enriched in brain) and negatively affected by TSC1/TSC2 (tuberous sclerosis complex 1 and 2) complex (Oshiro et al., 2007). The inhibitory function of PRAS40 on mTORC1 is relieved through binding of phosphorylated PRAS40 to 14-3-3 (cytosolic anchor protein) and induces PRAS40 to dissociate from raptor. Moreover, PRAS40 has been found to be a substrate of Akt/PKB that in response to insulin treatment is phosphorylated on Thr246 in a wortmannin-dependent but rapamycin-independent manner and as a result mTORC1 activity is de-repressed through the association of PRAS40 to 14-3-3 (Fonseca et al., 2007; Kovacina et al., 2003; Oshiro et al., 2007; Sancak et al., 2007; Vander Haar et al., 2007; Wang et al., 2007). Both mTORC1 (stimulated by nutrients) and Akt/PKB (stimulated by insulin) phosphorylate and regulate PRAS40 binding to 14-3-3 and thus relieving the inhibitory constraint to mTORC1.

Under nutrient replete conditions mTORC1 negatively regulates the catabolic process macroautophagy (commonly termed autophagy), bulk degradation of cytoplasmic components such as organelles and proteins. Autophagy is upregulated during periods of starvation resulting in the sequestration of cytoplasmic components into a double-membrane vacuolar structure termed autophagosome. Upon fusion with a lysosome an autolysosome is formed, where its content is degraded providing a nutrient source to sustain anabolic processes such as protein synthesis and energy production that will allow cell survival until nutrients become available again (Codogno and Meijer, 2005; Klionsky, 2007; Simonsen and Tooze, 2009). Autophagy is controlled by mTORC1 through the regulation of the protein complex composed of Ser/Thr kinase ULK1 (unc-51-like kinase, yeast Atg1 homologue), Atg13 (autophagy-related gene 13) and FIP200 (focal adhesion kinase family-interacting proteine of 200 kDa, yeast Atg17 homologue) (Stipanuk, 2009). ULK1 kinase activity is regulated by Atg13 and FIP200 and the heterotrimeric complex is essential for the initiation of autophagosome formation (Stipanuk, 2009). Under condition of high nutrient availability mTORC1 phosphorylates both ULK1 and Atg13 and negatively affects the kinase activity of ULK1 thus repressing the initiation of autophagy (Stipanuk, 2009).

The cellular function of mTORC2 is less clear but it is involved in the reorganization of the cytoskeleton and cell survival (Jacinto et al., 2004; Sarbassov et al., 2004). mTORC2 has been shown to phosphorylate the hydrophobic motifs in Akt/PKB, PKCα (protein kinase C α) and SGK1 (serum- and glucocorticoid-induced protein kinase 1) (Guertin and Sabatini, 2005), all members of the AGC protein kinase family (Pearce et al., 2010). Akt/PKB is the best-characterized substrate of mTORC2 and lays downstream of the growth factor-activated PI3K pathway. mTORC2 phosphorylates Akt/PKB at Ser473 (Hresko and Mueckler, 2005) and facilitates PDK1 (3-phosphoinositide-dependent protein kinase 1) to phosphorylate Thr308 resulting in the full activation of Akt/PKB (Fig. 2). Activated Akt/PKB controls mTORC1 activity in response to growth factors, by releasing the inhibitory effect of the TSC1/TSC2 complex and PRAS40 (Inoki et al., 2002; Sancak et al., 2007; Vander Haar et al., 2007) (Fig. 2).

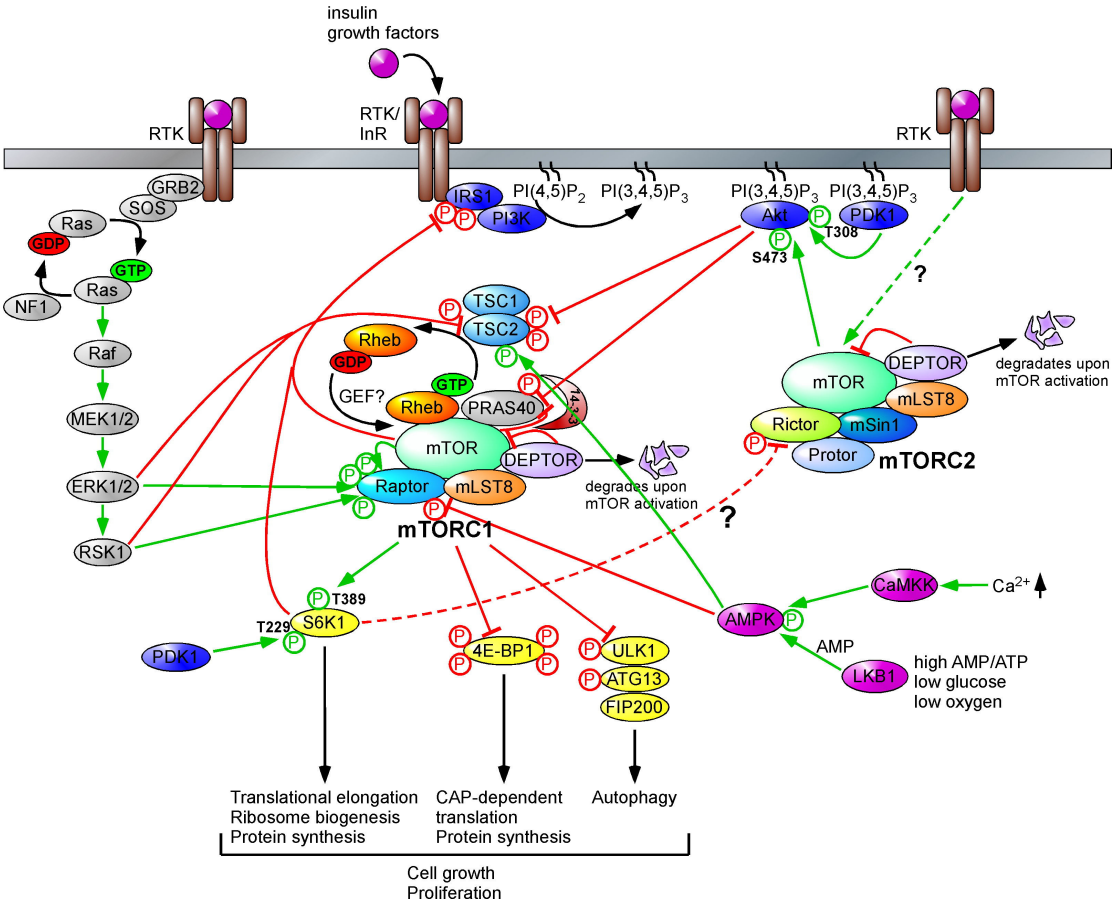

Fig. 2: The mTOR signaling pathway regulated by growth factors and energy status (simplified). Activated insulin receptor recruits and phosphorylates IRS1 that binds and activates PI3K. PI3K phosphorylates at the plasma membrane PtdIns(4,5)P_2 to generate PtdIns(3,4,5)P_3, which recruits Akt/PKB and PKD1 to the plasma membrane mediated by the binding of their pleckstrin homology (PH) domains to PtdIns(3,4,5)P_3. PDK1 phosphorylates the activation loop of Akt/PKB at Thr308 (T308). Growth factors also activate mTORC2 by an unknown mechanism near the plasma membrane, where mTORC2 may be recruited through binding of mSin1 to phospholipids, which allows mTORC2 to phosphorylate Akt/PKB on the hydrophobic motif Ser473 (S473). Active Akt/PKB phosphorylates TSC2 within the TSC1/TSC2 complex on multiple sites thereby blocking the GTPase-activating protein (GAP) activity in TSC2 to act towards Rheb, allowing Rheb-GTP to accumulate. Rheb-GTP activates mTORC1 that inactivates the inhibitor of translational initiation 4E-BP1 by phosphorylation on multiple sites, and activates the activator of translation S6K1 by phosphorylating the hydrophobic motif Thr389 (T389). PDK1 then phosphorylates the activation loop of S6K1 at Thr229 (T229) leading to the full activation of S6K1. mTORC1 blocks autophagy by phosphorylating both ULK1 and Atg13 thereby negatively affecting the kinase activity of ULK1. Together this leads to increased protein synthesis and cell growth. Akt/PKB can also directly activate mTORC1 by phosphorylating PRAS40 that gets sequestered by 14-3-3 proteins into the cytoplasm, thereby relieving the inhibitory constraint on mTORC1. DEPTOR is phosphorylated by mTOR leading to the release of DEPTOR from mTORC1 and to its degradation, thus further activating mTORC1 signaling. Once active, both mTORC1 and S6K1 phosphorylates IRS1 on multiple sites leading to the dissociation of IRS1 from the insulin receptor and to its degradation. This is a negative feedback mechanism in order to attenuate PI3K/Akt signaling. A second negative feedback loop has been proposed, where S6K1 phosphorylates rictor thereby negatively affecting Ser473

(Fig. 2 continued)
phosphorylation and activation of Akt/PKB.
The MAPK pathway also impinges positively on mTORC1 signaling. Both activated ERK1/2 and RSK1 can either activate mTORC1 indirectly by phosphorylating TSC2 and inactivating the GAP activity towards Rheb or directly by phosphorylating raptor on multiple sites.
To ensure that cells do not continue to grow under unfavorable conditions, as by withdrawal of glucose, amino acids, energy and oxygen, mTORC1 complex is rapidly inactivated by the LKB1/AMPK pathway. Upon LKB1- and AMP-dependent activation of AMPK, AMPK directly phosphorylates TSC2 within TSC1/TSC2 and activates the GAP activity of TSC2 towards Rheb, hydrolyzing Rheb-GTP to Rheb-GDP and thus inhibiting mTORC1 signaling. mTORC1 activity can also be directly suppressed by AMPK-dependent phosphorylation of raptor, which results in its binding to 14-3-3 proteins. AMPK can also be activated by CaMKK-dependent manner due to an increase in intracellular Ca^{2+} concentration.
RTK: receptor tyrosine kinase; InR: insulin receptor; IRS1: insulin receptor substrate 1; PI3K: phosphatidylinositol 3-kinase; PDK1: phosphoinositide dependent kinase 1; TSC: tuberous sclerosis complex; Rheb: Ras homologue enriched in brain; 4E-BP1: translation initiation factor 4E-binding protein 1; S6K: p70 ribosomal S6 kinase 1; ULK1: unc-51-like kinase 1; Atg13: autophagy-related gene 13; FIP200: focal adhesion kinase family interacting protein of 200 kDa; LKB1: liver kinase B1; AMPK: AMP protein kinase; AMP: adenosine monophosphate; CaMKK: calcium/calmodulin-dependent protein kinase kinase; GRB2: growth factor receptor-bound protein 2; SOS: son-of-sevenless; NF1: neurofibromin; MEK: MAPK/ERK kinase; ERK: extracellular-signal related kinase; RSK1: p90 ribosomal S6 kinase 1.

2.3 Upstream signals to mTOR complex1

A plethora of signals can activate mTORC1 including nutrients, growth factors and cellular energy levels, while stress conditions as nutrient starvation, osmotic stress and hypoxia (condition of low oxygen) inactivates mTORC1. In contrary, mTORC2 is activated only by growth factors by an unknown mechanism.

2.3.1 mTORC1 regulated by growth factors

The best described pathway that activates mTORC1 is via the growth factor insulin (Fig. 2). Insulin binds to its cognate tyrosine kinase receptor, the insulin receptor, promoting the activation of the receptor and the recruitment and activation of insulin receptor substrate 1 (IRS1). IRS1 recruits PI3K that phosphorylates phosphatidylinositol (4,5)-biphosphate [PtdIns(4,5)P_2] in the plasma membrane to phosphatidylinositol (3,4,5)-triphosphate [PtdIns(3,4,5)P_3]. Both Akt/PKB and PDK1 are then recruited to the plasma membrane through binding of their pleckstrin homology (PH) domains to PtdIns(3,4,5)P_3. This allows Akt/PKB to be activated

through phosphorylation on Thr308 by PDK1 and Ser473 by mTORC2, which is activated by growth factors by an unknown mechanism (Manning and Cantley, 2007). Once active, Akt/PKB phosphorylates many downstream targets including multiple sites in TSC2 as Ser939, Ser1130 and Thr1462, which forms a functional complex with TSC1 (Manning and Cantley, 2003; Manning et al., 2002). TSC2 contains a GTPase-activating protein (GAP) that, when in complex with TSC1 is active and stimulates the intrinsic GTPase activity of the small G-protein Rheb, thereby promoting the conversion of GTP-bound active Rheb into its GDP-bound inactive state (Manning and Cantley, 2003; Tee et al., 2003). Phosphorylation of TSC2 by Akt/PKB impairs the ability of the TSC1/TSC2 complex to act as a GAP towards Rheb, allowing GTP-bound Rheb to accumulate and to activate mTORC1 (Inoki et al., 2003a). Akt/PKB can also activate mTORC1 directly by phosphorylating and relieving the inhibitory constraint of PRAS40 on mTORC1 (Sancak et al., 2007; Vander Haar et al., 2007; Wang et al., 2007). The inhibitory constraint exerted by DEPTOR on mTORC1 is relieved through phosphorylation by mTOR that eventually leads to the release of DEPTOR from mTORC1 and to its degradation (Peterson et al., 2009). Active mTORC1 phosphorylates its downstream effectors S6K1 at Thr389 and 4E-BP1 on multiple sites (Thr37, Thr46, Ser65 and Thr70) promoting mRNA translation, ribosome biogenesis and protein synthesis (Burnett et al., 1998; Wang et al., 2005). PDK1 phosphorylates phospho Thr389-primed S6K1 on Thr229 in a reaction independent of PDK1 binding to PtdIns(3,4,5)P_3 leading to the full activation of S6K1 (Manning and Cantley, 2007). A negative feedback loop exists to attenuate the PI3K-Akt/PKB-mTORC1 signaling that involves phosphorylation of IRS1 by active S6K1 and mTORC1 on Ser302 and Ser636/Ser639, respectively (Harrington et al., 2004; Tzatsos and Kandror, 2006). Phosphorylated IRS1 is impaired to associate with the insulin receptor and is targeted for proteosomal degradation leading to the inability of insulin to activate PI3K and Akt/PKB (Harrington et al., 2004; Harrington et al., 2005; Manning, 2004; Tzatsos and Kandror, 2006).

Recently, another S6K1-mediated feedback mechanism has been identified that does not involve IRS1. S6K1 phosphorylates the mTORC2 component rictor on Thr1135 in a rapamycin-sensitive manner and thereby negatively regulating Akt/PKB phosphorylation and activation (Dibble et al., 2009; Julien et al., 2010) (Fig. 2). However, this mechanism needs still verification, because a recent report demonstrated that phosphorylation of rictor on Thr1135 does not attenuate Akt/PKB phosphorylation (Treins et al., 2010). Furthermore, the physiological importance of rictor phosphorylation is also unclear, inasmuch as Thr1135 phosphorylation does

neither affect mTORC2 assembly nor alter mTORC2 kinase activity (Dibble et al., 2009; Julien et al., 2010).

In addition to the above described PI3K-Akt/PKB pathway, activation of the Ras/MAPK (mitogen-activated protein kinase) pathway also leads to mTORC1 activation (Fig. 2). Growth factor activated receptor tyrosine kinase (RTK) recruits GRB2 (growth factor receptor-bound protein 2) followed by the recruitment of the Ras GEF (guanine nucleotide-exchange factor) son-of-sevenless (SOS) that activates Ras promoting a signaling cascade via Raf towards MEK1/2 (MAPK / ERK kinase) stimulating ERK1/2 (extracellular-signal related kinases 1 and 2, also referred as MAPK1/2) (Shaw and Cantley, 2006). Activated ERK interacts with and directly phosphorylates TSC2 at Ser664 leading to the disruption of the TSC1/TSC2 complex and therefore to the activation of mTORC1 signaling (Ma et al., 2005). The ERK1/2 substrate RSK1 (p90 ribosomal S6 kinase 1) also signals to the mTORC1 pathway by relieving the inhibitory effect of TSC1/TSC2 complex on mTORC1 by phosphorylating TSC2 at Ser1798 (Roux et al., 2004). Both ERK1/2 and RSK1 can also directly target mTORC1 by phosphorylating raptor on multiple sites, including Ser8, Ser696, Ser855 and Ser863 by ERK1/2 and on Ser719, Ser721 and Ser722 by RSK1 (Carriere et al., 2008; Carriere et al., 2011; Langlais et al., 2011). Raptor phosphorylation positively stimulates mTORC1 activity to its downstream effectors without influencing the association of raptor with mTOR or its substrates S6K1 and 4E-BP1 (Carriere et al., 2008; Carriere et al., 2011).
Interstingly, Ser863 on raptor has been reported to be phosphorylated by mTOR following insulin stimulation or under conditions of Rheb overexpression (Foster et al., 2010; Wang et al., 2009), which renders mTORC1 activity insensitive to serum and nutrient starvation (Long et al., 2005a; Long et al., 2005b). Together this suggests that the MAPK pathway and the PI3K-Akt/PKB synergize at the level of raptor phosphorylation to activate mTORC1 signaling and that MAPK pathway can independently of the PI3K-Akt/PKB pathway activate mTORC1 activity. Moreover, raptor, besides to its role in substrate binding seems to be an important integration site for mTORC1 regulation and activation.

2.3.2 mTORC1 regulated by energy status

Information regarding the intracellular energy and oxygen status of the cell is also sensed by mTORC1. In cases of stress such as energy depletion and hypoxia LKB1/AMPK pathway inhibits mTORC1 activity and cell growth (Fig. 2). LKB1 (liver kinase B1) is a key upstream activator of AMPK (adenosine monophosphate-activated protein kinase). LKB1 exists as a heterotrimeric protein complex with STRAD (STE20-related adaptor) and MO25 (mouse protein 25), two regulatory subunits required for the kinase activity of LKB1 (Shackelford and Shaw, 2009). Similar to LKB1, AMPK is a heterotrimer composed of a catalytic subunit (AMPKα) and two regulatory subunits (AMPKβ and AMPKγ) (Shackelford and Shaw, 2009). When the intracellular ratio AMP/ATP is high either due to an excessive ATP consumption or reduced aerobic ATP production, in case of hypoxia, AMP is bound by AMPKγ promoting the phosphorylation of AMPKα at Thr172 by LKB1 and thus activating AMPK (Shackelford and Shaw, 2009). Active AMPK directly phosphorylates TSC2 on Thr1227 and Ser1345 and activates the TSC1/TSC2 complex (Inoki et al., 2003b). As a result of TSC1/TSC2 activation GTP-bound Rheb is converted to the inactive GDP-bound Rheb resulting in the inhibition of mTORC1 signaling (Inoki et al., 2003b). Intriguingly, active AMPK can, independent of TSC1/TSC2 complex, directly block mTORC1 activity by phosphorylating raptor on two serines, Ser722 and Ser792 (Gwinn et al., 2008), which results in raptor binding to 14-3-3 and suppression of mTORC1 kinase activity (Gwinn et al., 2008). AMPK can also, independent of LKB1, be phosphorylated and activated by calcium/calmodulin-dependent protein kinase kinase (CaMKK), which is triggered through influx of calcium (van Veelen et al., 2011). The role of AMPK is to restore the cellular energy balance. Consistently, AMPK activation induces relocalization of the glucose importer GLUT4 to the plasma membrane of muscle cells to internalize glucose in order to gain energy through glycolysis (Hardie, 2007; van Veelen et al., 2011). Moreover, AMPK phosphorylates several targets to enhance energy-producing catabolism and suppress energy-consuming anabolism (Hardie, 2007).

2.3.3 mTORC1 regulated by amino acids

The components of the insulin/growth factor-mediated activation of mTORC1 are well characterized, while the elements mediating the nutrient input to mTORC1 have just started to be unraveled. Nutrients, such as amino acids, positively regulate mTORC1 activity and signaling. In the absence of amino acids the two best-characterized mTORC1 substrates, S6K1 and 4E-BP1, are rapidly dephosphorylated (Hara et al., 1998; Wang et al., 1998) due to the action of the protein phosphatase 2A (PP2A) (Peterson et al., 1999). Interestingly, amino acid-mediated activation of mTORC1 is dominant over the growth factor stimulated pathway (Hara et al., 1998), because in the absence of amino acids insulin treatment alone is insufficient to drive S6K1 and 4E-BP1 phosphorylation (Hara et al., 1998). The amino acid-sensing pathway to mTORC1 is distinct from that controlled by the growth factor-PI3K-Akt/PKB pathway. In agreement, it has been previously demonstrated that amino acids act on mTORC1 independent of the TSC1/TSC2 complex, as amino acid depletion can still inhibit mTORC1-mediated S6K1 phosphorylation in the absence of TSC2 (Nobukuni et al., 2005; Roccio et al., 2006; Smith et al., 2005). However, Rheb is absolutely required in the amino acid-mediated activation of mTORC1, inasmuch as in the absence of Rheb amino acid stimulation is ineffective in stimulating mTORC1 signaling (Sancak et al., 2010; Sancak et al., 2008). On the other hand, overexpression of Rheb overcomes the inhibitory constraint of amino acid withdrawal on mTORC1 activation (Long et al., 2005a; Long et al., 2005b). Nevertheless, Rheb does not activate mTORC1 signaling by altering the intracellular amino acid levels, because Rheb does not influence the uptake of amino acids or glucose (Hall et al., 2007). Moreover, depletion of Rheb or TOR has been demonstrated to decrease the rates of protein synthesis and ribosome production without altering the rates of amino acid import (Hall et al., 2007). Instead, Rheb activates mTORC1 through a direct association with the catalytic domain of mTOR in an amino acid-dependent manner (Long et al., 2005a). Interestingly, the ability of Rheb to associate with mTOR is not dependent on GTP loading (Long et al., 2005a; Long et al., 2005b). In contrast, guanyl nucleotide deficient Rheb mutant binds mTOR more tightly than wild type Rheb (Long et al., 2005a; Long et al., 2005b). Nevertheless, mTOR kinase activity is positively affected only by GTP-charged Rheb (Long et al., 2005a; Long et al., 2005b). Even though Rheb GTP loading is not affected by amino acid withdrawal, amino acid withdrawal inhibits the interaction between Rheb and mTOR (Long et al., 2005b). Consistently, upon amino acid stimulation mTORC1 has been demonstrated to translocate to

Rheb-positive late endosomes/lysosomes thereby facilitating the interaction between mTOR and Rheb and thereby activating mTORC1 (Sancak et al., 2010; Sancak et al., 2008).

Less is know about the GEF regulating the conversion of Rheb-GDP to Rheb-GTP. In *Drosophila* TCTP (translationally controlled tumor protein) has been found to be a GEF for Rheb (Hsu et al., 2007). However, follow up studies in mammalian cells revealed that reducing TCTP expression does not affect mTORC1 signaling in response to amino acid or insulin treatment (Rehmann et al., 2008; Wang et al., 2008b). The GDP/GTP ratio of Rheb bound nucleotide does not change in response to insulin in TCTP knockdown cells compared to control cells (Rehmann et al., 2008). Additionally, overexpresison of TCTP does not rescue mTORC1 signaling in amino acid-depleted cells (Wang et al., 2008b), and MEFs from TCTP null mice show normal mTORC1 activation upon serum stimulation (Chen et al., 2007). Together, this suggests that, at least in mammals, TCTP is unlikely a GEF for Rheb.

2.4 Intracellular amino acid sensing

2.4.1 Intracellular amino acid levels modulated by amino acid transporters

The question that has captivated many research groups in the last years is how amino acids regulate mTORC1 signaling. Unlike the insulin receptor that transduces the extracellular signal inside the cell via the PI3K/Akt pathway to mTORC1, there is no amino acid receptor that perceives variation in extracellular amino acid levels. Instead, mTORC1 senses intracellular amino acids levels (Beugnet et al., 2003; Christie et al., 2002). Nonetheless, extracellular amino acids modulate the levels of intracellular amino acids through amino acid transporters at the plasma membrane. In *Xenopus* oocytes, that are relative impermeable to amino acids and lack amino acid transporters, extracellular leucine is unable to stimulate mTORC1 activity (Christie et al., 2002). But expression of a System L amino acid transporter (also known as LAT1), which is a transporter for neutral amino acids such as leucine, enables *Xenopus* oocytes to respond to extracellular leucine by S6K1 phosphorylation in a rapamycin-dependent manner (Christie et al., 2002). Furthermore, in mammalian cells starved for amino acids, mTORC1 signaling is inactive and unresponsive to insulin (Hara et al., 1998). However, treatment with

translation inhibitors such as cycloheximide to block protein synthesis allows insulin-dependent activation of mTORC1 even in the absence of amino acids in the medium, inasmuch as protein synthesis inhibition results in an accumulation of intracellular amino acids allowing mTORC1 signaling (Beugnet et al., 2003).

The main amino acids able to activate mTORC1 pathway are essential amino acids (EAA) such as leucine, tryptophan, phenylalanine and arginine (Blommaart et al., 1995; Hara et al., 1998; Wang et al., 1998). Nonetheless, addition of EAA alone to amino acid starved cells has little effect in mTORC1 activation (Nicklin et al., 2009) (Fig. 3). Instead, EAA has to act together with the nonessential amino acid glutamine in a two step transport mechanism to regulate mTORC1 activity (Nicklin et al., 2009). First, glutamine is transported into cells through the high affinity sodium (NA^+)-dependent glutamine transporter SLC1A5, a System ASC transporter (also named ASCT2). Second, intracellular glutamine is used as an efflux substrate to regulate the uptake of extracellular leucine through the heterodimeric SLC7A5/SLC3A2 antiporter, a System L transporter (also named LAT1/4F2hc), which subsequently leads to activation of mTORC1 (Nicklin et al., 2009) (Fig. 3). Intriguingly, there are some tumor lines such as the breast cancer cell line MCF7 that have elevated intracellular glutamine levels allowing EAA alone in a one transport mechanism to activate mTORC1 pathway (Nicklin et al., 2009). In addition, it has been reported that in some tumors glutamine synthetase is overexpressed (reviewed in Nicklin et al., 2009) or amino acid transporters are upregulated (Fuchs and Bode, 2005; Yanagida et al., 2001) probably to sustain the increased protein synthesis for continuous growth and proliferation of tumors.

Together, this implies the existence of an intracellular amino acid sensor that acts upstream of mTORC1 (Fig. 3). However, the mode of action of this amino acid sensor is unknown. Candidate mediators acting downstream of amino acids have been identified, including Rag GTPases, p62, V-ATPase, PAT1 and PAT4, Vps34, the sterile 20 (STE20) family kinase mitogen-activated protein kinase kinase kinase kinase 3 (MAP4K3), Rab5, and Vps39. The mode of action of the potential amino acid mediators will be discussed in the following paragraphs and are summarized in Table 2.

Table 2: Proteins that might be involved in mTORC1 activation and subcellular localization by amino acids

Mammals	yeast	Function
TSC1/TSC2		Rheb GTPase-activating protein; no homologues in *Saccharomyces cerevisiae*
Rheb	ScRheb SpRhb1	Small GTPase; activates mTORC1 through direct interaction with mTOR; is important for development as Rheb knockout mice are embryonic lethal (Goorden et al., 2011); *Saccharomyces cerevisiae* Rheb is involved in the uptake of arginine and lysine (Urano et al., 2000). *Schizosaccharomyces pombe* Rhb1 (Rheb homologue) is essential for cell growth and division (Mach et al., 2000).
RagA/B	Gtr1	Small GTP binding proteins; regulates mTORC1 activation by amino acids by guiding mTORC1 to the Rheb-containing endosomal compartment; function as a heterodimer where RagA/B has a dominant function over RagC/D and RagA/B^{GTP}-RagC/D^{GDP} combination is the most active.
RagC/D	Gtr2	
p18, p14, MP1 (Ragulator)	Ego1, Ego3 (Sc Ragulator)	Rag GTPases interacting complex; anchors TORC1 to late endosomes/lysosomes via Rag proteins
Vps39 / Vam6	Vps39 / Vam6	Vam6 functions as a Gtr1 GEF in *Saccharomyces cerevisiae*; in mammalian cells no Rag GEF has been found yet. GEF for Rab7; required for the conversion of early endosomes to late endosomes; deletion impairs amino acid- and insulin-stimulated mTORC1 activity.
V-ATPase		Localized on endosomal membranes such as lysosomes; hydrolysis of ATP; involved in mTORC1 activation by amino acids.
PATs		Localized on endosomal compartment; senses amino acids availability to mTORC1 by an unknown mechanism.
p62		Similar function as the Ragulator; required for the Rag-mTORC1 interaction and directs mTORC1 to lysosomes.
Vps34	Vps34	Class III PI3K; generates PtdIns(3)P from PtdIns; might be involved in the amino acid sensing through mTORC1 either acting as an potential amino acid signaling mediator or by regulating the formation of late endosomes/lysosomes, where mTORC1 can interact with Rheb.
p150 / Vps15	Vps15	Ser/Thr-like kinase; Vps34 adaptor protein; localizes Vps34 to cellular membranes.
MAP4K3	Ste20-related	Protein kinase; signals nutrient availability to mTORC1.
$PP2A_{T61\varepsilon}$		Ser/Thr protein phosphatase; inhibits MAP4K3 by dephosphorylation.
PLD		Hydrolysis of PC to PA; amino acid- and mitogenic-dependent activation; regulates mTORC1 signaling; involved in autophagy.
Rab5		Early endosomal marker; constitutive active Rab5 impairs amino acid- and insulin-stimulated mTORC1 activity.

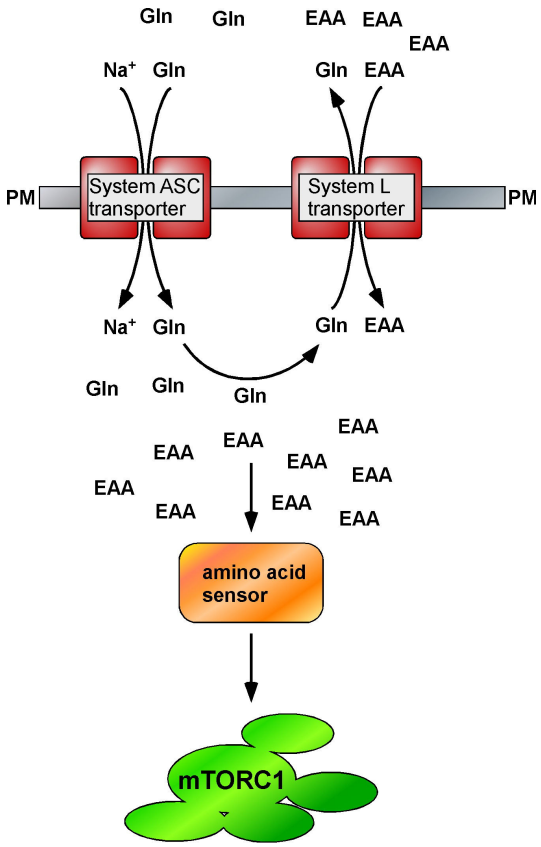

Fig. 3: Intracellular accumulation of amino acids positively signals to mTORC1 through a putative intracellular amino acid sensor. In a two step transport mechanism amino acids, especially essential amino acids such as leucine, are enriched intracellularly involving a System ASC transporter, for glutamine uptake, coupled to a bidirectional System L transporter. Glutamine (Gln) is transported through the System ASC transporter into cells in a Na^+-dependent manner. Next glutamine is exported through the system L transporter in exchange for extracellular essential amino acids that accumulate within cells. A putative amino acid sensor senses intracellular amino acids and activates mTORC1 through an unknown pathway. Cells starved for glutamine are unable to take up essential amino acids, which results in the inhibition of mTORC1. Gln: glutamine; EAA: essential amino acids; PM: plasma membrane.

2.4.2 mTORC1 regulated by Rag GTPases

Key components in the regulation of the amino acid-dependent mTORC1 activation are the Ras-related small GTP-binding (Rag) proteins. Mammals express four Rag proteins (RagA, RagB, RagC and RagD), with high sequence similarity between RagA and RagB (97%) and RagC and RagD (81%) (Sekiguchi et al., 2001). The Rag proteins function as heterodimers, RagA or RagB dimerizes with RagC or RagD and unlike most Ras family GTPases, Rag proteins lack any membrane targeting sequences (Sekiguchi et al., 2001). Another interesting aspect is that in the heterodimer one Rag is GTP- and the other is GDP-charged.

Two recent reports have provided evidence that the Rag proteins (Rag heterodimers) are required for amino acids to activate mTORC1 signaling in *Drosophila* and in mammalian cells (Kim et al., 2008; Sancak et al., 2008). Rag proteins interact with mTORC1 in an amino acid-dependent manner mediated by the interaction with raptor (Sancak et al., 2008). Furthermore, the GTP/GDP loading status of the Rag proteins is crucial for the association with mTORC1. The heterodimer with RagA/B in the GTP and RagC/D in the GDP form is active and strongly binds to raptor (Sancak et al., 2008). In response to amino acid treatment GTP charging of RagA/B increases and concomitantly augments the association of the Rag proteins with mTORC1.

Moreover, in respect to the intracellular localization of mTORC1, amino acids treatment relocates mTORC1 from tiny puncta distributed throughout the cytoplasm to late endosomes/lysosomes (Sancak et al., 2008), where Rheb resides thereby promoting mTORC1 activation. Interestingly, depletion of either the Rag proteins or of raptor by RNA interference (RNAi) prevents the recruitment of mTORC1 to late endosomes/lysosomes in response to amino acids and strongly reduces mTORC1 activity (Kim et al., 2008; Sancak et al., 2008). Additionally, expression of constitutive active RagA/B renders mTORC1 activity insensitive to amino acid starvation (Kim et al., 2008; Sancak et al., 2008). A direct relationship of Rag proteins and TORC1 activation is also phenotypically visible in *Drosophila*, where overexpression of constitutive active dRagA increases cell size under starvation conditions, while dominant-negative dRagA decreases cell size under nutrient-rich conditions (Kim et al., 2008). Therefore, the Rag proteins are specifically involved in the amino acid-dependent mTORC1 signaling pathway and the following mechanism has been proposed how amino acids positively regulate mTORC1 signaling (Fig. 4A). Upon amino acid stimulation RagA/B becomes GTP charged, promoting Rag heterodimer to interact with raptor and eventually recruiting mTORC1 to late endosomes/lysosomes, where Rheb resides thereby promoting interaction with and activation of mTORC1 (Sancak et al., 2008). This model explains why TSC2 knockout MEFs, which have constitutive active Rheb, are still sensitive to amino acids starvation, and only by amino acid treatment mTORC1 comes together with Rheb on the same endosomal compartment where they can interact.

Since Rag proteins lack any membrane anchoring sequences (Sekiguchi et al., 2001), the question is how mTORC1 is targeted by the Rag proteins to endosomal membranes. Membrane anchorage is mediated by the Ragulator (Rag and mTORC1 regulator), a heterotrimeric complex composed of MP1, p14 and p18 (Sancak et al., 2010). p18 is myristoylated and palmitoylated and is localized on late endosomes/lysosomes (Nada et al., 2009). Moreover, p18 is the principal Rag-binding subunit of the Ragulator (Sancak et al., 2010) thereby anchoring the Rag proteins on late endosomes/lysosomes. The association between Ragulator and the Rag proteins is constitutive, inasmuch as it is independent of the amino acid availability and of the GTP/GDP charged status of the Rag proteins (Sancak et al., 2010). But Ragulator-Rag complex is an amino acid-regulated docking site for mTORC1 on late endosomal/lysosomal membranes as upon amino acid treatment RagA/B is GTP loaded and binds to mTORC1 (via raptor) thereby relocalizing mTORC1 to Rheb-containing late endosomes/lysosomes (Sancak et al., 2010) (Fig.

4A). Consisting with this model, artificial targeting of raptor to late endosomes/lysosomes constitutively localizes mTORC1 to late endosomes/lysosomes and renders mTORC1 activity resistant to amino acid starvation and eliminates the requirement of the Ragulator-Rag complex in mTORC1 signaling (Sancak et al., 2010). Nonetheless, mTORC1 localization alone is not sufficient for its activation, because deletion of Rheb expression blocks mTORC1 activation in response to amino acids (Sancak et al., 2010).

Interestingly, Rag GTPases homologous has been observed in yeast and, alike in *Drosophila* and mammalian cells, they function in the amino acid-dependent TORC1 activation (Binda et al., 2009). Gtr1 is homologous to RagA/B and Gtr2 to RagC/D, and the heterodimer is active when Gtr1 is GTP- and Gtr2 is GDP-loaded. Alike RagA/B, Gtr1 interacts with and activates TORC1 in an amino acid-sensitive manner, and Gtr1 in its GTP-charged form can physically interact to TORC1 (Binda et al., 2009). TORC1 and the Gtr proteins localize on the vacuolar membrane, the yeast equivalent of lysosomes (Binda et al., 2009). Homologous of the Ragulator subunits have not been found in yeast, but the mammalian Ragulator-Rag complex may be functionally similar to the yeast EGO (exit from growth arrest) complex. The EGO complex consists of Ego1, Ego3, Gtr1 and Gtr2, and like p18 in mammalian cells, Ego1 is myristoylated and targets the EGO complex to the vacuole (De Virgilio and Loewith, 2006). Moreover, Ego3 displays structural conservation to MP1 and p14 (Kogan et al., 2010) indicating Ego1 and Ego3 being the potential yeast Ragulator. Despite these similarities, TOR1 localization is not dependent on amino acid availability, inasmuch as leucine deprivation does not alter the localization of TOR1, Gtr1 or Ego1, even though amino acids control the association of TORC1 with Gtr1 (Binda et al., 2009). Nonetheless, structural conservation of TOR membrane-targeting constituents between yeast and mammalian cells suggests a common mechanism for sensing and signaling amino acids availability to TORC1.

In response to amino acid stimulation RagA/B is GTP charged but a Rag GEF has not been found yet. However, a good candidate is found in *Saccharomyces cerevisiae* where Vps39 (vacuolar protein sorting 39; also named Vam6) has been found to be the GEF for Gtr1p (Binda et al., 2009). The mammalian Vps39 seems not to act as a Rag GEF, although knockdown of Vps39 reduces mTORC1 activity (Flinn et al., 2010).

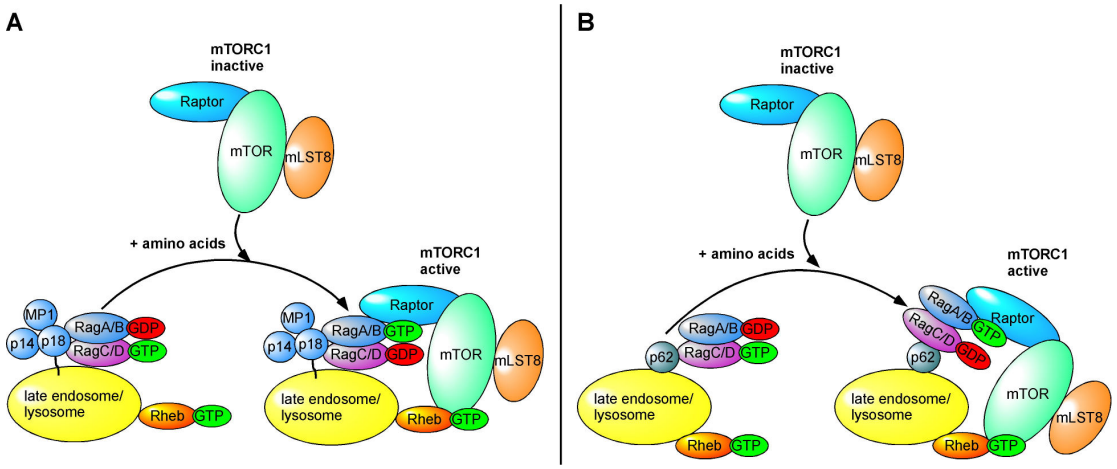

Fig. 4: Amino acid-induced mTORC1 activation via Rag GTPases (two complexes are proposed). (A) In amino acid-starved cells, the complex consisting of Ragulator (p18-p14-MP1) and the inactive RagA/B^{GDP}-RagC/D^{GTP} heterodimer is localized on the late endosome/lysosome, while mTORC1 is absent. Upon amino acid stimulation active RagA/B^{GTP}-RagC/D^{GDP} heterodimer is formed and raptor binds to RagA/B^{GTP} thereby guiding mTORC1 from an unknown cellular compartment to the late endosomal/lysosomal membrane, where mTORC1 interacts with Rheb and promotes mTORC1 activation and signaling. (B) A distinct complex composed of p62 and Rag heterodimer recruits mTORC1 to late endosomes/lysosomes by amino acid treatment in an analogous manner as the Ragulator-Rag complex, resulting in the association between Rheb and mTORC1 and eventually to the activation of mTORC1.

A distinct complex consisting of p62 and the Rag proteins has been recently reported to recruit mTORC1 to the late endosome/lysosome in response to amino acids without the involvement of the Ragulator (Duran et al., 2011) (Fig. 4B). p62 is an adaptor protein that interacts with different signaling proteins to regulate cellular functions (reviewed in Duran et al., 2011). Here, p62 specifically associates with mTORC1, but not mTORC2, through its interaction with raptor and is selectively required for mTORC1 activation in response to amino acid but not to insulin treatment (Duran et al., 2011). Moreover, p62 selectively interacts with RagC/D but not with RagA/B (Duran et al., 2011). Like raptor, p62 preferentially interacts with active RagA/B^{GTP}-RagC/D^{GDP} heterodimer, while interaction with one of the Ragulator components (p18, p14, MP1) has not been observed. Overexpression of p62 promotes GTP-loading of RagB in amino acid starved cells thus mimicking amino acid stimulation (Duran et al., 2011). Interestingly, p62 and RagC colocalizes on late endosomes/lysosomes membranes independently of amino acid availability (Duran et al., 2011), which is reminiscent of the localization of the Ragulator and Rag proteins (Sancak et al., 2010). Consistently, amino acid stimulation leads to the translocation of mTORC1 to p62 containing late endosomes/lysosomes, while in p62 deficient cells late endosomes/lysosomes localization of mTORC1 is abrogated

(Duran et al., 2011). Therefore, p62 promotes the formation of an active Rag complex to induce Rag-mTORC1 interactions and translocation of mTORC1 to late endosomes/lysosomes. Consequently, p62 provides a second docking site for mTORC1 activation. However, it is unclear what the cellular purpose is to have two distinct complexes (p62/Rags vs. Ragulator/Rags) with apparently similar functions.
There are several open questions as how do Rag GTPases sense amino acid availability within a cell and how are they GTP and GDP loaded? Is there a mammalian Rag GTPase GEF that is activated by amino acid sufficiency? Conversely, is there a Rag GTPase GAP that switch off the amino acid signal?

Recently, the activity of vacuolar H^+-adenosine triphosphatase ATPase (V-ATPase) has been found to be necessary for mTORC1 activation by amino acids (Zoncu et al., 2011). Inhibition of the V-ATPase, either by pharmacological inhibition or gene silencing, prevents amino acid-induced mTORC1 translocation onto lysosomes and activation of mTORC1 signaling. However, the overexpression of GTP-charged RagB can bypass the need of V-ATPase function. Therefore, the author placed V-ATPase downstream of amino acids but upstream of Rag proteins (Zoncu et al., 2011). But how mechanistically V-ATPase can activate mTORC1 is not known. V-ATPase physically interacts with Ragulator and Rag GTPases and amino acid stimulation induces a structural rearrangement of the V-ATPase-Ragulator-Rag complex that somehow activates mTORC1. Furthermore, the authors claim that sensing of intralysosomally accumulated amino acids initiates signaling to mTORC1, inasmuch as overexpression of PAT1 (proton-assisted amino acid transporter 1; a lysosomal localized symporter of amino acids and protons) (Boll et al., 2004), or permeabilized lysosomal membrane empties the lysosomes of amino acids and blocks mTORC1 activity (Zoncu et al., 2011). How exactly amino acids within the lysosomal lumen are sensed is not known, but a good candidate could be the PATs by themselves. PAT1 and PAT4 have recently been demonstrated to be indispensable in amino acid induced mTORC1 activation. Interestingly, the effect of PATs has not been dependent on their ability to shuttle amino acids (Heublein et al., 2010). The ability of the PATs to sense amino acids is probably due to their endosomal localization but how they mechanistically do it is not known. Alternatively, they may facilitate amino acid transport across endomembranes where mTORC1 resides in order to directly promote mTORC1 signaling.

2.4.3 mTORC1 regulated by Vps34

Vps34 (vacuolar protein sorting 34) has been originally identified in *Saccharomyces cerevisiae* as a protein involved in the transport of newly synthesized soluble hydrolases from the Golgi to the lysosome-like vacuole (Herman and Emr, 1990). Mammalian Vps34 has been cloned and shown to be ubiquitously expressed (Volinia et al., 1995). Vps34 exclusively phosphorylates phosphatidylinositol (PtdIns) to generated phosphatidylinositol 3-phosphate [PtdIns(3)P]. In both yeast and mammals, Vps34 exists in a complex with Vps15 (in mammals also named p150), a N-terminal myristoylated Ser/Thr-like protein kinase (Stack et al., 1993; Volinia et al., 1995). Due to this myristoylation moiety in Vps15, Vps34 is targeted to cellular membranes where PtdIns resides (Christoforidis et al., 1999; Murray et al., 2002; Stack et al., 1993; Stein et al., 2003). Additionally, Vps15 serves to regulate the lipid kinase activity of Vps34 in yeast and probably also in mammals (Panaretou et al., 1997; Petiot et al., 2000; Stack et al., 1993).

In addition to play a role in vesicular trafficking, Vps34 has been shown to be required for the initiation of the autophagic pathway (Simonsen and Tooze, 2009) and it has been proposed to mediate the amino acid signal to mTORC1 (Byfield et al., 2005; Nobukuni et al., 2005). Deletion of Vps34 by small interference RNA (siRNA) blocks amino acid- and insulin-stimulated mTORC1 activation, whereas insulin-stimulated Akt/PKB phosphorylation on Ser473 is not affected (Byfield et al., 2005; Nobukuni et al., 2005). In the presence of amino acids, overexpression of epitope-tagged Vps34 leads to a marked increase in mTORC1 activity compared to control cells (Nobukuni et al., 2005). Sequester of the Vps34 lipid product PtdIns(3)P by ectopic expression of a tandem FYVE domain (from Fab1p, YOTB, Vac1p, EEA1 (early endosomal antigen 1)) reduces amino acid-induced mTORC1 activation (Nobukuni et al., 2005). Moreover, amino acid treatment of starved cells leads to an increase in Vps34 activity and in intracellular PtdIns(3)Ps (Nobukuni et al., 2005) further underscoring the link between Vps34 and mTORC1 in the amino acid-dependent pathway. Furthermore, a mechanism has been proposed how extracellular amino acids can regulate Vps34 activity in a Ca^{2+}-dependent manner (Gulati et al., 2008). Amino acids induce an extracellular Ca^{2+} influx into the cell inducing Ca^{2+}/calmodulin (CaM) complex formation. Ca^{2+}/CaM binds to and activates Vps34 leading to increased PtdIns(3)P generation and eventually to mTORC1 activation (Gulati et al., 2008). However, there are several concerns in presenting Vps34 as an amino acids sensor towards mTORC1. (1) Yan et al. (2009) questioned the Ca^{2+} mechanism (Gulati et al., 2008) by demonstrating that Vps34 activity is not

affected by Ca^{2+} chelators or CaM inhibitors (Yan et al., 2009). (2) Overexpression of hVps34 increases mTORC1 activity only in the presence, but not in the absence of amino acids (Nobukuni et al., 2005). Overexpression of kinase inactive version of Vps34 has never been analyzed in order to determine whether the increase of mTORC1 activity was due to Vps34 kinase activity or just an off-target effect. (3) Increased PtdIns(3)P levels due to amino acid stimulation have not been quantified. (4) In mammalian C2C12 cells, amino acid treatment appears to inhibit rather than to activate Vps34 (Tassa et al., 2003). (5) In yeast, Vps34 mutants (severe defects in vacuolar protein sorting, temperature-sensitive growth defect, defect in osmoregulation and in vacuole segregation during mitosis) do not recapitulate the phenotypes of TOR1 and TOR2 mutants (cell cycle arrest in G1) (Barbet et al., 1996; Herman and Emr, 1990). (6) In a *Drosophila* study, Vps34 loss-of-function mutants display disrupted autophagy and endocytosis but TORC1 signaling pathway is not affected (Juhasz et al., 2008).

Recently, Vps34 knockout mice have been generated showing that they die between E7.5 and E8.5 of embryogenesis (Zhou et al., 2011). Vps34 mutant embryos have reduced proliferation and drastically decreased mTORC1 activity, determined by the phosphorylation of ribosomal S6, the downstream target of S6K1 (Zhou et al., 2011). Decreased mTORC1 activity signifies reduced availability of amino acids. It is known that during early stages of development the embryo is dependent on amino acids and glucose (Martin and Sutherland, 2001), and the period just before implantation of the embryo into the uterus, amino acid uptake is inhibited (reviewed in Martin and Sutherland, 2001). Therefore, the only way to acquire amino acids is through catabolic processes such as autophagy. During autophagy proteins and organelles are sequestered into autophagosomes that deliver their content to lysosomes for degradation into amino acids to be re-used for protein synthesis and ATP generation. Vps34 is involved in both the autophagic process and vesicular trafficking to lysosomes (Simonsen and Tooze, 2009). Consequently, it might be possible that the phospho-S6 phenotype in Vps34 mutant embryos (Zhou et al., 2011) is rather a consequence of nutrient shortage due to disrupted autophagy and vesicular trafficking than a direct involvement of Vps34 on mTORC1. Mice have been generated where Vps34 was conditionally deleted in postmitotic sensory neurons (Zhou et al., 2010). These Vps34-deleted neurons have been demonstrated to accumulate ubiquitin-positive aggregates and enlarged vesicles (Zhou et al., 2010), which is indicative of a blocked transport to lysosomes thus supporting a defect in vesicular transport.

2.4.4 mTORC1 regulated by MAP4K3

MAP4K3 is another possible mediator of the amino acid-induced mTORC1 activation. MAP4K3, a *Ste20*-related MAP4K3, has been identified in a screen of *Drosophila* protein kinases required for signaling to dS6K (Findlay et al., 2007). Overexpression of MAP4K3 activates mTORC1 in serum-starved cells leading to the phosphorylation of S6K1 and 4E-BP1, while depletion of MAP4K3 by siRNA suppresses mTORC1 activity induced by amino acid stimulation. Moreover, activity of MAP4K3 *per se* is regulated by amino acid sufficiency but not by insulin stimulation or rapamycin treatment, placing MAP4K3 downstream of amino acids but upstream of mTORC1 (Findlay et al., 2007). Ser170 in the kinase domain of MAP4K3 has been identified to be critical for kinase activity (Yan et al., 2010). Depriving cells of amino acids inhibits MAP4K3 Ser170 phosphorlyation, while amino acids addition reversed the response. Importantly, insulin has no effect on Ser170 phosphorylation. Moreover, mutation of Ser170 to alanine abolishes MAP4K3 activity and blocks mTORC1-mediated phosphorylation of S6K1 in response to amino acids. Ser170 phosphorylation is transphosphorylated by another MAP4K3, whereas dephosphorylation is mediated by the Ser/Thr phosphatase $PP2A_{T61\varepsilon}$. In response to amino acid withdrawal, the regulatory/targeting subunit PR61ε of $PP2A_{T61\varepsilon}$ associates with MAP4K3 thereby recruiting MAP4K3 to $PP2A_{T61\varepsilon}$ leading to a rapid Ser170 dephosphorylation and suppression of mTORC1 activity (Yan et al., 2010). A model has been proposed that upon amino acid withdrawal, $PP2A_{T61\varepsilon}$ associates with MAP4K3 and dephosphorylates Ser170 therefore inactivating MAP4K3 and signaling to mTORC1 (Yan et al., 2010). Interestingly, the ability of MAP4K3 to activate mTORC1 is impaired when RagC and RagD are suppressed (Yan et al., 2010) indicating that either MAP4K3 lies downstream of the Rag proteins or MAP4K3 is not the major regulator of the amino acid input to mTORC1.

2.4.5 mTORC1 regulated by phospholipase D (PLD) and phosphatidic acid (PA)

mTORC1 can also be activated by phosphatidic acid (PA) generated through the hydrolysis of phosphatidylcholine catalyzed by phospholipase D (PLD). Overexpression of PLD1 activates mTORC1, while PLD1 knockdown blocks mitogenic activation of mTORC1 signaling (Fang et al., 2003). Similarly, exogenous added PA to serum-starved cells stimulates mTORC1 activity in a rapamycin-

dependent manner, whereas inhibition of cellular PA accumulation by 1-butanol treatment reduces serum-stimulated mTORC1 activity (Fang et al., 2001). Interestingly, the stimulatory effect of PA is absent in cells deprived of amino acids (Fang et al., 2001), indicating that an amino acid signal is required for the action of PA. PA regulates mTORC1 through a direct interaction with the FRB domain of mTOR and competes with the FKBP12-rapamycin complex for binding to mTOR (Fang et al., 2001). Consistently, elevated cellular PA levels render cells less sensitive to rapamycin (Chen et al., 2003). Mutational analysis has demonstrated that Arg2109 in the mTOR FRB domain is critical for the interaction with PA. Because the catalytic activity of mTOR is not affect by PA stimulation or by disrupting PA binding (Fang et al., 2001), it is not known how PA mechanistically activates mTORC1 signaling. But, it has been reported that Rheb interacts with and activates PLD1 in a GTP-dependent manner (Sun et al., 2008) generating PA that binds to and activates mTORC1. The production of PA by Rheb-meditated activation of PLD1 is therefore an additional mode of how Rheb can regulate mTORC1, besides its direct interaction with mTOR (Long et al., 2005a; Long et al., 2005b). Because both PLD1 and mTOR are localized on intracellular membranes, there is a possibility that both localize in close proximity. Therefore, when PLD1 is activated by Rheb, PA is produced and that due to its appropriate cellular localization can bind to mTOR and activate mTORC1 kinase. Indeed, Yoon et al. has recently shown that in response to amino acids stimulation, PLD1 translocates from a cytoplasmic compartment to lysosomal membranes that is paralleled by the lysosomal translocation of mTORC1 (Yoon et al., 2011). Lysosomal translocation requires PtdIns(3)P generated by human Vps34 (hVps34) (Yoon et al., 2011). Additionally, PLD1 is activated by amino acids in a hVps34- and PtdIns(3)P-dependent manner. Both amino acid-dependent lysosomal translocation and activation of PLD1 are needed to activate mTORC1. Interestingly, translocation of PLD1 is independent of Rag proteins, Ragulator and raptor suggesting that a Vps34-PLD1 pathway exists that activates mTORC1 in parallel to the Rag pathway (Yoon et al., 2011). Nevertheless, there are some concerns about the Vps34-PLD1 connection in the activation of mTORC1. Translocation and activation of PLD1 are supposed to be mediated by the phox (PX) homology domain of PLD1 through binding to PtdIns(3)P (Yoon et al., 2011). However, there is evidence that PX of PLD1 does not bind to PtdIns(3)P (Du et al., 2003). The isolated PLD1-PX domain localizes to endosomal compartments that do not colocalize with EEA1, a protein that binds specifically to PtdIns(3)P through its FYVE domain. Moreover, treatment with wortmannin does not affect PLD1-PX localization, unlike to p40-PX (phox domain of p40 that also specifically binds to PtdIns(3)P) that upon

wortmannin treatment delocalizes to the cytoplasm (Du et al., 2003). It should also be considered that membrane association can be mediated independently of the PX domain, either through the PH or a PtdIns(4,5)P_2 binding motif that are found in PLD1 (Du et al., 2003; Frohman and Morris, 1999). In addition being activated by amino acids (Xu et al., 2011; Yoon et al., 2011), PLD1 activity is also enhanced by nutrient deprivation (Dall'Armi et al., 2010) suggesting a role of PLD1 in the regulation of autophagy. Indeed, PLD1-deficient MEFs or PLD1-deleted liver tissues exhibit defects in starvation-induced autophagy (Dall'Armi et al., 2010). PLD1 stability seems to be dependent on Vps34, because silencing of Vps34 dramatically decreases the levels of ectopically expressed and of endogenous PLD1 (Dall'Armi et al., 2010) explaining why in Yoon et al. PLD1 activity is Vps34 dependent (Yoon et al., 2011). Together, this indicates that Vps34 and PLD1 are involved in both the regulation of autophagy and mTORC1 signaling.

2.4.6 mTORC1 regulated by endosomal trafficking

There are numerous evidences connecting mTORC1 signaling with endosomes (Flinn et al., 2010; Hennig et al., 2006; Sancak et al., 2010; Sancak et al., 2008; Takahashi et al., 2012), thereby indicating that vesicular trafficking might be important for proper mTORC1 activation. In fact, constitutive active Rab5 (meaning GTP-charged Rab5), a small GTPase that regulates membrane transport through early endosomes (Callaghan et al., 1999; Simonsen et al., 1998), inhibits insulin- and amino acids-dependent mTORC1 activation (Flinn et al., 2010; Li et al., 2010), while the insulin-stimulated Akt/PKB activation (phosphorylation on Thr308) is not affected (Flinn et al., 2010) excluding a block in the growth factor signaling. In addition, overexpression of Gapex-5, a GEF for Rab5, blocks amino acid-mediated mTORC1 activation further supporting a role of Rab5 in mTORC1 regulation (Li et al., 2010). The effect of Rab5 is specific on mTORC1, because in resting cells constitutive active Rab5 does not affect mTORC2-mediated Akt/PKB Ser473 phosphorylation, while mTORC1-mediated S6K1 Thr389 phosphorylation is blocked (Li et al., 2010). Interestingly, constitutive active Rab5 blocks mTORC1 signaling induced by constitutive active RagA in the presence and in the absence of amino acids (Li et al., 2010), while it does not block mTORC1 activity induced by Rheb overexpression (Flinn et al., 2010; Li et al., 2010) most likely due to the mislocalization of overexpressed Rheb to other mTOR-containing compartments.

In cells, early endosomes (Rab5 positive) are converted into late endosomes (Rab7 positive). This maturation process is referred to as Rab5-to-Rab7 conversion, because Rab5 is replaced by Rab7 on the same endosome (Rink et al., 2005). This Rab5-to-Rab7 conversion can be blocked by constitutive active Rab5 thereby forming a Rab5/Rab7 hybrid endosome (Flinn et al., 2010; Rink et al., 2005). Similar to the constitutive active Rab5 phenotype, knockdown of Vps39 blocks Rab5-to-Rab7 conversion (Flinn et al., 2010; Rink et al., 2005) and inhibits mTORC1 activation in response to insulin stimulation (Flinn et al., 2010). Vps39 has GEF activity toward Rab7 (Rink et al., 2005; Wurmser et al., 2000) and is a subunit of the class C VPS/HOPS (homotypic fusion and protein sorting) complex that is necessary to elicit Rab5-to-Rab7 conversion (Rink et al., 2005). The Rab5-to-Rab7 conversion is a sequential and complicated processes simplified as follows: The class C VPS/HOPS complex and Rab7-GDP are recruited by Rab5-GTP to the early endosome (Rink et al., 2005) thereby forming a hybrid endosome containing both Rab5 and Rab7. Vps39 subunit of the class C VPS/HOPS complex activates Rab7 to the GTP form (Rink et al., 2005; Wurmser et al., 2000), Rab5 is then converted to the inactive GDP form and displaced from the hybrid endosome thereby creating a late endosome (Fig. 5). Constitutive active Rab5 or deletion of Vps39 leads to the formation of a hybrid Rab5/Rab7 positive endosome (Flinn et al., 2010; Rink et al., 2005) that is unable to proceed to a late endosome, where mTORC1 should interact with Rheb upon amino acid stimulation (Fig. 5). Therefore, it is possible that the formation of late endosomes is a prerequisite for amino acid- and insulin-dependent mTORC1 activation, as it is the place where the Ragulator-Rag-mTORC1 complex is assembled. Therefore, Vps39, Rab5 and Rab7 are more likely involved in the progression from early to late endosomes, rather than being engaged in nutrient signaling to mTORC1. With this in mind, Vps34 might also participate in the same endosomal processing as it controls vesicular transport (Stack et al., 1995) and therefore affecting mTORC1 signaling indirectly.

If late endosomes function as a “signaling platform” for mTORC1, how can then mTORC1 regulatory proteins such as Rheb, Ragulator/Rag proteins recognize late endosomes among the plethora of different organelles within a cell? Can they sense differences in intraluminal pH value between early and late endosomes? Or can they recognize different lipid compositions on the endosomal membrane?

Alike Rab5-to-Rab7 conversion, the PtdIns(3)P-to-PtdIns(3,5)P_2 conversion plays an indisputable role in the early to late endosome conversion. PtdIns(3)P and PtdIns(3,5)P_2 are two phospholipids that contribute to the identity of early and late

endosomes. PtdIns(3)P is mostly found on early endosomal membranes and synthesized by Vps34 (Schu et al., 1993), while PtdIns(3,5)P_2 is generated by the PtdIns(3)P 5-kinase PIKfyve (Fab1 in yeast) on cellular membranes as late endosomes and multivesicular bodies (MVBs) (Michell et al., 2006; Vicinanza et al., 2008). It is possible that PIKfyve might also be involved in the maturation process, as PIKfyve dysfunction impairs normal endosomal processing (Shisheva, 2008). Therefore, PIKfyve could impinge on the mTORC1 late endosomal localization and signaling. So far, there is no data available dealing with an involvement of PIKfyve, directly or indirectly, in the mTORC1 signaling pathway and it would be of great interest to find a possible connection between PIKfyve and mTORC1.

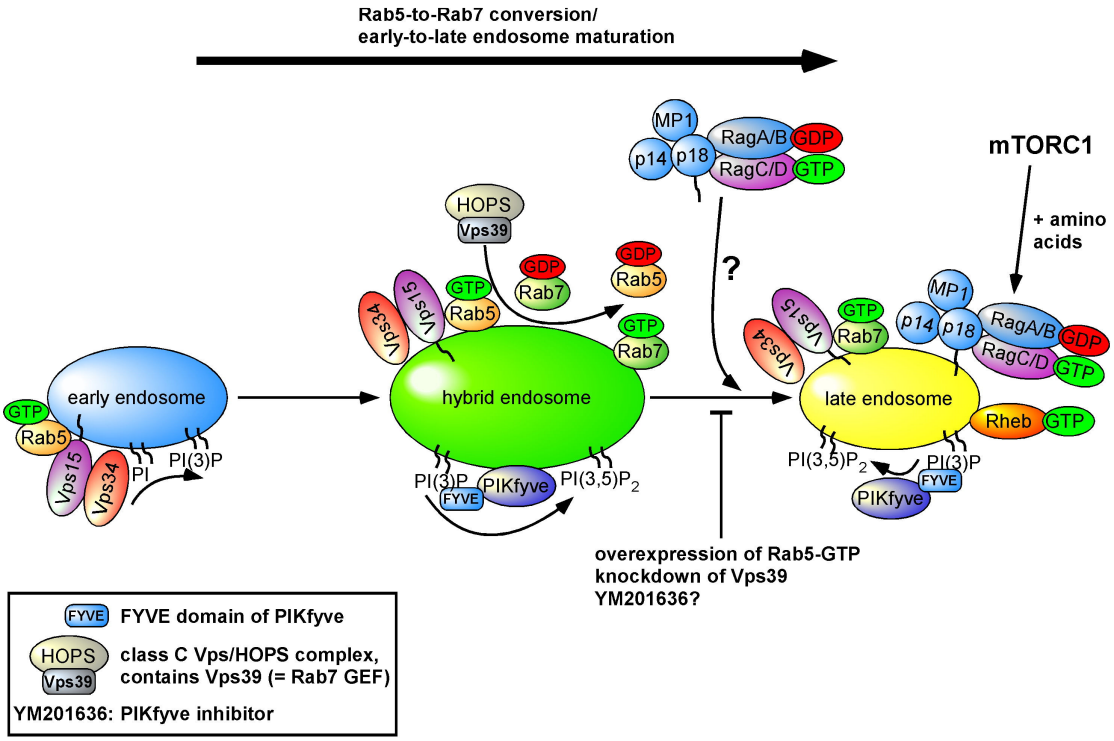

Fig. 5: Continuous endosomal transport/maturation required to set up an amino acid signaling platform on late endosomes for mTORC1 localization and signaling (hypothetical). During maturation from early to late endosomes, Rab5 is substituted for Rab7. An early endosome is defined through the associated components such as Rab5 and the phosphoinositide PtdIns(3)P generated by the early endosomal localized Vps34, while late endosomes contain Rab7. The formation of a late endosome is likely preceded by the transiently formed hybrid Rab5/Rab7 endosome. Rab5-GTP recruits Rab7-GDP and the class C Vps/HOPS complex to the early endosome thereby forming the hybrid endosome (Rink et al., 2005). The class C Vps/HOPS complex subunit Vps39 (also named Vam6) has GEF activity towards Rab7 and activates it to the GTP form (Rink et al., 2005; Wurmser et al., 2000), while Rab5 is converted to the inactive GDP form and removed from the hybrid endosome leading to the formation of a late endosome, where Ragulator (p18-p14-MP1)-Rag complex can be assembled in order to recruit mTORC1 upon amino acid stimulation. Rab5-to-Rab7 conversion is paralleled by the PtdIns(3)P-to-PtdIns(3,5)P_2 conversion implicating PIKfyve in the conversion process as it generates

(Fig. 5 continued)

PtdIns(3,5)P_2 from PtdIns(3)P. Vps34 is found on both early and late endosomes, where it generates PtdIns(3)P that serves first in the recruitment of PIKfyve to late endosomes and probably also to the hybrid endosome via its FYVE domain and second as substrate for the generation of PtdIns(3,5)P_2.
Maturation of an early endosome to a late endosome can be blocked at the hybrid endosome level by overexpressing Rab5-GTP that impedes Rab5 to be removed, or by Vps39 deletion that keeps Rab7 in its inactive state. Together, this hinders the hybrid endosome to proceed to a late endosome and most probably the Ragulator-Rag complex to be assembled and eventually blocking mTORC1 activation. Hypothetically, pharmacological inhibition of PIKfyve by YM201636 treatment should also block early to late endosome maturation at the hybrid endosome stage.
Vps: vacuolar protein sorting; HOPS: homotypic fusion and vacuole protein sorting; PIKfyve: PtdIns(3)P 5-kinase.

Amino acid-induced activation of mTORC1 is a hot topic research field at the moment. As outlined above many molecules that transmit the amino acid signal to mTORC1 have been identified. Moreover, mTORC1 regulation has been linked to endosomal compartments. Consistently, PtdIns(3)P, which is predominantly found on early endosomes, has been proposed to be implicated in mTORC1 signaling. However, PtdIns(3,5)P_2 that is found on late endosomes, the compartment where mTORC1 interacts with Rheb, has not been ascribed a regulatory role to mTORC1 yet. Figure 5 shows a hypothetical connection between mTORC1 and PtdIns(3,5)P_2 generated by PIKfyve, which needs verification.

2.5 References

Abraham, R.T. (2004). PI 3-kinase related kinases: 'big' players in stress-induced signaling pathways. DNA Repair (Amst) *3*, 883-887.

Andrade, M.A., and Bork, P. (1995). HEAT repeats in the Huntington's disease protein. Nat Genet *11*, 115-116.

Barbet, N.C., Schneider, U., Helliwell, S.B., Stansfield, I., Tuite, M.F., and Hall, M.N. (1996). TOR controls translation initiation and early G1 progression in yeast. Mol Biol Cell *7*, 25-42.

Berchtold, D., and Walther, T.C. (2009). TORC2 plasma membrane localization is essential for cell viability and restricted to a distinct domain. Mol Biol Cell *20*, 1565-1575.

Beugnet, A., Tee, A.R., Taylor, P.M., and Proud, C.G. (2003). Regulation of targets of mTOR (mammalian target of rapamycin) signalling by intracellular amino acid availability. Biochem J *372*, 555-566.

Binda, M., Peli-Gulli, M.P., Bonfils, G., Panchaud, N., Urban, J., Sturgill, T.W., Loewith, R., and De Virgilio, C. (2009). The Vam6 GEF controls TORC1 by activating the EGO complex. Mol Cell *35*, 563-573.

Blommaart, E.F., Luiken, J.J., Blommaart, P.J., van Woerkom, G.M., and Meijer, A.J. (1995). Phosphorylation of ribosomal protein S6 is inhibitory for autophagy in isolated rat hepatocytes. J Biol Chem *270*, 2320-2326.

Boll, M., Daniel, H., and Gasnier, B. (2004). The SLC36 family: proton-coupled transporters for the absorption of selected amino acids from extracellular and intracellular proteolysis. Pflugers Arch *447*, 776-779.

Burnett, P.E., Barrow, R.K., Cohen, N.A., Snyder, S.H., and Sabatini, D.M. (1998). RAFT1 phosphorylation of the translational regulators p70 S6 kinase and 4E-BP1. Proc Natl Acad Sci U S A *95*, 1432-1437.

Byfield, M.P., Murray, J.T., and Backer, J.M. (2005). hVps34 is a nutrient-regulated lipid kinase required for activation of p70 S6 kinase. J Biol Chem *280*, 33076-33082.

Callaghan, J., Nixon, S., Bucci, C., Toh, B.H., and Stenmark, H. (1999). Direct interaction of EEA1 with Rab5b. Eur J Biochem *265*, 361-366.

Carriere, A., Cargnello, M., Julien, L.A., Gao, H., Bonneil, E., Thibault, P., and Roux, P.P. (2008). Oncogenic MAPK signaling stimulates mTORC1 activity by promoting RSK-mediated raptor phosphorylation. Curr Biol *18*, 1269-1277.

Carriere, A., Romeo, Y., Acosta-Jaquez, H.A., Moreau, J., Bonneil, E., Thibault, P., Fingar, D.C., and Roux, P.P. (2011). ERK1/2 phosphorylate Raptor to promote Ras-dependent activation of mTOR complex 1 (mTORC1). J Biol Chem *286*, 567-577.

Chen, S.H., Wu, P.S., Chou, C.H., Yan, Y.T., Liu, H., Weng, S.Y., and Yang-Yen, H.F. (2007). A knockout mouse approach reveals that TCTP functions as an essential factor for cell proliferation and survival in a tissue- or cell type-specific manner. Mol Biol Cell *18*, 2525-2532.

Chen, Y., Zheng, Y., and Foster, D.A. (2003). Phospholipase D confers rapamycin resistance in human breast cancer cells. Oncogene *22*, 3937-3942.

Christie, G.R., Hajduch, E., Hundal, H.S., Proud, C.G., and Taylor, P.M. (2002). Intracellular sensing of amino acids in Xenopus laevis oocytes stimulates p70 S6 kinase in a target of rapamycin-dependent manner. J Biol Chem *277*, 9952-9957.

Christoforidis, S., Miaczynska, M., Ashman, K., Wilm, M., Zhao, L., Yip, S.C., Waterfield, M.D., Backer, J.M., and Zerial, M. (1999). Phosphatidylinositol-3-OH kinases are Rab5 effectors. Nat Cell Biol *1*, 249-252.

Codogno, P., and Meijer, A.J. (2005). Autophagy and signaling: their role in cell survival and cell death. Cell Death Differ *12 Suppl 2*, 1509-1518.

Dall'Armi, C., Hurtado-Lorenzo, A., Tian, H., Morel, E., Nezu, A., Chan, R.B., Yu, W.H., Robinson, K.S., Yeku, O., Small, S.A.*, et al.* (2010). The phospholipase D1 pathway modulates macroautophagy. Nat Commun *1*, 142.

De Virgilio, C., and Loewith, R. (2006). The TOR signalling network from yeast to man. Int J Biochem Cell Biol *38*, 1476-1481.

Dibble, C.C., Asara, J.M., and Manning, B.D. (2009). Characterization of Rictor phosphorylation sites reveals direct regulation of mTOR complex 2 by S6K1. Mol Cell Biol *29*, 5657-5670.

Drenan, R.M., Liu, X., Bertram, P.G., and Zheng, X.F. (2004). FKBP12-rapamycin-associated protein or mammalian target of rapamycin (FRAP/mTOR) localization in the endoplasmic reticulum and the Golgi apparatus. J Biol Chem *279*, 772-778.

Du, G., Altshuller, Y.M., Vitale, N., Huang, P., Chasserot-Golaz, S., Morris, A.J., Bader, M.F., and Frohman, M.A. (2003). Regulation of phospholipase D1 subcellular cycling through coordination of multiple membrane association motifs. J Cell Biol *162*, 305-315.

Duran, A., Amanchy, R., Linares, J.F., Joshi, J., Abu-Baker, S., Porollo, A., Hansen, M., Moscat, J., and Diaz-Meco, M.T. (2011). p62 Is a Key Regulator of Nutrient Sensing in the mTORC1 Pathway. Mol Cell *44*, 134-146.

Fang, Y., Park, I.H., Wu, A.L., Du, G., Huang, P., Frohman, M.A., Walker, S.J., Brown, H.A., and Chen, J. (2003). PLD1 regulates mTOR signaling and mediates Cdc42 activation of S6K1. Curr Biol *13*, 2037-2044.

Fang, Y., Vilella-Bach, M., Bachmann, R., Flanigan, A., and Chen, J. (2001). Phosphatidic acid-mediated mitogenic activation of mTOR signaling. Science *294*, 1942-1945.

Findlay, G.M., Yan, L., Procter, J., Mieulet, V., and Lamb, R.F. (2007). A MAP4 kinase related to Ste20 is a nutrient-sensitive regulator of mTOR signalling. Biochem J *403*, 13-20.

Fingar, D.C., Salama, S., Tsou, C., Harlow, E., and Blenis, J. (2002). Mammalian cell size is controlled by mTOR and its downstream targets S6K1 and 4EBP1/eIF4E. Genes Dev *16*, 1472-1487.

Flinn, R.J., Yan, Y., Goswami, S., Parker, P.J., and Backer, J.M. (2010). The late endosome is essential for mTORC1 signaling. Mol Biol Cell *21*, 833-841.

Fonseca, B.D., Smith, E.M., Lee, V.H., MacKintosh, C., and Proud, C.G. (2007). PRAS40 is a target for mammalian target of rapamycin complex 1 and is required for signaling downstream of this complex. J Biol Chem *282*, 24514-24524.

Foster, K.G., Acosta-Jaquez, H.A., Romeo, Y., Ekim, B., Soliman, G.A., Carriere, A., Roux, P.P., Ballif, B.A., and Fingar, D.C. (2010). Regulation of mTOR complex 1 (mTORC1) by raptor Ser863 and multisite phosphorylation. J Biol Chem *285*, 80-94.

Frias, M.A., Thoreen, C.C., Jaffe, J.D., Schroder, W., Sculley, T., Carr, S.A., and Sabatini, D.M. (2006). mSin1 is necessary for Akt/PKB phosphorylation, and its isoforms define three distinct mTORC2s. Curr Biol *16*, 1865-1870.

Frohman, M.A., and Morris, A.J. (1999). Phospholipase D structure and regulation. Chem Phys Lipids *98*, 127-140.

Fuchs, B.C., and Bode, B.P. (2005). Amino acid transporters ASCT2 and LAT1 in cancer: partners in crime? Semin Cancer Biol *15*, 254-266.

Gangloff, Y.G., Mueller, M., Dann, S.G., Svoboda, P., Sticker, M., Spetz, J.F., Um, S.H., Brown, E.J., Cereghini, S., Thomas, G.*, et al.* (2004). Disruption of the mouse mTOR gene leads to early postimplantation lethality and prohibits embryonic stem cell development. Mol Cell Biol *24*, 9508-9516.

Gingras, A.C., Raught, B., and Sonenberg, N. (2001). Regulation of translation initiation by FRAP/mTOR. Genes Dev *15*, 807-826.

Goorden, S.M., Hoogeveen-Westerveld, M., Cheng, C., van Woerden, G.M., Mozaffari, M., Post, L., Duckers, H.J., Nellist, M., and Elgersma, Y. (2011). Rheb is essential for murine development. Mol Cell Biol *31*, 1672-1678.

Groves, M.R., Hanlon, N., Turowski, P., Hemmings, B.A., and Barford, D. (1999). The structure of the protein phosphatase 2A PR65/A subunit reveals the conformation of its 15 tandemly repeated HEAT motifs. Cell *96*, 99-110.

Guertin, D.A., and Sabatini, D.M. (2005). An expanding role for mTOR in cancer. Trends Mol Med *11*, 353-361.

Guertin, D.A., Stevens, D.M., Thoreen, C.C., Burds, A.A., Kalaany, N.Y., Moffat, J., Brown, M., Fitzgerald, K.J., and Sabatini, D.M. (2006). Ablation in mice of the mTORC components raptor, rictor, or mLST8 reveals that mTORC2 is required for signaling to Akt-FOXO and PKCalpha, but not S6K1. Dev Cell *11*, 859-871.

Gulati, P., Gaspers, L.D., Dann, S.G., Joaquin, M., Nobukuni, T., Natt, F., Kozma, S.C., Thomas, A.P., and Thomas, G. (2008). Amino acids activate mTOR complex 1 via Ca2+/CaM signaling to hVps34. Cell Metab *7*, 456-465.

Gwinn, D.M., Shackelford, D.B., Egan, D.F., Mihaylova, M.M., Mery, A., Vasquez, D.S., Turk, B.E., and Shaw, R.J. (2008). AMPK phosphorylation of raptor mediates a metabolic checkpoint. Mol Cell *30*, 214-226.

Hall, D.J., Grewal, S.S., de la Cruz, A.F., and Edgar, B.A. (2007). Rheb-TOR signaling promotes protein synthesis, but not glucose or amino acid import, in Drosophila. BMC Biol *5*, 10.

Hara, K., Maruki, Y., Long, X., Yoshino, K., Oshiro, N., Hidayat, S., Tokunaga, C., Avruch, J., and Yonezawa, K. (2002). Raptor, a binding partner of target of rapamycin (TOR), mediates TOR action. Cell *110*, 177-189.

Hara, K., Yonezawa, K., Weng, Q.P., Kozlowski, M.T., Belham, C., and Avruch, J. (1998). Amino acid sufficiency and mTOR regulate p70 S6 kinase and eIF-4E BP1 through a common effector mechanism. J Biol Chem *273*, 14484-14494.

Hardie, D.G. (2007). AMP-activated/SNF1 protein kinases: conserved guardians of cellular energy. Nat Rev Mol Cell Biol *8*, 774-785.

Harrington, L.S., Findlay, G.M., Gray, A., Tolkacheva, T., Wigfield, S., Rebholz, H., Barnett, J., Leslie, N.R., Cheng, S., Shepherd, P.R.*, et al.* (2004). The TSC1-2 tumor suppressor controls insulin-PI3K signaling via regulation of IRS proteins. J Cell Biol *166*, 213-223.

Harrington, L.S., Findlay, G.M., and Lamb, R.F. (2005). Restraining PI3K: mTOR signalling goes back to the membrane. Trends Biochem Sci *30*, 35-42.

Heitman, J., Movva, N.R., and Hall, M.N. (1991). Targets for cell cycle arrest by the immunosuppressant rapamycin in yeast. Science *253*, 905-909.

Hennig, K.M., Colombani, J., and Neufeld, T.P. (2006). TOR coordinates bulk and targeted endocytosis in the Drosophila melanogaster fat body to regulate cell growth. J Cell Biol *173*, 963-974.

Herman, P.K., and Emr, S.D. (1990). Characterization of VPS34, a gene required for vacuolar protein sorting and vacuole segregation in Saccharomyces cerevisiae. Mol Cell Biol *10*, 6742-6754.

Heublein, S., Kazi, S., Ogmundsdottir, M.H., Attwood, E.V., Kala, S., Boyd, C.A., Wilson, C., and Goberdhan, D.C. (2010). Proton-assisted amino-acid transporters are conserved regulators of proliferation and amino-acid-dependent mTORC1 activation. Oncogene *29*, 4068-4079.

Hresko, R.C., and Mueckler, M. (2005). mTOR.RICTOR is the Ser473 kinase for Akt/protein kinase B in 3T3-L1 adipocytes. J Biol Chem *280*, 40406-40416.

Hsu, Y.C., Chern, J.J., Cai, Y., Liu, M., and Choi, K.W. (2007). Drosophila TCTP is essential for growth and proliferation through regulation of dRheb GTPase. Nature *445*, 785-788.

Iiboshi, Y., Papst, P.J., Kawasome, H., Hosoi, H., Abraham, R.T., Houghton, P.J., and Terada, N. (1999). Amino acid-dependent control of p70(s6k). Involvement of tRNA aminoacylation in the regulation. J Biol Chem *274*, 1092-1099.

Inoki, K., Li, Y., Xu, T., and Guan, K.L. (2003a). Rheb GTPase is a direct target of TSC2 GAP activity and regulates mTOR signaling. Genes Dev *17*, 1829-1834.

Inoki, K., Li, Y., Zhu, T., Wu, J., and Guan, K.L. (2002). TSC2 is phosphorylated and inhibited by Akt and suppresses mTOR signalling. Nat Cell Biol *4*, 648-657.

Inoki, K., Zhu, T., and Guan, K.L. (2003b). TSC2 mediates cellular energy response to control cell growth and survival. Cell *115*, 577-590.

Jacinto, E., Facchinetti, V., Liu, D., Soto, N., Wei, S., Jung, S.Y., Huang, Q., Qin, J., and Su, B. (2006). SIN1/MIP1 maintains rictor-mTOR complex integrity and regulates Akt phosphorylation and substrate specificity. Cell *127*, 125-137.

Jacinto, E., and Hall, M.N. (2003). Tor signalling in bugs, brain and brawn. Nat Rev Mol Cell Biol *4*, 117-126.

Jacinto, E., Loewith, R., Schmidt, A., Lin, S., Ruegg, M.A., Hall, A., and Hall, M.N. (2004). Mammalian TOR complex 2 controls the actin cytoskeleton and is rapamycin insensitive. Nat Cell Biol *6*, 1122-1128.

Jefferies, H.B., Fumagalli, S., Dennis, P.B., Reinhard, C., Pearson, R.B., and Thomas, G. (1997). Rapamycin suppresses 5'TOP mRNA translation through inhibition of p70s6k. EMBO J *16*, 3693-3704.

Juhasz, G., Hill, J.H., Yan, Y., Sass, M., Baehrecke, E.H., Backer, J.M., and Neufeld, T.P. (2008). The class III PI(3)K Vps34 promotes autophagy and endocytosis but not TOR signaling in Drosophila. J Cell Biol *181*, 655-666.

Julien, L.A., Carriere, A., Moreau, J., and Roux, P.P. (2010). mTORC1-activated S6K1 phosphorylates Rictor on threonine 1135 and regulates mTORC2 signaling. Mol Cell Biol *30*, 908-921.

Kim, D.H., Sarbassov, D.D., Ali, S.M., King, J.E., Latek, R.R., Erdjument-Bromage, H., Tempst, P., and Sabatini, D.M. (2002). mTOR interacts with raptor to form a nutrient-sensitive complex that signals to the cell growth machinery. Cell *110*, 163-175.

Kim, D.H., Sarbassov, D.D., Ali, S.M., Latek, R.R., Guntur, K.V., Erdjument-Bromage, H., Tempst, P., and Sabatini, D.M. (2003). GbetaL, a positive regulator of the rapamycin-sensitive pathway required for the nutrient-sensitive interaction between raptor and mTOR. Mol Cell *11*, 895-904.

Kim, E., Goraksha-Hicks, P., Li, L., Neufeld, T.P., and Guan, K.L. (2008). Regulation of TORC1 by Rag GTPases in nutrient response. Nat Cell Biol *10*, 935-945.

Klionsky, D.J. (2007). Autophagy: from phenomenology to molecular understanding in less than a decade. Nat Rev Mol Cell Biol *8*, 931-937.

Kogan, K., Spear, E.D., Kaiser, C.A., and Fass, D. (2010). Structural conservation of components in the amino acid sensing branch of the TOR pathway in yeast and mammals. J Mol Biol *402*, 388-398.

Kovacina, K.S., Park, G.Y., Bae, S.S., Guzzetta, A.W., Schaefer, E., Birnbaum, M.J., and Roth, R.A. (2003). Identification of a proline-rich Akt substrate as a 14-3-3 binding partner. J Biol Chem *278*, 10189-10194.

Kunz, J., Henriquez, R., Schneider, U., Deuter-Reinhard, M., Movva, N.R., and Hall, M.N. (1993). Target of rapamycin in yeast, TOR2, is an essential phosphatidylinositol kinase homolog required for G1 progression. Cell *73*, 585-596.

Kunz, J., Schneider, U., Howald, I., Schmidt, A., and Hall, M.N. (2000). HEAT repeats mediate plasma membrane localization of Tor2p in yeast. J Biol Chem *275*, 37011-37020.

Langlais, P., Yi, Z., and Mandarino, L.J. (2011). The identification of raptor as a substrate for p44/42 MAPK. Endocrinology *152*, 1264-1273.

Li, L., Kim, E., Yuan, H., Inoki, K., Goraksha-Hicks, P., Schiesher, R.L., Neufeld, T.P., and Guan, K.L. (2010). Regulation of mTORC1 by the Rab and Arf GTPases. J Biol Chem *285*, 19705-19709.

Liu, X., and Zheng, X.F. (2007). Endoplasmic reticulum and Golgi localization sequences for mammalian target of rapamycin. Mol Biol Cell *18*, 1073-1082.

Loewith, R., Jacinto, E., Wullschleger, S., Lorberg, A., Crespo, J.L., Bonenfant, D., Oppliger, W., Jenoe, P., and Hall, M.N. (2002). Two TOR complexes, only one of which is rapamycin sensitive, have distinct roles in cell growth control. Mol Cell *10*, 457-468.

Long, X., Lin, Y., Ortiz-Vega, S., Yonezawa, K., and Avruch, J. (2005a). Rheb binds and regulates the mTOR kinase. Curr Biol *15*, 702-713.

Long, X., Ortiz-Vega, S., Lin, Y., and Avruch, J. (2005b). Rheb binding to mammalian target of rapamycin (mTOR) is regulated by amino acid sufficiency. J Biol Chem *280*, 23433-23436.

Long, X., Spycher, C., Han, Z.S., Rose, A.M., Muller, F., and Avruch, J. (2002). TOR deficiency in C. elegans causes developmental arrest and intestinal atrophy by inhibition of mRNA translation. Curr Biol *12*, 1448-1461.

Ma, L., Chen, Z., Erdjument-Bromage, H., Tempst, P., and Pandolfi, P.P. (2005). Phosphorylation and functional inactivation of TSC2 by Erk implications for tuberous sclerosis and cancer pathogenesis. Cell *121*, 179-193.

Mach, K.E., Furge, K.A., and Albright, C.F. (2000). Loss of Rhb1, a Rheb-related GTPase in fission yeast, causes growth arrest with a terminal phenotype similar to that caused by nitrogen starvation. Genetics *155*, 611-622.

Manning, B.D. (2004). Balancing Akt with S6K: implications for both metabolic diseases and tumorigenesis. J Cell Biol *167*, 399-403.

Manning, B.D., and Cantley, L.C. (2003). Rheb fills a GAP between TSC and TOR. Trends Biochem Sci *28*, 573-576.

Manning, B.D., and Cantley, L.C. (2007). AKT/PKB signaling: navigating downstream. Cell *129*, 1261-1274.

Manning, B.D., Tee, A.R., Logsdon, M.N., Blenis, J., and Cantley, L.C. (2002). Identification of the tuberous sclerosis complex-2 tumor suppressor gene product tuberin as a target of the phosphoinositide 3-kinase/akt pathway. Mol Cell *10*, 151-162.

Martin, P.M., and Sutherland, A.E. (2001). Exogenous amino acids regulate trophectoderm differentiation in the mouse blastocyst through an mTOR-dependent pathway. Dev Biol *240*, 182-193.

Michell, R.H., Heath, V.L., Lemmon, M.A., and Dove, S.K. (2006). Phosphatidylinositol 3,5-bisphosphate: metabolism and cellular functions. Trends Biochem Sci *31*, 52-63.

Murakami, M., Ichisaka, T., Maeda, M., Oshiro, N., Hara, K., Edenhofer, F., Kiyama, H., Yonezawa, K., and Yamanaka, S. (2004). mTOR is essential for growth and proliferation in early mouse embryos and embryonic stem cells. Mol Cell Biol *24*, 6710-6718.

Murray, J.T., Panaretou, C., Stenmark, H., Miaczynska, M., and Backer, J.M. (2002). Role of Rab5 in the recruitment of hVps34/p150 to the early endosome. Traffic *3*, 416-427.

Nada, S., Hondo, A., Kasai, A., Koike, M., Saito, K., Uchiyama, Y., and Okada, M. (2009). The novel lipid raft adaptor p18 controls endosome dynamics by anchoring the MEK-ERK pathway to late endosomes. EMBO J *28*, 477-489.

Nicklin, P., Bergman, P., Zhang, B., Triantafellow, E., Wang, H., Nyfeler, B., Yang, H., Hild, M., Kung, C., Wilson, C.*, et al.* (2009). Bidirectional transport of amino acids regulates mTOR and autophagy. Cell *136*, 521-534.

Nobukuni, T., Joaquin, M., Roccio, M., Dann, S.G., Kim, S.Y., Gulati, P., Byfield, M.P., Backer, J.M., Natt, F., Bos, J.L.*, et al.* (2005). Amino acids mediate mTOR/raptor signaling through activation of class 3 phosphatidylinositol 3OH-kinase. Proc Natl Acad Sci U S A *102*, 14238-14243.

Nojima, H., Tokunaga, C., Eguchi, S., Oshiro, N., Hidayat, S., Yoshino, K., Hara, K., Tanaka, N., Avruch, J., and Yonezawa, K. (2003). The mammalian target of rapamycin (mTOR) partner, raptor, binds the mTOR substrates p70 S6 kinase and 4E-BP1 through their TOR signaling (TOS) motif. J Biol Chem *278*, 15461-15464.

Oldham, S., Montagne, J., Radimerski, T., Thomas, G., and Hafen, E. (2000). Genetic and biochemical characterization of dTOR, the Drosophila homolog of the target of rapamycin. Genes Dev *14*, 2689-2694.

Oshiro, N., Takahashi, R., Yoshino, K., Tanimura, K., Nakashima, A., Eguchi, S., Miyamoto, T., Hara, K., Takehana, K., Avruch, J.*, et al.* (2007). The proline-rich Akt substrate of 40 kDa (PRAS40) is a physiological substrate of mammalian target of rapamycin complex 1. J Biol Chem *282*, 20329-20339.

Panaretou, C., Domin, J., Cockcroft, S., and Waterfield, M.D. (1997). Characterization of p150, an adaptor protein for the human phosphatidylinositol (PtdIns) 3-kinase. Substrate

presentation by phosphatidylinositol transfer protein to the p150.Ptdins 3-kinase complex. J Biol Chem *272*, 2477-2485.

Pearce, L.R., Huang, X., Boudeau, J., Pawlowski, R., Wullschleger, S., Deak, M., Ibrahim, A.F., Gourlay, R., Magnuson, M.A., and Alessi, D.R. (2007). Identification of Protor as a novel Rictor-binding component of mTOR complex-2. Biochem J *405*, 513-522.

Pearce, L.R., Komander, D., and Alessi, D.R. (2010). The nuts and bolts of AGC protein kinases. Nat Rev Mol Cell Biol *11*, 9-22.

Peterson, R.T., Desai, B.N., Hardwick, J.S., and Schreiber, S.L. (1999). Protein phosphatase 2A interacts with the 70-kDa S6 kinase and is activated by inhibition of FKBP12-rapamycinassociated protein. Proc Natl Acad Sci U S A *96*, 4438-4442.

Peterson, T.R., Laplante, M., Thoreen, C.C., Sancak, Y., Kang, S.A., Kuehl, W.M., Gray, N.S., and Sabatini, D.M. (2009). DEPTOR is an mTOR inhibitor frequently overexpressed in multiple myeloma cells and required for their survival. Cell *137*, 873-886.

Petiot, A., Ogier-Denis, E., Blommaart, E.F., Meijer, A.J., and Codogno, P. (2000). Distinct classes of phosphatidylinositol 3'-kinases are involved in signaling pathways that control macroautophagy in HT-29 cells. J Biol Chem *275*, 992-998.

Polak, P., Cybulski, N., Feige, J.N., Auwerx, J., Ruegg, M.A., and Hall, M.N. (2008). Adipose-specific knockout of raptor results in lean mice with enhanced mitochondrial respiration. Cell Metab *8*, 399-410.

Rehmann, H., Bruning, M., Berghaus, C., Schwarten, M., Kohler, K., Stocker, H., Stoll, R., Zwartkruis, F.J., and Wittinghofer, A. (2008). Biochemical characterisation of TCTP questions its function as a guanine nucleotide exchange factor for Rheb. FEBS Lett *582*, 3005-3010.

Rink, J., Ghigo, E., Kalaidzidis, Y., and Zerial, M. (2005). Rab conversion as a mechanism of progression from early to late endosomes. Cell *122*, 735-749.

Roccio, M., Bos, J.L., and Zwartkruis, F.J. (2006). Regulation of the small GTPase Rheb by amino acids. Oncogene *25*, 657-664.

Roux, P.P., Ballif, B.A., Anjum, R., Gygi, S.P., and Blenis, J. (2004). Tumor-promoting phorbol esters and activated Ras inactivate the tuberous sclerosis tumor suppressor complex via p90 ribosomal S6 kinase. Proc Natl Acad Sci U S A *101*, 13489-13494.

Sabatini, D.M., Barrow, R.K., Blackshaw, S., Burnett, P.E., Lai, M.M., Field, M.E., Bahr, B.A., Kirsch, J., Betz, H., and Snyder, S.H. (1999). Interaction of RAFT1 with gephyrin required for rapamycin-sensitive signaling. Science *284*, 1161-1164.

Sancak, Y., Bar-Peled, L., Zoncu, R., Markhard, A.L., Nada, S., and Sabatini, D.M. (2010). Ragulator-Rag complex targets mTORC1 to the lysosomal surface and is necessary for its activation by amino acids. Cell *141*, 290-303.

Sancak, Y., Peterson, T.R., Shaul, Y.D., Lindquist, R.A., Thoreen, C.C., Bar-Peled, L., and Sabatini, D.M. (2008). The Rag GTPases bind raptor and mediate amino acid signaling to mTORC1. Science *320*, 1496-1501.

Sancak, Y., Thoreen, C.C., Peterson, T.R., Lindquist, R.A., Kang, S.A., Spooner, E., Carr, S.A., and Sabatini, D.M. (2007). PRAS40 is an insulin-regulated inhibitor of the mTORC1 protein kinase. Mol Cell *25*, 903-915.

Sarbassov, D.D., Ali, S.M., Kim, D.H., Guertin, D.A., Latek, R.R., Erdjument-Bromage, H., Tempst, P., and Sabatini, D.M. (2004). Rictor, a novel binding partner of mTOR, defines a rapamycin-insensitive and raptor-independent pathway that regulates the cytoskeleton. Curr Biol *14*, 1296-1302.

Sarbassov, D.D., Guertin, D.A., Ali, S.M., and Sabatini, D.M. (2005). Phosphorylation and regulation of Akt/PKB by the rictor-mTOR complex. Science *307*, 1098-1101.

Schalm, S.S., and Blenis, J. (2002). Identification of a conserved motif required for mTOR signaling. Curr Biol *12*, 632-639.

Schmelzle, T., and Hall, M.N. (2000). TOR, a central controller of cell growth. Cell *103*, 253-262.

Schroder, W., Cloonan, N., Bushell, G., and Sculley, T. (2004). Alternative polyadenylation and splicing of mRNAs transcribed from the human Sin1 gene. Gene *339*, 17-23.

Schroder, W.A., Buck, M., Cloonan, N., Hancock, J.F., Suhrbier, A., Sculley, T., and Bushell, G. (2007). Human Sin1 contains Ras-binding and pleckstrin homology domains and suppresses Ras signalling. Cell Signal *19*, 1279-1289.

Schu, P.V., Takegawa, K., Fry, M.J., Stack, J.H., Waterfield, M.D., and Emr, S.D. (1993). Phosphatidylinositol 3-kinase encoded by yeast VPS34 gene essential for protein sorting. Science *260*, 88-91.

Sekiguchi, T., Hirose, E., Nakashima, N., Ii, M., and Nishimoto, T. (2001). Novel G proteins, Rag C and Rag D, interact with GTP-binding proteins, Rag A and Rag B. J Biol Chem *276*, 7246-7257.

Shackelford, D.B., and Shaw, R.J. (2009). The LKB1-AMPK pathway: metabolism and growth control in tumour suppression. Nat Rev Cancer *9*, 563-575.

Shaw, R.J., and Cantley, L.C. (2006). Ras, PI(3)K and mTOR signalling controls tumour cell growth. Nature *441*, 424-430.

Shisheva, A. (2008). PIKfyve: Partners, significance, debates and paradoxes. Cell Biol Int *32*, 591-604.

Simonsen, A., Lippe, R., Christoforidis, S., Gaullier, J.M., Brech, A., Callaghan, J., Toh, B.H., Murphy, C., Zerial, M., and Stenmark, H. (1998). EEA1 links PI(3)K function to Rab5 regulation of endosome fusion. Nature *394*, 494-498.

Simonsen, A., and Tooze, S.A. (2009). Coordination of membrane events during autophagy by multiple class III PI3-kinase complexes. J Cell Biol *186*, 773-782.

Smith, E.M., Finn, S.G., Tee, A.R., Browne, G.J., and Proud, C.G. (2005). The tuberous sclerosis protein TSC2 is not required for the regulation of the mammalian target of rapamycin by amino acids and certain cellular stresses. J Biol Chem *280*, 18717-18727.

Sonenberg, N., and Gingras, A.C. (1998). The mRNA 5' cap-binding protein eIF4E and control of cell growth. Curr Opin Cell Biol *10*, 268-275.

Stack, J.H., Herman, P.K., Schu, P.V., and Emr, S.D. (1993). A membrane-associated complex containing the Vps15 protein kinase and the Vps34 PI 3-kinase is essential for protein sorting to the yeast lysosome-like vacuole. EMBO J *12*, 2195-2204.

Stack, J.H., Horazdovsky, B., and Emr, S.D. (1995). Receptor-mediated protein sorting to the vacuole in yeast: roles for a protein kinase, a lipid kinase and GTP-binding proteins. Annu Rev Cell Dev Biol *11*, 1-33.

Stein, M.P., Feng, Y., Cooper, K.L., Welford, A.M., and Wandinger-Ness, A. (2003). Human VPS34 and p150 are Rab7 interacting partners. Traffic *4*, 754-771.

Stipanuk, M.H. (2009). Macroautophagy and its role in nutrient homeostasis. Nutr Rev *67*, 677-689.

Sun, Y., Fang, Y., Yoon, M.S., Zhang, C., Roccio, M., Zwartkruis, F.J., Armstrong, M., Brown, H.A., and Chen, J. (2008). Phospholipase D1 is an effector of Rheb in the mTOR pathway. Proc Natl Acad Sci U S A *105*, 8286-8291.

Takahashi, Y., Nada, S., Mori, S., Nagae, T., Oneyama, C., and Okada, M. (2012). The late endosome/lysosome-anchored p18-mTORC1 pathway controls terminal maturation of lysosomes. Biochem Biophys Res Commun.

Tassa, A., Roux, M.P., Attaix, D., and Bechet, D.M. (2003). Class III phosphoinositide 3-kinase--Beclin1 complex mediates the amino acid-dependent regulation of autophagy in C2C12 myotubes. Biochem J *376*, 577-586.

Tee, A.R., Manning, B.D., Roux, P.P., Cantley, L.C., and Blenis, J. (2003). Tuberous sclerosis complex gene products, Tuberin and Hamartin, control mTOR signaling by acting as a GTPase-activating protein complex toward Rheb. Curr Biol *13*, 1259-1268.

Thedieck, K., Polak, P., Kim, M.L., Molle, K.D., Cohen, A., Jeno, P., Arrieumerlou, C., and Hall, M.N. (2007). PRAS40 and PRR5-like protein are new mTOR interactors that regulate apoptosis. PLoS One *2*, e1217.

Treins, C., Warne, P.H., Magnuson, M.A., Pende, M., and Downward, J. (2010). Rictor is a novel target of p70 S6 kinase-1. Oncogene *29*, 1003-1016.

Tzatsos, A., and Kandror, K.V. (2006). Nutrients suppress phosphatidylinositol 3-kinase/Akt signaling via raptor-dependent mTOR-mediated insulin receptor substrate 1 phosphorylation. Mol Cell Biol *26*, 63-76.

Urano, J., Tabancay, A.P., Yang, W., and Tamanoi, F. (2000). The Saccharomyces cerevisiae Rheb G-protein is involved in regulating canavanine resistance and arginine uptake. J Biol Chem *275*, 11198-11206.

van Veelen, W., Korsse, S.E., van de Laar, L., and Peppelenbosch, M.P. (2011). The long and winding road to rational treatment of cancer associated with LKB1/AMPK/TSC/mTORC1 signaling. Oncogene.

Vander Haar, E., Lee, S.I., Bandhakavi, S., Griffin, T.J., and Kim, D.H. (2007). Insulin signalling to mTOR mediated by the Akt/PKB substrate PRAS40. Nat Cell Biol *9*, 316-323.

Vezina, C., Kudelski, A., and Sehgal, S.N. (1975). Rapamycin (AY-22,989), a new antifungal antibiotic. I. Taxonomy of the producing streptomycete and isolation of the active principle. J Antibiot (Tokyo) *28*, 721-726.

Vicinanza, M., D'Angelo, G., Di Campli, A., and De Matteis, M.A. (2008). Function and dysfunction of the PI system in membrane trafficking. EMBO J *27*, 2457-2470.

Volinia, S., Dhand, R., Vanhaesebroeck, B., MacDougall, L.K., Stein, R., Zvelebil, M.J., Domin, J., Panaretou, C., and Waterfield, M.D. (1995). A human phosphatidylinositol 3-kinase complex related to the yeast Vps34p-Vps15p protein sorting system. EMBO J *14*, 3339-3348.

Wang, L., Harris, T.E., and Lawrence, J.C., Jr. (2008a). Regulation of proline-rich Akt substrate of 40 kDa (PRAS40) function by mammalian target of rapamycin complex 1 (mTORC1)-mediated phosphorylation. J Biol Chem *283*, 15619-15627.

Wang, L., Harris, T.E., Roth, R.A., and Lawrence, J.C., Jr. (2007). PRAS40 regulates mTORC1 kinase activity by functioning as a direct inhibitor of substrate binding. J Biol Chem *282*, 20036-20044.

Wang, L., Lawrence, J.C., Jr., Sturgill, T.W., and Harris, T.E. (2009). Mammalian target of rapamycin complex 1 (mTORC1) activity is associated with phosphorylation of raptor by mTOR. J Biol Chem *284*, 14693-14697.

Wang, X., Beugnet, A., Murakami, M., Yamanaka, S., and Proud, C.G. (2005). Distinct signaling events downstream of mTOR cooperate to mediate the effects of amino acids and insulin on initiation factor 4E-binding proteins. Mol Cell Biol *25*, 2558-2572.

Wang, X., Campbell, L.E., Miller, C.M., and Proud, C.G. (1998). Amino acid availability regulates p70 S6 kinase and multiple translation factors. Biochem J *334 (Pt 1)*, 261-267.

Wang, X., Fonseca, B.D., Tang, H., Liu, R., Elia, A., Clemens, M.J., Bommer, U.A., and Proud, C.G. (2008b). Re-evaluating the roles of proposed modulators of mammalian target of rapamycin complex 1 (mTORC1) signaling. J Biol Chem *283*, 30482-30492.

Wullschleger, S., Loewith, R., and Hall, M.N. (2006). TOR signaling in growth and metabolism. Cell *124*, 471-484.

Wullschleger, S., Loewith, R., Oppliger, W., and Hall, M.N. (2005). Molecular organization of target of rapamycin complex 2. J Biol Chem *280*, 30697-30704.

Wurmser, A.E., Sato, T.K., and Emr, S.D. (2000). New component of the vacuolar class C-Vps complex couples nucleotide exchange on the Ypt7 GTPase to SNARE-dependent docking and fusion. J Cell Biol *151*, 551-562.

Xu, L., Salloum, D., Medlin, P.S., Saqcena, M., Yellen, P., Perrella, B., and Foster, D.A. (2011). Phospholipase D mediates nutrient input to mammalian target of rapamycin complex 1 (mTORC1). J Biol Chem *286*, 25477-25486.

Yan, L., Mieulet, V., Burgess, D., Findlay, G.M., Sully, K., Procter, J., Goris, J., Janssens, V., Morrice, N.A., and Lamb, R.F. (2010). PP2A T61 epsilon is an inhibitor of MAP4K3 in nutrient signaling to mTOR. Mol Cell *37*, 633-642.

Yan, Y., Flinn, R.J., Wu, H., Schnur, R.S., and Backer, J.M. (2009). hVps15, but not Ca2+/CaM, is required for the activity and regulation of hVps34 in mammalian cells. Biochem J *417*, 747-755.

Yanagida, O., Kanai, Y., Chairoungdua, A., Kim, D.K., Segawa, H., Nii, T., Cha, S.H., Matsuo, H., Fukushima, J., Fukasawa, Y*., et al.* (2001). Human L-type amino acid transporter 1 (LAT1): characterization of function and expression in tumor cell lines. Biochim Biophys Acta *1514*, 291-302.

Yang, Q., Inoki, K., Ikenoue, T., and Guan, K.L. (2006). Identification of Sin1 as an essential TORC2 component required for complex formation and kinase activity. Genes Dev *20*, 2820-2832.

Yoon, M.S., Du, G., Backer, J.M., Frohman, M.A., and Chen, J. (2011). Class III PI-3-kinase activates phospholipase D in an amino acid-sensing mTORC1 pathway. J Cell Biol *195*, 435-447.

Zhang, H., Stallock, J.P., Ng, J.C., Reinhard, C., and Neufeld, T.P. (2000). Regulation of cellular growth by the Drosophila target of rapamycin dTOR. Genes Dev *14*, 2712-2724.

Zhou, X., Takatoh, J., and Wang, F. (2011). The mammalian class 3 PI3K (PIK3C3) is required for early embryogenesis and cell proliferation. PLoS One *6*, e16358.

Zhou, X., Wang, L., Hasegawa, H., Amin, P., Han, B.X., Kaneko, S., He, Y., and Wang, F. (2010). Deletion of PIK3C3/Vps34 in sensory neurons causes rapid neurodegeneration by disrupting the endosomal but not the autophagic pathway. Proc Natl Acad Sci U S A *107*, 9424-9429.

Zoncu, R., Bar-Peled, L., Efeyan, A., Wang, S., Sancak, Y., and Sabatini, D.M. (2011). mTORC1 senses lysosomal amino acids through an inside-out mechanism that requires the vacuolar H-ATPase. Science *334*, 678-683.

Zoncu, R., Efeyan, A., and Sabatini, D.M. (2011a). mTOR: from growth signal integration to cancer, diabetes and ageing. Nat Rev Mol Cell Biol *12*, 21-35.

3 Aims

The components involved in the growth factor-induced signaling pathway to mTORC1 are well-characterized, while the ones in the amino acid pathway have only recently started to be uncovered. The importance of amino acids in regulating mTORC1 has been substantiated by the fact that in cells deprived of amino acids, growth factor stimulation cannot induce mTORC1 activation (Hara et al., 1998). It is unclear how mammalian cells perceive variation of intracellular amino acid concentrations, determined by the extracellular amino acid supply and by rates of protein synthesis and degradation. But recently different molecules have been identified mediating the amino acid signal to mTORC1, including the Rag GTPases, MAP4K3 and hVps34 with its lipid product PtdIns(3)P (Byfield et al., 2005; Findlay et al., 2007; Nobukuni et al., 2005; Sancak et al., 2010; Sancak et al., 2008; Yan et al., 2010). To our opinion the involvement of hVps34 in the amino acid sensing pathway to mTORC1 is controversial.

Therefore as a first aim we re-analyzed the connection between hVps34 and mTORC1 by examining the effect of either ectopic expression of wild type and kinase-dead hVps34, or RNAi-induced deletion of hVps34 on amino acid-induced mTORC1 signaling. We could show that independently of the catalytic activity of hVps34 overexpression had no effect, while hVps34 deletion only partially affected mTORC1 activity, which is consistent with the observed PtdIns(3)P generation.

Since both class II PI3K isoforms PI3K-C2α and PI3K-C2β have been shown to form PtdIns(3)P *in vivo* (Falasca and Maffucci, 2007; Maffucci et al., 2005) we aimed to investigate their role in mTORC1 signaling by RNAi knockdown. Surprisingly, while PI3K-C2α knockdown increased mTORC1 activity, PI3K-C2β caused only a modest decrease in mTORC1 activation.

PtdIns(3)P has been proposed to be involved in mTORC1 regulation (Byfield et al., 2005; Nobukuni et al., 2005). Despite targeting PtdIns(3)P-generating enzymes we were not able to observe a clear cut connection to mTORC1. Therefore we attempted to directly affecting intracellular PtdIns(3)Ps by either reducing the availability of free PtdIns(3)P or by acutely increasing PtdIns(3)P levels, which caused a strong decrease or increase in mTORC1 activity, respectively.

PtdIns(3)P is phosphorylated by PIKfyve to form PtdIns(3,5)P_2 (Ikonomov et al., 2001; Sbrissa et al., 1999; Shisheva et al., 2001), and both phospholipids are involved in endosomal membrane transports (Michell et al., 2006; Odorizzi et al., 2000). Moreover, mTORC1 signaling seems to be coordinated at endosomal compartments (Flinn et al., 2010; Sancak et al., 2010; Sancak et al., 2008). Collectively, this would suggest a possible implication of PIKfyve and its PtdIns(3,5)P_2 in mTORC1 signaling. Therefore we subjected PIKfyve to pharmacologic inhibition demonstrating a connection to mTORC1 signaling.

References

Byfield, M.P., Murray, J.T., and Backer, J.M. (2005). hVps34 is a nutrient-regulated lipid kinase required for activation of p70 S6 kinase. J Biol Chem *280*, 33076-33082.

Falasca, M., and Maffucci, T. (2007). Role of class II phosphoinositide 3-kinase in cell signalling. Biochem Soc Trans *35*, 211-214.

Findlay, G.M., Yan, L., Procter, J., Mieulet, V., and Lamb, R.F. (2007). A MAP4 kinase related to Ste20 is a nutrient-sensitive regulator of mTOR signalling. Biochem J *403*, 13-20.

Flinn, R.J., Yan, Y., Goswami, S., Parker, P.J., and Backer, J.M. (2010). The late endosome is essential for mTORC1 signaling. Mol Biol Cell *21*, 833-841.

Hara, K., Yonezawa, K., Weng, Q.P., Kozlowski, M.T., Belham, C., and Avruch, J. (1998). Amino acid sufficiency and mTOR regulate p70 S6 kinase and eIF-4E BP1 through a common effector mechanism. J Biol Chem *273*, 14484-14494.

Ikonomov, O.C., Sbrissa, D., and Shisheva, A. (2001). Mammalian cell morphology and endocytic membrane homeostasis require enzymatically active phosphoinositide 5-kinase PIKfyve. J Biol Chem *276*, 26141-26147.

Maffucci, T., Cooke, F.T., Foster, F.M., Traer, C.J., Fry, M.J., and Falasca, M. (2005). Class II phosphoinositide 3-kinase defines a novel signaling pathway in cell migration. J Cell Biol *169*, 789-799.

Michell, R.H., Heath, V.L., Lemmon, M.A., and Dove, S.K. (2006). Phosphatidylinositol 3,5-bisphosphate: metabolism and cellular functions. Trends Biochem Sci *31*, 52-63.

Nobukuni, T., Joaquin, M., Roccio, M., Dann, S.G., Kim, S.Y., Gulati, P., Byfield, M.P., Backer, J.M., Natt, F., Bos, J.L., *et al.* (2005). Amino acids mediate mTOR/raptor signaling through activation of class 3 phosphatidylinositol 3OH-kinase. Proc Natl Acad Sci U S A *102*, 14238-14243.

Odorizzi, G., Babst, M., and Emr, S.D. (2000). Phosphoinositide signaling and the regulation of membrane trafficking in yeast. Trends Biochem Sci *25*, 229-235.

Sancak, Y., Bar-Peled, L., Zoncu, R., Markhard, A.L., Nada, S., and Sabatini, D.M. (2010). Ragulator-Rag complex targets mTORC1 to the lysosomal surface and is necessary for its activation by amino acids. Cell *141*, 290-303.

Sancak, Y., Peterson, T.R., Shaul, Y.D., Lindquist, R.A., Thoreen, C.C., Bar-Peled, L., and Sabatini, D.M. (2008). The Rag GTPases bind raptor and mediate amino acid signaling to mTORC1. Science *320*, 1496-1501.

Sbrissa, D., Ikonomov, O.C., and Shisheva, A. (1999). PIKfyve, a mammalian ortholog of yeast Fab1p lipid kinase, synthesizes 5-phosphoinositides. Effect of insulin. J Biol Chem *274*, 21589-21597.

Shisheva, A., Rusin, B., Ikonomov, O.C., DeMarco, C., and Sbrissa, D. (2001). Localization and insulin-regulated relocation of phosphoinositide 5-kinase PIKfyve in 3T3-L1 adipocytes. J Biol Chem *276*, 11859-11869.

Yan, L., Mieulet, V., Burgess, D., Findlay, G.M., Sully, K., Procter, J., Goris, J., Janssens, V., Morrice, N.A., and Lamb, R.F. (2010). PP2A T61 epsilon is an inhibitor of MAP4K3 in nutrient signaling to mTOR. Mol Cell *37*, 633-642.

4 Results

Manuscript in preparation

Regulation of mTORC1 by PtdIns(3)P and PtdIns(3,5)P_2

Anna Melone[1], Romina Marone[1], Devaraj Subramanian[2], Carsten Schultz[2], Matthias P. Wymann[1]*

[1]Institute of Biochemistry and Genetics, Department of Biomedicine, University of Basel, Mattenstrasse 28, CH-4058 Basel, Switzerland. [2]European Molecular Biology Institute (EMBL), Cell Biology and Biophysics Unit, Heidelberg, Germany.

***To whom correspondence should be addressed:**
Matthias P. Wymann
Inst. Biochemistry and Genetics
Dept. Biomedicine
Mattenstrasse 28
CH-4058 Basel, Switzerland
Matthias.Wymann@UniBas.CH

4.1 Abstract

The mammalian target of rapamycin (mTOR) serine/threonine kinase is the catalytic component of two functional distinct complexes, mTOR complex 1 (mTORC1) and mTORC2. mTORC1 integrates signals emerging from growth factors and nutrients such as amino acids to regulate cell proliferation and cell growth. In contrary to the growth factor-initiated pathway, the components of the amino acid signaling pathway to mTORC1 are poorly characterized and only in recent years they have started to be uncovered. In this study we analyzed two different phosphoinositides (PIs), PtdIns(3)P and PtdIns(3,5)P_2, in the regulation of mTORC1 signaling in response to amino acid stimulation. The role of PtdIns(3)P was analyzed by targeting PtdIns(3)P-generating enzymes, human vacuolar protein sorting 34 (hVps34) and class II phosphatidylinositol 3-kinase (PI3K). In contrary to previous reports, we found that downregulation of hVps34 does not completely blunt mTORC1 signaling and that overexpression of hVps34 kinase-dead mutant affects mTORC1 activation similarly as wild type hVps34 does. Unexpectedly, silencing of class II PI3Ks results in an isoform-specific activation of mTORC1 where PI3K-C2α knockdown increases, while PI3K-C2β knockdown modestly decreases mTORC1 activity. Nevertheless, by affecting PtdIns(3)P directly either by masking or by acute treatment with synthetic PtdIns(3)P strongly inhibits or increases mTORC1 activity, respectively. Surprisingly, pharmacologic inhibition of the PtdIns(3,5)P_2-synthesizing enzyme PIKfyve decreases mTORC1 signaling that is paralleled by diminished late endosomal localization of mTOR.

Our data confirm a positive role of PtdIns(3)P in the mTORC1 pathway and demonstrate a novel role for PIKfyve and its phospholipid PtdIns(3,5)P_2 in the regulation of mTORC1 signaling in response to amino acids, which is consistent with the regulation of mTORC1 on endosomal membranes.

4.2 Introduction

Mammalian target of rapamycin (mTOR) is a Ser/Thr kinase playing a central role in the regulation of cell metabolism, growth, proliferation and survival (Corradetti and Guan, 2006; Guertin and Sabatini, 2007; Wullschleger et al., 2006). mTOR is found in two functionally distinct and independently regulated complexes, termed mTOR complex 1 (mTORC1) and mTORC2 (Jacinto et al., 2004; Loewith et al., 2002; Sarbassov et al., 2004). mTORC1 consists of mTOR, raptor, mLST8, PRAS40 and DEPTOR and is sensitive to rapamycin (Hara et al., 2002; Kim et al., 2002; Kim et al., 2003; Loewith et al., 2002; Peterson et al., 2009; Sancak et al., 2007). mTORC2 shares mTOR, mLST8 and DEPTOR with mTORC1, while rictor, mSIN1 and Protor are unique components (Frias et al., 2006; Jacinto et al., 2006; Jacinto et al., 2004; Pearce et al., 2007; Peterson et al., 2009; Sarbassov et al., 2004; Yang et al., 2006). In contrary to mTORC1, mTORC2 is insensitive to rapamycin, although long-term rapamycin treatment disrupts mTORC2 assembly in certain cell lines (Sarbassov et al., 2006).

Different upstream signals such as growth factors, amino acid availability, intracellular energy levels and stress control mTORC1 activation (Hay and Sonenberg, 2004; Wullschleger et al., 2006). In responses to these signals, mTORC1 controls many cellular processes that contribute to cell growth, including protein synthesis, ribosome biogenesis, nutrient transport and autophagy (Hay and Sonenberg, 2004; Martin and Hall, 2005; Wullschleger et al., 2006). The two best-characterized downstream targets of mTORC1 are S6K1 (p70 ribosomal S6 kinase 1) and 4E-BP1 (eukaryotic initiation factor 4E binding protein 1) via which mTORC1 controls protein synthesis (Burnett et al., 1998; Hay and Sonenberg, 2004; Wullschleger et al., 2006). The mechanism how growth factors regulate mTORC1 downstream targets is well-characterized, while the amino acid signaling pathway to mTORC1 is at its infancy. It is known that amino acids regulate mTORC1-mediated S6K1 and 4E-BP1 phosphorylation (Hara et al., 1998; Kim et al., 2002). However, how amino acids are sensed and how this information is transmitted to mTORC1 is poorly understood.

Intracellular molecules have recently been identified that may sense amino acid sufficiency to mTORC1. The class III phosphatidylinositol 3-kinase (PI3K), Vps34 (vacuolar protein sorting 34), which was identified as a protein regulating vesicular trafficking (Herman and Emr, 1990; Stack et al., 1993) and autophagy (Simonsen and Tooze, 2009), has recently been proposed to mediate the amino acid signal to

mTORC1 (Byfield et al., 2005; Gulati et al., 2008; Nobukuni et al., 2005). Especially its phospholipid product phosphatidylinositol 3-phosphate [PtdIns(3)P] seems to be required in the amino acid-induced mTORC1 activation (Nobukuni et al., 2005; Yoon et al., 2011).

An important step in the amino acid-dependent activation of mTORC1 is the recruitment of mTORC1 to late endosomal/lysosomal membranes, where it interacts with Rheb thereby promoting mTORC1 activation. This translocation is mediated by a complex composed of heterodimeric Rag GTPases and the p18-p14-MP1 complex (also termed Ragulator) that anchors the Rag GTPases on late endosomes/lysosomes (Sancak et al., 2010; Sancak et al., 2008). The Rag GTPases-Ragulator complex is constitutively localized on late endosomes/lysosomes (Sancak et al., 2010) and in response to amino acid stimulation Rag GTPases are activated allowing to interact with mTORC1 via raptor, thereby re-localizing mTORC1 to late endosomes/lysosomes (Sancak et al., 2010; Sancak et al., 2008).

There are evidences indicating that continuous intracellular trafficking is important for mTORC1 signaling. It is known that during early to late endosome maturation, Rab5 is substituted for Rab7 and that either active Rab5 mutants or deletion of Rab7 GEF (guanine exchange factor) Vps39 block early to late endosomal conversion (Rink et al., 2005). Concerning mTORC1, overexpression of constitutive active Rab5 has been demonstrated to impair amino acid- and insulin-induced mTORC1 activation similarly to Vps39 knockdown (Flinn et al., 2010; Li et al., 2010). Because PtdIns(3)P and PtdIns(3,5)P_2 contribute to the identity of early and late endosomes, respectively (Huotari and Helenius, 2011), early-to-late endosomal conversion might be paralleled by the PtdIns(3)P-to-PtdIns(3,5)P_2 conversion implicating PIKfyve (mammalian homologue of yeast Fab1) in this process, as it is the PtdIns(3)P 5-kinase that generates PtdIns(3,5)P_2 from PtdIns(3)P (Dove et al., 2009; Ikonomov et al., 2001; Sbrissa et al., 1999; Shisheva et al., 2001).

In this present study we re-ananlyzed the role of hVps34 (human Vps34) and its phospholipid product PtdIns(3)P in the nutrient sensing pathway to mTORC1, especially because the Vps34-mTORC1 connection has been shown to be controversial (Juhasz et al., 2008). Additionally, the role of PtdIns(3)P and PtdIns(3,5)P_2 were investigated in the amino acid sensing pathway to mTORC1. In contrary to recent reports (Byfield et al., 2005; Nobukuni et al., 2005) we were unable to reproduce a clear hVps34-mTORC1 connection. Nonetheless, we could demonstrate that PtdIns(3)P is important for mTORC1 activation. Surprisingly, pharmacologic inhibition of PIKfyve impairs mTORC1 activation and mTOR

localization to late endosomes. This is the first report demonstrating that PIKfyve and PtdIns(3,5)P_2 are implicated in mTORC1 signaling.

4.3 Materials and Methods

Chemicals

DMSO, phosphatidylserine (PS) and phosphatidylinositol (PI) were purchased from Sigma. Rapamycin and ZSTK474 were purchased from LC Laboratories. Wortmannin was purchased from Sandoz. NVP-BEZ235 was from Novartis Institutes for BioMedical research (Basel, Switzerland). PI-103 was purchased from Enzo. pp242 and YM201636 were purchased from Chemdea. PtdIns(3)P/AM was synthesized by D. Subramanian (EMBL Heidelberg, Germany). [γ-^{32}P]-ATP was purchased from Perkin Elmer.

Plasmids and plasmid generation

pRK5-Myc-S6K1 was obtained from G. Thomas (Cincinnati, USA), pEGFP-2xFYVE^{HRS} wt and C215S mutant from H. Stenmark (Oslo, Norway), pRK5-HA-Raptor and pEGFP-Rheb were from M. Hall (Basel, Switzerland), pEGFP-PH^{Btk} from T. Balla (Bethesda, USA) and pEGFP-PH^{TAPP1} was from laboratory plasmid collection. pRK5-HA-Raptor-Rheb15 was generated by subcloning the C-terminal tail of pEGFP-Rheb containing the last 15 amino acids of Rheb (I-D-G-A-A-S-Q-G-K-S-S-C-S-V-M) to the C-terminus of pRK5-HA-Raptor. Kinase-dead pcDNA3-GST-hVps34^{K636R} was cloned by introducing three point mutations into pcDNA3-GST-hVps34^{wt} ($_{3587}$AAG$_{3589}$ -> $_{3587}$CGC$_{3589}$) by site-directed mutagenesis. pEGFP-Rab5a and pEGFP-Rab7 were generated by subcloning Rab5a and Rab7 cDNA (from Missoury S&T Resource Center) into pEGFP-C1 (Clontech), respectively.

Cells, cell culture and transfection

HEK293 and HER911 cells were cultured in DMEM containing 10% heat-inactivated fetal calf serum (HIFCS, Sigma), 2mM L-glutamine (L-Gln, Sigma) and 1% penicillin-streptomycin solution (PEST, Sigma). The human melanoma cell line A375 was cultured in RPMI 1640 containing 10% HIFCS, 2mM L-Gln and 1% PEST at 37°C in 5% CO_2 atmosphere. shRNA mock and shRNA hVps34 HEK29 and A375 cells were cultured in complete medium as described before supplemented with 1µg/ml puromycin.

Transfections were carried out with JetPEI (Brunschwig) according to manufacturer's guidelines.

Mammalian lentiviral shRNA and siRNA targeting sequences

The sequences of shRNA targeting hVps34 (Sigma), siRNA targeting hVps34 (Invitrogen), and PI3K-C2α and PI3K-C2β (Invitrogen) were as follows:

shRNA hVps34: CCACGAGAGATCAGTTAAATA
siRNA PI3K C2A#1: GGAAUAUGGUGUGACAGGAUCCUUU
siRNA PI3K C2A#2: GGAUGUAGCAGAGUGUGAUCUUGUU
siRNA PI3K C2A#3: UCAACUUGAGCAAAGAGACGGUUAA
siRNA PI3K C2B#1: GAGAGAUGAGGAGGUUGCUGCAUUU
siRNA PI3K C2B#2: UGGCUGAUGGAGACUUCCCACUGAA
siRNA PI3K C2B#3: CAGCGCCCGUUGGAGUGCACCUAAU

siRNA-mediated silencing of class II PI3K

After Myc-S6K1 transfection, cells were transfected with siRNA using Lipofectamine RNAiMAX (Invitrogen) as described in the manufacturer's guideline. Briefly, 180,000 HEK293 cells were plated per well in 6-well culture plates in complete medium without antibiotics. Twenty-four hours later cells were transfected with 100 ng pRK5-Myc-S6K1 using JetPEI and medium replaced 7 hours later with complete medium without antibiotics. The following day, cells were either transfected with 10 nM control siRNA, siRNA C2A#1-3 or siRNA C2B#1-3 and 5 hours later medium replaced. After 48 h cells were O/N serum starved and subjected to amino acid starvation and amino acid stimulation as described below.

Amino acid and serum starvation and stimulation of cells

Cells were washed once with PBS and incubated O/N (16-18h) in serum-free culture medium supplemented with 2 mM L-glutamine. The following day cells were washed twice with PBS and incubated for 2h in amino acid free buffer (homemade: 1.8 mM $CaCl_2$, 0.248 µM $Fe(NO_3)_3$, 810 µM $MgSO_4$, 5.37 mM KCl, 44 mM $NaHCO_3$, 109.5 mM NaCl, 906 µM NaH_2PO_4, 25 mM Glucose, 4x MEM vitamins) followed by amino acid stimulation with serum-free culture medium supplemented with 2 mM L-glutamine for 30 min.

For IGF-II stimulation, cells were O/N serum starved in serum-free culture medium supplemented with 2 mM L-glutamine and stimulated with 50 ng/ml IGF-II (Sigma) for 5 min.

MTT-based cell proliferation assay

For proliferation HEK293 or A375 cells were plated in quadruplicate at 3,000 or 1,000 cells per well in 96-well tissue culture plates in 100 µl culture medium. At day 0, 24h after plating, inhibitors (1 µM BEZ235, 100 nM Rapamycin, 1 µM pp242, 1 µM ZSTK474, and 1 µM YM201636) were added to cells. To each well 11 µl MTT (Sigma, diluted in PBS to 5 mg/ml) was added and plate shaken carefully. After incubation for 2h at 37°C and 5% CO_2, 100 µl solubilization solution (95% isopropanol, 5% formic acids) was added to each well and pipetted up and down several times to dissolve the formazan salt. After 10 min of gently mixing absorbance was measured at 570 nm and background absorbance at 690 nm.

Lipid kinase assay

GST-hVps34^{wt} and GST-hVps34^{K636R} were GST pulled down and resuspended in 40µl kinase buffer (20 mM HEPES (pH 7.4)/5mM $MnCl_2$) and pre-treated with either DMSO or 100nM wortmannin while vigorously shaking for 15 min at 37°C. Afterwards, 10 µl of PS/PtdIns (1µg/µl) vesicles and 10 µl [γ-^{32}P]-ATP/ATP solution (2µCi [γ-^{32}P]-ATP and 60 µM cold ATP) were added and mixed constantly for 10 min at 30°C. Reaction was stopped by the addition of 100 µl 1 M HCl and lipid extracted with 200 µl Chloroform:Methanol (1:1, v/v). PtdIns(3)Ps were resolved by thin layer chromatography and visualized by phosphoimager and autoradiography.

Preparation of cell lysates

Cells were washed twice with ice-cold PBS and scraped in ice-cold NP40-based lysis buffer (20 mM Tris-HCl pH 8.0, 138 mM NaCl, 2.7 mM KCl, 5% glycerol, 1% NP-40, 40 mM NaF, 2mM Na_3VO_4, 20 µM Leupeptin, 18 µM Pepstatin, 5 µM Aprotinin, 1 mM PMSF, 1 mM $MgCl_2$, 1 mM $CaCl_2$, 5 mM EDTA). Cell lysates were cleared by centrifugation at 13,200 rpm for 15 min and denatured by the addition of 5x sample buffer and boiling for 6 min.

Western blotting analysis and antibodies

Equal amount of proteins were subjected to SDS-PAGE and transferred to Immobilon PVDF membranes (Millipore). Primary antibodies to pS6K Thr389 (1A5), S6K1, pPKB Ser473 (193H12), pPKB Thr308 (244F9) and Myc (9B11) were from Cell signaling Technology; primary antibodies to PI3-Kinase C2α and PI3-Kinase C2β were from BD Transduction Laboratories; primary antibody to PKB (19G7/C7) was a kind gift of E. Hirsch (Turin, Italy); primary antibody to GFP (clone 7.1 and 13.1) was

from Roche; primary antibody to Tubulin (DM1A) was from Sigma; primary antibody to hVps34 was from Zymed Laboratories/Invitrogen; and primary antibody to HA (HA.11) was from Lucerna Chem. Secondary antibodies such as horseradish peroxidase (HRP)-conjugated goat anti-mouse IgG and goat anti-rabbit IgG (Sigma) were visualized using enhanced chemiluminescence (Millipore).

Immunofluorescence of cells and quantification of colocalization

For staining, cells were grown in a 12-well plate on glass coverslips. After transfection with appropriate plasmids (total 1 μg), starvation and stimulation, cells were washed twice with PBS and fixed with 3% paraformaldehyde for 10 min at 37°C. After two times washing with PBS cells were quenched with 100 mM Glycine in PBS for 5min and washed an additional time with PBS. For intracellular staining, cells were permeabilized with 0.1% (w/v) saponin (Sigma) in PBS for 20 min at RT, and washed once with PBS and blocked with 5% goat serum in PBS (5% GS/PBS) for 20 min at RT. Cells were incubated with primary antibody (anti-HA (HA.11, Lucerna Chem); anti-TOR (7C10) (Cell Signaling Technology)) diluted in 5% GS/PBS for 1h at RT, washed twice with PBS and incubated with secondary antibody (AlexaFluor568 goat anti-rabbit IgG (H+L) and AlexaFluor568 goat anti-mouse IgG (H+L) from Molecular Probes) diluted in 5% GS/PBS for 1h at RT in dark. After two times wash with PBS, nuclei were stained with 1 μM Hoechst 33342 (Juro supply) diluted in PBS for 15 min at RT in dark. After washing twice with PBS, glass coverslips were mounted with Mowiol and cells imaged on a Zeiss LSM 510 Meta confocal laser scanning microscope attached to an Axiovert 200 inverted microscope using an oil-immersed 63x/1.40 numerical aperture objective (Carl Zeiss).

All images were analyzed with ImageJ except for Pearson's correlation coefficient analysis where colocalization threshold plugin of FiJi was used. For colocalization analysis, ROI (region of interest) of individual cells was selected and Pearson's coefficient correlation performed from at least 10 cells.

Statistical analysis

Data are shown as means and error bars indicate standard error of the mean (SEM). Data analysis was carried out using a two-tailed Student's t-test and are considered significant at *P<0.05, **P<0.01 and ***P<0.001.

4.4 Results

Implication of hVps34 in the amino acid-dependent activation of mTORC1

The Vps34 is the sole class III phosphatidylinositol 3-kinase (PI3K) and exclusively synthesizes PtdIns(3)P from PtdIns (Stack and Emr, 1994; Volinia et al., 1995). In addition in regulating autophagy and vesicular transport such as homotypic early endosomal fusion, formation of internal vesicles in multivesicular bodies and transport of the PDGF receptor through the early endosome (Christoforidis et al., 1999; Futter et al., 2001; Siddhanta et al., 1998; Simonsen and Tooze, 2009; Stein et al., 2003), Vps34 has been demonstrated to be involved in the activation of mTORC1 by amino acids, and in particular its lipid product PtdIns(3)P seems to positively regulate mTORC1 (Byfield et al., 2005; Nobukuni et al., 2005; Yoon et al., 2011). To investigate the role of PtdIns(3)P in the amino acid sensing pathway to mTORC1, we first re-examined the connection between the PtdIns(3)P-generating Vps34 and mTORC1. GST-tagged human Vps34 (hVps34) wild type and kinase-dead mutant (K636R) were ectopically expressed in HEK293 cells in increasing amounts and Thr389 phosphorylation of Myc-S6K1 was measured as a readout for mTORC1 activation (Fig. 1). Amino acid stimulation resulted in an increase in Thr389 phosphorylation, but no concentration dependence was observed as evidenced in the western blotting and from the quantification (Fig. 1A and 1B). Intriguingly, cells expressing the hVps34 KR mutant, that is devoid of kinase activity (Fig. 1C), also resulted in S6K1 Thr389 phosphorylation by amino acid stimulation (Fig. 1A and 1B). Probably, the PtdIns(3)P that is generated by the endogenous hVps34 (Fig. 1A) is most likely enough to induce mTORC1-mediated S6K1 phosphorylation. Furthermore, it is known that membrane targeting of hVps34 is accomplished by its adaptor protein hVps15 (also called p150) (Christoforidis et al., 1999; Murray et al., 2002; Stack et al., 1993; Stein et al., 2003) and that coexpression of hVps34 with hVps15 increases the activity of hVps34 (Yan et al., 2009). Therefore, it is conceivable that overexpression of Vps34 alone results in its mislocalization, from where hVps34 cannot properly function.

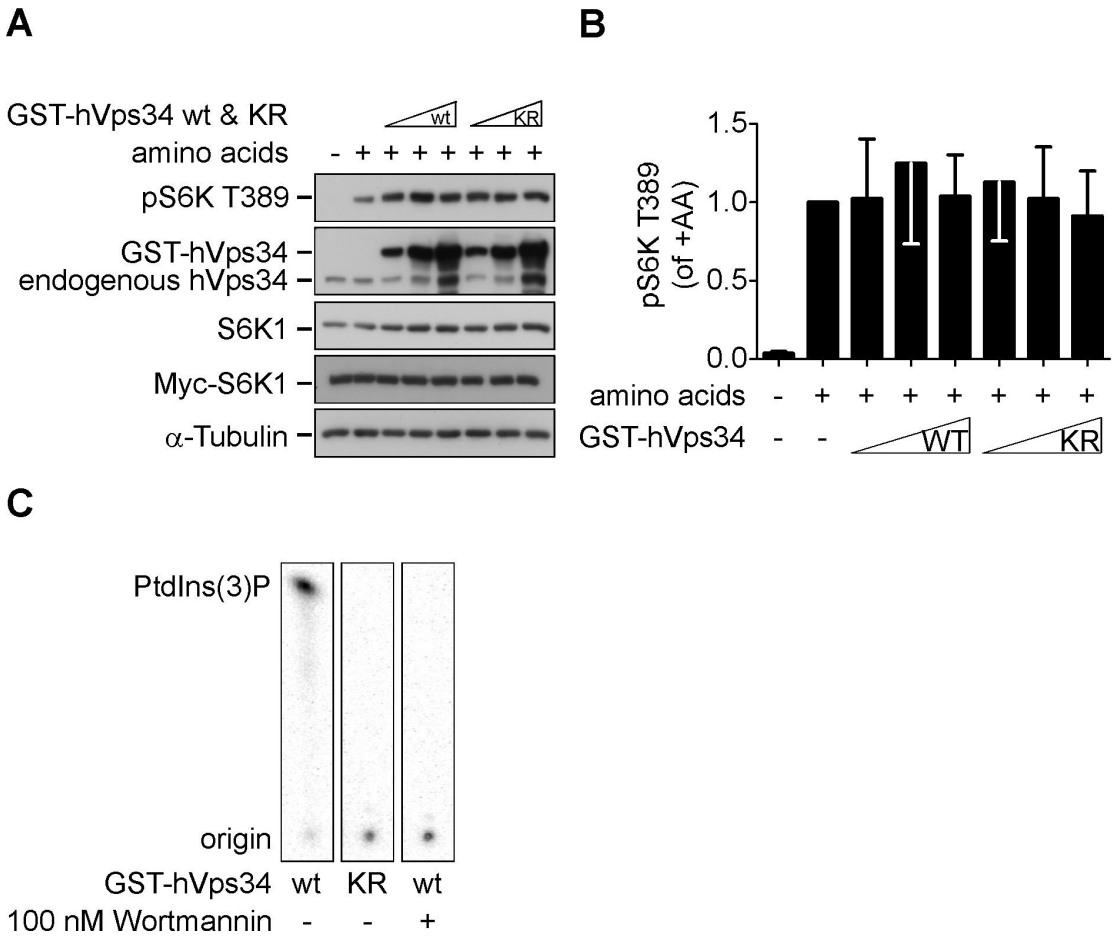

Fig. 1: Ectopic expression of GST-hVps34 wild type or kinase-dead does not influence mTORC1 activity.

(A) HEK293 cells ectopically co-expressing Myc-S6K1 and increasing amounts of wild type (wt) or kinase-dead (KR) GST-hVps34 were serum starved over night, amino acid deprived for 2h (-AA) and stimulated with amino acids (+AA) for 30min. Cell lysates were subjected to SDS-PAGE and indicated proteins were analyzed by western blotting. Phosphorylated Thr389 S6K1 was assessed for mTORC1 activity and amount of hVps34 determined with anti-hVps34. Anti-α-Tubulin was used as loading control. (B) Levels of phosphorylated S6K1 Thr389 from experiment described in (B) were densitometric quantified using ImageJ and normalized to the levels of S6K1. Data represented as mean ± SEM of n = 3 experiments.

(C) *In vitro* PI3K lipid kinase assay. GST pulldowns were prepared from HEK293 cells ectopically expressing GST-tagged wild type (wt) or kinase-dead mutant (KR) hVps34 and analyzed for kinase activity in an *in vitro* lipid kinase assay. GST pulldowns were pre-treated either with DMSO or 100 nM wortmannin for 15 min at 30°C, followed by the kinase assay in the presence of 2 μCi [γ-^{32}P] ATP/10 μM cold ATP and 10 μg PtdIns/PS vesicles for 10 min at 30°C. Extracted lipids were separated on TLC and analyzed by phosphoimager.

To further investigate the connection between hVps34 and mTORC1, we depleted hVps34 by RNA interference (RNAi) in two completely different cell lines, HEK293 and A375 (a human melanoma cell line) (Figs. 2A-2D and 2E-2H, respectively).

Silencing of hVps34 markedly decreased the expression of hVps34 in both cell lines (reduced to 6.7 % in HEK293 and 3.4% in A375 cells) (Figs. 2A and 2E) and decreased amino acid-stimulated S6K1 Thr389 phosphorylation (Figs. 2B and 2F). In HEK293 cells Thr389 phosphorylation decreased significantly to 55% (Fig. 2C), while in A375 decreased to 67% (Fig. 2G). In contrary to hVps34 silencing, pharmacologic inhibition of PtdIns(3)P synthesis by wortmannin treatment, a pan PI3K inhibitor, completely abrogated S6K1 Thr389 phosphorylation (Figs. 2B-2C and 2F-2G). To find an explanation why hVps34 silencing did not completely abrogate mTORC1 activity and considering that PtdIns(3)P is most likely required for mTORC1 activation (Byfield et al., 2005; Nobukuni et al., 2005; Yoon et al., 2011), we examined whether PtdIns(3)P generation is abrogated in hVps34 deleted cells (Fig. S1). To visualize PtdIns(3)P by microscopy, we ectopically expressed EGFP-tagged tandem FYVE domain (named after the first four proteins in which it was identified: Fab1/YOTB/Vac1/EEA1) of HRS (hepatocyte growth factor-regulated tyrosine kinase substrate) (EGFP-2xFYVE^{HRS}), which is known to specifically bind to PtdIns(3)P (Gillooly et al., 2000) (Fig. S1). In both control and hVps34 depleted A375 cells, EGFP-2xFYVE^{HRS} localized on intracellular vesicles indicating that in hVps34 knockdown cells PtdIns(3)P is still formed, whereas treatment with wortmannin resulted into a diffused cytoplasmic distribution (Fig. S1). This is consistent with a previous report, where suppression of hVps34 by RNAi did not disrupt the PtdIns(3)P-dependent localization of the early endosomal antigene 1 (EEA1) in U-251 glioblastoma (Johnson et al., 2006). This explains, why in the hVps34 knockdown cells mTORC1 was still able to phosphorylate S6K1 (Figs. 2B and 2F), although hVps34 expression was almost completely suppressed (Figs. 2A and 2E). Therefore, it is possible that another PI3K can compensate for the loss of hVps34 to generate PtdIns(3)P.

Consistent with the remaining S6K1 Thr389 phosphorylation signal, knockdown of hVps34 did not affect cell proliferation in HEK293 and A375 cells (Figs. 2D and 2H), while pharmacological inhibition of the mTOR kinase by BEZ235, rapamycin and pp242 treatment completely blocked proliferation (Figs. 2D and 2H). Together, hVps34 knockdown negatively, but not completely, affects mTORC1 activation in presence of amino acids, whereas cell proliferation is not affected.

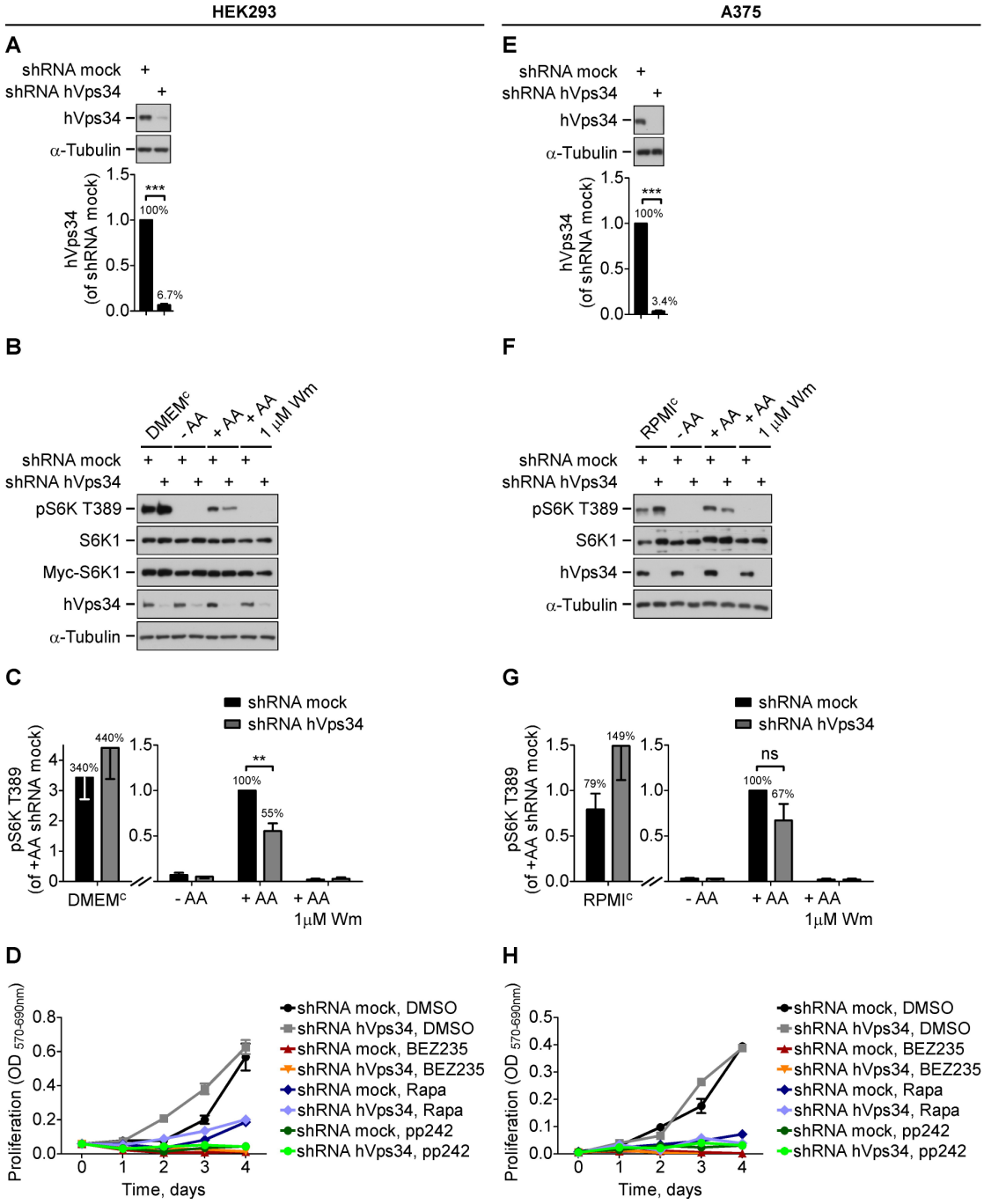

Fig. 2: Implication of hVps34 knockdown on amino acid-stimulated mTORC1 signaling.

(A and E) Degree of hVps34 knockdown. HEK293 (A) and A375 (E) cells were transduced with lentivirus expressing shRNA against hVps34 (shRNA hVps34) or empty vector (shRNA mock) as control and selected with puromycin. Cell lysates were subjected to SDS-PAGE and hVps34 levels determined by western blotting with anti-hVps34 and quantified using ImageJ. Anti-α-Tubulin was used as loading control. Data represented as mean ± SEM of n > 3 experiments. *** P<0.001.

(B and F) Effect of hVps34 silencing on mTORC1 by amino acid stimulation. HEK293 (B) and A375 (F) cells were transduced with lentivirus as described above and transiently transfected with Myc-S6K1. Cells were kept either in complete medium (DMEM^C for HEK293 and RPMI^C for A375; DMEM or RPMI medium supplemented with 2 mM L-glutamine and 10% FCS) or serum starved over night, amino acids deprived for 2h (-AA) and re-stimulated with amino acids (+AA) for 30 min. Prior to amino acid

(Fig. 2 continued)

stimulation cells were pre-treated with 1 μM wortmannin, where indicated. Cell lysates were subjected to SDS-PAGE and indicated proteins were analyzed by western blotting. Phosphorylated Thr389 S6K1 was assessed for mTORC1 activity and abundance of hVps34 was determined with anti-Vps34. Anti-α-Tubulin was used as loading control.

(C and G) Levels of phosphorylated S6K1 Thr389 from experiments described in (B) and (F) were quantified using ImageJ and data represented as mean ± SEM of n = 3 experiments. ** P<0.01.

(D and H) MTT-based proliferation assay. Lentivirus transduced HEK293 (D) and A375 (H) cells expressing shRNA against hVps34 (shRNA hVps34) or empty vector (shRNA mock) were treated with either DMSO, 1 μM BEZ235, 100 nM rapamycin or 1 μM pp242 and proliferation monitored for 4 days. Data represented as mean ± SEM of n = 4 experiments.

Class II PI3K isoforms differentially affect mTORC1 signaling by amino acid treatment

Since hVps34 silencing did not affect endomembrane localization of EGFP-2xFYVE^{HRS} (Fig. S1) and cell proliferation (Figs. 2D and 2H) and only partially decreased amino acid-stimulated S6K1 Thr389 phosphorylation (Figs. 2B and 2F), we wondered whether another PI3K might generate PtdIns(3)P that can contribute to mTORC1 activity. A possible candidate could be class II PI3K, which consists of three isoforms; PI3K-C2α, PI3K-Cβ and PI3K-C2γ. While PI3K-C2α and PI3K-Cβ are ubiquitously expressed, PI3K-C2γ expression is tissue restricted mostly in the liver, breast, prostate and salivary glands (Kok et al., 2009). They phosphorylate *in vitro* PtdIns and PtdIns(4)P to generate PtdIns(3)P and PtdIns(3,4)P_2, respectively, but evidences suggest that *in vivo* they synthesize PtdIns(3)P (Falasca and Maffucci, 2007; Maffucci et al., 2005; Wen et al., 2008). Furthermore, class II PI3Ks seem to be associated with intracellular membranes (Arcaro et al., 1998; Domin et al., 2000; Prior and Clague, 1999). Therefore, we hypothesize that class II PI3Ks can compensate for the loss of hVps34 and generate PtdIns(3)P, which will then be required for mTORC1 activation. Hence, we targeted PI3K-C2α and PI3K-C2β by small interference RNA (siRNA) in HEK293 cells and analyzed Myc-S6K1 Thr389 phosphorylation by western blotting (Fig. 3). Interestingly, knockdown of PI3K-C2α (Fig. 3A) and PI3K-C2β (Fig. 3B), respectively, had an isoform specific effect on mTORC1 activity. In the presence of amino acids, knockdown of PI3K-C2α caused an increase in S6K1 Thr389 phosphorylation (Fig. 3A), while loss of PI3K-C2β, in particular targeting sequences C2B#1 and C2B#2, decreased S6K1 Thr389 phosphorylation to approximate 50% (Fig. 3B). The observed increase in Thr389 phosphorylation by PI3K-C2α deletion could be due to a defect in the endocytosis of

amino acid transporters. PI3K-C2α is known to be a component of the clathrin-mediated transport machinery at the plasma membrane and in the trans-Golgi network (Domin et al., 2000) and therefore one can speculate that PI3K-C2α might be involved in endocytosis. In *Drosophila* increased levels of Slimfast, a cationic-dependent amino acid transporter, at the cell surface correlates with increased TOR activity, while reduction in TOR activity results in decreased levels of Simfast (Hennig et al., 2006). Therefore, it is conceivable that upon PI3K-C2α deletion, amino acid transporters remain at the plasma membrane leading to increased mTORC1 activity.

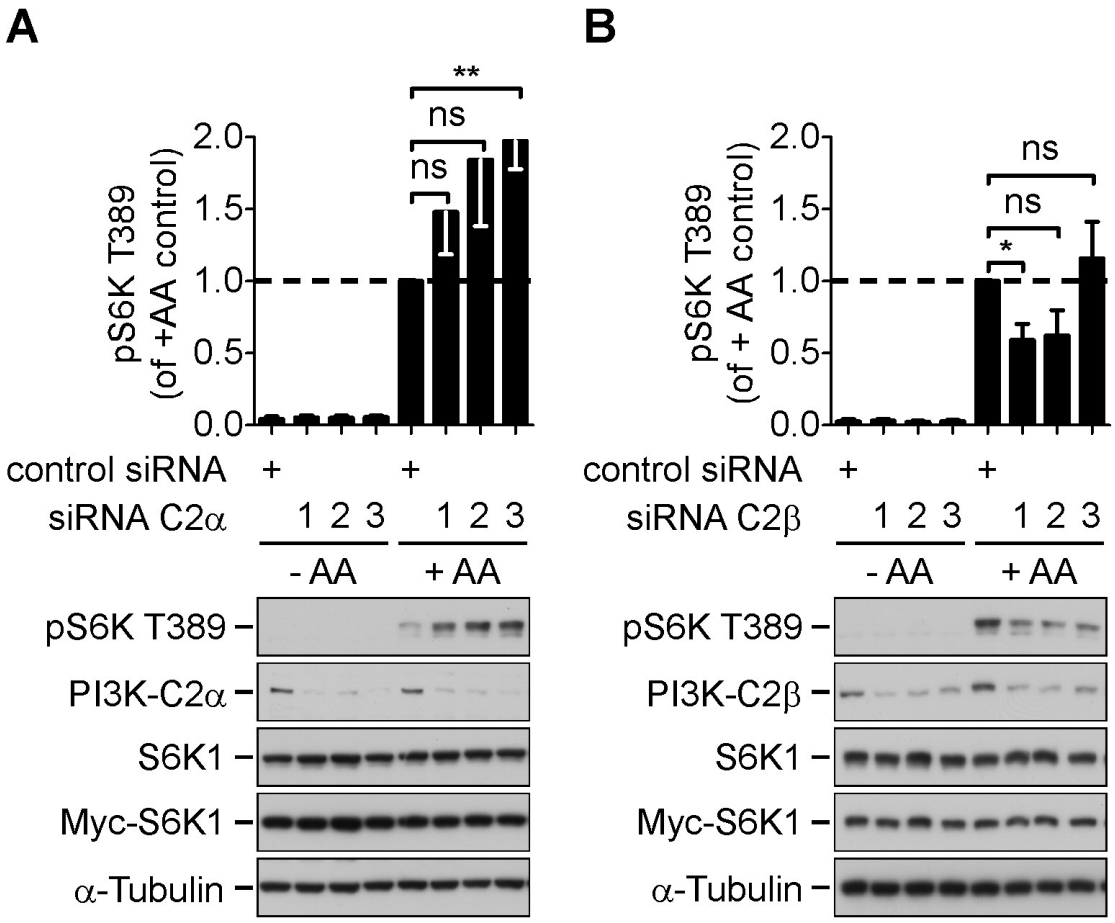

Fig. 3: Silencing of PI3K-C2α and PI3K-C2β has an isoform specific effect on mTORC1 signaling. Twenty-four hours after Myc-S6K1 transfection, HEK293 cells were transfected with three different siRNA duplexes against either PI3K-C2α (A) or PI3KC-2β (B). 48 h later cells were serum starved over night, amino acids deprived for 2h (-AA) and stimulated with amino acids (+AA) for 30 min. Cell lysates were subjected to SDS-PAGE and indicated proteins were analyzed by western blotting. PI3K-C2α (A) and PI3K-C2β (B) knockdown were assessed with anti-PI3KC2α and anti PI3KC2β and anti-α-Tubulin used as loading control. mTORC1 activity was measured by Thr389 S6K1 phosphorylation. Thr389 levels were quantified using ImageJ and normalized to the levels of Myc-S6K1. Data represented as mean ± SEM of n = 9 for PI3K-C2α and n = 6 for PI3K-C2β experiments. *P<0.05; **P<0.01.

In contrary to amino acid treatment, IGF-II stimulation of serum-starved cells did not markedly affect S6K1 Thr389 phosphorylation by either PI3K-C2α (Fig. S2A) or PI3K-C2β (Fig. S2B) silencing indicating that IGF-II stimulation goes via the canonical PI3K/PKB pathway to mTORC1, which is consistent with the unaltered PKB/Akt Thr308 and Ser473 phosphorylations (Figs. S2).

Together, it is still enigmatic which PI3K is responsible for the PtdIns(3)P generation that is required for mTORC1 activity. The modest decrease in mTORC1 activity induced through the RNAi-mediated deletion of hVps34 or PI3K-C2β suggests that loss of one PI3K can probably be complemented by another PI3K class.

PtdIns(3)P-dependent activation of mTORC1

Since targeting of hVps34 and PI3K-C2β did not markedly affect S6K1 Thr389 phosphorylation (Fig. 1B and Fig. 2B) we chose another approach to investigate the role of PtdIns(3)P in the amino acid sensing pathway to mTORC1. PtdIns(3)P is highly enriched on early endosomes and is involved in recruiting proteins containing FYVE or phox (PX) homology domains to endosomal membranes. FYVE domain containing proteins as hepatocyte growth factor-regulated tyrosine kinase substrate (HRS) and early endosomal antigen 1 (EEA1) are used as PtdIns(3)P sensors (Gillooly et al., 2000; Lemmon, 2003). However, we utilized the FYVE domain to mask PtdIns(3)P in order to disrupt PtdIns(3)P-dependent signaling (Byfield et al., 2005; Nobukuni et al., 2005; Yoon et al., 2011). Ectopic expression of EGFP-2xFYVE^{HRS} decreased amino acid-induced Thr389 phosphorylation in a concentration-dependent manner in two different cell lines, HEK293 (Fig. 4A) and HER911 cells (Fig. S3A). Unlike EGFP-2xFYVE^{HRS} wild type, the PtdIns(3)P binding-deficient mutant EGFP-2xFYVE^{HRS} C215S did not impair amino acid-induced S6K1 Thr389 phosphorylation in HEK293 (Fig. 4B) and HER911 cells (Fig. S3B). Together, this confirms a PtdIns(3)P-dependent mechanism in the activation of mTORC1 by amino acid treatment. To exclude that other 3-phosphorylated phosphoinositides might be involved in mTORC1 signaling, the PH domain of TAPP1 (tandem PH domain containing protein 1) and Btk (Bruton's tyrosine kinase), which specifically binds to PtdIns(3,4)P_2 and PtdIns(3,4,5)P_3 (Lemmon, 2003), respectively, were overexpressed in HEK293 cells (Fig. 4C). Both PH domains, unlike the tandem FYVE domain, were not able to ablate S6K1 Thr389 phosphorylation induced by amino acid treatment. The requirement of PtdIns(3)P for mTORC1 signaling is also necessary during growth factor such as IGF-II stimulation and at steady-state conditions (cells

maintained in complete medium) (Fig. 4D). Interestingly, PKB/Akt Thr308 phosphorylation was not affected by masking PtdIns(3)P (Fig. 4D), indicating that the canonical PI3K/PKB pathway was not influenced. Consequently, PtdIns(3)P is an important phospholipid in the regulation of mTORC1 and it regulates mTORC1 independent of the kind of stimulation.

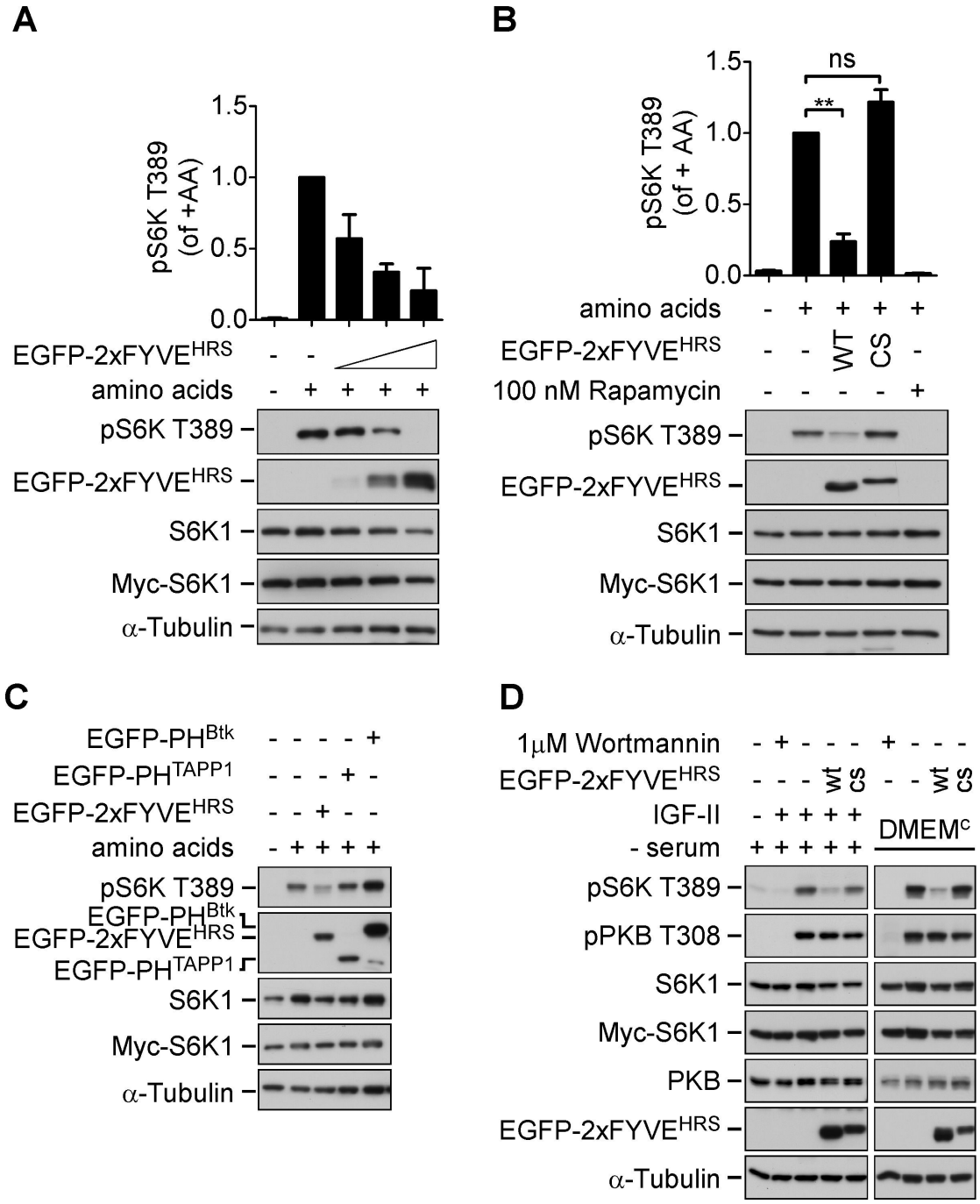

Fig. 4: PtdIns(3)P-dependent activation of mTORC1.

(A) Concentration-dependent sequester of PtdIns(3)P inhibits amino acid-induced mTORC1 activation in a concentration-dependent manner. HEK293 cells were co-transfected with Myc-S6K1 and increasing amounts of EGFP-2xFYVE^{HRS}. Thirty hours later cells were serum starved over night, amino acid

(Fig. 4. continued)

depleted for 2h and re-stimulated with amino acids for 30 min. Cell lysates were processed for SDS-PAGE and the indicated proteins were analyzed by western blotting. Anti-α-Tubulin was used as loading control and mTORC1 activity measured by S6K1 Thr389 phosphorylation. Levels of phosphorylated Thr389 were quantified using ImageJ and normalized to the levels of Myc-S6K1. Data represented as mean ± SEM of n = 3 experiments.

(B) Masking PtdIns(3)P negatively affects mTORC1 activity. EGFP-2xFYVE^{HRS} wild type (wt) and lipid-binding deficient mutant (CS) were co-transfected with Myc-S6K1 in HEK293 cells. Cells were starved and stimulated as described in (A). Where indicated, cells were pre-treated with 100nM rapamycin for 15 min prior to amino acid stimulation. Cells and western blotting were processed and analyzed as described in (A). Data represented as mean ± SEM of n = 3 experiments. **P<0.01.

(C) Masking different 3-phosphorylated phosphoinositides other than PtdIns(3)P does not affect mTORC1 signaling by amino acid stimulation. HEK293 cells were co-transfected with Myc-S6K1 and plasmids encoding for different EGFP-tagged phosphoinositide-binding modules as EGFP-2xFYVE^{HRS} (PtdIns(3)P binding), EGFP-PH^{TAPP1} (PtdIns(3,4)P_2 binding) and EGFP-PH^{Btk} (PtdIns(3,4,5)P_3 binding). Thirty hours later, cells were serum starved over night, amino acid depleted for 2h and stimulated with amino acids for 30 min. Cell lysates and western blotting were processed as described above. One representative experiment of three is shown.

(D) Sequester of PtdIns(3)P affects mTORC1 signaling by IGF-II stimulation and at steady-state condition. EGFP-2xFYVE^{HRS} wild type (wt), lipid-binding deficient mutant (CS) or empty vector were co-transfected with Myc-S6K1 in HEK293 cells and 30h later cells were either serum starved over night (-serum) and stimulated with 50 ng/ml IGF-II for 5 min (on the left) or maintained in complete medium (DMEM^{C}; on the right). Cell lysates were processed as described above. mTORC1 activity was measured by S6K1 Thr389 phosphorylation and PI3K activity by PKB/Akt Thr308 phosphorylation. Anti-α-Tubulin was used as loading control. One representative experiment of three is shown.

To further prove the connection between PtdIns(3)P and mTORC1, we acutely increased intracellular PtdIns(3)P levels by using a synthetic membrane-permeant PtdIns(3)P/AM (Subramanian et al., 2010), which chemical structure is depicted in figure 5A. The mode of action of the synthetic phospholipid is as follows: The negative charged phosphate groups of PtdIns(3)P/AM are masked with acetoxymethyl ester (AM) groups and the hydroxyl groups by butyrates that allow the uncharged lipid to pass the lipid membrane. Once inside the cell, the negative charges are regenerated by the action of endogenous esterases and lipases that remove the AM esters and butyrates and therefore making the lipid biological active (Subramanian et al., 2010). Treatment with synthetic PtdIns(3)P/AM increased almost 2-fold S6K1 Thr389 phosphorylation by amino acid stimulation, while in the absence of amino acids PtdIns(3)P/AM treatment could not induce Thr389 phosphorylation as evidenced by western blotting (Figs. 5B and 5C). Collectively, an amino acid input has to exist in order that PtdIns(3)P can activate mTORC1.

Moreover, the positive effect of synthetic PtdIns(3)P/AM on Thr389 phosphorylation was blocked by the overexpression of EGFP-2xFYVE^{HRS} (Figs. 5B and 5C) further confirming that 2xFYVE^{HRS} specifically binds to PtdIns(3)P and negatively affects mTORC1 signaling.

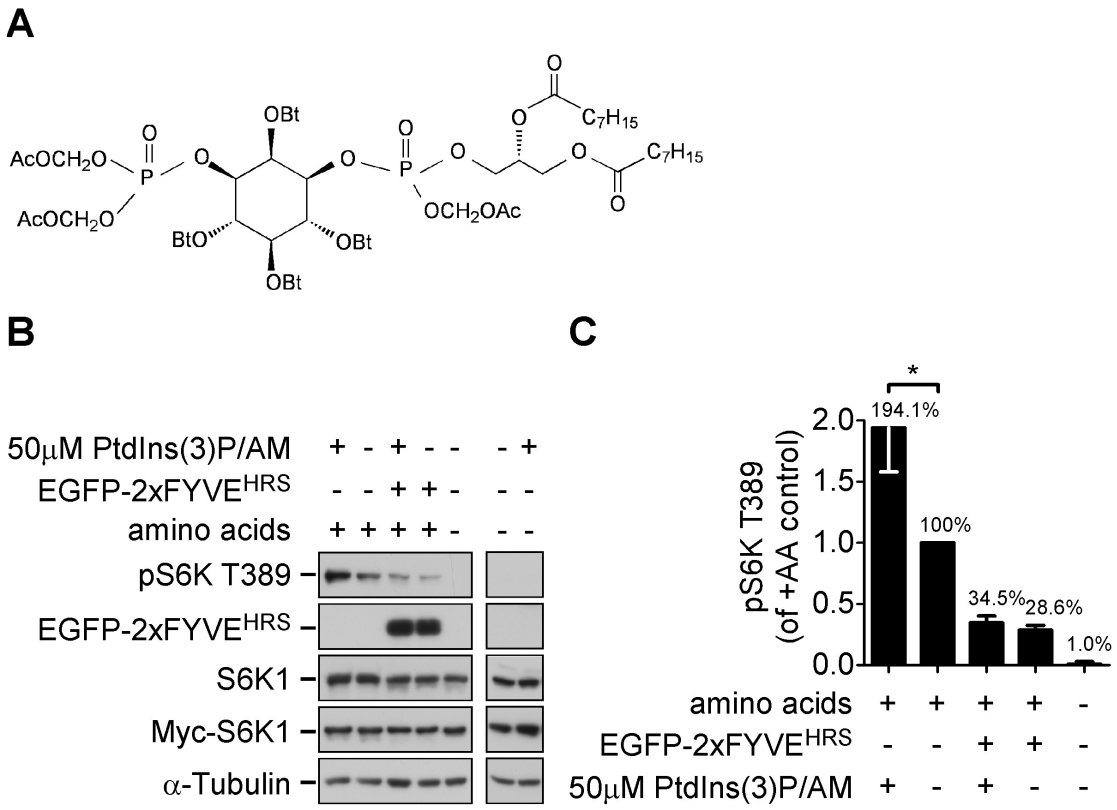

Fig. 5: Acute treatment with PtdIns(3)P increases mTORC1 signaling in response to amino acid stimulation.

(A) Chemical structure of synthetic, membrane-permeant PtdIns(3)P/AM.

(B) Treatment with PtdIns(3)P/AM positively affects mTORC1. HEK293 cells were co-transfected with EGFP-2xFYVE^{HRS} or empty vector together with Myc-S6K1. Thirty hours later, cells were serum starved over night, amino acids depleted for 1 ½ h, pre-treated with either 50 μM PtdIns(3)P/AM or carrier for 30 min and subsequently stimulated with amino acids for 30 min. Cell lysates were processed for SDS-PAGE and the indicated proteins analyzed by western blotting. mTORC1 activity was assessed by S6K1 Thr389 phosphorylation and anti-α-Tubulin used as loading control.

(C) Thr389 phosphorylation levels were quantified using ImageJ. Data are represented as mean ± SEM of n = 4 experiments, except 2xFYVE^{HRS} experiments that were done n = 3. A one tailed t-test was performed, where *P< 0.05.

Positioning mTORC1 to endosomal membranes renders its activation independent of PtdIns(3)P

Recent studies have demonstrated that by amino acid stimulation, mTORC1 is translocated from an unknown compartment to late endosomes/lysosomes, where mTORC1 can interact with and be activated by Rheb (Sancak et al., 2010; Sancak et al., 2008). To confirm the translocation, we analyzed the localization of mTOR in respect to Rab5a and Rab7 in amino acid-starved and amino acid-stimulated cells, with or without treatment by rapamycin or wortmannin (Fig. 6A and Fig. S4). For that purpose, A375 cells expressing EGFP-tagged Rab5a and Rab7 were stained for endogenous mTOR by anti-mTOR and colocalization between mTOR and EGFP-Rab5a or Rab7 analyzed by confocal microscopy (Fig. 6A and Fig. S4 showing representative microscopy pictures). As summarized in the Δ Pearson's correlation coefficient, mTOR localized to both Rab5a- and Rab7-positive endosomes in amino acid-starved, amino acid-stimulated conditions as well as at steady-state conditions (Fig. 6A). However, independently of the stimulation, the degree of mTOR localization on Rab7-positive late endosomes was significantly higher than on Rab5a-positive early endosomes. Moreover, upon amino acid stimulation mTOR localization on Rab7 endosomes significantly increased compared to amino acid-starved cells, while on Rab5a endosomes the degree of mTOR localization remained unchanged (Fig. 6A). Interestingly, rapamycin or wortmannin treatment did not affect mTOR translocation to Rab7 endosomes by amino acid stimulation (Fig. 6A) indicating that the translocation process is mTORC1 and PI3K independent. Together these data confirm that late endosomes are the cellular compartments, where mTOR translocates upon amino acid stimulation.

With in mind that PtdIns(3)P (this work; Nobukuni et al., 2005; Yoon et al., 2011) and that late endosomal translocation of mTOR (Sancak et al., 2010; Sancak et al., 2008) are required for mTORC1 signaling, we wondered whether mTORC1 activation can be made independent of PtdIns(3)P. For that purpose we made use of a system developed in Sabatini's lab (Sancak et al., 2010), where they artificially targeted raptor to late endosomal/lysosomal membranes thereby rendering mTORC1 constitutive active and resistant to amino acid starvation. Therefore, we generated HA-tagged raptor fusion protein containing at its C-terminus the last 15 amino acids of Rheb, which confers membrane targeting. For simplicity and in analogy to Sancak et al. we named this construct HA-Raptor-Rheb15 (Sancak et al., 2010). To investigate whether HA-Raptor-Rheb15, and therefore mTORC1, was localized on late endosomes we ectopically expressed EGFP-Rab5a or EGPF-Rab7 together with

HA-Raptor-Rheb15 or HA-Raptor in HEK293 and A375 cells and analyzed their colocalization to EGFP-Rab5a or EGPF-Rab7 by anti-HA staining and confocal microscopy (Fig. 6B and Fig. S5). As evidenced in the Δ Pearson's correlation coefficient summarizing the colocalization analysis, both HA-Raptor-Rheb15 and HA-Raptor localized on Rab5a early and Rab7 late endosomes in both cell lines (Fig. 6B; representative microscopy pictures are shown in Fig. S5). Nonetheless, HA-Raptor-Rheb15 was significantly more abundant on these endosomal membranes than HA-Raptor (Fig. 6B). Intriguingly, the targeting sequence of Rheb guided raptor on both early and late endosomes. So far, it was assumed that the C-terminus of Rheb is a late endosome/lysosome targeting sequence (Sancak et al., 2010). Considering mTORC1 signaling, ectopic expression of HA-Raptor-Rheb15 in HEK293 cells, unlike control samples (empty vector and HA-Raptor), resulted in S6K1 Thr389 phosphorylation in the absence of amino acids (Fig. 6C), thereby confirming that endosomal targeted raptor renders mTORC1 constitutive active and resistant to amino acid starvation. Interestingly, in HA-Raptor-Rheb15 expressing cells amino acid stimulation significantly increased Thr389 phosphorylation compared to amino acid starved cells, indicating that besides being constitutive active mTORC1 is still sensitive to amino acid stimulation (Fig. 6C).

Simultaneous expression of HA-Raptor-Rheb15 and sequester of PtdIns(3)P by ectopic expression of EGFP-2xFYVE^{HRS} significantly increased S6K1 Thr389 phosphorylation by amino acid stimulation compared to cells expressing HA-Raptor-Rheb15 alone or HA-Raptor/EGFP-2xFYVE^{HRS} (Fig. 6C). These data suggest that, when mTORC1 is guided artificially to endosomal membranes, PtdIns(3)P becomes dispensable for mTORC1 activation. Interestingly, by simultaneous masking of PtdIns(3)P by 2xFYVE^{HRS} and by HA-Raptor-Rheb15 expression S6K1 Thr389 phosphorylation increased, probably because either an inhibitory effect of PtdIns(3)P on mTORC1 was relieved or because due to complete shielding of early endosomes by 2xFYVE^{HRS} more HA-Raptor-Rheb15 and therefore more mTORC1 was targeted to late endosomes, where mTORC1 is believed to interact with Rheb (Sancak et al., 2010; Sancak et al., 2008).

In contrary to EGFP-2xFYVE^{HRS}/HA-Raptor-Rheb15 expression, EGFP-2xFYVE^{HRS} alone is inhibitory to mTORC1 signaling (Fig. 4) probably because either early endosomes are not able to mature into late endosomes when PtdIns(3)P is masked by 2xFYVE^{HRS} and therefore preventing mTORC1 to interact with and be activated by Rheb, or because mTORC1 needs PtdIns(3)P as a docking platform to associate with endosomal compartments.

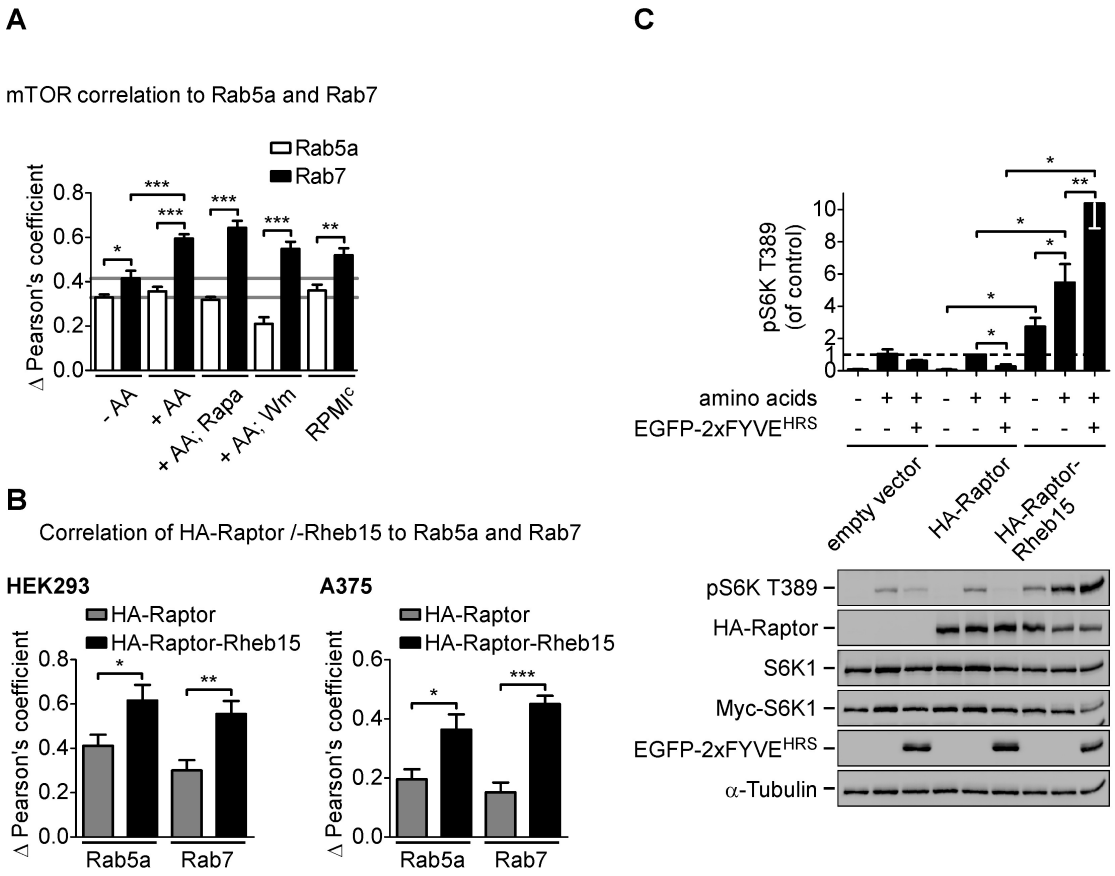

Fig. 6: Positioning mTORC1 on endosomes renders mTORC1 signaling independent of PtdIns(3)P.

(A) Amino acid stimulation induces translocation of mTOR to late endosomes. A375 cells were transfected with either EGFP-Rab5a or EGFP-Rab7 and 30h later, cells were either serum starved over night, depleted of amino acids for 2h (-AA) and re-stimulated with amino acids for 30min (+AA) or maintained in complete medium (RPMI^c). Where indicated, prior to amino acid stimulation cells were pre-treated with 100 nM rapamycin (Rapa) or 1 μM wortmannin (Wm) for 15 min and included during amino acid stimulation. Following fixation, cells were immunostained for endogenous mTOR followed by AlexaFluor568-coupled secondary antibody. Images were acquired with a Zeiss confocal microscope and degree of mTOR colocalization to either EGFP-Rab5a (Rab5a) or EGFP-Rab7 (Rab7) was determined by Δ Pearson's correlation coefficient of at least 10 different cells. Representative pictures for each treatment used for quantification are depicted in the supplementary figures (Fig. S4). Data are represented as mean ± SEM. Horizontal grey lines demarcate the levels amino acid-starved Rab5a- or Rab7-positive cells from the other stimulated cells. *P<0.05, **P<0.01, ***P<0.001.

(B) HA-Raptor-Rheb15 targets mTOR to endosomal membranes. Both HEK293 and A375 cells were co-transfected with HA-Raptor and HA-Raptor-Rheb15 with either EGFP-Rab5a or EGFP-Rab7. Thirty hours later, cells were serum starved over night, amino acids depleted for 2h and cells were fixed and immunostained for HA followed by AlexaFluor568-coupled secondary antibody. Images were acquired with a Zeiss confocal microscope and degree of colocalization of either HA-Raptor-Rheb15 or HA-Raptor to EGFP-Rab5a (Rab5a) and EGFP-Rab7 (Rab7) was determined by Δ Pearson's correlation coefficient of at least 10 different cells. Representative pictures used for quantification are depicted in the supplementary figures (Fig. S5). Data represented as mean ± SEM. *P<0.05, **P<0.01, ***P<0.001.

(Fig. 6 continued)

(C) Endosomal targeting renders mTORC1 activity independent of PtdIns(3)P. HEK293 cells were co-transfected with empty vector, HA-Raptor, HA-Raptor-Rheb15 and Myc-S6K1 together with or without EGFP-2xFYVE^{HRS}. Thirty hours later cells were serum starved over night, amino acids depleted for 2h and re-stimulated with amino acids for 30 min. Cell lysates were processed for SDS-PAGE and the indicated proteins were analyzed by western blotting. S6K1 Thr389 phosphorylation was assessed for mTORC1 activity and anti-α-Tubulin used as loading control. Levels of phosphorylated Thr389 were quantified using ImageJ and normalized to Myc-S6K1. Data represented as mean ± SEM of n = 4 experiments. *P<0.05, **P<0.01.

Inhibiting PtIns(3,5)P_2 synthesis by treatment with the PIKfyve inhibitor YM201636, impairs amino acid-induced mTORC1 activation and late endosomal mTOR localization

PtdIns(3,5)P_2 along with PtdIns(3)P are fundamental for endomembrane sorting and endomembrane homeostasis (Michell et al., 2006). PtdIns(3,5)P_2 is synthesized by the PtdIns(3)P 5-kinase PIKfyve (Fab1 in yeast) that catalyzes the 5-phosphorylation of PtdIns(3)P (Dove et al., 2009; Ikonomov et al., 2001; Sbrissa et al., 1999; Shisheva et al., 2001). PIKfyve is a fundamental kinase as genetic deletion in mice and *C. elegans* is embryonic lethal (Ikonomov et al., 2011; Nicot et al., 2006). Furthermore, cells having a defective PIKfyve kinase display a characteristic vacuolar phenotype. Overexpression of a catalytic inactive PIKfyve mutant or knockdown of PIKfyve results in swollen cytoplasmic vacuoles in many cell types and decreased PtdIns(3,5)P_2 levels (Ikonomov et al., 2003; Ikonomov et al., 2006; Jefferies et al., 2008; Rutherford et al., 2006). Enlarged vacuoles and decreased PtdIns(3,5)P_2 have also been observed in different cell lines by pharmacologic inhibition of PIKfyve with the pyridofuropyrimidine compound YM201636, a specific PIKfyve inhibitor (Jefferies et al., 2008). The generation of these large vacuoles is regarded as a functional indication of reduced PtdIns(3,5)P_2 levels or lost PIKfyve activity (Ikonomov et al., 2011). Treatment of HEK293 and A375 cells with YM201636 for different times led to the formation of the well-characterized vacuolization phenotype (Fig. S6, see transmission pictures) thereby indicating a loss of PIKfyve activity. To investigate whether PtdIns(3,5)P_2 might be required for amino acid-induced mTORC1 signaling, HEK293 and A375 cells were treated with different concentrations of YM201636 and Myc-S6K1 Thr389 phosphorylation analyzed by western blotting (Figs. 7A and Fig. 7B). Already a low dose of 0.5 μM YM201636 almost completely blocked amino acid-induced S6K1 Thr389 phosphorylation in HEK293 cells (Fig. 7A), while in A375 cells treatment with 1 μM YM201636 significantly decreased Thr389 phosphorylation to

50% (Fig. 7B). Over night treatment with 1 μM YM201636 in A375 could not further decrease Thr389 phosphorylation (Fig. 7B). The differential behavior in S6K1 Thr389 phosphorylation observed between A375 and HEK293 cells is probably dependent on the constitutive active MAPK pathway in A375 cells due to V600E mutation in B-Raf. It is known that active ERK and RSK either indirectly, via inhibition of the TSC1/TSC2 complex, or directly, via phosphorylation of raptor, activate mTORC1 signaling (Carriere et al., 2008; Carriere et al., 2011; Langlais et al., 2011; Roux et al., 2004). Collectively, YM201636 almost completely blocks mTORC1-mediated S6K1 Thr389 phosphorylation in amino acid-stimulated HEK293 cells, while in A375 cells the suppression is less pronounced probably due to the constitutive active MAPK pathway.

Consistent with mTOR translocation to late endosomes being required for mTORC1 signaling (Sancak et al., 2010; Sancak et al., 2008), we investigated whether YM201636 treatment affected the localization of mTOR in respect to Rab7. EGFP-Rab7 was ectopically expressed in A375 cells and localization of endogenous mTOR examined by anti-mTOR antibody and by confocal microscopy (Fig. 7C). Interestingly, mTOR localization to Rab7 endosomes was significantly reduced by YM201636 treatment in amino acid stimulated cells compared to vehicle treated cells as evidenced in the Δ Pearson's correlation coefficient (Fig. 7C; representative microscopy pictures are shown in Fig. S7). The colocalization between mTOR and Rab7 after YM201636 treatment resembled that of amino acid starved cells (Fig. 7C). Together, PtdIns(3,5)P_2 regulates mTORC1 signaling either by serving as a docking platform for mTORC1 association on late endosomes or as an important phospholipid involved in the maturation of early to late endosomes. Concerning endosome maturation, Flinn et al. claimed that when maturation from early to late endosome is blocked by constitutive active Rab5 or by deleting the Rab7 GEF (guanine exchange factor) Vps39, mTORC1 signaling is negatively affected (Flinn et al., 2010). PIKfyve has been shown to be required in the early-to-late endosome traffic and is essential for the organization of late endosomal/lysosomal compartment (Ikonomov et al., 2003; Ikonomov et al., 2006) consequently favoring the maturation process for mTORC1 regulation.

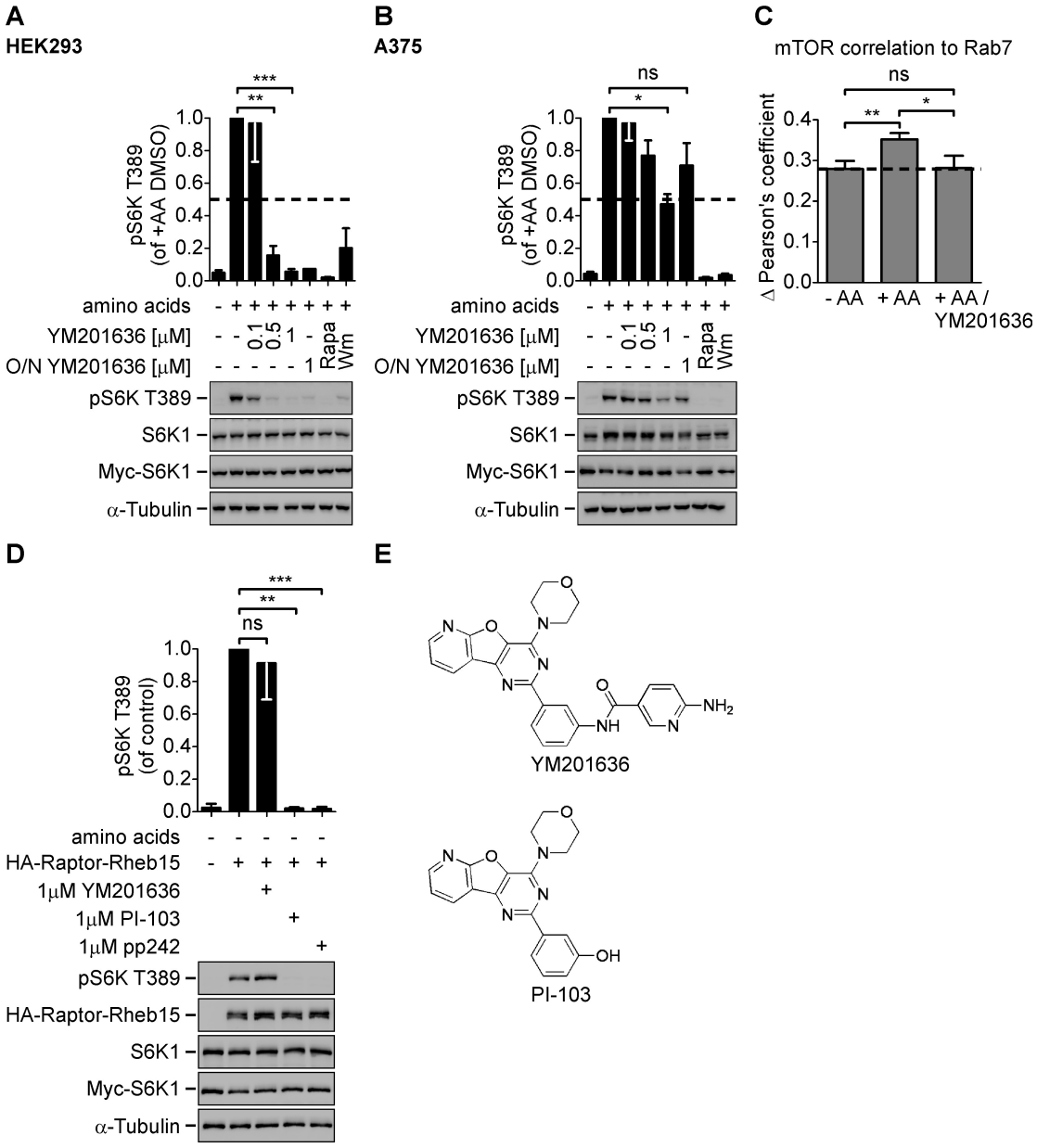

Fig. 7: Inhibiting PtIns(3,5)P_2 generation by treatment with the PIKfyve inhibitor YM201636, impairs amino acid-induced mTORC1 activation and late endosomal mTOR localization.

(A and B) PIKfyve inhibition by YM201636 negatively affects amino acid-induced mTORC1 activation. Following 30h of Myc-S6K1 transfection, HEK293 (A) and A375 (B) cells were serum starved over night, amino acid depleted for 2h and re-stimulated with amino acids for 30 min. Where indicated, cells were either pre-treated with DMSO, different concentrations of YM201636 (0.1 μM, 0.5 μM and 1 μM), 100nM rapamycin (Rapa) or 1μM wortmannin (Wm) for 15 min prior to amino acid stimulation and inhibitors were re-added during amino acid stimulation. For over night (O/N) YM201636 treatment, 1 μM YM201636 was added each time to the cells when medium condition was changed. Cell lysates were processed for SDS-PAGE and indicated proteins analyzed by western blotting. Anti-α-Tubulin was used as loading control. S6K1 Thr389 phosphorylation was assessed for mTORC1 activity and Thr389 levels quantified using ImageJ and normalized to Myc-S6K1. Data are represented as mean ± SEM of n = 3 experiments, exception O/N YM201636 treatment done n = 1 in HEK293 (A) and n = 2 in A375 (B) cells. *P<0.05, **P<0.01, ***P<0.001.

(Fig. 7 continued)

(C) PIKfyve inhibition by YM201636 treatment affects mTOR localization on late endosomes. A375 cells were transfected with EGFP-Rab7 and 30h later cells were serum starved over night, amino acids depleted for 2h (-AA) and stimulated with amino acids for 30min (+AA). Prior to amino acid stimulation cells were pre-treated with 1 μM YM201636 for 15 min and re-added during amino acid stimulation, where indicated. After fixation, cells were immunostained for endogenous mTOR followed by AlexaFluor568-coupled secondary antibody. Images were acquired with a Zeiss confocal microscope and degree of mTOR colocalization to EGFP-Rab7 was determined by Δ Pearson's correlation coefficient of at least 16 different cells. Data are represented as mean ± SEM (*P<0.05, **P<0.01). Horizontal line demarcates the level of amino acid-starved cells from amino acid-stimulated cells treated with or without YM201636. Representative pictures used for quantification are depicted in supplementary figures (Fig. S7).

(D) YM201636 is not an mTOR kinase inhibitor. HEK293 cells were co-transfected with HA-Raptor-Rheb15 and Myc-S6K1 and 30 h later cells were over night serum starved and amino acid depleted for 2h. Where indicated 1μM YM201636, 1μM PI-103 and 1μM pp242 were included during the last 45 min of amino acid depletion. Cell lysates and western blotting were processed as described above. Data are represented as mean ± SEM of n = 3 experiments, exception PI-103 and amino acid starved experiments done n = 2. **P<0.01, ***P<0.001.

E) Chemical structures of YM201636 and PI-103.

Because of the negative effect of YM201636 treatment on mTORC1 signaling and late endosomal mTOR localization (Figs. 7A-7C), we wondered whether these effects were due to the inhibition of the catalytic activity of mTOR. For that purpose we tested YM201636 in the absence of amino acids on constitutive active mTORC1, induced through the expression of HA-Raptor-Rheb15 in HEK293 cells (Fig. 7D). S6K1 Thr389 phosphorylation was completely blocked by two mTOR kinase inhibitors, pp242 and PI-103, the latter one being structurally related to YM201636 (Fig. 7E), while YM201636 had no effect on mTORC1 activity (Fig. 7D). Consequently, YM201636 inhibits mTORC1 signaling by preventing the translocation of mTOR to late endosomes but not by inhibiting the kinase activity of mTOR.

To exclude any effect of YM201636 treatment on PtdIns(3)P generation, we examined the intracellular distribution of EGFP-2xFYVE^{HRS} in HEK293 and A375 cells by confocal microscopy (Fig. S6). YM201636 did not affect endosomal localization of EGFP-2xFYVE^{HRS} in both cells lines, while wortmannin treatment resulted in a diffused cytoplasmic localization of EGFP-2xFYVE^{HRS} due to the inhibition of PtdIns(3)P synthesis (Fig S6). Interestingly, EGFP-2xFYVE^{HRS} positive endosomes increased in size over time of YM201636 treatment either due to increased homotypic early endosome fusion or due to a block in forward membrane

transport from early to late endosomes. The latter would be consistent with a defect in membrane transport (Ikonomov et al., 2003; Ikonomov et al., 2006).

Together, PIKfyve inhibition by YM201636 treatment negatively affects amino acid-induced mTORC1 signaling by preventing the amino acid-induced translocation of mTOR on late endosomes rather than by blocking mTOR kinase activity or PtdIns(3)P synthesis. However, YM201636 is less effective in A375 cells than in HEK293 most probably due to the constitutive active MAPK pathway in A375 cells.

4.5 Discussion

In this study, we have characterized the role of PtdIns(3)P and PtdIns(3,5)P_2 in the amino acid-dependent activation of mTORC1 and described how targeting PtdIns(3)P- and PtdIns(3,5)P_2-generating kinases or changing intracellular levels of freely available PtdIns(3)P affects mTORC1 activity.

We provide evidence that PIKfyve, the sole PtdIns(3)P 5-kinase, that synthesizes PtdIns(3,5)P_2 from PtdIns(3)P (Dove et al., 2009; Ikonomov et al., 2001; Sbrissa et al., 1999; Shisheva et al., 2001), is implicated in the amino acid signaling pathway to mTORC1. PIKfyve and its phospholipid product PtdIns(3,5)P_2 are mostly found on late endocytic compartments (Sbrissa et al., 2002; Shisheva et al., 2001). PIKfyve is necessary for several membrane trafficking pathways as retrograde transport from early/late endosomes to the trans-Golgi network (TGN) (Ikonomov et al., 2003b), morphogenesis of multivesicular bodies (Ikonomov et al., 2003), insulin-regulated GLUT4 vesicle transport (Berwick et al., 2004) and early-to-late endosome traffic (Ikonomov et al., 2003; Ikonomov et al., 2006). Here, we have assessed that PIKfyve is also involved in mTORC1 signaling. Inhibition of PIKfyve by YM201636 treatment, a PIKfyve inhibitor that specifically blocks PtdIns(3,5)P_2 synthesis (Jefferies et al., 2008), blunts amino acid-induced mTORC1 activation by preventing mTOR translocation to late endosomes, but without affecting mTOR kinase activity and PtdIns(3)P generation. Previous reports have shown that recruitment of mTOR to late endosomes/lysosomes by amino acid stimulation is important for mTORC1 activation (Sancak et al., 2010; Sancak et al., 2008). Conceivably, PtdIns(3,5)P_2 might serve as a docking platform for mTORC1 association on late endocytic compartments. On the other hand intracellular trafficking, especially maturation of early to late endosomes also impinges on mTORC1 activation (Flinn et al., 2010; Li et al., 2010). When early to late endosome conversion is blocked by ectopic expression of constitutive active Rab5 or by knockdown of Rab7 GEF hVps39 mTORC1 activation is blunted, probably due to the formation of a hybrid endosome that contain both markers for both early and late endosomes (Flinn et al., 2010). PIKfyve regulated PtdIns(3)P-to-PtdIns(3,5)P_2 transition has been shown to be important for the organization of late endosomes/lysosomes (Ikonomov et al., 2006), therefore it might be possible that PIKfyve is involved in the early-to-late endosome maturation process. Consistently, by inhibiting PIKfyve, increased EGFP-2xFYVE^{HRS}-positive endosomes have been observed that were generated probably due to a defect in membrane transport. This

would explain why inhibition of PIKfyve impairs amino acid-induced mTORC1 activation.

Similarly to PIKfyve inhibition, masking PtdIns(3)P by EGFP-FYVE^{HRS} expression inhibits mTORC1 activation possibly by affecting membrane transport. Consistently, it has been demonstrated that EGFR (epidermal growth factor receptor) stays trapped in early endosomes by EGFP-2FYVE^{HRS} overexpression (Petiot et al., 2003). Moreover, PIKfyve uses PtdIns(3)P as a substrate for the formation of PtdIns(3,5)P_2 (Sbrissa et al., 1999; Shisheva et al., 1999) and as a membrane docking through its FYVE finger domain (Sbrissa et al., 2002; Shisheva et al., 1999). Masking PtdIns(3)P by 2xFYVE^{HRS} deprives PIKfyve of its substrate and displaces PIKfyve from its membrane localization and consequently PtdIns(3,5)P_2 production is lost.
Interestingly, we demonstrated that acute treatment with the membrane permeant PtdIns(3)P/AM increases almost 2-fold amino acid-induced S6K1 Th389 phosphorylation compared to control. Cell fractionation studies have demonstrated that PIKfyve is to 70% cytosolic (Sbrissa et al., 2002), therefore acute PtdIns(3)P/AM treatment can lead to higher mobilization of PIKfyve to endomembrane compartments and therefore to increased PtdIns(3,5)P_2 formation and consequently to increased mTORC1 activation.

PtdIns(3,5)P_2 is derived from the sequential phosphorylation of PtdIns. hVps34 catalyzes the 3-phosphorylation of PtdIns to form PtdIns(3)P that is eventually used for 5-phosphorylation catalyzed by PIKfyve resulting in PtdIns(3,5)P_2 formation. Therefore, manipulation of PtdIns(3)P levels by deleting the expression of hVp34 is expected to have a negative effect on mTORC1 activation as has been demonstrated previously (Byfield et al., 2005; Nobukuni et al., 2005; Yoon et al., 2011). However, unlike to these reports, we were unable to see a complete decrease in amino acid-induced mTORC1 activation by depleting hVps34 expression in HEK293 and A375 melanoma cells. Similarly, Xu et al were not able to see a significant reduction in amino acid-induced S6K1 Thr389 phosphorylation by hVps34 knockdown in T24 bladder cancer cells, but only by deleting hVps15/p150, the adaptor of hVps34, a marked reduction in mTORC1 activation was observed (Xu et al., 2011). Elimination of hVps34 is expected to deplete intracellular PtdIns(3)P similar to wortmannin treatment. Despite hVps34 knockdown, PtdIns(3)P was still formed as demonstrated by the endosomal localization of EGFP-2xFYVE^{HRS}. This result might explain why mTORC1 activity was still present in the Vps34 depleted cells. Moreover, hVps34 knockdown cells proliferated similarly to control cells.

The connection between hVps34 and mTORC1 in the amino acid pathway has been shown to be controversial. Genetic elimination of Vps34 in *Drosophila* has no impact on dTORC1 signaling, while autophagy and endocytosis are affected (Juhasz et al., 2008). Recently, Vps34 knock out mice have been generated, where homozygous Vps34 null mice are embryonic lethal and die between E7.5 and E8.5 of embryogenesis due to severely reduced cell proliferation (Zhou et al., 2011). Additionally, phospho-S6 staining in E6.5 Vps34 null embryos is drastically reduced compared to control embryos thereby providing evidence that mTORC1 signaling is reduced in Vps34 mutant embryos (Zhou et al., 2011). This result suggests that in mammalian cells, Vps34 is implicated in the mTORC1 signaling. However, during early stages of development the embryo is dependent on branched chain amino acids and glucose (Martin and Sutherland, 2001). During these early stages autophagy provides the embryo with the required nutrients. Since Vps34 is involved in the autophagic process (Simonsen and Tooze, 2009), it is conceivable that the phospho-S6 phenotype observed in Vps34 null embryos is a consequence of nutrient shortage due to the disrupted autophagy rather than a direct involvement of Vps34 in the nutrient regulation to mTORC1.

In cells, PtdIns(3)P generation is not exclusively dependent on hVps34. In *C. elegans* RNAi-mediated deletion of myotubularin 6 (MTM6), a PtdIns(3)P phosphatase, in Vps34 knockout larvae (let-512 mutants) restored PtdIns(3)P levels and rescued lethality of the let-512 mutants (Xue et al., 2003). Interestingly, the kinase responsible for the generation of PtdIns(3)P in the let-512 mutants has been shown to be class II PI3K (Xue et al., 2003). Therefore, it is possible that the class II PI3K might compensate for the loss of hVps34 in the amino acid signaling pathway to mTORC1. Class II PI3Ks are poorly understood kinases, but there are some evidences that they preferentially generate PtdIns(3)P *in vivo* (Falasca and Maffucci, 2007; Maffucci et al., 2005; Wen et al., 2008). To our surprise depletion of PI3K-C2α and PI3K-C2β resulted in an isoform specific effect on amino acid-dependent mTORC1 activation. While knockdown of PI3K-C2α increased mTORC1 activation, knockdown of PI3K-C2β decreased it to approximate 50% similar to the result obtained by silencing hVps34. However, when performing a double PI3K-C2β/hVps34 knockdown no additional decrease in amino acid-induced mTORC1 activation could be observed (unpublished data).

There are alternative pathways for the generation of PtdIns(3)P that do not require the direct 3-phosphorylation of PtdIns, which might have an impact on mTORC1. It

has been shown that PtdIns(3,4,5)P_3 generated by class IA PI3Kβ, p110β, is sequentially dephosphorylated by phosphoinositide 4- and 5-phosphatases (Shin et al., 2005). Alternatively, type I alpha inositol polyphosphate 4-phosphatase has been found to be localized on early and recycling endosomes and forms PtdIns(3)P by dephosphorylating PtdIns(3,4)P_2 (Ivetac et al., 2005).

In these report we show a mechanistic role of PtdIns(3)P and PtdIns(3,5)P_2 in the regulation of mTORC1 by amino acid stimulation. With in mind that progression of early endosomes to late endosome is involved in amino acids signaling to mTORC1 (Flinn et al., 2010), the PtdIns(3)P-to-PtdIns(3,5)P_2 transition might be involved in the same process.

PtdIns(3)P and PtdIns(3,5)P_2 do not directly affect mTORC1 activation rather they are involved in the formation of late endosomes that might serve as a signaling platform for mTORC1. However, when HA-Raptor-Rheb15 is ectopically expressed, mTORC1 activity is independent of PtdIns(3)P and PtdIns(3,5)P_2, probably because the targeting sequence of Rheb fused to raptor guides mTORC1 to Rheb-containing endosomal compartments allowing mTORC1 to be activated by Rheb.

We are the first to show that the PIKfyve inhibitor YM201636 blocks amino acid-induced mTORC1 activation but without affecting the mTOR kinase activity. Our preliminary data further show that YM201636 negatively affects proliferation in HEK293 cells without affecting the canonical PI3K/PKB pathway (data not shown). The implication of PIKfyve in cell proliferative capacity has also been demonstrated in PIKfyve null MEFs, where they have a profound arrest in DNA synthesis (Ikonomov et al., 2011). However, PIKfyve is likely not suitable as a cancer target. In A375 melanoma cells, that have a constitutive active MAPK kinase pathway, the effect of YM201636 treatment on mTORC1 activity is less pronounced. Additionally, A375 cells proliferate undisturbed by YM20636 treatment (data not shown). A combinatorial treatment of YM201636 with a MAPK kinase inhibitor might be more effective in blocking mTORC1 activity and proliferation.

4.6 Supplementary figures

Suppl. Fig. 1

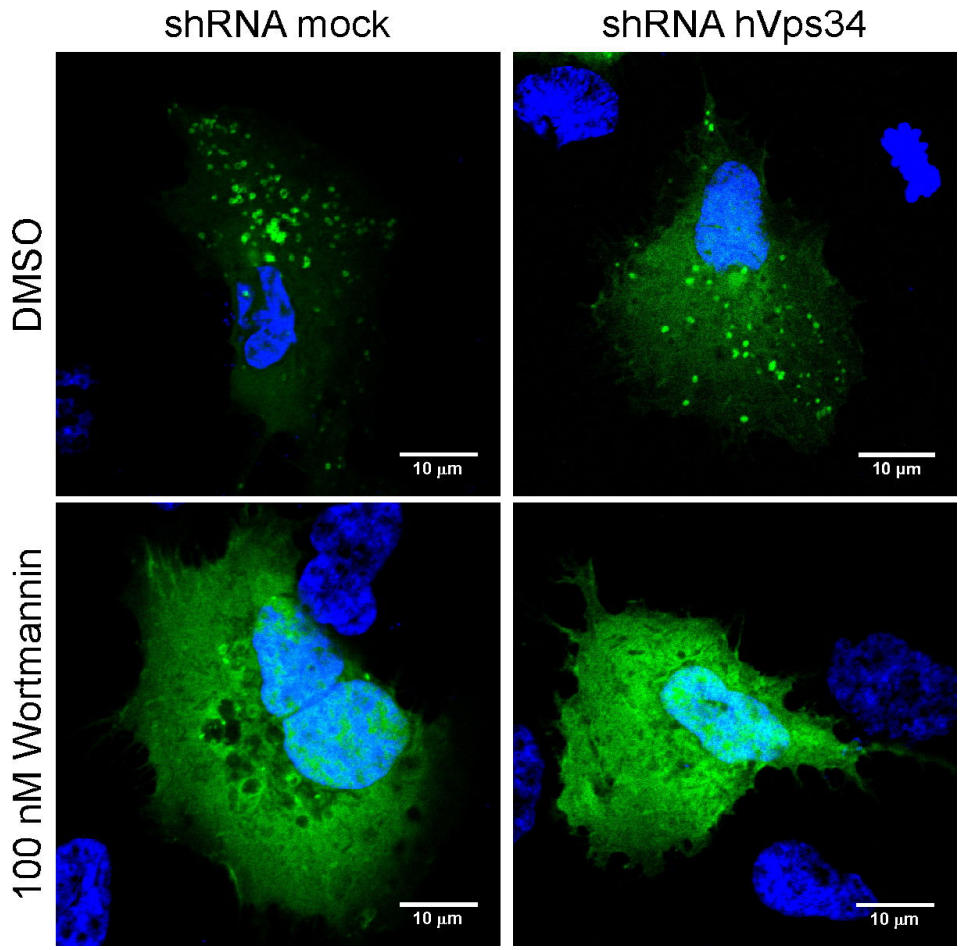

Fig. S1 (related to Fig. 2): Silencing of hVps34 does not affect PtdIns(3)P generation.

A375 cells were transduced with lentivirus with shRNA against hVps34 (shRNA hVps34) and empty vector (shRNA mock) and selected with puromycin followed by EGFP-2xFYVE^{HRS} transfection in order to visualize PtdIns(3)P-containing endosomes. Cells were maintained in complete medium (RPMI supplemented with 2 mM L-glutamine and 10% FCS) and 48h later cells were either treated with DMSO or 100nM wortmannin for 30min. After fixation, nuclei were stained with Hoechst and cells imaged with a Zeiss confocal microscope. Scale bars represent 10 µm.

Suppl. Fig. 2

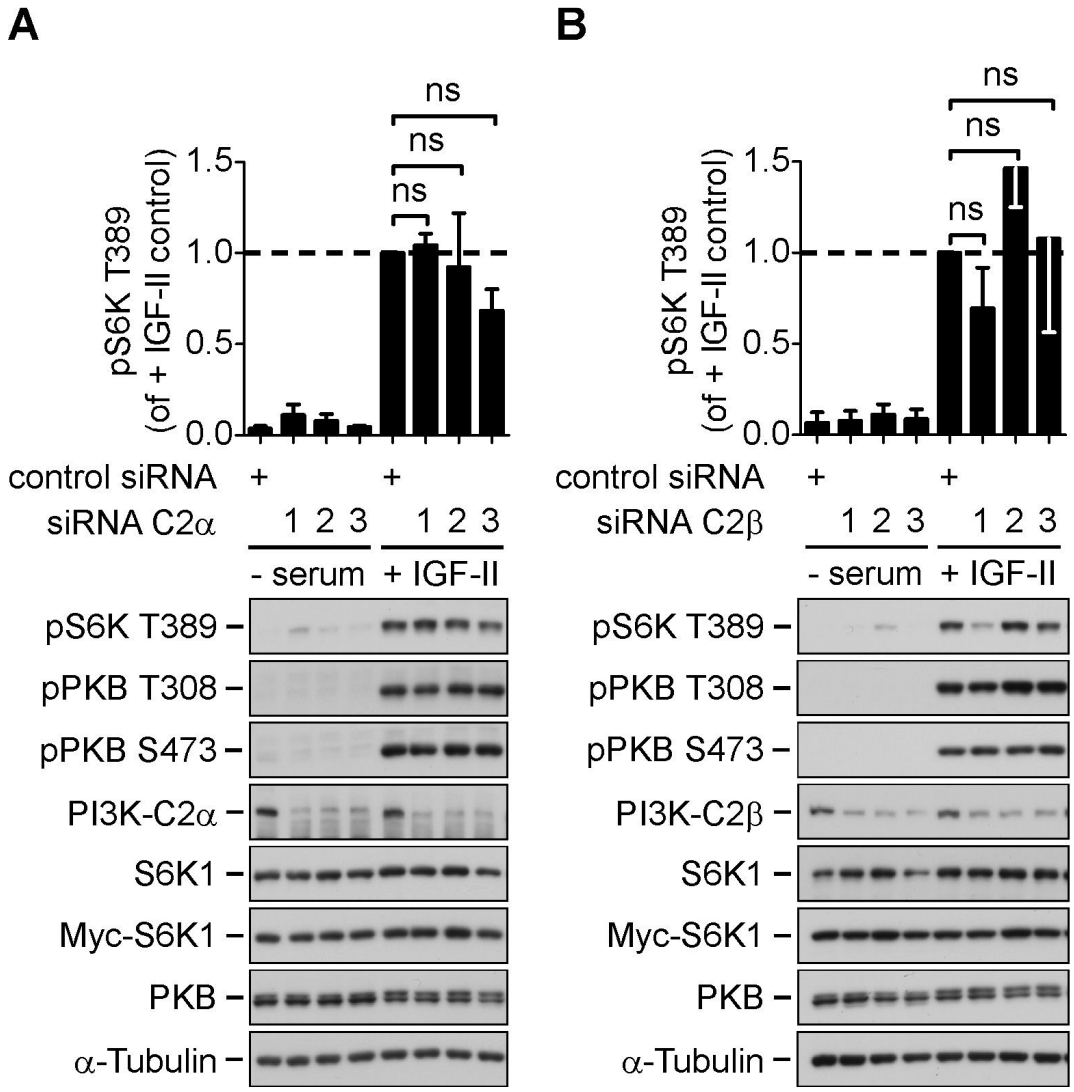

Fig. S2 (related to Fig. 3): PI3K-C2α and PI3K-C2β are not involved in the growth factor-induced mTORC1 and PI3K activation.

HEK293 cells were transfected with Myc-S6K1 followed 24h later by siRNA transfection with three different siRNA duplexes against either PI3K-C2α (siRNA C2α #1, #2 and #3) (A) or PI3K-C2β (siRNA C2β #1, #2 and #3) (B) and siRNA control duplex was included as negative control (control siRNA). After 48h, cells were over night serum starved (-serum) and stimulated with 50 ng/ml IGF-II for 5 min (+IGF-II). Cell lysates were processed for SDS-PAGE and indicated proteins analyzed by western blotting. Anti-α-Tubulin was used as loading control. mTORC1 activity was assessed by S6K1 Thr389 phosphorylation and PI3K activity by PKB Thr308 and Ser473 phosphorylation. Levels of phosphorylated Thr389 were quantified using ImageJ and normalized to Myc-S6K1. Data are represented as mean ± SEM of n = 3 experiments.

Suppl. Fig. 3

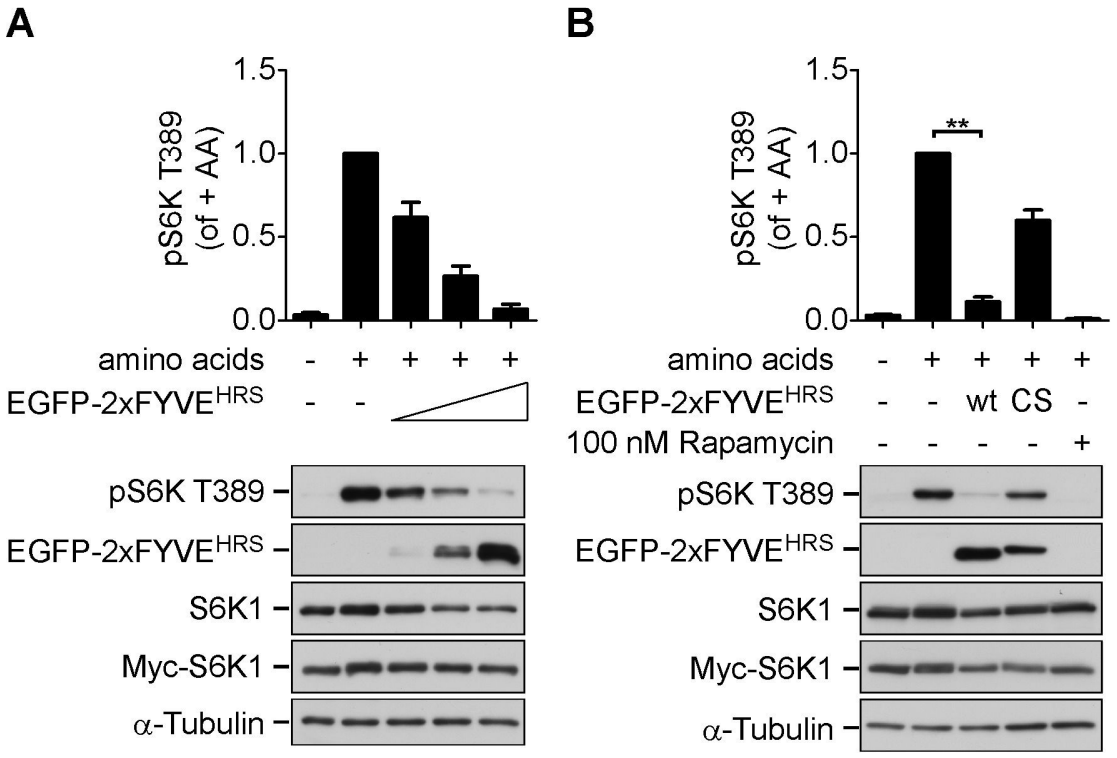

Fig. S3 (related to Fig. 4): PtdIns(3)P-dependent activation of mTORC1 in HER911 cells.

(A) Concentration-dependent sequester of PtdIns(3)P inhibits amino acid-induced mTORC1 activation in a concentration-dependent manner. HER911 cells were co-transfected with Myc-S6K1 and increasing amounts of EGFP-2xFYVE^{HRS}. Thirty hours later cells were serum starved over night, amino acid depleted for 2h and re-stimulated with amino acids for 30 min. Cell lysates were processed for SDS-PAGE and the indicated proteins were analyzed by western blotting. Anti-α-Tubulin was used as loading control and mTORC1 activity measured by S6K1 Thr389 phosphorylation. Levels of phosphorylated Thr389 were quantified using ImageJ and normalized to the levels of Myc-S6K1. Data represented as mean ± SEM of n = 3 experiments.

(B) Masking PtdIns(3)P negatively affects mTORC1 activity. HER911 cells were co-transfected with Myc-S6K together either EGFP-2xFYVE^{HRS} wild type (wt), EGFP-2xFYVE^{HRS} lipid-binding deficient mutant (CS) or empty vector. Cells were starved and stimulated as described in (A). Where indicated, cells were pre-treated with 100nM rapamycin for 15 min prior to amino acid stimulation. Cells and western blotting were processed and analyzed as described in (A). Data represented as mean ± SEM of n = 3 experiments. **P<0.01.

Suppl. Fig. 4

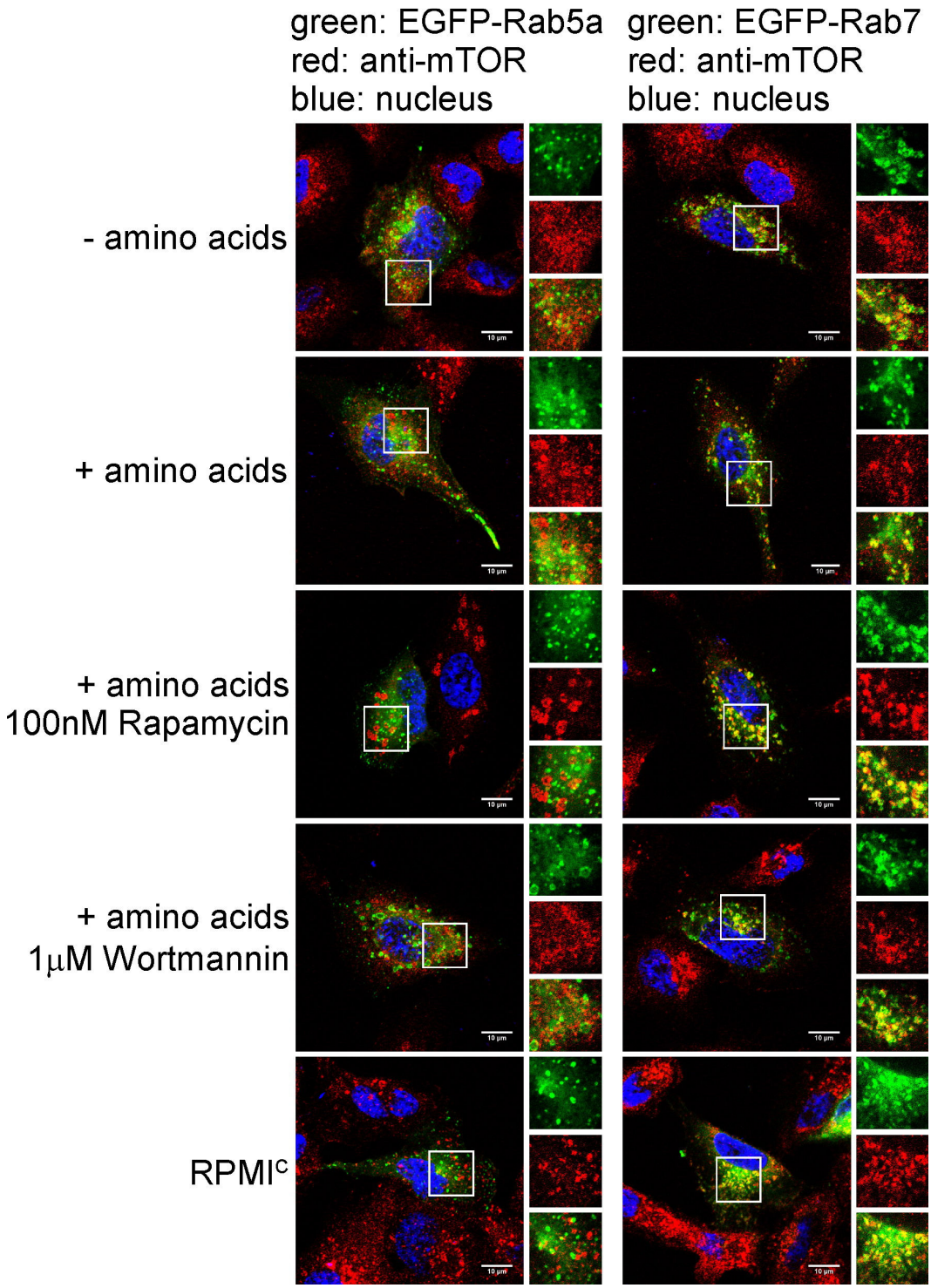

Fig. S4 (related to Fig. 6A): Translocation of mTOR to late endosomes by amino acid stimulation.

A375 cells were transfected and processed as described in Fig. 6A. Images of A375 cells expressing EGFP-Rab5a (green) or EGFP-Rab7 (green) immunostained for endogenous mTOR (red) after amino acid starvation, amino acid stimulation with or without treatment with 100 nM rapamycin or 1 μM wortmannin and maintained in complete medium ($RPMI^C$). Nuclei were stained with Hoechst and colocalization depicted in the merge pictures. Scale bars represent 10 μm.

Suppl. Fig. 5

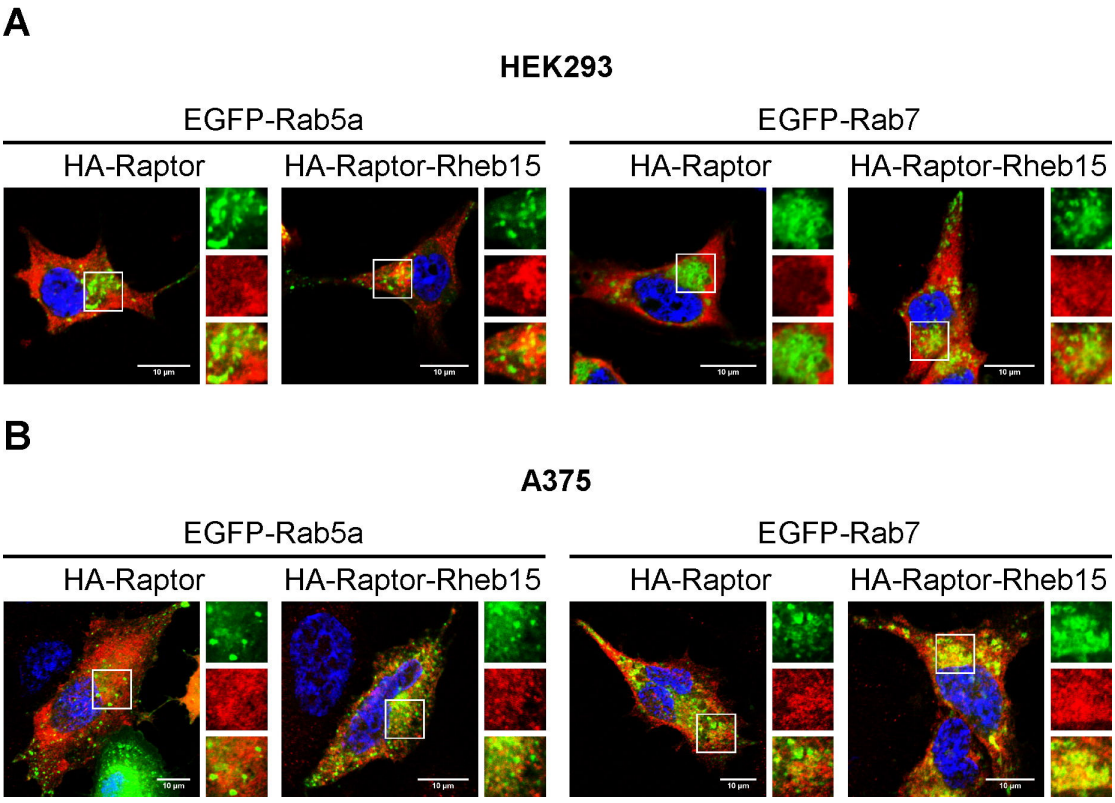

Fig. S5 (related to Fig. 6B): HA-Raptor-Rheb15 targets mTOR to endosomal membranes.

(A and B) HEK293 (A) and A375 (B) cells were transfected and processed as described in Fig. 6B. Images of HEK293 (A) and A375 (B) cells co-expressing EGFP-Rab5a (green) and EGFP-Rab7 (green) with HA-Raptor or HA-Raptor-Rheb15 immunostained for HA (red) after amino acid starvation. Nuclei were stained with Hoechst and colocalization depicted in the merge pictures. Scale bars represent 10μm.

Suppl. Fig. 6

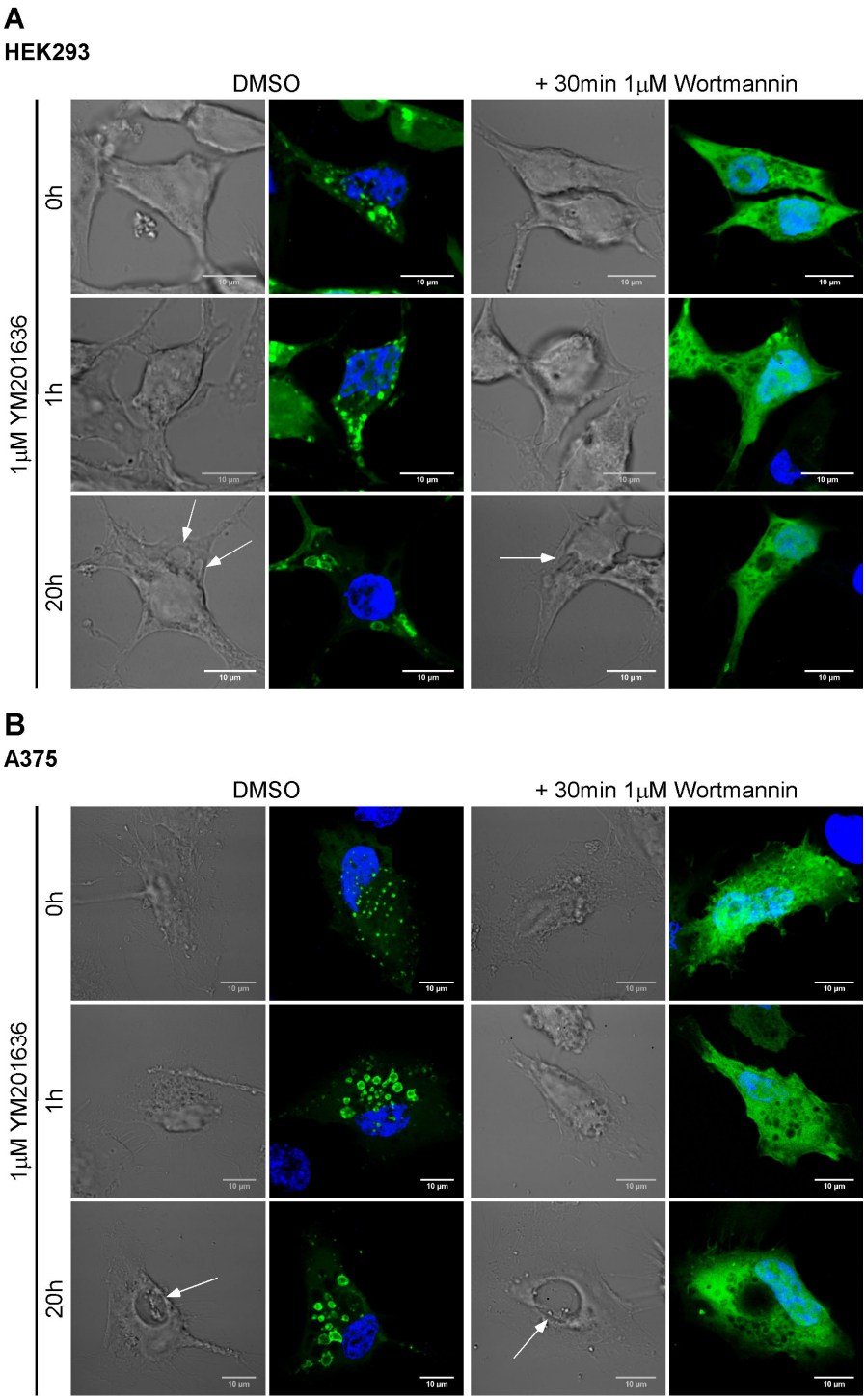

Fig. S6 (related to Fig. 7): PIKfyve inhibition by YM201636 treatment does not block PtdIns(3)P generation

HEK293 (A) and A375 (B) cells were transfected with the PtdIns(3)P probe EGFP-2xFYVE^{HRS} and maintained in complete medium (DMEM^{C} for HEK293 and RPMI^{C} for A375 cells supplemented with 2 mM L-glutamine and 10% FCS). After 48h, cells were incubated with 1 μM YM201636 for different time points (0, 1 and 20h) followed by a 30 min treatment with either DMSO or 1 μM wortmannin. Cells were fixed and nuclei stained with Hoechst. Images were acquired with a Zeiss confocal microscope. Arrows indicate swollen vacuoles in the transmission figure. Scale bars represent 10 μm.

Suppl. Fig. 7

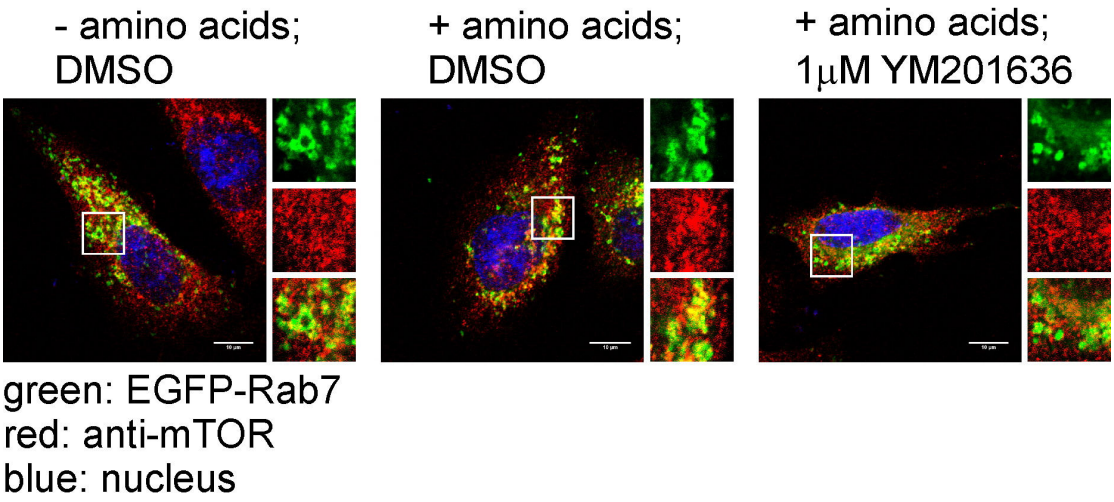

Fig. S7 (related to Fig. 7C): PIKfyve inhibition by YM201636 treatment affects mTOR localization on late endosomes.

A375 cells were transfected and processed as described in Fig. 7C. Images of A375 cells expressing EGFP-Rab7 (green) immunostained for endogenous mTOR (red) after amino acid starvation and amino acid re-stimulation with DMSO or 1 μM YM201636. Nuclei were stained with Hoechst and colocalization depicted in the merge pictures. Scale bars represent 10 μm.

4.7 References

Arcaro, A., Volinia, S., Zvelebil, M.J., Stein, R., Watton, S.J., Layton, M.J., Gout, I., Ahmadi, K., Downward, J., and Waterfield, M.D. (1998). Human phosphoinositide 3-kinase C2beta, the role of calcium and the C2 domain in enzyme activity. J Biol Chem *273*, 33082-33090.

Berwick, D.C., Dell, G.C., Welsh, G.I., Heesom, K.J., Hers, I., Fletcher, L.M., Cooke, F.T., and Tavare, J.M. (2004). Protein kinase B phosphorylation of PIKfyve regulates the trafficking of GLUT4 vesicles. J Cell Sci *117*, 5985-5993.

Burnett, P.E., Barrow, R.K., Cohen, N.A., Snyder, S.H., and Sabatini, D.M. (1998). RAFT1 phosphorylation of the translational regulators p70 S6 kinase and 4E-BP1. Proc Natl Acad Sci U S A *95*, 1432-1437.

Byfield, M.P., Murray, J.T., and Backer, J.M. (2005). hVps34 is a nutrient-regulated lipid kinase required for activation of p70 S6 kinase. J Biol Chem *280*, 33076-33082.

Carriere, A., Cargnello, M., Julien, L.A., Gao, H., Bonneil, E., Thibault, P., and Roux, P.P. (2008). Oncogenic MAPK signaling stimulates mTORC1 activity by promoting RSK-mediated raptor phosphorylation. Curr Biol *18*, 1269-1277.

Carriere, A., Romeo, Y., Acosta-Jaquez, H.A., Moreau, J., Bonneil, E., Thibault, P., Fingar, D.C., and Roux, P.P. (2011). ERK1/2 phosphorylate Raptor to promote Ras-dependent activation of mTOR complex 1 (mTORC1). J Biol Chem *286*, 567-577.

Christoforidis, S., Miaczynska, M., Ashman, K., Wilm, M., Zhao, L., Yip, S.C., Waterfield, M.D., Backer, J.M., and Zerial, M. (1999). Phosphatidylinositol-3-OH kinases are Rab5 effectors. Nat Cell Biol *1*, 249-252.

Corradetti, M.N., and Guan, K.L. (2006). Upstream of the mammalian target of rapamycin: do all roads pass through mTOR? Oncogene *25*, 6347-6360.

Domin, J., Gaidarov, I., Smith, M.E., Keen, J.H., and Waterfield, M.D. (2000). The class II phosphoinositide 3-kinase PI3K-C2alpha is concentrated in the trans-Golgi network and present in clathrin-coated vesicles. J Biol Chem *275*, 11943-11950.

Dove, S.K., Dong, K., Kobayashi, T., Williams, F.K., and Michell, R.H. (2009). Phosphatidylinositol 3,5-bisphosphate and Fab1p/PIKfyve underPPIn endo-lysosome function. Biochem J *419*, 1-13.

Falasca, M., and Maffucci, T. (2007). Role of class II phosphoinositide 3-kinase in cell signalling. Biochem Soc Trans *35*, 211-214.

Flinn, R.J., Yan, Y., Goswami, S., Parker, P.J., and Backer, J.M. (2010). The late endosome is essential for mTORC1 signaling. Mol Biol Cell *21*, 833-841.

Frias, M.A., Thoreen, C.C., Jaffe, J.D., Schroder, W., Sculley, T., Carr, S.A., and Sabatini, D.M. (2006). mSin1 is necessary for Akt/PKB phosphorylation, and its isoforms define three distinct mTORC2s. Curr Biol *16*, 1865-1870.

Futter, C.E., Collinson, L.M., Backer, J.M., and Hopkins, C.R. (2001). Human VPS34 is required for internal vesicle formation within multivesicular endosomes. J Cell Biol *155*, 1251-1264.

Gillooly, D.J., Morrow, I.C., Lindsay, M., Gould, R., Bryant, N.J., Gaullier, J.M., Parton, R.G., and Stenmark, H. (2000). Localization of phosphatidylinositol 3-phosphate in yeast and mammalian cells. EMBO J *19*, 4577-4588.

Guertin, D.A., and Sabatini, D.M. (2007). Defining the role of mTOR in cancer. Cancer Cell *12*, 9-22.

Gulati, P., Gaspers, L.D., Dann, S.G., Joaquin, M., Nobukuni, T., Natt, F., Kozma, S.C., Thomas, A.P., and Thomas, G. (2008). Amino acids activate mTOR complex 1 via Ca2+/CaM signaling to hVps34. Cell Metab *7*, 456-465.

Hara, K., Maruki, Y., Long, X., Yoshino, K., Oshiro, N., Hidayat, S., Tokunaga, C., Avruch, J., and Yonezawa, K. (2002). Raptor, a binding partner of target of rapamycin (TOR), mediates TOR action. Cell *110*, 177-189.

Hara, K., Yonezawa, K., Weng, Q.P., Kozlowski, M.T., Belham, C., and Avruch, J. (1998). Amino acid sufficiency and mTOR regulate p70 S6 kinase and eIF-4E BP1 through a common effector mechanism. J Biol Chem *273*, 14484-14494.

Hay, N., and Sonenberg, N. (2004). Upstream and downstream of mTOR. Genes Dev *18*, 1926-1945.

Hennig, K.M., Colombani, J., and Neufeld, T.P. (2006). TOR coordinates bulk and targeted endocytosis in the Drosophila melanogaster fat body to regulate cell growth. J Cell Biol *173*, 963-974.

Herman, P.K., and Emr, S.D. (1990). Characterization of VPS34, a gene required for vacuolar protein sorting and vacuole segregation in Saccharomyces cerevisiae. Mol Cell Biol *10*, 6742-6754.

Huotari, J., and Helenius, A. (2011). Endosome maturation. EMBO J *30*, 3481-3500.

Ikonomov, O.C., Sbrissa, D., Delvecchio, K., Xie, Y., Jin, J.P., Rappolee, D., and Shisheva, A. (2011). The phosphoinositide kinase PIKfyve is vital in early embryonic development: preimplantation lethality of PIKfyve-/- embryos but normality of PIKfyve+/- mice. J Biol Chem *286*, 13404-13413.

Ikonomov, O.C., Sbrissa, D., Foti, M., Carpentier, J.L., and Shisheva, A. (2003). PIKfyve controls fluid phase endocytosis but not recycling/degradation of endocytosed receptors or sorting of procathepsin D by regulating multivesicular body morphogenesis. Mol Biol Cell *14*, 4581-4591.

Ikonomov, O.C., Sbrissa, D., Mlak, K., Deeb, R., Fligger, J., Soans, A., Finley, R.L., Jr., and Shisheva, A. (2003b). Active PIKfyve associates with and promotes the membrane attachment of the late endosome-to-trans-Golgi network transport factor Rab9 effector p40. J Biol Chem *278*, 50863-50871.

Ikonomov, O.C., Sbrissa, D., and Shisheva, A. (2001). Mammalian cell morphology and endocytic membrane homeostasis require enzymatically active phosphoinositide 5-kinase PIKfyve. J Biol Chem *276*, 26141-26147.

Ikonomov, O.C., Sbrissa, D., and Shisheva, A. (2006). Localized PtdIns 3,5-P2 synthesis to regulate early endosome dynamics and fusion. Am J Physiol Cell Physiol *291*, C393-404.

Ivetac, I., Munday, A.D., Kisseleva, M.V., Zhang, X.M., Luff, S., Tiganis, T., Whisstock, J.C., Rowe, T., Majerus, P.W., and Mitchell, C.A. (2005). The type Ialpha inositol polyphosphate 4-phosphatase generates and terminates phosphoinositide 3-kinase signals on endosomes and the plasma membrane. Mol Biol Cell *16*, 2218-2233.

Jacinto, E., Facchinetti, V., Liu, D., Soto, N., Wei, S., Jung, S.Y., Huang, Q., Qin, J., and Su, B. (2006). SIN1/MIP1 maintains rictor-mTOR complex integrity and regulates Akt phosphorylation and substrate specificity. Cell *127*, 125-137.

Jacinto, E., Loewith, R., Schmidt, A., Lin, S., Ruegg, M.A., Hall, A., and Hall, M.N. (2004). Mammalian TOR complex 2 controls the actin cytoskeleton and is rapamycin insensitive. Nat Cell Biol *6*, 1122-1128.

Jefferies, H.B., Cooke, F.T., Jat, P., Boucheron, C., Koizumi, T., Hayakawa, M., Kaizawa, H., Ohishi, T., Workman, P., Waterfield, M.D.*, et al.* (2008). A selective PIKfyve inhibitor blocks PtdIns(3,5)P(2) production and disrupts endomembrane transport and retroviral budding. EMBO Rep *9*, 164-170.

Johnson, E.E., Overmeyer, J.H., Gunning, W.T., and Maltese, W.A. (2006). Gene silencing reveals a specific function of hVps34 phosphatidylinositol 3-kinase in late versus early endosomes. J Cell Sci *119*, 1219-1232.

Juhasz, G., Hill, J.H., Yan, Y., Sass, M., Baehrecke, E.H., Backer, J.M., and Neufeld, T.P. (2008). The class III PI(3)K Vps34 promotes autophagy and endocytosis but not TOR signaling in Drosophila. J Cell Biol *181*, 655-666.

Kim, D.H., Sarbassov, D.D., Ali, S.M., King, J.E., Latek, R.R., Erdjument-Bromage, H., Tempst, P., and Sabatini, D.M. (2002). mTOR interacts with raptor to form a nutrient-sensitive complex that signals to the cell growth machinery. Cell *110*, 163-175.

Kim, D.H., Sarbassov, D.D., Ali, S.M., Latek, R.R., Guntur, K.V., Erdjument-Bromage, H., Tempst, P., and Sabatini, D.M. (2003). GbetaL, a positive regulator of the rapamycin-sensitive pathway required for the nutrient-sensitive interaction between raptor and mTOR. Mol Cell *11*, 895-904.

Kok, K., Geering, B., and Vanhaesebroeck, B. (2009). Regulation of phosphoinositide 3-kinase expression in health and disease. Trends Biochem Sci *34*, 115-127.

Langlais, P., Yi, Z., and Mandarino, L.J. (2011). The identification of raptor as a substrate for p44/42 MAPK. Endocrinology *152*, 1264-1273.

Lemmon, M.A. (2003). Phosphoinositide recognition domains. Traffic *4*, 201-213.

Li, L., Kim, E., Yuan, H., Inoki, K., Goraksha-Hicks, P., Schiesher, R.L., Neufeld, T.P., and Guan, K.L. (2010). Regulation of mTORC1 by the Rab and Arf GTPases. J Biol Chem *285*, 19705-19709.

Loewith, R., Jacinto, E., Wullschleger, S., Lorberg, A., Crespo, J.L., Bonenfant, D., Oppliger, W., Jenoe, P., and Hall, M.N. (2002). Two TOR complexes, only one of which is rapamycin sensitive, have distinct roles in cell growth control. Mol Cell *10*, 457-468.

Maffucci, T., Cooke, F.T., Foster, F.M., Traer, C.J., Fry, M.J., and Falasca, M. (2005). Class II phosphoinositide 3-kinase defines a novel signaling pathway in cell migration. J Cell Biol *169*, 789-799.

Martin, D.E., and Hall, M.N. (2005). The expanding TOR signaling network. Curr Opin Cell Biol *17*, 158-166.

Martin, P.M., and Sutherland, A.E. (2001). Exogenous amino acids regulate trophectoderm differentiation in the mouse blastocyst through an mTOR-dependent pathway. Dev Biol *240*, 182-193.

Michell, R.H., Heath, V.L., Lemmon, M.A., and Dove, S.K. (2006). Phosphatidylinositol 3,5-bisphosphate: metabolism and cellular functions. Trends Biochem Sci *31*, 52-63.

Murray, J.T., Panaretou, C., Stenmark, H., Miaczynska, M., and Backer, J.M. (2002). Role of Rab5 in the recruitment of hVps34/p150 to the early endosome. Traffic *3*, 416-427.

Nicot, A.S., Fares, H., Payrastre, B., Chisholm, A.D., Labouesse, M., and Laporte, J. (2006). The phosphoinositide kinase PIKfyve/Fab1p regulates terminal lysosome maturation in Caenorhabditis elegans. Mol Biol Cell *17*, 3062-3074.

Nobukuni, T., Joaquin, M., Roccio, M., Dann, S.G., Kim, S.Y., Gulati, P., Byfield, M.P., Backer, J.M., Natt, F., Bos, J.L.*, et al.* (2005). Amino acids mediate mTOR/raptor signaling through activation of class 3 phosphatidylinositol 3OH-kinase. Proc Natl Acad Sci U S A *102*, 14238-14243.

Pearce, L.R., Huang, X., Boudeau, J., Pawlowski, R., Wullschleger, S., Deak, M., Ibrahim, A.F., Gourlay, R., Magnuson, M.A., and Alessi, D.R. (2007). Identification of Protor as a novel Rictor-binding component of mTOR complex-2. Biochem J *405*, 513-522.

Peterson, T.R., Laplante, M., Thoreen, C.C., Sancak, Y., Kang, S.A., Kuehl, W.M., Gray, N.S., and Sabatini, D.M. (2009). DEPTOR is an mTOR inhibitor frequently overexpressed in multiple myeloma cells and required for their survival. Cell *137*, 873-886.

Petiot, A., Faure, J., Stenmark, H., and Gruenberg, J. (2003). PI3P signaling regulates receptor sorting but not transport in the endosomal pathway. J Cell Biol *162*, 971-979.

Prior, I.A., and Clague, M.J. (1999). Localization of a class II phosphatidylinositol 3-kinase, PI3KC2alpha, to clathrin-coated vesicles. Mol Cell Biol Res Commun *1*, 162-166.

Rink, J., Ghigo, E., Kalaidzidis, Y., and Zerial, M. (2005). Rab conversion as a mechanism of progression from early to late endosomes. Cell *122*, 735-749.

Roux, P.P., Ballif, B.A., Anjum, R., Gygi, S.P., and Blenis, J. (2004). Tumor-promoting phorbol esters and activated Ras inactivate the tuberous sclerosis tumor suppressor complex via p90 ribosomal S6 kinase. Proc Natl Acad Sci U S A *101*, 13489-13494.

Rutherford, A.C., Traer, C., Wassmer, T., Pattni, K., Bujny, M.V., Carlton, J.G., Stenmark, H., and Cullen, P.J. (2006). The mammalian phosphatidylinositol 3-phosphate 5-kinase (PIKfyve) regulates endosome-to-TGN retrograde transport. J Cell Sci *119*, 3944-3957.

Sancak, Y., Bar-Peled, L., Zoncu, R., Markhard, A.L., Nada, S., and Sabatini, D.M. (2010). Ragulator-Rag complex targets mTORC1 to the lysosomal surface and is necessary for its activation by amino acids. Cell *141*, 290-303.

Sancak, Y., Peterson, T.R., Shaul, Y.D., Lindquist, R.A., Thoreen, C.C., Bar-Peled, L., and Sabatini, D.M. (2008). The Rag GTPases bind raptor and mediate amino acid signaling to mTORC1. Science *320*, 1496-1501.

Sancak, Y., Thoreen, C.C., Peterson, T.R., Lindquist, R.A., Kang, S.A., Spooner, E., Carr, S.A., and Sabatini, D.M. (2007). PRAS40 is an insulin-regulated inhibitor of the mTORC1 protein kinase. Mol Cell *25*, 903-915.

Sarbassov, D.D., Ali, S.M., Kim, D.H., Guertin, D.A., Latek, R.R., Erdjument-Bromage, H., Tempst, P., and Sabatini, D.M. (2004). Rictor, a novel binding partner of mTOR, defines a rapamycin-insensitive and raptor-independent pathway that regulates the cytoskeleton. Curr Biol *14*, 1296-1302.

Sarbassov, D.D., Ali, S.M., Sengupta, S., Sheen, J.H., Hsu, P.P., Bagley, A.F., Markhard, A.L., and Sabatini, D.M. (2006). Prolonged rapamycin treatment inhibits mTORC2 assembly and Akt/PKB. Mol Cell *22*, 159-168.

Sbrissa, D., Ikonomov, O.C., and Shisheva, A. (1999). PIKfyve, a mammalian ortholog of yeast Fab1p lipid kinase, synthesizes 5-phosphoinositides. Effect of insulin. J Biol Chem *274*, 21589-21597.

Sbrissa, D., Ikonomov, O.C., and Shisheva, A. (2002). Phosphatidylinositol 3-phosphate-interacting domains in PIKfyve. Binding specificity and role in PIKfyve. Endomenbrane localization. J Biol Chem *277*, 6073-6079.

Shin, H.W., Hayashi, M., Christoforidis, S., Lacas-Gervais, S., Hoepfner, S., Wenk, M.R., Modregger, J., Uttenweiler-Joseph, S., Wilm, M., Nystuen, A.*, et al.* (2005). An enzymatic cascade of Rab5 effectors regulates phosphoinositide turnover in the endocytic pathway. J Cell Biol *170*, 607-618.

Shisheva, A., Rusin, B., Ikonomov, O.C., DeMarco, C., and Sbrissa, D. (2001). Localization and insulin-regulated relocation of phosphoinositide 5-kinase PIKfyve in 3T3-L1 adipocytes. J Biol Chem *276*, 11859-11869.

Shisheva, A., Sbrissa, D., and Ikonomov, O. (1999). Cloning, characterization, and expression of a novel Zn2+-binding FYVE finger-containing phosphoinositide kinase in insulin-sensitive cells. Mol Cell Biol *19*, 623-634.

Siddhanta, U., McIlroy, J., Shah, A., Zhang, Y., and Backer, J.M. (1998). Distinct roles for the p110alpha and hVPS34 phosphatidylinositol 3'-kinases in vesicular trafficking, regulation of the actin cytoskeleton, and mitogenesis. J Cell Biol *143*, 1647-1659.

Simonsen, A., and Tooze, S.A. (2009). Coordination of membrane events during autophagy by multiple class III PI3-kinase complexes. J Cell Biol *186*, 773-782.

Stack, J.H., and Emr, S.D. (1994). Vps34p required for yeast vacuolar protein sorting is a multiple specificity kinase that exhibits both protein kinase and phosphatidylinositol-specific PI 3-kinase activities. J Biol Chem *269*, 31552-31562.

Stack, J.H., Herman, P.K., Schu, P.V., and Emr, S.D. (1993). A membrane-associated complex containing the Vps15 protein kinase and the Vps34 PI 3-kinase is essential for protein sorting to the yeast lysosome-like vacuole. EMBO J *12*, 2195-2204.

Stein, M.P., Feng, Y., Cooper, K.L., Welford, A.M., and Wandinger-Ness, A. (2003). Human VPS34 and p150 are Rab7 interacting partners. Traffic *4*, 754-771.

Subramanian, D., Laketa, V., Muller, R., Tischer, C., Zarbakhsh, S., Pepperkok, R., and Schultz, C. (2010). Activation of membrane-permeant caged PtdIns(3)P induces endosomal fusion in cells. Nat Chem Biol *6*, 324-326.

Volinia, S., Dhand, R., Vanhaesebroeck, B., MacDougall, L.K., Stein, R., Zvelebil, M.J., Domin, J., Panaretou, C., and Waterfield, M.D. (1995). A human phosphatidylinositol 3-kinase complex related to the yeast Vps34p-Vps15p protein sorting system. EMBO J *14*, 3339-3348.

Wen, P.J., Osborne, S.L., Morrow, I.C., Parton, R.G., Domin, J., and Meunier, F.A. (2008). Ca2+-regulated pool of phosphatidylinositol-3-phosphate produced by phosphatidylinositol 3-kinase C2alpha on neurosecretory vesicles. Mol Biol Cell *19*, 5593-5603.

Wullschleger, S., Loewith, R., and Hall, M.N. (2006). TOR signaling in growth and metabolism. Cell *124*, 471-484.

Xu, L., Salloum, D., Medlin, P.S., Saqcena, M., Yellen, P., Perrella, B., and Foster, D.A. (2011). Phospholipase D mediates nutrient input to mammalian target of rapamycin complex 1 (mTORC1). J Biol Chem *286*, 25477-25486.

Xue, Y., Fares, H., Grant, B., Li, Z., Rose, A.M., Clark, S.G., and Skolnik, E.Y. (2003). Genetic analysis of the myotubularin family of phosphatases in Caenorhabditis elegans. J Biol Chem *278*, 34380-34386.

Yan, Y., Flinn, R.J., Wu, H., Schnur, R.S., and Backer, J.M. (2009). hVps15, but not Ca2+/CaM, is required for the activity and regulation of hVps34 in mammalian cells. Biochem J *417*, 747-755.

Yang, Q., Inoki, K., Ikenoue, T., and Guan, K.L. (2006). Identification of Sin1 as an essential TORC2 component required for complex formation and kinase activity. Genes Dev *20*, 2820-2832.

Yoon, M.S., Du, G., Backer, J.M., Frohman, M.A., and Chen, J. (2011). Class III PI-3-kinase activates phospholipase D in an amino acid-sensing mTORC1 pathway. J Cell Biol *195*, 435-447.

Zhou, X., Takatoh, J., and Wang, F. (2011). The mammalian class 3 PI3K (PIK3C3) is required for early embryogenesis and cell proliferation. PLoS One *6*, e16358.

5 General discussion and conclusion

In mammalian cells, mTORC1 senses intracellular amino acid status through a still undefined mechanism and regulates translation by phosphorylating key regulatory proteins such as S6K1 and 4E-BP1. Cultured cells can be easily manipulated and by withdrawing amino acids from the culture medium, mTORC1 signaling is completely inhibited thereby blocking cell growth and activating the catabolic process autophagy in order to produce energy during this period of stress. However, in higher organism such as humans, the bloodstream supplies the body constantly with nutrients. There are fluctuations in nutrient levels during food intake, but the organism will never suffer from complete nutrient deprivation. Nonetheless, it is important to elucidate in a cellular context how amino acid sufficiency is sensed, especially with in mind that cancers/tumors increase amino acids uptake via upregulating the expression of amino acid transporters (Fuchs and Bode, 2005) presumably to sustain their continuous growth. Elevated expression of the system L transporter LAT1 is associated with advanced glioblastoma and poorer prognosis (reviewed in Edinger, 2007). Pharmacologic inhibition of LAT1 leads to inhibition of cancer cell growth thereby defining amino acid transporters as drug targets for cancer chemotherapy (Ganapathy et al., 2009). Alternatively, the intracellular amino acid sensor might also be a good candidate as a cancer drug target. However, an amino acid sensor has not been characterized yet. But it is known that cells somehow sense amino acid sufficiency and transmit the signal to mTORC1 (Beugnet et al., 2003; Christie et al., 2002). In the recent years, proteins mediating the amino acid input to mTORC1 have started to be uncovered. Of great interest are the recently identified Rag GTPases and their role in translocating mTORC1 from an unknown compartment to late endosomes/lysosomes in response to amino acid stimulation, thereby bringing mTORC1 close to its activator Rheb (Sancak et al., 2010; Sancak et al., 2008). Other potential amino acid mediators such as MAP4K3, hVps34 and PLD1 have also been identified to be implicated in mTORC1 activation (Byfield et al., 2005; Findlay et al., 2007; Nobukuni et al., 2005; Xu et al., 2011; Yan et al., 2010; Yoon et al., 2011). It is unknown whether a relationship between these proteins and Rag GTPases exist, or whether they function in a parallel pathway to the Rag GTPase as it was recently proposed for PLD1 (Yoon et al., 2011).

The role of hVps34 in mediating the amino acid signal to mTORC1 is in my opinion still unclear. Experimental evidences demonstrate that PtdIns(3)P, which is formed

by hVps34 (Stack and Emr, 1994; Volinia et al., 1995), is important in the activation of mTORC1 (this present study; Nobukuni et al., 2005; Yoon et al., 2011). However, deletion of either hVps34 or class II PI3K isoforms, which might also generate PtdIns(3)P in vivo (Falasca and Maffucci, 2007; Maffucci et al., 2005; Wen et al., 2008), do not completely abrogate mTORC1 signaling, probably because cells find alternative pathways in synthesizing PtdIns(3)P to compensate for the loss of PtdIns(3)P (Ivetac et al., 2005; Shin et al., 2005). Indeed, confocal microscopy analyses revealed that in hVps34 knockdown cells the PtdIns(3)P sensor EGFP-2FYVE^{HRS} still localizes to endomembrane compartments as in control cells. However, the importance of PtdIns(3)P in regulating amino acid-induced mTORC1 activation is demonstrated by the sequester of PtdIns(3)P using 2xFYVE^{HRS}. The specificity of PtdIns(3)P in regulating mTORC1 is further underscored by the finding that masking other 3-phosphorylated PIs such as PtdIns(3,4)P_2 and PtdIns(3,4,5)P_3 does not affect mTORC1 signaling. Interestingly, the role of PtdIns(3)P in regulating mTORC1 activation is not only restricted to amino acid stimulation, but is also needed during IGF-II stimulation of serum starved cells and at steady-state conditions. Conceivably, PtdIns(3)P does not function as a amino acid mediator but owing to its role in endosomal membrane transport (Odorizzi et al., 2000; Reaves et al., 1996) might be involved in regulating the intracellular localization of mTORC1. On the other hand, PtdIns(3)P might be required to recruit effector proteins that somehow are involved in the regulation of mTORC1.

Another phosphoinositide involved in membrane transport is PtdIns(3,5)P_2 (Ikonomov et al., 2003; Ikonomov et al., 2006), and similarly to PtdIns(3)P might also affect mTORC1 signaling. Indeed, blocking PtdIns(3,5)P_2 formation by pharmacologic inhibition of PIKfyve blunts amino acid-induced mTORC1 activation by diminishing the degree of late endosomal localization of mTOR rather than by blocking mTOR kinase activity. From our experiments, however, it is not obvious whether PIKfyve inhibition blocks translocation of mTOR to late endosomes or formation of late endosomes, where mTOR should translocate to. The formation of increased EGFP-2xFYVE^{HRS} positive vesicles indicates a block in membrane transport at the early endosomal level and therefore in a possible block of late endosome formation. In this respect, blocking the maturation of early endosome to late endosome prevents mTORC1 activation by amino acid or insulin stimulation (Flinn et al., 2010). However, it is not clear how formation of late endosomes might facilitate mTORC1 activation. Since endogenous farnesylated Rheb is believed to localize on late endosmes/lysosomes (Buerger et al., 2006; Sancak et al., 2008), the formation of

late endosomes increases the ability of Rheb to interact with mTORC1. This would explain why overexpression of Rheb activates mTORC1 in the absence of amino acids. Presumably due to overexpression, Rheb overflows the cell and randomly interacts with and activates mTORC1 without the requirement of amino acid-stimulated translocation of mTORC1 to late endosomes. Similarly, artificial positioning of mTORC1 to late endosomes/lysosomes, induced through the expression of HA-Raptor-Rheb15, renders mTORC1 resistant to amino acid starvation or to treatment with the PIKfyve inhibitor.

Concern exists in using YM201636 (PIKfyve inhibitor) as a cancer drug. While PIKfyve inhibition in HEK293 cells almost completely blocks amino acid-induced mTORC1 activation, in A375 melanoma cell line, which has a constitutive active MAPK kinase pathway, the effect on mTORC1 signaling is less pronounced. A combination of YM201636 and a MAPK or B-Raf inhibitor would most probably blunt mTORC1 activation. Therefore YM201636 cannot be regarded as an exclusive drug against cancer.

With in mind that PIKfyve inhibition most probably affects early to late endosome maturation, it might also affect early to late phagosome maturation. This is of special interest in cells of the innate immune system that take up invading microorganisms through phagocytosis into a so-called phagosome, which through maturation becomes competent to fuse with lysosomes where microorganisms will eventually be degraded (Pieters, 2001). Microorganisms, such as *Mycobacterium tuberculosis*, once inside a phagosome have developed means to circumvent this maturation process thereby becoming intracellular parasites (Sundaramurthy and Pieters, 2007). Therefore, treatment with YM201636 would favor the survival of engulfed microorganism and thereby negatively affecting the innate immune system.

References

Beugnet, A., Tee, A.R., Taylor, P.M., and Proud, C.G. (2003). Regulation of targets of mTOR (mammalian target of rapamycin) signalling by intracellular amino acid availability. Biochem J *372*, 555-566.

Buerger, C., DeVries, B., and Stambolic, V. (2006). Localization of Rheb to the endomembrane is critical for its signaling function. Biochem Biophys Res Commun *344*, 869-880.

Byfield, M.P., Murray, J.T., and Backer, J.M. (2005). hVps34 is a nutrient-regulated lipid kinase required for activation of p70 S6 kinase. J Biol Chem *280*, 33076-33082.

Christie, G.R., Hajduch, E., Hundal, H.S., Proud, C.G., and Taylor, P.M. (2002). Intracellular sensing of amino acids in Xenopus laevis oocytes stimulates p70 S6 kinase in a target of rapamycin-dependent manner. J Biol Chem *277*, 9952-9957.

Edinger, A.L. (2007). Controlling cell growth and survival through regulated nutrient transporter expression. Biochem J *406*, 1-12.

Falasca, M., and Maffucci, T. (2007). Role of class II phosphoinositide 3-kinase in cell signalling. Biochem Soc Trans *35*, 211-214.

Findlay, G.M., Yan, L., Procter, J., Mieulet, V., and Lamb, R.F. (2007). A MAP4 kinase related to Ste20 is a nutrient-sensitive regulator of mTOR signalling. Biochem J *403*, 13-20.

Flinn, R.J., Yan, Y., Goswami, S., Parker, P.J., and Backer, J.M. (2010). The late endosome is essential for mTORC1 signaling. Mol Biol Cell *21*, 833-841.

Fuchs, B.C., and Bode, B.P. (2005). Amino acid transporters ASCT2 and LAT1 in cancer: partners in crime? Semin Cancer Biol *15*, 254-266.

Ganapathy, V., Thangaraju, M., and Prasad, P.D. (2009). Nutrient transporters in cancer: relevance to Warburg hypothesis and beyond. Pharmacol Ther *121*, 29-40.

Ikonomov, O.C., Sbrissa, D., Foti, M., Carpentier, J.L., and Shisheva, A. (2003). PIKfyve controls fluid phase endocytosis but not recycling/degradation of endocytosed receptors or sorting of procathepsin D by regulating multivesicular body morphogenesis. Mol Biol Cell *14*, 4581-4591.

Ikonomov, O.C., Sbrissa, D., and Shisheva, A. (2006). Localized PtdIns 3,5-P2 synthesis to regulate early endosome dynamics and fusion. Am J Physiol Cell Physiol *291*, C393-404.

Ivetac, I., Munday, A.D., Kisseleva, M.V., Zhang, X.M., Luff, S., Tiganis, T., Whisstock, J.C., Rowe, T., Majerus, P.W., and Mitchell, C.A. (2005). The type Ialpha inositol polyphosphate 4-phosphatase generates and terminates phosphoinositide 3-kinase signals on endosomes and the plasma membrane. Mol Biol Cell *16*, 2218-2233.

Maffucci, T., Cooke, F.T., Foster, F.M., Traer, C.J., Fry, M.J., and Falasca, M. (2005). Class II phosphoinositide 3-kinase defines a novel signaling pathway in cell migration. J Cell Biol *169*, 789-799.

Nobukuni, T., Joaquin, M., Roccio, M., Dann, S.G., Kim, S.Y., Gulati, P., Byfield, M.P., Backer, J.M., Natt, F., Bos, J.L.*, et al.* (2005). Amino acids mediate mTOR/raptor signaling through activation of class 3 phosphatidylinositol 3OH-kinase. Proc Natl Acad Sci U S A *102*, 14238-14243.

Odorizzi, G., Babst, M., and Emr, S.D. (2000). Phosphoinositide signaling and the regulation of membrane trafficking in yeast. Trends Biochem Sci *25*, 229-235.

Pieters, J. (2001). Entry and survival of pathogenic mycobacteria in macrophages. Microbes Infect *3*, 249-255.

Reaves, B.J., Bright, N.A., Mullock, B.M., and Luzio, J.P. (1996). The effect of wortmannin on the localisation of lysosomal type I integral membrane glycoproteins suggests a role for phosphoinositide 3-kinase activity in regulating membrane traffic late in the endocytic pathway. J Cell Sci *109 (Pt 4)*, 749-762.

Sancak, Y., Bar-Peled, L., Zoncu, R., Markhard, A.L., Nada, S., and Sabatini, D.M. (2010). Ragulator-Rag complex targets mTORC1 to the lysosomal surface and is necessary for its activation by amino acids. Cell *141*, 290-303.

Sancak, Y., Peterson, T.R., Shaul, Y.D., Lindquist, R.A., Thoreen, C.C., Bar-Peled, L., and Sabatini, D.M. (2008). The Rag GTPases bind raptor and mediate amino acid signaling to mTORC1. Science *320*, 1496-1501.

Shin, H.W., Hayashi, M., Christoforidis, S., Lacas-Gervais, S., Hoepfner, S., Wenk, M.R., Modregger, J., Uttenweiler-Joseph, S., Wilm, M., Nystuen, A*., et al.* (2005). An enzymatic cascade of Rab5 effectors regulates phosphoinositide turnover in the endocytic pathway. J Cell Biol *170*, 607-618.

Stack, J.H., and Emr, S.D. (1994). Vps34p required for yeast vacuolar protein sorting is a multiple specificity kinase that exhibits both protein kinase and phosphatidylinositol-specific PI 3-kinase activities. J Biol Chem *269*, 31552-31562.

Sundaramurthy, V., and Pieters, J. (2007). Interactions of pathogenic mycobacteria with host macrophages. Microbes Infect *9*, 1671-1679.

Volinia, S., Dhand, R., Vanhaesebroeck, B., MacDougall, L.K., Stein, R., Zvelebil, M.J., Domin, J., Panaretou, C., and Waterfield, M.D. (1995). A human phosphatidylinositol 3-kinase complex related to the yeast Vps34p-Vps15p protein sorting system. EMBO J *14*, 3339-3348.

Wen, P.J., Osborne, S.L., Morrow, I.C., Parton, R.G., Domin, J., and Meunier, F.A. (2008). Ca2+-regulated pool of phosphatidylinositol-3-phosphate produced by phosphatidylinositol 3-kinase C2alpha on neurosecretory vesicles. Mol Biol Cell *19*, 5593-5603.

Xu, L., Salloum, D., Medlin, P.S., Saqcena, M., Yellen, P., Perrella, B., and Foster, D.A. (2011). Phospholipase D mediates nutrient input to mammalian target of rapamycin complex 1 (mTORC1). J Biol Chem *286*, 25477-25486.

Yan, L., Mieulet, V., Burgess, D., Findlay, G.M., Sully, K., Procter, J., Goris, J., Janssens, V., Morrice, N.A., and Lamb, R.F. (2010). PP2A T61 epsilon is an inhibitor of MAP4K3 in nutrient signaling to mTOR. Mol Cell *37*, 633-642.

Yoon, M.S., Du, G., Backer, J.M., Frohman, M.A., and Chen, J. (2011). Class III PI-3-kinase activates phospholipase D in an amino acid-sensing mTORC1 pathway. J Cell Biol *195*, 435-447.

6 Material and methods

6.1 Reagents

AccuGel 29:1, ultra pure (40 % acrylamide stock)	National Diagnostics
Acetic acid	Scharlau
Acetone, analytical grade	Scharlau
Adenosine-5'-triphosphate (ATP)	Roche
^{32}P-γ Adenosine-5'-triphosphate (^{32}P-γ-ATP)	Perkin Elmer
Agar, technical grade	Difco
Agarose, standard	Eurobio
Albumin from bovine serum, BioChemika fraction V	Fluka
Ammonia solution 25 %	Merck
Ammonium persulfate (APS)	Bio-Rad
Ampicillin trihydrate	Fluka
Aprotinin	Fluka
Bacto-Tryptone	BD
Bacto-Yeast Extract	BD
Bromophenole blue sodium salt	Riedel-de Haen
Calcium chloride ($CaCl_2$ x $2H_2O$)	Fluka
Chloroform	Scharlau
Coomaasie brilliant blue R-250	Serva
Deoxynucleotides (dNTPs)	Sigma
Dimethylsulfoxide (DMSO)	Sigma
Dithiothreitol (DTT)	Eurobio
DNA AluI marker (low range)	Fermentas
DNA Lambda molecular weight marker (high range)	LabForce
T4 DNA ligase	NEB
Ethanol, absolute, HPLC grade	Scharlau
Ethidium bromide	Sigma
Ethylene diamine tetraacetate (EDTA)	Fluka
Fetal calf serum	Sigma
D (+)-glucose-monohydrate	Fluka
L-Glutamine, 200mM	Sigma
Glycerol, anhydrous	Fluka

Glycine	Fluka
HEPES	Fluka
HOECHST 33342	Juro Supply
Hydrochloric acid (HCl)	Merck
Iron(III)nitrate nonahydrate (FeN_3O_9 x $9H_2O$)	Fluka
Isopropanol, analytical grade	Scharlau
Kanamycin sulfate	Fluka
Leupeptin	Alexis Corporation
Lithium chloride, anhydrous	Fluka
Magnesium chloride hexahydrate ($MgCl_2$ x $6H_2O$)	Fluka
Magnesium sulphate heptahydrate ($MgSO_4$ x $7H_2O$)	Fluka
Manganese chloride tetrahydrate ($MnCl_2$ x $4H_2O$)	Merck
MEM Vitamin solution	Amimed
β-mercaptoethanol	Sigma
Methanol, HPLC grade	Scharlau
3-Methyladenine	Fluka
Milk powder (non-fat)	Migros
Mowiol	Clariant
Nonidet P40 (NP-40)	Fluka
Paraffin	Richard-Allan Scientific
Paraformaldehyde, powder, 95% pure	Sigma
PCR primers	Microsynth
Penicillin-Streptomycin solution	Sigma
Pepstatin A	Alexis Corporation
Phenylmethylsulfonylfluoride (PMSF)	Fluka
L-α-Phosphatidylinositol (PI)	Sigma
Phosphatidyl-L-Serine (PS)	Sigma
Potassium chloride (KCl)	Fluka
Potassium dihydrogen phosphate (KH_2PO_4)	Fluka
Potassium hydroxide (KOH)	Merck
Pwo DNA Polymerase	Roche
Restriction Enzymes	New England Biolabs
Saponin (from Quillaja bark)	Sigma
SDS-PAGE prestained molecular weight marker (27 kDa-180 kDa)	Sigma
Sodium acetate (CH_3COONa)	Fluka
Sodium azide (NaN_3)	Sigma
Sodium chloride (NaCl)	Fluka

Sodium dihydrogen phosphate dihydrate (NaH_2PO_4 x $2H_2O$)	Fluka
Sodium dodecyl sulfate (SDS)	Fluka
Sodium fluoride (NaF)	Fluka
Sodium hydrogen carbonate ($NaHCO_3$)	Fluka
Sodium hydroxide (NaOH)	Merck
Sodium orthovanadate (Na_3VO_4)	Sigma
N,N,N',N'tetramethylenethylenediamine (TEMED)	Bio-Rad
Triton X-100	Fluka
Trizma Base (Tris)	Sigma
Trypsin-EDTA solution (10x)	Sigma
Tween 20	Fluka
Water, endotoxin-free	Sigma
Xylene Cyanol FF	Fluka
Xylene	Sigma

6.2 Inhibitors

3-Methyladenine	Fluka/Sigma
NVP-BAG956	Novartis, Basel
NVP-BBD130	Novartis, Basel
NVP-BEZ235	Novartis, Basel
NVP-BGT226	Novartis Basel
PI-103	Enzo
pp242	Chemdea
Rapamycin	LC Laboratories
Wortmannin	Sandoz
YM201636	Chemdea
ZSTK474	LC Laboratories

6.3 Kits

Bio-Rad Protein Assay	Bio-Rad
Protein G Sepharose 4 Fast Flow GE Healthcare	GE Healthcare
GenElute Gel Extraction Kit	Sigma
GenElute HP Endotoxin-Free Plasmid Maxiprep Kit	Sigma

GenElute Plasmid Miniprep Kit	Sigma
Glutathione Sepharose 4B beads	Amersham Biosciences
Immobilon Western, Chemiluminescent HRP Substrate	Millipore
JetPEI DNA transfection agent	Polyplus
Min Elute PCR purification Kit	Qiagen
Pwo DNA Polymerase and PCR buffer	Roche
QIAGEN Plasmid Maxi Kit	Qiagen
QIAGEN Spin, Miniprep Kit	Qiagen
QIAquick Gel Extraction Kit	Qiagen
Taq DNA polymerase and PCR buffer	New England Biolabs

6.4 General buffers and solutions

Blue Juice (10x) (DNA loading buffer)	80% glycerol 20% EDTA of 0.5M pH 8.0 1 spatula Bromophenole blue 1 spatula Xylene Cyanol FF
Coomassie blue staining solution	0.1% Coomassie blue R-250 50% methanol 7% acetic acid 43% ddH_2O
Destaining solution for membrane	90% ethanol 2% acetic acid 8% ddH_2O
Stripping buffer	62.5mM Tris-HCl pH 6.7 2% SDS 100 mM β-Mercaptoethanol
10x PBS	28.4 g $Na_2HPO_4 \times 2H_2O$ 3.8 g KH_2PO_4 3.8 g KCl 159 g NaCl pH adjusted to 7.4 filled up to 2 liters with ddH_2O sterilized by autoclaving
10x TBS	24.2 g Trizma Base 80 g NaCl pH adjusted to 7.6 with HCl filled up to 1 liter with ddH_2O
1x TBS-T	1x TBS + 0.1% (v/v) Tween 20

5x sample buffer	2.5 ml of 1.25 M Tris-HCl pH 6.8 1 g SDS 2.5 ml β-Mercaptoethanol 5.8 ml of 87% glycerol 5 mg bromophenol blue 35 ml ddH_2O stirred until SDS and bromophenol blue had dissolved and filled up to 50 ml with ddH_2O. Stored at -20°C
1M Tris-HCl	121.14 g Trizma Base dissolved in 800 ml ddH_2O and pH adjusted to the desired value by adding HCl. Volume adjusted to 1 l with ddH_2O. Sterilized by autoclaving.
Standard lysis buffer	20 mM Tris-HCl pH 8.0 138 mM NaCl 2.7 mM KCl 5% glycerol 1% NP-40
100x Leupeptin (2mM)	dissolved in ddH_2O
100x Pepstatin (1.8mM)	dissolved in methanol
100x PMSF (100mM)	dissolved in ethanol
1000x Aprotinin (1 mg/ml)	dissolved in ddH_2O
500 mM NaF	dissolved in ddH_2O
100 mM Na_3VO_4	dissolved in ddH_2O
10x electrode buffer (Tris-Glycine)	30.3 g Tris-HCl (250mM Tris-HCl) 144.2 g glycine (1.92 M glycine) 10 g SDS (1% SDS) dissolved in 800 µl dH_2O and filled up to 1 l with ddH_2O (pH approx. 8.3)
10x transfer buffer	250 mM Tris-HCl 1.92 M glycine For 1x transfer buffer, methanol added to a final concentration of 20% (v/v)
50x TAE (5 liters)	1.21 kg Trizma base dissolved in H_2O, 500ml 500 mM EDTA pH 8.0 and 285.5 ml glacial acetic acid added, volume adjusted to 5 l with ddH_2O
10x TE pH 7.5	100 mM Tris-HCl pH 7.5 10 mM EDTA pH 8.0

3% paraformaldehyde (PFA) in PBS (20 ml)	18 ml ddH_2O and 7.5 µl 1 M NaOH added to 600 mg PFA, stirring on a hot plate until PFA is dissolved, 2ml 10x PBS pH 6.55 added, mixed, cooled to 37°C and pH adjusted to pH 7.2

6.5 Bacterial media and supplements

LB Miller	10 g NaCl 5 g yeast extract 10 g Bacto-Tryptone 5 ml 1 M NaOH filled up to 1 l with ddH_2O and sterilized by autoclaving.
LB Miller agar	LB Miller + 12.5 g agar after autoclaving, medium cooled down to 60°C, appropriate antibiotics added, plate poured and stored at 4°C
1 liter SOC	20 g Bacto-Tryptone 5 g yeast extract 0.5 g NaCl 2.5 ml 1M KCl 10ml 1M MgCl2 200 µl 5 M NaOH 980 ml ddH_2O sterilized by autoclaving 20 ml sterile 1 M glucose added
Ampicillin (1000x)	stock 100 mg/ml in ddH_2O (complete solubilization achieved by adding NaOH), used for cultures at 100 µg/ml
Kanamycin (1000x)	stock 25 mg/ml in ddH_2O, used for cultures at 25 µg/ml

6.6 Mammalian cell culture media and supplements

DMEM	Sigma
RPMI-1640	Sigma
Fetal calf serum (FCS)	Sigma
100x L-Glutamine (200 mM)	Sigma
100x Penicillin-Streptomycin solution	Sigma
100x MEM vitamin solution	Amimed
Puromycin	Clontech, stock in distilled ddH_2O at 1 mg/ml, used for cultures at 1 µg/ml
10x Trypsin-EDTA solution	Sigma
Amino acid depleting buffer (- AA buffer); 500ml	900 µl 1 M $CaCl_2$ 100 µl 0.5 mg/ml $Fe(NO_3)_3$ 405 µl 1 M MgSO4 2.685 ml 1 M KCl 22 ml 1 M $NaHCO_3$ 18.22 ml 3 M NaCl 181.2 µl 2.5 M NaH_2PO_4 12.5 ml 1 M Glucose 20 ml 100x MEM vitamins ddH_2O filled up to 500 ml pH adjusted to 7.4 and sterilized by filtrating through a 0.22 µm filter (Steritop, Millipore)

6.7 Vectors

Name	Vector	Insert	Constructor (reference)	Application
pcDNA3__p9	pcDNA3		www.invitrogen.com	Subcloning and transfection
pRK5_Myc-S6K1__p237	pRK5	S6K1	George Thomas University of Cincinnati (Cincinnati Ohio, USA)	Expression of myc-tagged S6K1 in mammalian cells for western blotting purpose
pcDNA3_tkGST-hVps34 _EcoRI__p256	pcDNA3	hVps34	Laboratory plasmid collection Matthias P. Wymann University of Basel (Switzerland)	Expression of GST-hVps34 in mammalian cells
pEGFP-N1_PH-Btk__p530	pEGFP-N1	PH Btk	Tamas Balla National institute of child health and human development (NICHD) (Bethesda Maryland, USA)	PtdIns(3,4,5)P_3 sensor Expression of EGFP-PH-Btk in mammalian cells for western blotting purpose
pcDNA3_p110g wt-CAAX-KI__p594	pcDNA3	p110 wt-CAAX	Laboratory plasmid collection Matthias P. Wymann University of Basel (Switzerland)	Subcloning CAAX box of K-Ras to c-terminus of Raptor (into plasmid #1275)
pEGFP-C1__p601	pEGFP-C1		www.clonetech.com	Subcloning, GFP expression
pEGFP-C2_2xFYVEHRS__p607	pEGFP-C2	2xFYVE HRS	Laboratory plasmid collection Matthias P. Wymann University of Basel (Switzerland)	PtdIns(3)P sensor Expression of EGFP-2xFYVE-HRS in eukaryotic cells for microscopy and western blotting purpose
pEGFP-C1_PH-TAPP1__p705	pEGFP-C1	PH TAPP1	Laboratory plasmid collection Matthias P. Wymann University of Basel (Switzerland)	PtdIns(3,4)P_2 sensor Expression of EGFP-PH-TAPP1 in mammalian cells for western blotting purpose
pcDNA3_tkHA-hVps34 wt__p1033	pcDNA3	hVps34	Anna Melone	Expression of wild type HA-hVps34 in mammalian cells
pcDNA3_tkGST-hVps34 K636R__p1122	pcDNA3	hVps34 K636R	Anna Melone	Expression of kinase-dead GST-hVps34 in mammalian cells
pcDNA3_tkHA-hVps34 K636R__p1130	pcDNA3	hVps34 K636R	Anna Melone	Expression of kinase inactive HA-hVps34 in mammalian cells
pRK5_HA-Raptor__p1275	pRK5	HA-Raptor	Mike Hall University of Basel (Switzerland)	Subcloning and expression of HA-tagged Raptor in mammalian cells
pEGFP-C1_Rheb1__p1277	pEGFP-C1	Rheb1	Mike Hall University of Basel (Switzerland)	Subcloning the very last 15 amino acids of Rheb to the C-terminus of Raptor (into plasmid #1275)
pcDNA3.1_Rab5a__p1287	pcDNA3.1	Rab5a	Missouri S&T Resource Center, www.cdna.org	Subcloning into pEGFP-C1 expression vector
pcDNA3.1_Rab7__p1289	pcDNA3.1	Rab7	Missouri S&T Resource Center, www.cdna.org	Subcloning into pEGFP-C1 expression vector
pEGFP-C1_Rab5a__p1313	pEGFP-C1	Rab5a	Anna Melone	Detection of EGFP-Rab5a compartments by microscopy
pEGFP-C1_Rab7__p1315	pEGFP-C1	Rab7	Anna Melone	Detection of EGFP-Rab7 compartments by microscopy
pRK5_HA-Raptor-CAAX__p1320	pRK5	HA-Raptor-CAAX	Anna Melone	Expression of HA-tagged Raptor-CAAX (K-Ras) in mammalian cells for western blotting purpose
pRK5_HA-Raptor-Rheb15__p1321	pRK5	HA-Raptor-Rheb15	Anna Melone	Expression of HA-tagged Raptor-Rheb15 in mammalian cells for western blotting and microscopy purposes
pEGFP-C2_2xFYVEHRS C215S__p1332	pEGFP-C2	2xFYVE HRS C215S	Harald Stenmark University of Oslo (Norway)	PtdIns(3)P binding-deficient mutant Expression of EGFP-2xFYVE-HRS C215S in mammalian cells for microscopy and western blotting purposes

Plasmid maps can be found in Appendix 7.3.

6.8 Primers

Name	Sequence (5'-3')	Source	Application
GPO-1#135	ACT CCT ACG GGA GGC AGC AGT A	Emilio Hirsch University of Torino (Italy)	Testing for mycoplasma contamination
MGSO#136	TGC ACC ATC TGT CAC TCT GTT AAC CTC	Emilio Hirsch University of Torino (Italy)	Testing for mycoplasma contamination
spV34BEf#475	TTA GAG GAA TAA TTC CGG AAA CAG CT	Anna Melone	Sequencing primer upstream of *BspE*I site in human Vps34
sphV34Bef#599	GAA GGC AGT ACA ACG CGA AAG TGG	Anna Melone	Forward sequencing primer for the generation of K636R hVps34 by SOE-PCR
mpV34KRf#717	CCA GTT ATA TTT **CGC** CAT GGA GAT GAT TTA CGT CAA GAT CA	Anna Melone	Forward mutagenesis primer for the generation of K636R hVps34 by SOE-PCR
mpV34KRr#718	ATC TCC ATG **GCG** AAA TAT AAC TGG ATA TTT GCC TCC ATC	Anna Melone	Reverse mutagenesis primer for the generation of K636R hVps34 by SOE-PCR
spV34BHr#719	AAG AGG CTT TGG ATC CCG ACC CA	Anna Melone	Reverse sequencing primer for the generation of K636R hVps34 by SOE-PCR
sppRK5r#860	CGC CGA ATT AAT TCC CGA TCC AGA	Anna Melone	Reverse sequencing primer for pRK5 plasmids reading into the insert's c-terminus
spRAPTORf#863	GGA GAG CTC ATC AAC AAC ATC AAG T	Anna Melone	Forward sequencing primer reading from human Raptor's C-terminus into its 3'UTR
spRapBEf#873	TGC TGA TTT GGA AAA GAA CCC AGA G	Anna Melone	Forward sequencing primer upstream of *BstE*II site in human Raptor
spCAAXXor#874	CCC TCT AGA TGC ATG CTC GAG TC	Anna Melone	Reverse sequencing primer for K-Ras CAAX box
mpCAAXRapf#875	***ACT CGG TGG AGA AGC GTG TCA GA***G GTA CCG ATA TCA ATG CTT GCA CG	Anna Melone	Forward mutagenesis primer for CAAX box containing C-terminus of Raptor (to generate Raptor-CAAX by SOE-PCR)
mpRapCAAXr#876	CGT GCA AGC ATT GAT ATC GGT ACC ***TCT GAC ACG CTT CTC CAC CGA GT***	Anna Melone	Reverse mutagenesis primer for Raptor's C-terminus containing initial part of CAAX box (to generate Raptor-CAAX by SOE-PCR)
mpRhebXor#877	GCG CTC T*CT CGA G*CC TCA CAT CAC CGA GCA CGA AGA C	Anna Melone	Reverse mutagenesis primer to append *Xho*I restriction site after stop codon of Rheb1
mpRhebRapf#878	***ACT CGG TGG AGA AGC GTG TCA GA***G GTA CCA TTG ACG GAG CGG CTT CAC AAG G	Anna Melone	Forward mutagenesis primer to generate Raptor-Rheb15 fusion protein by SOE-PCR primer contains C-terminus of Raptor, *Kpn*I site and Rheb appendage
mpRapRhebr#879	CCT TGT GAA GCC GCT CCG TCA ATG GTA CC***T CTG ACA CGC TTC TCC ACC GAG T***	Anna Melone	Reverse mutagenesis primer to generate Raptor-Rheb15 fusion protein by SOE-PCR primer contains C-terminus of Raptor, *Kpn*I site, Rheb appendage
spRaptorf#880	CGA GGG TCA CTG CCA TGG AGT ATC	Anna Melone	forward sequencing primer for Raptor (for sequencing of pRK5<HA-Raptor-CAAX >#1320 and pRK5<HA-Raptor-Rheb15>#1321)

Remarks: underlined bold letters mark introduced point mutations; italic and bold letters mark Raptor appendages; underlined letters mark *Kpn*I restriction site; underlined italic letters mark *Xho*I restriction site
Primers were obtained from Microsynth GmbH, Balgach, Switzerland

6.9 siRNA duplex targeting sequences for human PI3Ks

PI3Ks	Oligo ID:	Oligo	Sequence (5'->3')		Targeting site (see Fig.1)
PIK3C2A (PI3K-C2α)	HSS107992	#1	sense	GGAAUAUGGUGUGACAGGAUCCUUU	PI3K catalytic domain
			anti-sense	AAAGGAUCCUGUCACACCAUAUUCC	
	HSS107993	#2	sense	GGAUGUAGCAGAGUGUGAUCUUGUU	Phox domain
			anti-sense	AACAAGAUCACACUCUGCUACAUCC	
	HSS107994	#3	sense	UCAACUUGAGCAAAGAGACGGUUAA	C2 domain (the 2nd at the c-terminus)
			anti-sense	UUAACCGUCUCUUUGCUCAAGUUGA	
PIK3C2B (PI3K-C2β)	HSS107995	#1	sense	GAGAGAUGAGGAGGUUGCUGCAUUU	before the Ras-binding domain
			anti-sense	AAAUGCAGCAACCUCCUCAUCUCUC	
	HSS107997	#2	sense	UGGCUGAUGGAGACUUCCCACUGAA	between the Ras-binding domain and the C2 domain
			anti-sense	UUCAGUGGGAAGUCUCCAUCAGCCA	
	HSS182304	#3	sense	CAGCGCCCGUUGGAGUGCACCUAAU	between the C2 domain and the accessory domain
			anti-sense	AUUAGGUGCACUCCAACGGGCGCUG	
PIK3C3 (hVps34)	HSS108003	#3	sense	CCUCCACCUGCGAAGGUAUUCUAAU	c-terminal lobe of the catalytic domain c-terminal lobe
			anti-sense	AUUAGAAUACCUUCGCAGGUGGAGG	

Remarks: all siRNA duplex were purchased from Invitrogen

6.10 Lentiviral shRNA targeting sequence for hVps34

Name	Vector	shRNA insert (5'->3')	Targeting site (see Fig. 1)	Constructor (reference)	Application
pLKO.1#1283	pLKO.1	No insert		addgene (www.addgene.org)	Generation of shRNA mock cells
shRNA pLK1_hVps34 #1340	pLKO.1	**CCGG**CCACGAGAGATCAGT TAAATA***CTCGAG***TATTTAACT GATCTCTCGTGG**TTTTTG**	Shortly before the accessory domain	Sigma Aldrich TRCN0000037794	For hVps34 gene targeting in human cells

Remarks:
- underlined bold letters mark plasmid overhang
- italic bold letters mark loop

Fig.1:Targeting sites of the single RNAi targeting sequences in PI3K-C2α, PI3K-C2β and hVps34

Arrow heads point to the sites where the single RNAis are targeted within the protein.

siRNA PI3K-C2α: C2A#1-3

siRNA PI3K-C2β: C2B#1-3

siRNA hVps34: V34#3

shRNA hVps34: shV34-pLK1

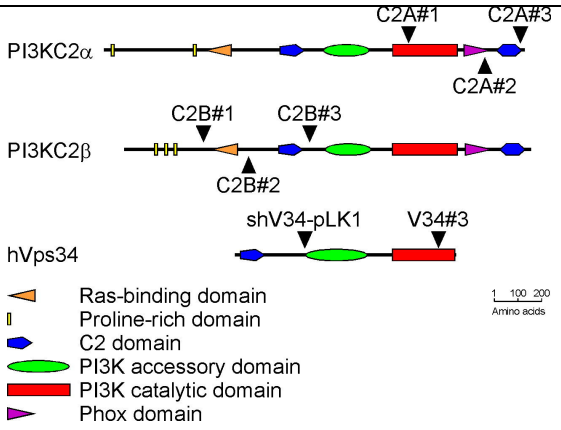

6.11 Antibodies

Name	Isotype	Antigen/Target	Source	Application (dilution)
anti-phospho p70 S6 Kinase Thr389 (1A5) #9206	mouse, monoclonal IgG2a	Phospho-p70 S6 kinase Thr389	Cell Signaling Technology	Western blot (1:2000)
anti-p70 S6 Kinase #9202	rabbit, polyclonal	S6K	Cell Signaling Technology	Western blot (1:1000)
anti-phospho-Akt Ser473 (193H12) #4058	rabbit, polyclonal	Phospho-Akt/PKB Ser473	Cell Signaling Technology	Western blot (1:2000)
anti-phospho-Akt Thr308 (244F9)#4056	rabbit, polyclonal	Phospho-Akt/PKB Thr308	Cell Signaling Technology	Western blot (1:1000)
anti-PKB (19G7/C7)	mouse, monoclonal	PKB	Gift from Emilio Hirsch University of Torino (Italy)	Western blot (1:5000)
anti-Myc-Tag (9B11)	mouse, monoclonal IgG2a	Myc	Cell Signaling Technology	Western blot (1:20'000) Immunoprecipitation (1:1000)
anti-GFP (mixture of clones 7.1 and 13.1)	mouse, monoclonal IgG1	GFP	Roche	Western blot (1:5000)
anti-α-tubulin (DM1A) #T9026	mouse, monoclonal IgG1	α-Tubulin	Sigma	Western blot (1:50'000)
anti-mTOR (7C10) #2983	rabbit, monoclonal IgG	mTOR	Cell Signaling Technology	Immunofluorescence (1:75) Western blot (1:2000)
anti-hVps34 #38-2100	rabbit, polyclonal	hVps34	Zymed Laboratories/ Invitrogen	Western blot (1:2000)
anti-PI3-Kinase p170 #611043	mouse, monoclonal IgG1	PI3 Kinase C2 alpha	BD Transduction Laboratories	Western blot (1:1000)
anti-human PI3-Kinase C2β #611342	mouse, monoclonal IgG1	PI3 Kinase C2 beta	BD Transduction Laboratories	Western blot (1:2000)
anti-HA.11 (16B12) #MMs-101R	mouse, monoclonal IgG1	HA	LucernaChem	Western blot (1:5000) Immunoprecipitation (1:150) Immunofluorescence (1:1000)
anti-Glutathione-S-Transferase #A190-122A	rabbit polyclonal, IgG	GST	Bethyl Laboratories Inc.	Western blot (1:10'000)
AlexaFluor568 goat anti-rabbit IgG (H+L) #A11036	goat, polyclonal	rabbit IgG (heavy and light chains)	Molecular Probes	Immunofluorescence (1:200)
AlexaFluor568 goat anti-mouse IgG (H+L) #A11031	goat, polyclonal	mouse IgG (heavy and light chains)	Molecular Probes	Immunofluorescence (1:200)
anti-rabbit IgG peroxidase conjugate #A6154	goat, polyclonal	Rabbit IgG	Sigma	Western blot (1:5000)
anti-mouse IgG peroxidase conjugate #A4416	goat, polyclonal	Mouse IgG	Sigma	Western blot (1:5000)

6.12 Bacterial strains and culture conditions

Name	Source	Culture medium	Culture conditions	Application
E.coli XL1-Blue	G. Christophori Centre of Biomedicine University of Basel	LB-Miller	37°C , 250 rpm	Propagation of plasmid DNA and cloning purposes

6.13 Mammalian cells and culture conditions

Name	Cell type	Source	Culture medium	Application
HeLa	Human cervical cancer cell line	ATCC	DMEM 10% FCS 2mM L-glutamine 1% penicillin/streptomycin (100U/ml)	- Transfection and gene expression - Nutrient stimulation - Immunofluorescence microscopy
HER911	Human embryonic retinoblast cell line	Sandro Rusconi University of Fribourg (Switzerland)	DMEM 10% FCS 2mM L-glutamine 1% penicillin/streptomycin (100U/ml)	- Transfection and gene expression - Nutrient stimulation
HEK293	Human embryonic kidney cell line	ATCC	DMEM 10% FCS 2mM L-glutamine 1% penicillin/streptomycin (100U/ml)	- Transfection and gene expression - Nutrient stimulation - Proliferation - siRNA-mediated gene silencing of PI3K-C2α and PI3K-C2β
HEK293 shRNA mock	Human embryonic kidney cells with empty pLKO.1 vector	Ann Mertz Biro	DMEM 10% FCS 2mM L-glutamine 1% penicillin/streptomycin (100U/ml) 1 µg/ml puromycin (added to the cell every second day)	- Transfection and gene expression - Nutrient stimulation - Proliferation
HEK293 shRNA Vps34	Human embryonic kidney cells with silenced hVps34	Ann Mertz Biro	DMEM 10% FCS 2mM L-glutamine 1% penicillin/streptomycin (100U/ml) 1 µg/ml puromycin (added to the cell every second day)	- Transfection and gene expression - Nutrient stimulation - Proliferation
A375	Human malignant melanoma cell line PTEN wt BRafV600E NRas wt p53 wt	Johannes Norgauer Friedrich-Schiller Universität (Germany)	RPMI 10% FCS 2mM L-glutamine 1% penicillin/streptomycin (100U/ml)	- Knockdown of hVps34 - Transfection and gene expression - Nutrient stimulation - Immunofluorescence microscopy - Proliferation
A375 shRNA mock	Human malignant melanoma cells with empty pLKO.1 vector PTEN wt BRafV600E NRas wt p53 wt	Ann Mertz Biro	RPMI 10% FCS 2mM L-glutamine 1% penicillin/streptomycin (100U/ml) 1 µg/ml puromycin (added to the cell every second day)	- Transfection and gene expression - Nutrient stimulation - Immunofluorescence microscopy - Proliferation
A375 shRNA Vps34	Human malignant melanoma cells with silenced hVps34 PTEN wt BRafV600E NRas wt p53 wt	Ann Mertz Biro	RPMI 10% FCS 2mM L-glutamine 1% penicillin/streptomycin (100U/ml) 1 µg/ml puromycin (added to the cell every second day)	- Transfection and gene expression - Nutrient stimulation - Immunofluorescence microscopy - Proliferation

Cells and cell lines were cultured at 37°C in a humified atmosphere at 5% CO_2.

6.14 Molecular biological methods

6.14.1 Agarose gel electrophoresis of DNA fragments

Agarose gel electrophoresis was performed for either analytical or preparative purposes prepared in 1 x TAE buffer containing ethidium bromide (10µg/ml). Agarose gels of 1% were used to separate fragments of 10-0.5 kb size and 2% for fragments of 2.5-0.1 kb size. DNA samples were prepared for gel electrophoresis by adding 10x blue juice. Electrophoresis was performed at 80 V in gel electrophoresis chambers (Werkstatt, Institute of Biochemistry Fribourg).

6.14.2 Preparation of $CaCl_2$-competent *E.coli* XL-1 Blue

Materials:
- 50 mM $CaCl_2$ (cooled to 4°C)
- 50 mM $CaCl_2$/10% glycerol (cooled to 4°C)

A 100 ml pre-culture derived from a single colony and grown o/n at 37°C and 300 rpm was used to inoculate 1L of LB-Miller (1:100). The culture was grown at 37°C with vigorous shaking to an OD_{600} of 0.6, and then the flask was placed on ice for 20 min. All of the following steps were carried out at 4°C. Bacteria were pelleted at 3000 rpm at 4°C for 20 min (Sorvall RC5C, rotor SLC4000). The pellet resuspended in 500 ml ice-cold $CaCl_2$ and mixed strongly and stored a few hours at 4°C while mixing occasionally. The bacteria were centrifuged at 3000 rpm for 15 min, and the pellet resuspended in 100 ml $CaCl_2$/glycerol. Aliquots of 500 µl were prepared to be used for transformation, flash-frozen in liquid nitrogen and stored at -80°C.

6.14.3 Transformation of $CaCl_2$-competent *E.coli* XL-1 Blue

A 500 µl aliquot of $CaCl_2$-competent *E.coli* was thawed on ice (15-20 min) and 100 µl of it were added to 4 µl ligation mix and mixed by flicking the tube. After 20 min incubation on ice, the bacteria were heat-shocked for 2 min at 42°C, incubated for 2 min on ice and 800 µl of pre-warmed SOC medium added. After shaking (250 rpm) for 1 h at 37°C, bacteria were spun down (8000 rpm, 5 min, RT), resuspended in

100µl LB-Miller medium and plated onto LB-Miller agar containing the appropriate antibiotic. After O/N incubation at 37°C, single colonies were picked, expanded in liquid culture and DNA isolated and analyzed for correct ligation by restriction enzyme digest

6.14.4 General cloning procedures

6.14.4.1 Preparation of plasmid DNA from *E.coli* cultures

Plasmid DNA from *E.coli* was prepared by using commercially available kits from QIAGEN (Maxi, Mini) and Sigma (Maxi Endofree, Mini) according to the manufacture's protocols. Purified plasmids were dissolved in TE buffer for long storage at 4°C.

6.14.4.2 Isopropanol precipitation of DNA

Precipitation of plasmid DNA was performed by adding 0.1 volume of 3 M sodium acetate pH 5.2 and 0.7 volume of isopropanol to the DNA. After mixing by inverting the tube, DNA was pelleted by centrifugation (20'000 x g, 30 min, 4°C), washed once with 1.5 ml 70% ethanol and centrifuged as before for 10 min. The DNA pellet was air-dried and dissolved in TE buffer to a final concentration of 1 µg/µl.

6.14.4.3 Restriction enzyme digestion of plasmid DNA and PCR products

For analytical purposes 0.25-1 µg plasmid DNA was digested with the appropriate restriction enzyme (5 U/µg DNA) for 1 h at 37°C in a total volume of 20 µl. For preparative purposes 2 µg vector or PCR product were digested with 20 U/µg of the appropriate enzyme for 1-2 h at 37°C in a total volume of 40 µl. All restriction enzymes were purchased from New England Biolabs (NEB).

6.14.4.4 Purification of DNA from agarose gel

Under UV illumination, bands of interests were quickly excised from the gel and DNA fragments purified from agarose gels using either QIAquick gel extraction kit (QIAGEN) or GenElute Gel Extraction kit (Sigma) according to the manufacturer's protocol.

6.14.4.5 Ligation of DNA fragments into vectors

Ligation of DNA fragments with cohesive ends was performed at a molar ratio between vector and insert of 1:2 in a reaction volume of 20 µl using the T4 DNA ligase (NEB). The ligation reactions were set up as follows:

x µl vector (50 ng)
x µl insert DNA
2 µl 10x ligation buffer
0.5 µl T4 DNA ligase (400 U/µl)
filled up to 20 µl with ddH_2O

The ligation mix were incubated either for 1 h at RT or O/N at 4°C to obtain a maximum number of transformants. Four µl of the reaction were transformed into $CaCl_2$-competent *E.coli*.

6.14.4.6 Polymerase chain reaction (PCR)

Materials:
- Endotoxin-free water (Sigma)
- 10 mM dNTPs mix (Sigma)
- 5 U/µl Pwo Polymerase (Roche)
- Primer (10 µM in endotoxin-free water)
- T3 thermocycler (Biometra)

PCR was performed with the Pwo Polymerase (Roche) to introduce appropriate restriction sites for subcloning the PCR products. Two reaction mixes were prepared on ice in 200 µl PCR tubes as follows:

<u>Mix 1:</u>

template DNA (10 ng/µl)	1 µl (10 ng)
10 mM dNTPs mix	1 µl (200 µM final concentration)
10 µM forward primer	1 µl (200 nM final concentration)
10 µM reverse primer	1 µl (200 nM final concentration)
ddH_2O filled up to 25 µl	21 µl

Mix 2:

Pwo Polymerase 5U/µl	0.5 µl
10x PCR buffer with 20 mM $MgCl_2$	5 µl
ddH_2O filled up to 25 µl	19.5 µl

Mix 1 and 2 were combined on ice, vortexed gently and spun down. The PCR was performed on a T3 thermocycler (Biometra) using the following protocol:

1. initial denaturation of DNA	95°C	5 min	
2. denaturation of DNA	95°C	20 sec	
3. annealing*	55-68°C	30 sec	(temperature depending on primer)
4. elongation	72°C	50 sec	
30 cycles			
5. final elongation	72°C	7 min	
6. cooling	4°C	∞	

After the reaction, the PCR product was analyzed by gel electrophoresis, purified using Min Elute PCR purification kit (QIAGEN) according to manufacture's protocol and digested with the appropriate enzyme for cloning.

6.14.4.7 Generation of GST-hVps34^{K636R} kinase-dead mutant by site-directed mutagenesis using sequence-overlap extension PCR (SOE-PCR)

For generation of kinase-dead GST-hVps34^{K636R} three point mutations ($_{3587}AAG_{3589}$ -> $_{3587}CGC_{3589}$) were inserted by SOE-PCR in plasmid pcDNA3_tkGST-hVps34__p256. In a first PCR, the coding sequence for the N-terminal region including the three point mutations was generated using the primer pair sphV34BEf#595/mpV34KRr#718 resulting in the BspEI-hVps34^{KR} fragment. The coding sequence for the C-terminal region including the three point mutations was generated using the primer pair mpV34KRf#717/mpV34BHr#719 resulting in the hVps34^{KR}-BamHI fragment. In a second round of PCR, BspEI-hVps34^{KR} together with hVps34^{KR}-BamHI were used as templates and with primers sphV34BEf#595/mpV34BHr#719 the BspEI-hVps34^{KR}-BamHI fragment was amplified and afterwards subcloned into *BspE*I and *BamH*I restriction sites of pcDNA3_tkGST-hVps34__p256 vector.

6.14.4.8 Generation of HA-Raptor-CAAX and HA-Raptor-Rheb15 by SOE-PCR

For the generation of HA-Raptor-CAAX and HA-Raptor-Rheb15 the same approach as described above was undertaken.

Generation of HA-Raptor-CAAX:

- First round of PCR:

PCR with primers spRapBEf#873/mpRapCAAXr#876 on pRK5<HA-Raptor>#1275 and mpCAAXRapf#875/spCAAXXor#874 on pcDNA3<p110 wt-CAAX KI>#594 resulted into fragments BstEII-Raptor-CAAX and Raptor-CAAX-XhoI, respectively.

- Second round of PCR:

Primer pair spRapBEf#873/spCAAXXor#874 and templates BstEII-Raptor-CAAX and Raptor-CAAX-XhoI were used resulting into BstEII-Raptor-CAAX-XhoI fragment. After digestion with *BstE*II and *Xho*I restriction enzymes, the fragment was subcloned into *BstE*II and *Xho*I restriction sites of pRK5_HA-Raptor__p1275.

Generation of HA-Raptor-Rheb15:

- First round of PCR:

PCR with primers spRapBEf#873/mpRapRhebr#879 on pRK5_HA-Raptor__p1275 and mpRhebRapf#878/mpRhebXor#877 on pEGFP-C1<Rheb>#1277 resulted into fragments BstEII-Raptor-Rheb15 and Raptor-Rheb15-XhoI, respectively.

- Second round of PCR:

Primer pair spRapBEf#873/mpRhebXor#877 and templates BstEII-Raptor-Rheb15 and Raptor-Rheb15-XhoI were used resulting into BstEII-Raptor-Rheb15-XhoI fragment. After digestion with *BstE*II and *Xho*I restriction enzymes, the fragment was subcloned into *BstE*II and *Xho*I restriction sites of pRK5_HA-Raptor__p1275.

6.14.4.9 Sequencing of plasmid DNA

Sequencing of plasmid DNA was performed at Microsynth GmbH (Balgach, Switzerland). For economy run sequencing following mixture was set up:

0.8 µg plasmid DNA	x µl
50 µM primer	0.4 µl (2 µM final concentration)
endotoxin-free H_2O	filled up to 10 µl

Sequences were analyzed using DNA Strider (version 1.4f13) or Serial Cloner 2.1.

6.15 Cell culture methods

6.15.1 Determination of cell numbers

The number of viable cells was determined using the CASY Cell Counter (Schärfe Systems, Reutlingen, Germany). Fifty µl of cell suspension was diluted into 10 ml CASYton dilution solution, mixed by inversion and cell number counted using a cell specific program.

6.15.2 Freezing and thawing of cells

For freezing, a cell suspension was prepared, centrifuged (900rpm, 5min, RT) and the pellet resuspended in freezing medium (10% (v/v) DMSO in FCS) at a minimal density of 5-10 x 10^6 cells/ml. Then 1 ml aliquots were transferred to 2 ml cryotubes (Nunc), placed into a freezing container (Nalgene) and put O/N at -80°C prior to the final storage in the liquid nitrogen.
Thawing of cells was performed by transferring cells from the liquid nitrogen into a 37°C water bath. Due to DMSO's toxicity, the cell suspension was immediately diluted in 10 ml of pre-warmed appropriate medium and centrifuged (900 rpm, 5 min, RT). The pellet was gently resuspended in medium and transferred into a culture flask.

6.15.3 Trypsinization of adherent cells for subculture

Adherent cells were washed 1x with PBS and trypsinized with 1x Trypsin/PBS for 3-5 min at 37°C until cells were detached from the culture surface. Afterwards Trypsin/PBS was quenched by adding 9 volumes of cell culture medium, cells resuspended and either splitted into new culture flasks or centrifuged for freezing (see above).

6.15.4 Testing cells for mycoplasma contamination

Cells were grown for a couple of days without changing the medium. 500 µl aliquot of the cell supernatants was boiled for 15 min at 95°C, centrifuged for 5 min at maximum speed and 5 µl used to run the PCR reaction. The PCR reaction was set as follows:

boiled medium	5 µl
dNTPs (10 mM)	1 µl
primer GPO-1#135 (50 µM)	1 µl
primer: MGSO#136 (50 µM)	1 µl
10x PCR buffer with 15 mM $MgCl_2$	5 µl
Taq Polymerase	0.5 µl
H_2O filled up to 50 µl	36.5 µl

The primers above amplify a 717 bp DNA fragment within the 16S rRNA gene, and should detect a wide range of mycoplasma (e.g. *Mycoplasma arginini*, *Acholeplasma laidlawii*, *Mycoplasma hyorhinis*, *Mycoplasma orale*, and *Mycoplasma fermentans*) (Dussurget and Roulland-Dussoix, 1994; Rawadi and Dussurget, 1995).

PCR Program:

1. pre-heat	94°C	4 min
2. denaturation of DNA	94°C	1 min
3. annealing	58°C	1.5 min
4. elongation	72°C	1.5 min
	30 cycles	
5. final elongation	72°C	10 min
6. cooling	4°C	∞

In case of mycoplasma contamination a band of approximate 700 bp size should be detectable.

6.15.5 Transfection of adherent cells with JetPEI™

For optimal transfection conditions, cells should be 50-60% confluent.

Number of cells to seed the day before transfection:

Culture vessel	**Number of cells to seed per well or dish**			
	HEK293	HeLa	HER911	A375
12 well	2×10^5	5×10^4	5×10^4	5×10^4
3.5 cm	0.3×10^6			
6 cm	0.6×10^6	0.25×10^6	2×10^5	0.35×10^6
10 cm	1.6×10^6	0.7×10^6	0.65×10^6	

Complex preparation for different cell culture formats:

	DNA solution		**JetPEI solution**		
Culture vessel	Amount of DNA (µg)	Volume of 150 mM NaCl (µl)	Volume of JetPEI reagent (µl)	Volume of 150 mM (µl)	Total volume of complexes per well
12 well	1 µg	40	2	40	80
3.5 cm	1.5 µg	50	3	50	100
6 cm	3 µg	100	6	100	200
10 cm	8 µg	270	16	270	540

Mixing of the JetPEI and DNA solutions was done as follows:
After vortexing for 10 sec and centrifugation the JetPEI solution was added to the DNA solution, vortexed for 10 sec and spun down. After 20 min incubation at RT the JetPEI/DNA mixture was added drop wise onto the cells. Medium was replaced 9 to 24 h later with complete medium. Cell lysis occurred various times after transfection.

6.15.6 siRNA transfection

Materials:
- RNAi duplex (20 µM stock solution, Invitrogen)
- Lipofectamine RNAiMAX (Invitrogen)
- Opti-MEM (Invitrogen)

Cells were plated into a 6-well plate (180.000 HEK293 cells/well) containing 1.5 ml DMEM/10% FCS/2mM Gln w/o antibiotics and let adhere O/N. The following two solutions were prepared for each well to be transfected:

a) To 150 µl Opti-MEM 0.9 µl siRNA (20 µM stock) were added and mixed gently by inverting the tubes several times.
b) To 150 µl Opti-MEM 3 µl Lipofectamine RNAiMAX was added and mixed gently by inverting the tubes several times.
The diluted RNAi duplex (solution a) was combined with the diluted Lipofectamine RNAiMAX (solution b), mixed gently and incubated for 20 min at RT. Afterwards the RNAi/Lipofectamine complexes were added onto the cells to give a final volume of 1.8 ml and a final RNA concentration of 10 nM. The plate was mixed gently by rocking back and forth and after incubation for 4 – 6 h at 37°C in a CO_2 incubator, medium was replaced with 1.5 ml DMEM/10% FCS/2mM Gln w/o antibiotics. Gene knockdown was assayed 48-72 h after transfection.

6.15.7 Proliferation assay

Materials:
- Cells: HEK293 and A375
- Medium: DMEM complete and RPMI complete
- CASY Cell Counter (Schärfe Systems, Reutlingen, Germany)
- CASYton dilution solution for cell culture

On day 0 either 1.5 x 10^5 cells/6cm dish for HEK293 or 1.2 x 10^5 cells/6cm for A375 were plated in triplicate in complete medium. At different time intervals cells were washed 1x in PBS, trypsinized, taken up in 4 ml complete medium and cell suspension transferred to a 15 ml tube. After centrifugation at 900 rpm for 5 min cells were resuspended in 1 ml complete medium and cell number and cell volume measured using the automated cell counter as described above.

6.15.8 MTT-based cell proliferation assay

Materials:
- MTT (Sigma, #5655) dissolved in PBS (5mg/ml)
- Solubilization buffer (95% isopropanol, 5% formic acids)
- 96 well-plate (flat bottom)
- HEK293 cells (normal, shRNA mock and shRNA hVps34)
- A375 cells (normal, shRNA mock ans shRNA hVps34)

- Inhibitors: 1μM NVP-BEZ235, 100nM Rapamycin, 1μM pp242, 1μM ZSTK474, 1μM YM201636 (indicated concentrations are the final concentrations in the assay)
- Spectrophotometer Spectra Max 340 (Molecular Devices) with software SoftMax Pro 4.8

Principle of the assay:
This is a colorimetric assay that measures the reduction of yellow 3-(4,5-dimethythiazol-2-yl)-2,5-diphenyl tetrazolium bromide (MTT) to purple formazan salts by mitochondrial succinate dehydrogenase. The formazan is then solubilised with acidified isopropanol and the concentration measured spectrophotometrically. Since reduction of MTT can only occur in metabolically active cells the level of activity is a measure of the viability of the cells.

Procedure:
Either 3000 HEK293 cells or 1000 A375 cells were plated per well in quadruplicate in 100 µl in 96-well tissue culture plates. On day zero 0.5µl inhibitors were added to cells with the final concentration as described above. Each inhibitor treatment was done in quadruplicate and MTT assay was performed each day from day 0 until day 4 post-inhibitor treatment as follows. To each well 11 µl MTT (10% of the culture medium volume) solution was added and plate shaken carefully. After incubation for 2h at 37°C and 5% CO_2, 100 µl solubilization solution was added to each well and pipetted up and down several times to dissolve the formazan salt. After 10 min of gently mixing on a table shaker absorbance was measured at 570 nm and background absorbance at 690 nm. After measurement solution was mixed again, incubated for 10 min and absorbance measured a second time as described before.

6.15.9 Amino acid and serum starvation and stimulation of cells

Materials:
- Culture medium: DMEM, RPMI
- Amino acid depletion buffer pH 7.4 (homemade, see chapter 6.6: 1.8 mM $CaCl_2$, 0.248 µM $Fe(NO_3)_3$, 810 µM $MgSO_4$, 5.37 mM KCl, 44 mM $NaHCO_3$, 109.5 mM NaCl, 906 µM NaH_2PO_4, 25 mM Glucose, 4x MEM vitamins)
- IGF-II (Sigma)
- Cells grown in 6 cm culture plates

The day before amino acid depletion, cells were washed 2x with PBS and incubated for 15-18 h in 3 ml serum-free culture medium supplemented with 2mM L-glutamine. Following 2x wash with PBS cells were incubated for 2 h in 3 ml amino acid depletion buffer. During the last 15 min of amino acid depletion cells were pre-treated either with DMSO or inhibitors. Afterwards, starvation buffer was replaced with 3 ml serum-free culture medium supplemented with 2mM L-glutamine containing either DMSO or inhibitors and incubated for 30 min at 37°C. Total cell lysis was performed as described below.
For IGF-II stimulation, cells were over night serum starved in serum-free culture medium supplemented with 2mM L-glutamine as described above and stimulated with 50 ng/ml IGF-II for 5 min at 37°C.

6.15.10 Treatment with synthetic membrane permeant PtdIns(3)P/AM

Materials:
- PtdIns(3)P/AM (kind gift from Carsten Schultz, EMBL, Germany), diluted to 20mM in DMSO
- Pluronic F-127 (kind gift from Carsten Schultz)
- HEK293 cells were grown in 6 cm cell culture plates

Preparation of PtdIns(3)P/AM shortly before use!
To 2.5 µl 20mM PtdIns(3)P/AM 1 µl pluronic F127 were added and mixed by pipetting up and down.

Serum starvation of HEK293 cells was performed as described above. After 2x wash with PBS, cells were incubated for 2 h in 1 ml amino acids depletion buffer. During the last 30 min of amino acid starvation cells were pre-treated with 50 µM PtdIns(3)P/AM as follows. To the above prepared PtdIns(3)P/AM 100 µl cell supernatant was added, pipetted up and down and re-added back to cells and mixed by carefully rocking back and forth. After 30 min incubation, starvation/PtdIns(3)P/AM buffer was replaced with 1 ml serum-free culture medium supplemented with 2mM L-glutamine and incubated for 30 min. Cell lysis was performed as described below.

6.16 Biochemical methods

6.16.1 Preparation of total cell lysates from adherent cells

Materials:
- NP-40 based lysis buffer (20 mM Tris-HCl pH 8.0, 138 mM NaCl, 2.7 mM KCl, 5% glycerol, 1% NP-40) supplemented with protease and phosphatase inhibitors (40 mM NaF, 2mM Na_3VO_4, 20 µM Leupeptin, 18 µM Pepstatin, 5 µM Aprotinin, 1 mM PMSF, 1 mM $MgCl_2$, 1 mM $CaCl_2$, 5 mM EDTA)
- PBS
- Plastic cell scrapers (SPL Life Sciences)

All works were performed on ice and in cooled centrifuges. Adherent cells were washed 2x with ice cold PBS, scraped in lysis buffer and cell lysate transferred to a 1.5 ml Eppendorf tube. After 10 min incubation on ice, cell lysate was cleared by centrifugation (13'2000 rpm, 15min, 4°C), supernatant transferred to a new 1.5 ml Eppendorf tube and protein concentration determined with the Bradford method. Equal amounts of proteins were mixed with 1/5th of 5x loading buffer, boiled for 6 min at 95°C, centrifuged and loaded onto SDS-PAGE.

6.16.2 Determination of protein concentrations

Materials:
- Cell lysates
- Semi-micro cuvette (1.6 ml, Greiner Bio-One)
- Bradford (Bio-Rad)
- BioPhotometer (Eppendorf)

Bradford reagent was prepared by diluting the dye reagent 1:5 with ddH_2O. To each cuvette containing 1 ml of Bradford reagent, 1 µl cell lysate was added and mixed by pipetting up and down. After 5 min incubation at RT, absorbance was measured with a spectrophotometer at 595 nm.

6.16.3 Immunoprecipitation

Materials:
- Protein G Sepharose 4 Fast Flow (GE Healthcare)
- Anti-myc antibody (Cell Signaling Technology)
- Wash buffer 1 (lysis buffer containing 1% NP-40, 40 mM NaF, 2 mM Na_3VO_4)
- Wash buffer 2 (0.1 M Tris-HCl pH 7.4/0.5 M LiCl)
- 1x PBS

Following cell lysis and determination of protein concentration 100-200 µg proteins were incubated with anit-myc antibody (diluted 1:1000) while rotating for 1h in the cold room (4°C). In the meantime protein G Sepharose beads were washed 3x in PBS and resuspended in lysis buffer containing protease and phosphatase inhibitors to give a 50% beads slurry. Afterwards 20 µl of 50% beads slurry were added to each sample and rotated for an additional 1 h in the cold room (4°C). Then the beads were washed 2x with wash buffer 1 (13'200 rpm, 1min, 4°C), 2x with wash buffer 2 (13'200 rpm, 1min, 4°C) and 1x with PBS (13'200 rpm, 1min, 4°C) using a volume of 500 µl each time. Then 12 µl of 2x concentrated SDS-sample buffer were added, samples boiled for 6 min at 95°C, centrifuged, resolved by SDS-PAGE and analyzed by western blotting.

6.16.4 GST pulldown

Materials:
- Glutathione Sepharose 4B (GE Healthcare)
- GST wash buffer (Lysis buffer, 1% NP-40, 1 mM DTT)
- Wash buffer 1 (lysis buffer containing 1% NP-40, 40 mM NaF, 2 mM Na_3VO_4)
- Wash buffer 2 (1mM Tris-HCl pH 7.4/0.5 M LiCl)
- 1x PBS
- Cells were grown in 10 cm culture dishes

Preparation of Glutathione Sepharose 4B:
Desired volume of 70% slurry was transferred into a 1.5 ml tube, washed 3x with GST wash buffer and resuspended in lysis buffer supplementend with protease and phosphatase inhibitors and 1 mM DTT to give a 50% slurry.

Following cell lysis and determination of protein concentration, 200-400 µg proteins were added to a 1.5 ml Eppendorf tube containing 20 µl 50% of glutathione sepharose slurry. After 2 h rotation in the cold room (4°C), beads were washed 2x with wash buffer 1 (13'200 rpm, 1min, 4°C), 2x with wash buffer 2 (13'200 rpm, 1min, 4°C) and 1x with PBS (13'200 rpm, 1min, 4°C) using 500 µl each time. Pulled down proteins were denatured by the addition of 12 µl 2x concentrated sample buffer and boiled for 6 min at 95°C, subjected to SDS-PAGE and analyzed by western blotting.

6.16.5 SDS polyacrylamide gel electrophoresis

The polyacrylamide gel for SDS-PAGE consists of two separate regions: the upper stacking gel and the lower separating. The stacking gel is less concentrated (larger pore size) than the separating gel and is prepared in a buffer of lower ionic strength and lower pH leading to a rapid movement of the proteins through the upper gel and therefore accumulating at the boundary between stacking and separating gel. The concentration of acrylamide in the separating gel is chosen based on the size of the proteins to be analyzed.

Preparation of ten minigels (8 cm x 10 cm x 0.75 cm)
Ten gels were cast up at once using the Mighty Small gel caster (Amersham Biosciences).
Following solutions were prepared for 10 gels:

	Separating gel (Total: 75 ml)					**Stacking gel (Total: 30 ml)**
	6%	**7.5%**	**10%**	**12%**	**15%**	**5%**
40% Acrylamide Stock	11.3 ml	14.1 ml	18.8 ml	22.5 ml	28.1 ml	4.8 ml
Distilled H_2O	47.7 ml	44.9 ml	40.2 ml	36.5 ml	30.9 ml	21.6 ml
Tris-HCl pH 8.8 (1.875 M)	15 ml	15 ml	15 ml	15 ml	15 ml	---
Tris-HCl pH 6.8 (1.25 M)	---	---	---	---	---	3 ml
10% (w/v) SDS	750 µl	750 µl	750 µl	750 µl	750 µl	300 µl
10% APS	250 µl	250 µl	250 µl	250 µl	250 µl	102 µl
TEMED	37.5 µl	37.5 µl	37.5 µl	37.5 µl	37.5 µl	30 µl

APS and TEMED were added just prior to pouring the gels. Separating gel solution was poured and overlaid with isopropanol to get a flat surface. After polymerization isopropanol was removed, gels rinsed with H_2O, stacking gel solution poured on top of the separating gel and combs inserted avoiding air bubbles.

Loading and running of gels

For Western blotting 10 µg proteins from cell lysates were loaded per lane. The appropriate sample volume were mixed with 5x sample buffer and heated for 6 min at 95°C while mixing, centrifuged briefly and loaded onto the gel. Running of the gels was carried out at 20 mA/minigel and 250 V for approximate 60 min.

6.16.6 Semi-dry transfer and western blotting

Materials:

- Transfer buffer (25 mM Tris, 192 mM Glycine, 20% methanol, pH 8.3)
- Immobilon P PVDF membrane (Millipore), cut 9 x 6.5 cm
- For 1 minigel 6x Whatman paper (Macherey & Nagel), cut 9 x 6.5 cm
- Semidry blotting device (Witec AG)
- TBS, 0.1% Tween (TBST)

Preparation for semi-dry transfer:

PVDF membrane was activated in 100% Methanol for 15 sec and equilibrated in 1x transfer buffer for at least 5 min. Filter papers were soaked in 1x transfer buffer.

Following gel electrophoresis, proteins were transferred onto a positively charged PVDF membrane using the semi-dry transfer technique. The blot was assembled on the lower electrode (anode) as follows: three Whatman papers, PVDF membrane, gel, three Whatman papers and the upper electrode (cathode). After removal of air bubbles, the transfer was run at 1 mA/cm^2 (65 mA/minigel) and 20 V for 75 min. Afterwards the membrane was blocked under agitation in TBS-Tween containing 5% non-fat milk (5% milk TBST) for at least 30 min and incubated with primary antibody diluted either in 5% milk TBST or 5% BSA TBST (for detection of phospho proteins) for 1h at RT or O/N at 4°C. Following three washes of 5 min with TBST, membrane was incubated with HRP-coupled secondary antibody (diluted in 5% milk TBST) for 1h and afterwards washed 6x 5 min with TBST. For immunodetection, the membrane was covered for 1 min with 2 ml chemiluminescent HRP substrate (Immobilon Western, Millipore). The membrane was placed in an autoradiography cassette and exposed to films for different times or detection was carried out with the Fusion Fx7 imaging system (analysis-software FUSION CAPT, version 15.16 for Windows).

6.16.7 Stripping of membranes for reprobing

In order to remove primary and secondary antibodies, the membrane was incubated under agitation in stripping buffer (100 mM β-mercaptoethanol, 2% SDS, 62.5 mM Tris-HCl pH 6.7) for 30 min at 50°C. After washing 3x 10 min with TBST, the membrane was blocked in 5% milk TBST for at least 30 min and western blotting was continued as described above.

6.16.8 Lipid kinase assay

Materials:

- GST-pull down of GST-hVps34^{wt} or GST-hVps34^{K636R}
- Sonicater (IKA Labortechnik, Staufen); settings: cycle = 1 and Amplitude = 50%
- Thermomixer (Eppendorf)
- Sped vac (UNIVAPO 150H)
- wash buffer (lysis buffer containing 1% NP-40, 40 mM NaF, 2 mM Na_3VO_4)
- 0.1 M Tris-HCl pH 7.4, 0.5 M LiCl (Tris-HCl/LiCl)
- Kinase buffer for hVps34: 20 mM HEPES pH 7.4, 5 mM $MnCl_2$
- Kinase buffer for p110α, p110β, p110δ: 20 mM HEPES pH 7.4, 1 mM $MgCl_2$
- Kinase buffer for p110γ: 20 mM HEPES pH 7.4, 5 mM $MgCl_2$
- Phosphatidyl-L-serine (PS; Sigma): 1 mg/ml in Chloroform:Methanol (2:1)
- L-α-Phosphatidyl-D-myo-inositol 5-monophosphate (PI; Sigma): 1 mg/ml in Chloroform:Methanol (2:1)
- [γ-^{32}P]-ATP (6000 Ci; Perkin Elmer)
- 6 mM ATP (Roche)
- 1 M HCl
- Chloroform:Methanol (1:1)

Preparation of 1ug/ul PS/PI lipid substrate solution:

PS/PI vesicles were generated by mixing 300 µl of PI (1mg/ml) and 300 µl of PS (1mg/1ml) together in a 1.5 ml Eppendorf tube. After drying under a N_2 stream, lipids were resuspended in 300 µl kinase buffer and shortly before starting the kinase assay lipids were extensively sonicated for a few seconds.

Preparation of [γ-^{32}P]-ATP/ATP solution:

Cold ATP (6mM, 100x) was diluted to 60 µM in kinase buffer and 2 µCi [^{32}P]-ATP/10µl was added.

Following GST pull-down of either GST-hVps34^{wt} or GST-hVps34^{K636R}, *in vitro* lipid kinase assay was performed as follows. GST pull-downs were washed 2x with wash buffer, 2x with Tris-HCl/LiCl and 2x with kinase buffer using 500 µl each time. After resuspending in 40 µl kinase buffer either DMSO or wortmannin were added and mixed extensively for 15 min at 37°C. Afterwards 10 µl of PS/PI vesicles and 10 µl [γ-^{32}P]-ATP/ATP solution were added and mixed constantly for 10 min at 30°C. Reaction was stopped by the addition of 100 µl 1 M HCl, mixed shortly and lipid extracted with 200 µl Chloroform:Methanol (1:1). Following vortexing and centrifugation (3000 rpm, 3 min, RT) the organic lower phase was transferred into a new 1.5 ml Eppendorf tube. After perforating the lid of the Eppendorf tube 3x with a needle, lipids were dried in a speed vac for 30 min and stored O/N or until use at -20°C.

6.16.9 Thin layer chromatography (TLC) for lipid separation

Materials:

- TLC plates, Silica gel 60 W F254s (Merck)
- Hamilton glass syringe with flat tip
- Chloroform:Methanol (2:1)
- Chloroform/Methanol/H_2O/NH_4OH (45:35:8.5:1.5)
- Films (Fuji)
- Phosphoimager screen (BioRad)

TLC plate was prepared by pre-heating (200°C) in the microwave in order to remove excess H_2O. To the dried lipids 20 µl Chloroform:Methanol (2:1) were added and mixed by tapping on the tube several times. Lipids were applied drop wise on TLC plate with a Hamilton syringe 2 cm from the bottom edge. Lipid resuspension and application on TLC plate was repeated a second time. Between samples Hamilton syringe was cleaned by overfilling 3 times with Chloroform:Methanol. When all samples were applied, the TLC plate was air dried and placed in a horizontal developing container containing solvent chloroform/methanol/H_2O/NH_4OH. When the solvent front had moved to about 2 cm of the top end of the plate (after 1 ½ h), the

TLC plate was removed from the developing container and dried at RT. PtdIns(3)-^{32}P was either visualized by autoradiography or by phosphoimager (Typhoon with IMAGE Quant software).

6.17 Microscopy

6.17.1 Indirect immunofluorescence of cells

Materials:
- Glass coverslips (round Ø 18 mm, Thermo Scientific)
- Microscope slides (Menzel-Gläser)
- Hoechst 33342 (Juro supply, stock solution 1 mM, diluted in ddH_2O)
- Parafilm
- Mowiol (Clariant GMBH)
- Confocal scanning laser microscope: Axiovert 200M and laser scanning module LSM 510 Meta (Zeiss) with LSM 510 software

Preparation of 3% (w/v) paraformaldehyde in PBS:
To prepare 20 ml of 3% paraformaldheyde, 18 ml of ddH_2O and 7.5 µl of 1 M NaOH were added to 600 mg paraformaldehyde and suspension was stirred on a hot plate (100°). After complete dissolution, 2 ml 10x PBS pH 6.55 were added, mixed, cooled to 37°C and pH adjusted to pH 7.2.

For staining, cells were grown in a 12-well plate on glass coverslips. The medium was aspirated from the cells and each well washed 2x with PBS (RT) and cells were fixed in freshly prepared pre-warmed 3% paraformaldehyde for 10 min at 37°C. Afterwards cells were washed 2x with PBS, quenched with PBS/50 mM glycine for 5 min at RT and washed 1x with PBS. For intracellular staining, cells were permeabilized for 20 min at RT with 0.1% (w/v) saponin dissolved in PBS (1 ml/well). After washing 1x with PBS coverslips were removed from the 12-well plate with a forceps and blocked with 250 µl 5% goat serum in PBS inverted on a layer of Parafilm for 20 min at RT. All the subsequent steps were performed with inverted coverslips on Parafilm. Following incubation with 60 µl primary antibody (diluted in 5% goat serum/PBS) for 1 h RT, cells were washed 2x with PBS (300 µl/cover slips) and incubated with 60 µl secondary antibody coupled to a fluorescent dye (diluted in

5% goat serum/PBS) for 1 h at RT in the dark. After 2x wash with PBS nuclei were stained with 300 µl Hoechst (final concentration 1 µM, diluted 1:1000 in PBS,) for 15 min at RT and washed 2x with PBS (300 µl/cover slip). For mounting a drop of Mowiol was added onto a microscope slide and coverslips were washed 1x with ddH_2O, residual liquid was soaked from the edge with a fine paper towel and placed upside down onto the Mowiol containing slide. Slides were stored at 4°C in the dark until usage for microscopy analysis.

6.18 References

Dussurget, O., and Roulland-Dussoix, D. (1994). Rapid, sensitive PCR-based detection of mycoplasmas in simulated samples of animal sera. Appl Environ Microbiol *60*, 953-959.

Rawadi, G., and Dussurget, O. (1995). Advances in PCR-based detection of mycoplasmas contaminating cell cultures. PCR Methods Appl *4*, 199-208.

7 Appendix

7.1 The seek for a hVps34-specific inhibitor

For quite a few months during my Ph.D. research period I was occupied with testing some PI3K inhibitors, which we had at that time in the lab, on their efficacies to block hVps34 catalytic activity. Since there is no Vps34-specific inhibitor available, most of the studies concerning Vps34 role in cellular functions are done with ectopic expressed Vps34 wild type or kinase-dead mutants and with RNAi-mediated Vps34 deletion. However, RNAi targeting does not result into a complete deletion of Vps34, so that there is still some Vps34 expression left. Ectopic expression leads presumably to a delocalization of Vps34 and therefore to off-target effects. With a specific Vps34 inhibitor one could circumvent these problems. At present wortmannin and 3-methyladenine are used to inhibit Vps34. However, wortmannin is a pan-PI3K inhibitor, while 3-methyladenine is used at 10 mM concentration and might influence other PI3Ks as well or have additional non-specific effects. Therefore, we undertook to test the efficacies of different PI3K inhibitors on inhibiting Vps34 in an *in vitro* lipid PI3K kinase assay and compared it with the inhibition of class IA PI3Kα, p110α. The idea was to find an inhibitor that might inhibit hVps34 at a low concentration, while for the inhibition of p110α a higher concentration is needed. Moreover, we examined whether 3-methyladenine might as well affect the catalytic activity of the class I PI3K isoforms.

Effect of different PI3K inhibitors on the catalytic activity of hVps34

Different PI3K and dual PI3K/mTOR inhibitors (see Table 1) were tested on their efficacies to inhibit the catalytic activity of hVps34 and p110α. An *in vitro* lipid kinase assay was performed with GST pulldown of ectopically expressed GST-hVps34 from HEK293 cells and with recombinant p110α (kind gift from Doriano Fabbro, Novartis Basel). Both kinases were pretreated either with DMSO or with 3 different concentrations of the indicated inhibitors (10μM, 1μM and 100nM for hVps34 and 100nM for p110α) (Fig. 1) for 10 min at 30°C, while vigorously shaking. After addition of 10 μg of unilaminar PtdIns/phosphatidylserine vesicles and 2 μCi [γ-^{32}ATP]/10 μM cold ATP, lipid kinase assay was performed at 30°C for 15 min while vigorously shaking. Lipids were extracted and separated on a thin layer chromatography (TLC) and PtdIns(3)P quantified by phosphoimager.

Table 1: Inhibitors used for the lipid kinase assays and for analyzing the effect on cellular distribution of EGFP-2xFYVE^{HRS}

Compound	Comments	Chemical structure
Wortmannin	Pan-PI3K inhibitor, also active against DNA-PK, mTOR, ATR, ATM	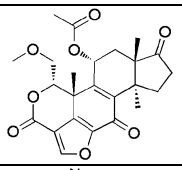
NVP-BAG956	Dual PI3K and PDK1 inhibitor	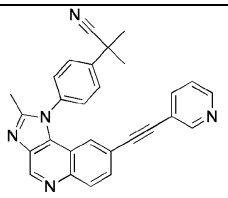
NVP-BBD130	Dual PI3K and mTOR inhibitor	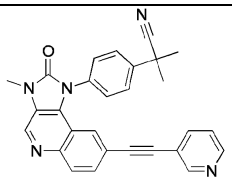
NVP-BEZ235	Dual PI3K and mTOR inhibitor	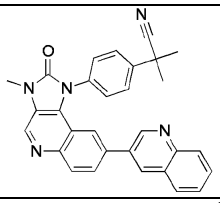
NVP-BGT226	Dual PI3K and mTOR inhibitor	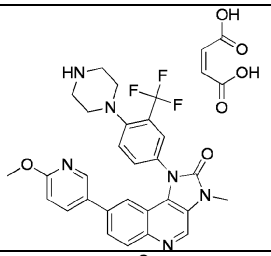
PI-103	Class I PI3K, mTORC1 and also DNA-PK inhibitor	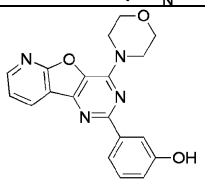
ZSTK474	Class I PI3K inhibitor	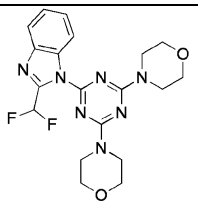
3-Methyladenine	Vps34 inhibitor, inhibitor of autophagy	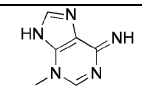

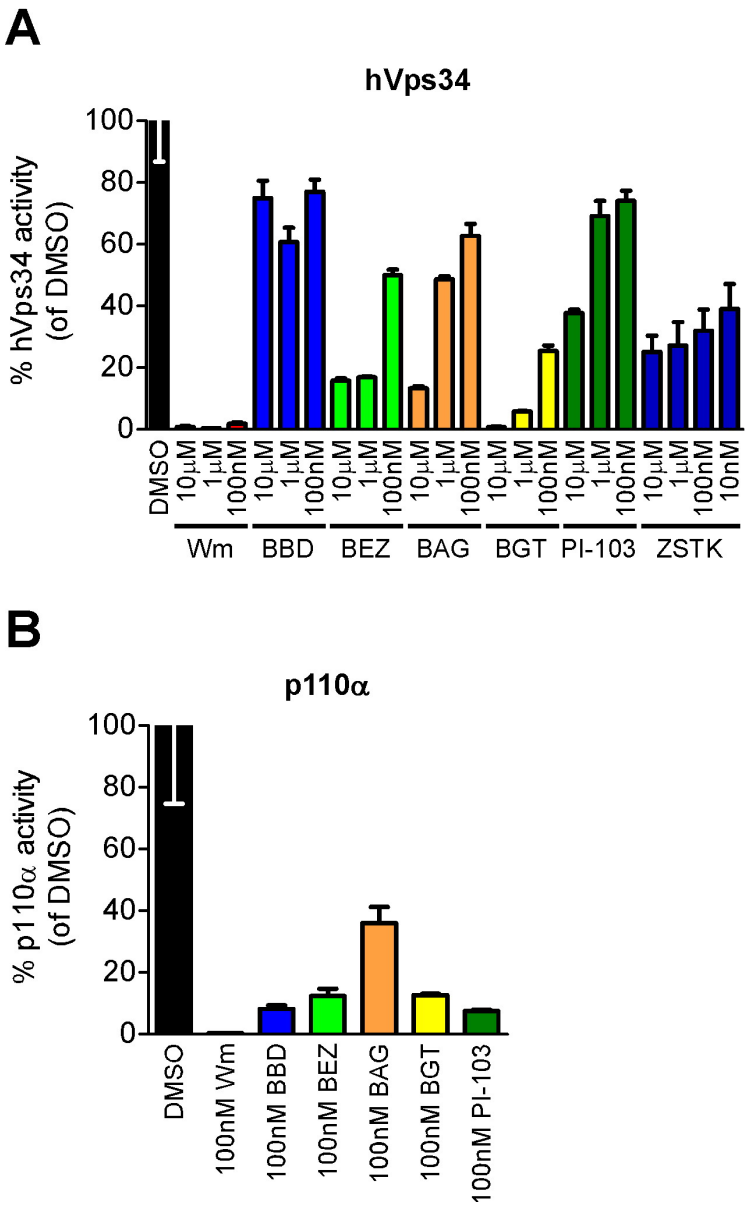

Fig. 1: Efficacies of different inhibitors in inhibiting hVps34 and p110α.

hVps34 (A) and p110α (B) were treated with different inhibitors as indicated and an *in vitro* lipid PI3K kinase assay performed. Quantification of n = 3 experiments are shown and data are represented as mean ± SEM.

Wm: wortmannin; BBD: NVP-BBD130; BEZ: NVP-BEZ235; BAG: NVP-BAG956; BGT: NVP-BGT226; ZSTK: ZSTK474.

Inhibitors at a low concentration of 100 nM, except wortmannin and BGT226, badly blocked the catalytic activity of hVps34, while the same concentration inhibited p110α to a much higher extent. Interestingly, BGT226 at 100 nM concentration blocked hVps34 to a similar extent as p110α. In parallel the vesicular distribution of EGFP-2xFYVE^{HRS}, which was used to detect PtdIns(3)P by microscopy, was

analyzed after inhibitor treatment in HeLa cells (Fig. 2). Similar to the lipid kinase assay, BGT226 treatment resulted in a diffused cytoplasmic localization of EGFP-2xFYVE^{HRS}, alike wortmannin treatment, indicating a block in PtdIns(3)P synthesis. BEZ235 and PI-103, which both blocked p110α to high extent but not hVps34, did not affect vesicular localization of EGFP-2xFYVE^{HRS}.

Consequently, the inhibitors tested here cannot be used at a low concentration to block solely hVps34 without affecting other PI3Ks as demonstrated with p110α (Fig.1).

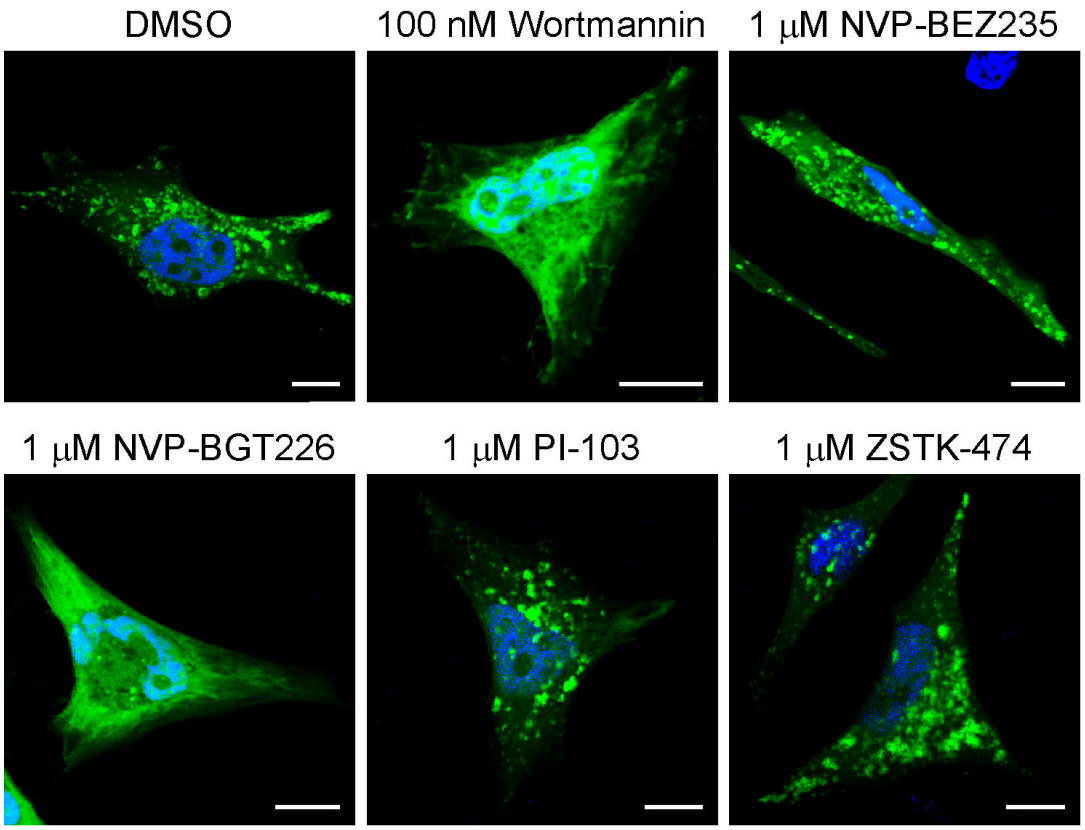

Fig. 2: Cellular distribution of the PtdIns(3)P sensor EGFP-FYVE^{HRS} after inhibitor treatment.
HeLa cells ectopically expressed EGFP-2xFYVE^{HRS} (green) in order to visualize PtdIns(3)P-containing endosomes. Cells were maintained in complete medium (DMEM supplemented with 2 mM L-glutamine and 10% FCS) and 48h after transfection cells were either treated with DMSO or with the indicated inhibitors for 30min. After fixation, nuclei were stained with Hoechst (blue) and cells imaged with a Zeiss confocal microscope. Scale bars represent 10 μm.

Effect of 3-methyladednine on class I PI3K isoforms and hVps34

3-Methyladenine is a compound used to block autophagy and as an hVps34 specific inhibitor (Li and Fan, 2010; Petiot et al., 2000). Because its working concentration is 10mM, we were wondering whether 3-methyladenine would also affect other PI3Ks. For that purpose *in vitro* lipid kinase assays were performed with recombinant class I PI3K isoforms (p110α, p110β, p110δ and p110γ) and with GST pull downed GST-hVps34 as described above. Interestingly, 10 mM 3-methyladenine effectively inhibited the catalytic activity of p110γ and hVps34 (Fig. 3), while p110α and p110δ were inhibited to 20% and p110β to around 25% in respect to DMSO treated controls (Fig. 3). Consequently, this result demonstrates that 3-methyladenine is not a hVps34 specific inhibitor, but it also negatively affects class I PI3K isoforms, especially p110γ. In support to our results, Ito et al. could demonstrate that 10 mM 3-methyladenine inhibits all 3 classes of PI3Ks as effective as 100 nM wortmannin (Ito et al., 2007).

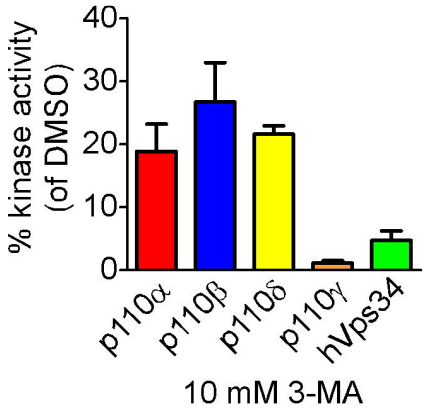

Fig. 3: 3-Methyladenine (3-MA) is not an hVps34 specific inhibitor.
Class I PI3K isoforms (p110α, p110β, p110δ and p110γ) and hVps34 were treated with 10mM 3-methyladenine in an *in vitro* lipid kinase assay. Quantification of n = 3 experiments are shown and data are represented as mean ± SEM.

Conclusion

PI3Ks class I isoform-specific inhibitors are available on the market but not for Vps34. Recently, the catalytic domain of *Drosophila* Vps34 has been crystallized (Miller et al., 2010), which will facilitate the design of selective Vps34 inhibitors. It has been demonstrated that Vps34 has a smaller ATP binding pocket compared to p110γ. The small size most probably restricts the binding of typical PI3K inhibitors such as PI-103 into the ATP binding pocket of Vps34 and thereby explaining why class I PI3K inhibitors have lower affinities for Vps34. The low molecular weight compound 3-methyladenine has been shown to accommodate very well into the ATP binding pocket of hVps34 (Miller et al., 2010). However, because of its smallness 3-methyladenine probably binds as well into the ATP binding cavities of the other

PI3Ks, especially p110γ, thereby blocking them. Nevertheless, thanks to the structural insights gained from the crystal structure of Vps34, Miller et al. were able to synthesize an analog of PIK93, termed PT210, that is 10-fold more selective for Vps34 (IC_{50} 450nM) than for p110γ (IC_{50} 4,428 nM) (Table 2). Moreover, the authors were able to reverse the selectivity of PIK93 for p110γ over Vps34 (Table 2) (Miller et al., 2010). Consequently, selective Vps34 inhibitors will sooner or later become available.

Table 2: Structural and IC_{50} comparison between PIK93 and PT210

PIK93	PT210
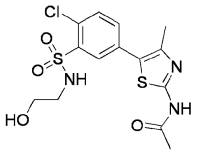	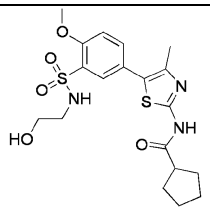
IC_{50} Vps34: 36 nM IC_{50} p110γ: 4 nM	IC_{50} Vps34: 450 nM IC_{50} p110γ: 4,428 nM

References

Ito, S., Koshikawa, N., Mochizuki, S., and Takenaga, K. (2007). 3-Methyladenine suppresses cell migration and invasion of HT1080 fibrosarcoma cells through inhibiting phosphoinositide 3-kinases independently of autophagy inhibition. Int J Oncol *31*, 261-268.

Li, X., and Fan, Z. (2010). The epidermal growth factor receptor antibody cetuximab induces autophagy in cancer cells by downregulating HIF-1alpha and Bcl-2 and activating the beclin 1/hVps34 complex. Cancer Res *70*, 5942-5952.

Miller, S., Tavshanjian, B., Oleksy, A., Perisic, O., Houseman, B.T., Shokat, K.M., and Williams, R.L. (2010). Shaping development of autophagy inhibitors with the structure of the lipid kinase Vps34. Science *327*, 1638-1642.

Petiot, A., Ogier-Denis, E., Blommaart, E.F., Meijer, A.J., and Codogno, P. (2000). Distinct classes of phosphatidylinositol 3'-kinases are involved in signaling pathways that control macroautophagy in HT-29 cells. J Biol Chem *275*, 992-998.

Peer-reviewed publication

7.2 Separation and detection of all phosphoinositide isomers by ESI-MS

Sabine Kiefer[a], Johannes Rogger[a], **Anna Melone[b]**, Ann C. Mertz[b], Anna Koryakina[a], Matthias Hamburger[a], Peter Küenzi[a]*

[a]Institute of Pharmaceutical Biology, University of Basel, Klingelbergstrasse 50, 4056 Basel, Switzerland. [b]Institute of Biochemistry and Genetics, Department of Biomedicine, University of Basel, Mattenstrasse 28, CH-4058 Basel, Switzerland.

***To whom correspondence should be addressed:**
Peter Künzi
CSL Behring
Wankdorfstrasse 10
3022 Bern, Switzerland
peter.kueenzi@cslbehring.com

Journal of Pharmaceutical and Biomedical Analysis 53 (2010) 552–558

Contents lists available at ScienceDirect

Journal of Pharmaceutical and Biomedical Analysis

journal homepage: www.elsevier.com/locate/jpba

Separation and detection of all phosphoinositide isomers by ESI-MS

Sabine Kiefer[a], Johannes Rogger[a], Anna Melone[b], Ann C. Mertz[b], Anna Koryakina[a], Matthias Hamburger[a], Peter Küenzi[a,*]

[a] Institute of Pharmaceutical Biology, University of Basel, Klingelbergstrasse 50, 4056 Basel, Switzerland
[b] Institute of Biochemistry and Genetics, Department of Biomedicine, University of Basel, Mattenstrasse 28, 4058 Basel, Switzerland

ARTICLE INFO

Article history:
Received 10 December 2009
Received in revised form 22 March 2010
Accepted 23 March 2010
Available online 30 March 2010

Keywords:
Phosphoinositides
Phosphatidylinositol 3,4,5 triphosphate
LC–MS
ESI
Reversed phase ion-pair chromatography

ABSTRACT

Phosphoinositides (PIs) play fundamental roles as signalling molecules in numerous cellular processes. Direct analysis of PIs is typically accomplished by metabolic labelling with ^{3}H-inositol or inorganic ^{32}P followed by deacylation, ion-exchange chromatography and flow scintillation detection. This analysis is laborious, time-consuming, and involves massive amounts of radioactivity. To overcome these limitations we established a robust, non-radioactive LC–ESI–MS assay for the separation and analysis of deacylated PIs that allows discrimination of all isomers without the need for radioactive labelling. We applied the method to various cell types to study the PI levels upon specific stimulation.

1. Introduction

The inositol containing glycerophospholipids, collectively known as phosphoinositides (PIs), play a fundamental role in diverse cellular functions such as cell growth and differentiation, motility, calcium mobilisation and oncogenesis [1,2]. The family of the phosphoinositides consists of the non-phosphorylated precursor phosphatidylinositol (PtdIns) and seven derivatives with different phosphorylation patterns on the myo-inositol ring, where the 3-, 4- and 5-positions can be phosphorylated by specific kinases (Fig. 1A).

PIs derived from PtdIns and its phosphorylation products phosphatidylinositol-4-phosphate (PtdIns4*P*) and phospha tidylinositol-4,5-bisphosphate (PtdIns(4,5)P_2) form the so called canonical pathway [3] and are believed to be kept at constant levels at the plasma membrane. The other PIs are considered to be low-abundant signalling molecules that transiently appear upon stimulation. Stimulation with growth factors or insulin leads to increased PtdIns(3,4,5)P_3 levels, which in turn produces specific cellular responses. The bisphosphorylated PIs containing PtdIns(3,4)P_2, PtdIns(4,5)P_2, and PtdIns(3,5)P_2 moieties play distinct roles in signal prolongation after PtdIns(3,4,5)P_3 inducing stimuli, regulation of the actin cytoskeleton and vesicle transport, respectively [4–8]. PIs containing phosphoinositide monophosphates were long thought to be mere intermediates in the pathway but are now recognised to possess specific functions by themselves in protein sorting, vesicular trafficking and in osmotic stress response [9–12].

Analysis of PIs has been achieved in several ways. Most frequently, metabolic radioisotope labelling with inorganic ^{32}P or ^{3}H-inositol, lipid extraction, hydrolysis followed by chromatographic separation and radiographic analysis of phosphoinositides has been used [13–15]. Metabolic labelling involves very high doses of radioactivity (GBq), long labelling times and only detects the turnover of PIs, whereas dormant pools of PIs remain unlabelled. More recent approaches include fluorescent-labelled binding proteins for specific PIs, and antibodies directed against PIs [16,17]. However, differentiation of all the mono- and bisphosphorylated positional isomer PIs, has not been achieved yet.

Two fundamentally different approaches have been pursued in PI analysis: (i) a comprehensive profiling of intact PIs [18–21] and (ii) head group analysis after cleavage of the lipid moieties [22,23]. The first approach used in lipidomics leads to a highly complex picture due to a plethora of closely related molecules that only vary in their lipid moieties. This approach including quantification has been successfully applied to cells producing phophoinositides with limited complexity in their lipid residues, such as platelets [24–26]. Even though the analysis of intact PIs would be the preferred approach, it is currently unsuitable for most cells due to the overwhelming complexity of their PI patterns. Therefore, separation and detection of the head groups following deacylation (Fig. 1B) is a more suitable approach if the focus lies on the detec-

* Corresponding author. Present address: CSL Behring, Wankdorfstrasse 10, 3022 Bern, Switzerland. Tel.: +41 31 344 40 48.
E-mail addresses: peter.kueenzi@cslbehring.com, peter.kueenzi@unibas.ch (P. Küenzi).

0731-7085/$ – see front matter © 2010 Elsevier B.V. All rights reserved.
doi:10.1016/j.jpba.2010.03.029

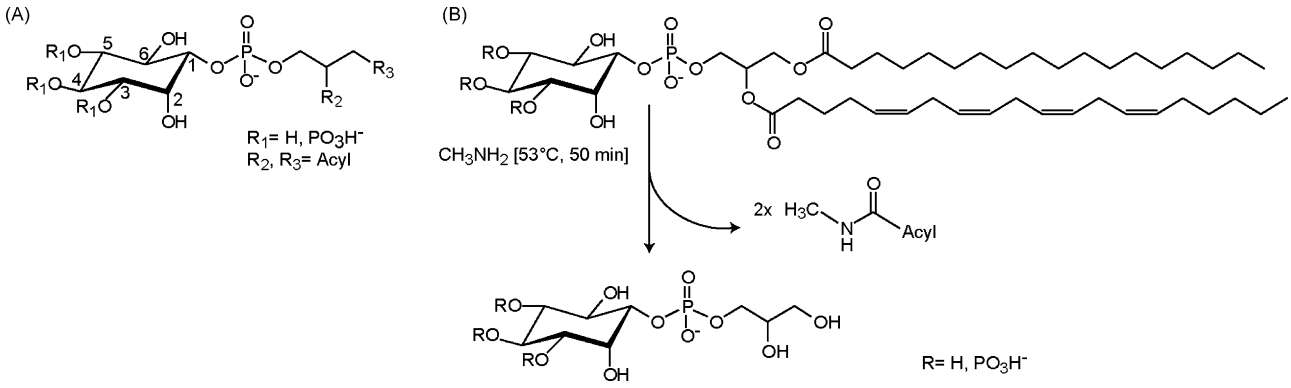

Fig. 1. (A) Structure of a typical PtdIns, sn-1-stearoyl-2-arachidonyl-phosphatidylinositol and the performed deacylation step, resulting in cleavage of the lipid moiety. (B) Structure of phosphatidylinositol-3,4,5-trisphosphate (PtdInsP_3); numbering of the myo-inositol ring is indicated.

tion of the change in phosphorylation pattern that exerts the major influence on the subsequently elicited signalling. Given the low abundance of certain PIs, even the analysis of deacylated lipids is highly challenging.

As alternatives to radioisotope labelling, analysis by mass spectrometry [27], suppressed conductivity detection [28] and evaporative light scattering detection (ELSD) [29] have been used. Unfortunately, none of these allowed a discrimination of all isomers. An LC–ESI–MS method for separation of deacylated PtdInsP_2 isomers has been recently published [14]. However, chromatography suffered from poor peak shape and co-elution of PtdIns(3,5)P_2 and PtdIns(3,4,5)P_3.

Since the PtdIns moieties of PIs can be interconverted by specific kinases and phosphatases, inhibition, stimulation, modification, or deletion of one of these enzymes may have profound implications on the biological response. Therefore, separation and simultaneous detection of all headgroups of PIs is of major importance for a better understanding of their biological roles, and a robust and sensitive method is of general interest to researchers involved in cell signalling.

2. Experimental

2.1. LC–MS instrumentation

HPLC separation was carried out on a series 1100 system equipped with degasser, binary high pressure mixing pump, and column thermostat (Agilent Technologies). A liquid handler 215 (Gilson) was used as autosampler. The HPLC was coupled to an Esquire 3000 ion trap mass spectrometer equipped with an electrospray (ESI) interface (Bruker Daltonics). Data acquisition and processing was performed using HyStar 3.0 software from Bruker Daltonics.

2.2. LC–MS method

2.2.1. Ion-pair chromatography

N,N-dimethylhexylamine (DMHA; Acros, Thermo Fisher) was used as ion-pair reagent. Mobile phase A consisted of water containing 5 mM DMHA and 4 mM glacial acetic acid (Sigma–Aldrich) and mobile phase B of acetonitrile or methanol with 5 mM DMHA and 4 mM glacial acetic acid. All solvents were from Scharlau (Scharlau, Barcelona, Spain).

2.2.2. Columns

Various columns were tested for suitability in phosphoinositide analysis, including Atlantis C18 (150 mm × 4.6 mm, 5 μm) and T3 (150 mm × 3.5 mm, 3 μm; Waters, Baden, Switzerland), Nucleosil C100 (250 mm × 4.6 mm, 5 μm; Macherey-Nagel, Düren, Germany), liChrospher diol (125mm × 4.0 mm, 5 μm; Merck, Darmstadt, Germany) and Aqua C18 (250 mm × 4.6 mm, 5 μm and 75 mm × 2.0 mm, 3 μm; Phenomenex, Torrance, CA).

2.2.3. Separation of phosphoinositides

2.2.3.1. Method 1. Separation of deacylated PIs with different numbers of phosphorylations; PtdIns, PtdIns*P*, PtdInsP_2 and PtdInsP_3, was achieved by ion-pair chromatography on a Aqua C18 column (3 μm, 125 Å, 75 mm × 2.0 mm). A gradient from mobile phase B (acetonitrile) 0.1 to 50% in 25 min and a wash step (50% B to 100% B in 3 min, 100% B for 12 min, 100% B to 0.1% B in 5 min, 0.1% B for 5 min) was applied.

2.2.3.2. Method 2. Separation of deacylated PIs with different numbers of phosphorylation plus additional separation of phosphoinositides bisphosphate isomers PtdIns(4,5)P_2, PtdIns(3,5)P_2, PtdIns(3,4)P_2, was achieved by ion-pair chromatography on an Aqua C18 column (125 Å, 250 mm × 4.6 mm, 5 μm). A gradient from mobile phase B (acetonitrile) 15 to 35% in 40 min followed by a wash sequence (35% B to 100% B in 2 min, 100% B for 15 min, 100% B to 15% B in 3 min, 15% B for 5 min) was applied.

2.2.3.3. Method 3. Separation of PtdIns(3)*P*, PtdIns(4)*P* and PtdIns(5)*P*, additionally to separation of all other PIs, was performed with methanol as mobile phase B and a gradient from 15 to 50% in 60 min, followed by a wash step (50% B to 100% B in 2 min, 100% B for 15 min, 100% B to 15% B in 3 min, 15% B for 5 min).

2.3. Mass spectrometry

Negative ion LC–MS spectra on the ion trap instrument were recorded after optimization of settings, under ion charge control conditions (ICC 20000) at a scan speed of 13,000 *m*/*z*/s, using a gauss filter width of 0.2 *m*/*z*. Nitrogen was used as a drying gas at a flow rate of 10 l/min and as a nebulizing gas at a pressure of 30 psi. The nebulizer temperature was set to 300 °C. Spectra were recorded in the range of *m*/*z* 200–600 in negative mode. Capillary voltage was at 4500 V, endplate offset at −500 V, capillary end voltage at −115.0 V, skimmer voltage −40.0 V and trap drive at 53.4.

2.4. Flow scintillation analysis

Levels of radioactively labelled intracellular phosphatidylinositides were determined essentially as described [30]. Briefly, 4 million cells were incubated with 500 μCi $^{32}P_i$ for 60 min at 37 °C. After removal of non-incorporated $^{32}P_i$, cells were extracted as described below. The column effluent was splitted and exam-

ined online with a FLO-ONE A500 β-detector (Packard–Perkin Elmer).

2.5. Chemicals and cell culture

Murine bone marrow cells were cultured in Iscove's Modified Dulbecco's medium (IMDM; Sigma–Aldrich) supplemented with 10% heat-inactivated fetal calf serum (FCS; Amimed, Basel, Switzerland), 100 U/ml penicillin/streptomycin and 2 mM L-glutamine (both from Invitrogen, Basel, Switzerland). Cells were grown in humified atmosphere containing 5% CO_2 and maintained with 2 ng/ml recombinant murine interleukin-3 (IL3; PeproTech EC Ltd., London, UK).

Human embryonic kidney cells HEK 293 were cultured in Dulbecco's Modified Eagle's Medium (DMEM; Sigma–Aldrich) supplemented with 10% FCS, 100 U/ml penicillin/streptomycin and 2 mM L-glutamine. Cells were transfected with jetPEI cationic polymer transfection reagent (Polyplus-Transfection, Illkirch, France) according to the manufacturers' instructions. Twenty-four hour before transfection, cells were plated at 10^6 cells/25 cm^2 flask, then transfected with 2.6 μg GST-Vps34 and 0.4 μg Myc-S6K. Thirty hour after transfection, cells were starved over night and experiments were performed the following day.

Platelets were isolated from blood of healthy donors. Blood samples were mixed with acid citrate dextrose ACD (10.1 mM glucose, 30 μM citric acid, pH 6.5 in 0.9% NaCl, all from Sigma–Aldrich) and centrifuged for 5 min at 1000 × *g* [31]. Platelet rich plasma was collected and washed in PBS.

Chemicals used for experiments were: adenosine (Ade), N-formyl-Met-Leu-Phe (fMLP), wortmannin (wort) (all from Sigma–Aldrich).

Phosphoinositide standards used were: Phosphoinositides sodium salt from bovine brain (Sigma–Aldrich), PtdIns(3,4)P_2, PtdIns(3,5)P_2 and PtdIns(3,4,5)P_2 as 1,2-dioctanoyl-sn-glycero-3-phosphoinositolphosphates ammonium salt and PtdIns3*P* and PtdIns5*P* as 1-heptadecanoyl-2-(5Z,8Z,11Z,14Z-eicosatetraenoyl)-sn-glycero-3-phosphoinositolphosphates ammonium salt from Avanti Polar Lipids (Avanti Polar Lipids, Alabaster, AL).

2.6. Extraction, deacylation and sample preparation

Extraction of PIs was adapted from Ogiso et al. [27], who described a modified acidic Bligh-Dyer extraction [32] with addition of NaCl to the aqueous phase to help reducing loss of PIs. Briefly, ca. 10^6 cells were extracted with 2 ml methanol, 2 ml 1 M HCl, 0.15 ml 2 M NaCl and 2 ml chloroform (solvents from Scharlau, other reagents from Sigma–Aldrich). Methanol was supplemented with PhosSTOP (Roche, Basel, Switzerland), 1 mM NaF, 3 mM BHT and 0.5 mM phosphatidic acid (all from Sigma–Aldrich). The two phases were mixed well and centrifuged shortly for separation. The lower organic phase was removed, evaporated by nitrogen stream and transferred to deacylation. Dried samples were incubated with methylamine solution in water/methanol/n-butanol (43:46:11) at 53 °C for 50 min, all solvent was evaporated under vacuum, and then extracted with a mixture of n-butanol/petrol ether 40–60°/ethyl formiate (20:4:1) and water [33]. The water-phase was dried in vacuum and the samples were dissolved in 40 μl of solvent A for LC–MS analysis.

3. Results and discussion

3.1. Separation of phosphoinositides in order of increasing phosphorylation

Separation of anionic or phosphorylated compounds is typically achieved by ion-exchange chromatography. However, typical ion-pairing reagents are not volatile and, hence, not compatible with LC–MS. We tested several volatile and MS-compatible ion-pairing reagents, such as formic acid, ammonium formiate and N,N-dimethyl-hexylamine (DMHA) and applied them on various columns (Nucleosil C100, LiChrospher Diol and Phenomenex Aqua C18). The only acceptable separation of a phosphoinositide reference mixture was achieved on a short (75 mm) Phenomenex Aqua C18 column with the addition of DMHA. Subsequently, we tested different gradient profiles, column temperatures, pH and concentrations of DMHA to optimize separation. Column temperature had a slight impact, and the best separation was obtained at 15 °C. In contrast, pH of the mobile phase was critical. Best results were obtained around pH 7, while lower pH values lead to peak tailing and split peaks and higher pH resulted in shorter retention times. Increase of DMHA concentration from 5 to 10 mM and 20 mM did not enhance the quality of the separation. A water-acetonitrile gradient was applied and the final gradient program was 0.1–50% ACN (containing 5 mM DMHA) in 25 min, leading to the separation of a PI standard mixture shown in Fig. 2A. Peaks shown resulted from 0.1 μg of deacylated PtdIns(3,4,5)P_3 standard mixed with 4 μg of deacylated phosphoinositde extract (mixture of PtdIns, PtdIns4*P* and PtdIns(4,5)P_2).

Separation of a mixture of PIs standards was also achieved under isocratic conditions (27% ACN and 73% water) but separation of biological samples, however, could not be achieved under these conditions, probably due to interference with the biological matrix.

To test the applicability of our method to biological samples, we analysed mast cell extracts. Mast cells are known to produce large amounts of PtdIns(3,4,5)P_3 upon activation that can be provoked *in vitro* by stimulation with adenosine [30]. Murine bone marrow derived mast cells (BMMCs) were stimulated with 5 μM adenosine for 30 s, the lipids were extracted, deacylated and analysed with method 1. Our method clearly succeeded in reproducing the increased amounts of PtdIns(3,4,5)P_3 upon stimulation of mast cells with adenosine, whereas peaks of PtdIns and PtdIns*P* remained constant (Fig. 2B and C).

3.2. Positional isomer separation of phosphatidylinositol bisphosphates

To achieve separation of PtdInsP_2 positional isomers various columns were tested, including Nucleosil C100, Atlantis C18, Atlantis T3 and Phenomenex Aqua C18. The separation was only achieved on a Phenomenex Aqua column (column length 250 mm) and a water–acetonitrile gradient (containing 5 mM DMHA as ion-pair reagent) (method 2). A mixture of standards of all PtdInsP_2 isomers was separated in the elution order of PtdIns(3,4)P_2, PtdIns(4,5)P_2 and PtdIns(3,5)P_2 (Fig. 3A and B). Peaks shown resulted from 0.1 μg of deacylated PtdIns(3,5)P_2 and PtdIns(3,4)P_2 standard mixed with 4 μg of deacylated phosphoinositde extract (mixture of PtdIns, PtdIns4*P* and PtdIns(4,5)P_2). Several other solvent mixtures and addition of modifiers were tested. A separation with a different elution order (PtdIns(3,4)P_2, PtdIns(3,5)P_2 and PtdIns(4,5)P_2) was obtained with a water–methanol gradient (containing 5 mM DMHA) (method 3) (Fig. 3C and D).

Vps34 transfected HEK 293 cells under hyperosmolar stress were used as a model to test the analysis of PtdIns(3,5)P_2 from biological samples. The PI3-kinase Vps34 is known to stimulate osmotic stress related production of PtdIns(3,5)P_2 in yeast [22,28]. HEK Vps34 were incubated for 10 min in a medium supplemented with 1 M NaCl solution to induce stimulation of Vps34, and generation of PtdIns3*P* leading to production of PtdIns(3,5)P_2. As can be seen in Fig. 4A and B, the transfection with Vps34 already induced some production of PtdIns(3,5)P_2, which was then further increased upon NaCl hyperosmotic stimulation.

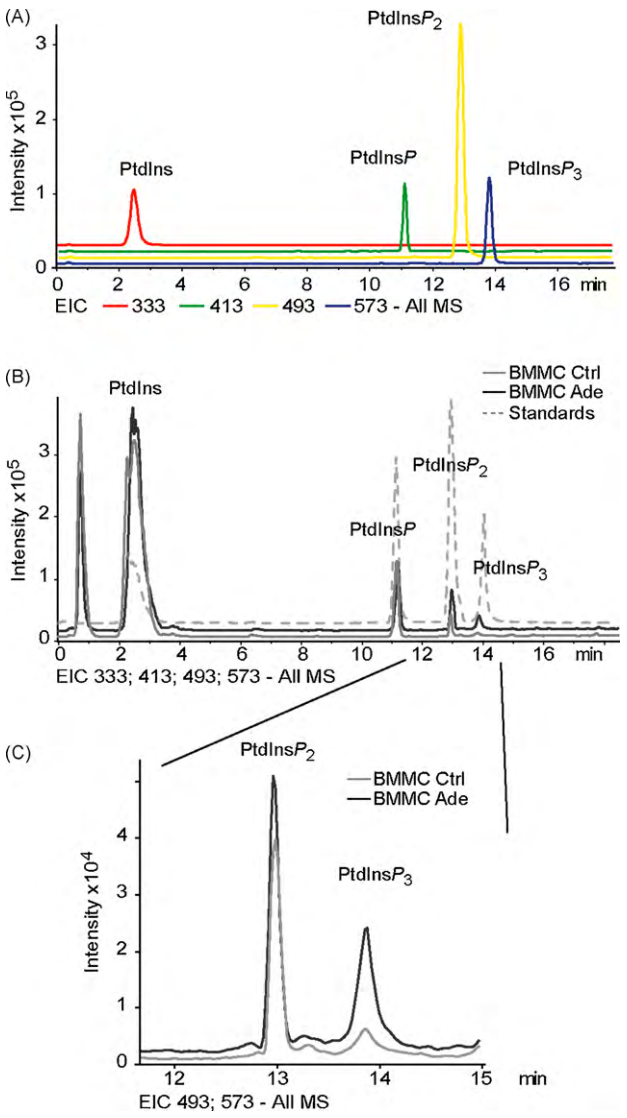

Fig. 2. (A) Extracted ion chromatogram (EIC) of deacylated phosphoinositide standards (PtdIns, PtdIns*P*, PtdInsP_2 and PtdInsP_3) mixture. (B) EIC of cell samples from 4 mio BMMC and standards. Cells were stimulated with adenosine (Ade) 5 μM for 30 s to induce production of PtdInsP_3. (C) Peaks of PtdInsP_2 and PtdInsP_3 from control cells in relation to stimulated cells, levels of PtdInsP_3 increased after stimulation with adenosine. Column: Phenomenex Aqua C18 (75 mm × 2 mm, 3 μm). Solvent A: H_2O (+5 mM DMHA), solvent B: acetonitrile (+5 mM DMHA). Gradient: 0.1% B to 50% B in 25 min.

Analysis of PtdIns(3,4)P_2 in biological samples was tested with human blood platelets. In comparison to many other cell models, platelets produce PtdIns(3,4)P_2 in relatively large amounts upon activation. PtdIns(3,4,5)P_3 is degraded to PtdIns(3,4)P_2 by the 5-phosphatase SHIP1 [34]. PtdIns(3,4)P_2 is responsible for the persistence of the signal induced by PtdIns(3,4,5)P_3 [8,35]. For detection of PtdIns(3,4)P_2, platelets were stimulated for 90 s with fMLP. This resulted in elevated amounts of PtdIns(3,4)P_2 which were not present in control cells (Fig. 4C and D).

3.3. Positional isomer separation of phosphatidylinositol monophosphates

Separation of the mono-phosphorylated isomers was only achieved with methanol–water mixtures as mobile phase (Fig. 5A and B), whereas the use of acetonitrile resulted in co-elution of PtdIns3*P* and PtdIns5*P*.

The method was applied to Vps34 transfected HEK cells as model. Vps34 is stimulated by amino acid addition through a yet unknown mechanism [36]. Starvation and subsequent amino acid supplementation stimulates Vps34 and induces the generation of PtdIns3*P* [37,38]. Thus, HEK Vps34 cells were serum and amino acid starved for 12 and 2 h, respectively. By addition of serum and amino acids, cells were stimulated for 30 min prior to extraction of lipids, deacylation and analysis. The stimulation with serum and amino acids induced production of PtdIns3*P*, which, in contrast, was inhibited by incubation with the PI3-kinase inhibitor wortmannin 15 min prior to and during stimulation with amino acids and serum (Fig. 5C and D).

3.4. Comparison with radiolabelling method

For comparison with the standard detection method of scintillation analysis, we applied radiolabelled samples to the newly developed HPLC method combined with subsequent scintillation analysis. This also gave a reconfirmation of the peaks measured with MS. The large loop size of 1 ml within the flow scintillation analyser and a flow rate of only 0.5 ml/min resulted in very broad and asymmetric peaks. Nevertheless, peaks of the major PIs could be detected (Fig. 6A and B). A radioactive labelled cell sample showed all major PI peaks (Fig. 6C) at the same retention times as when detected with MS. So did a radioactive labelled standard of PtdIns3*P* (Fig. 6C) that was clearly different to the retention time of the cellular PtdIns4*P* peak.

3.5. Discussion

The separation of PIs differing in number of phosphorylations was successfully achieved with method 1 and applied to analysis of phosphoinositides in cell samples. For analysis of PtdIns(3,4,5)P_3 this method offers a good alternative to the assay involving radiolabelling and anion-exchange HPLC. The short analysis time facilitates handling of large sample numbers.

Separation of isomers was achieved on the same column type, but of longer size and hence increased separation capacity (method 2). This assay offers new perspectives for research on phosphoinositide signalling. The low-abundant PtdInsP_2 isomers can now be separated and analysed without the need for radioactive labelling.

Replacing acetonitrile by methanol enabled the separation of PtdIns3*P*, PtdIns4*P* and PtdIns5*P* (method 3). This isomer separation has not been possible before. Also the PtdInsP_2 isomers could be separated with method 3, albeit in a different elution order when compared to method 2. This hampered a complete separation of the highly abundant PtdIns(4,5)P_2 from the trace isomer PtdIns(3,5)P_2. Therefore, analysis of the biologically important PtdIns(3,5)P_2 should be performed with method 2.

Separation of PtdInsP_2 isomers has been shown before on a cyclodextrin column [14], but co-eluting peaks of PtdIns(3,4,5)P_3 and PtdIns(3,5)P_2 limited the usefulness of the method. Also, separation of PtdIns*P* isomers was neither shown nor discussed in that publication. Compared to a cyclodextrin column the polar endcapped RP-column used here exhibits a more predictable chromatographic behaviour, offers more options for method refinement, and is widely applicable. Furthermore, robustness of the column and reproducibility and stability of separations are very high.

The methods presented here were successfully applied to relevant biological samples. The extraction procedure of PIs remains a major concern. As extensively discussed by Ogiso et al. [27], recovery rates of PIs are generally poor and decrease with increasing phosphorylation. Due to the amphiphilic properties these lipids are difficult to extract. The ionic headgroup adsorbs easily to glass surfaces, whereas the lipid moiety adsorbs to plastic. However,

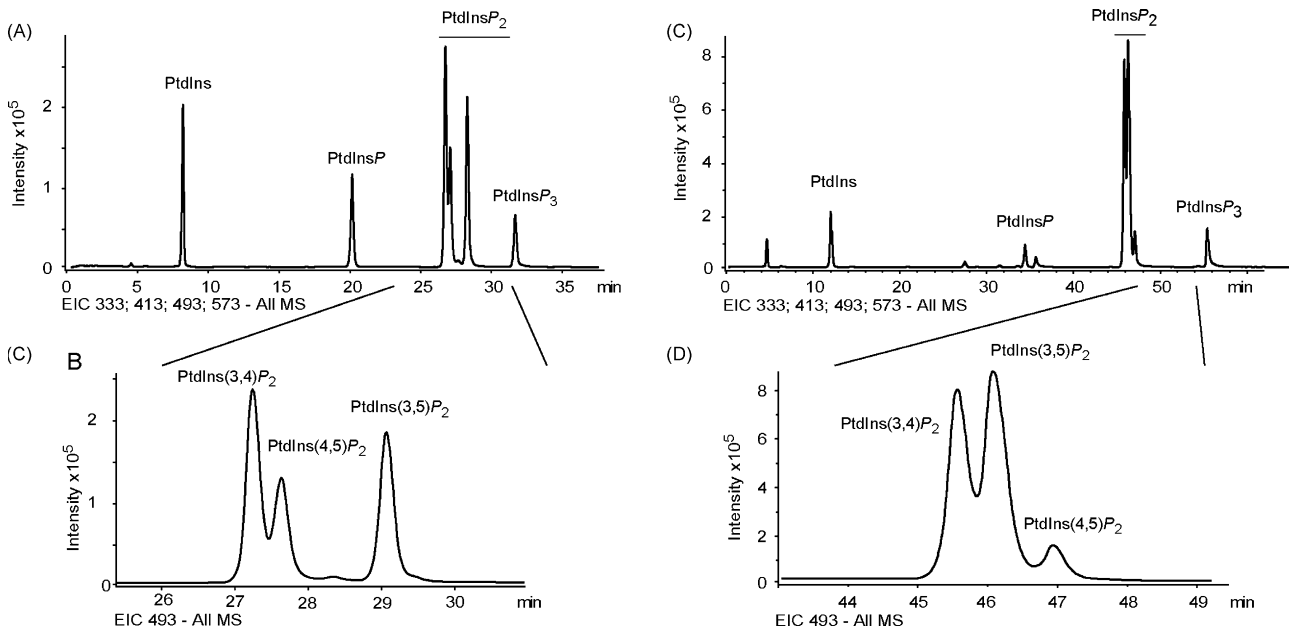

Fig. 3. (A and B) Separation of a standard mixture of PIs containing all PtdInsP_2 regioisomers. (B) Elution of the isomers of PtdInsP_2 in following order: PtdIns(3,4)P_2, PtdIns(4,5)P_2 and PtdIns(3,5)P_2. Column: Phenomenex Aqua C18 (250 mm × 4.6 mm, 5 μm). A: H_2O (+5 mM DMHA), B: acetonitrile (+5 mM DMHA). Gradient: 15% B to 35% B in 40 min. (C and D) Separation of a standard mixture of PIs containing all PtdInsP_2 regioisomers. (D) Separation of PtdInsP_2 isomers in sequence of PtdIns(3,4)P_2, PtdIns(3,5)P_2 and PtdIns(4,5)P_2. Column: Phenomenex Aqua C18 (250 mm × 4.6 mm, 5 μm). A: Methanol (+5 mM DMHA), B: acetonitrile (+5 mM DMHA). Gradient: 15% B to 50% B in 60 min.

measures can be taken to reduce loss of analytes, such as use of silanized glassware to prevent adsorption at glass surfaces [26], and lipid pre-treatment of plastic surfaces with lipids as adsorption protectants. We used plastic tubes, added lipids as adsorption protectants, and phosphatase inhibitors to prevent hydrolysis. These combined measures noticably increased extraction yields. However, further optimization is needed towards a robust and fully validated quantitative analysis of PI headgroups. This could be achieved by spiking with suitable internal standards at the beginning of the extraction procedure which ideally should be a PI with a stable-isotope labelled headgroup. However, such standards are not commercially available. An issue is the efficiency of extraction of phospholipids with different degrees of phosphorylation. There are clear indications that replacing the widely used extraction with chloroform/methanol by butanol increases the yield of highly phosphorylated PtdIns isoforms ([26], Traynor-Kaplan and

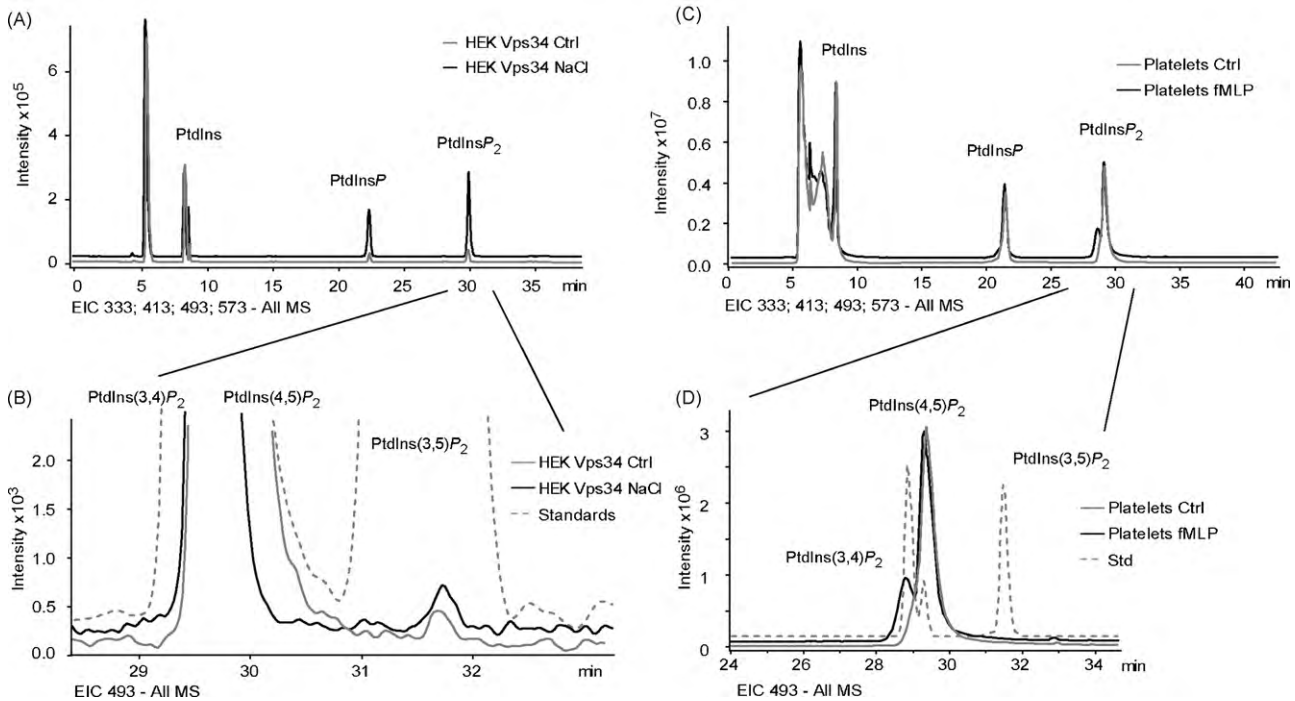

Fig. 4. Analysis of phosphoinositide cell samples. (A and B) Extracted ion chromatograms (EIC) of HEK Vps34 cell samples showed increased amounts of PtdIns(3,5)P_2, that were further increased by stimulation with 1 M NaCl for 10 min. (C and D) EIC of lipids extracted from platelets, control sample and stimulated with fMLP for 1 min. Stimulation induced generation of PtdIns(3,4)P_2 that was not present in the control sample. Column: Phenomenex Aqua C18 (250 mm × 4.6 mm, 5 μm). A: H_2O (+5 mM DMHA), B: acetonitrile (+5 mM DMHA). Gradient: 15% B to 35% B in 40 min.

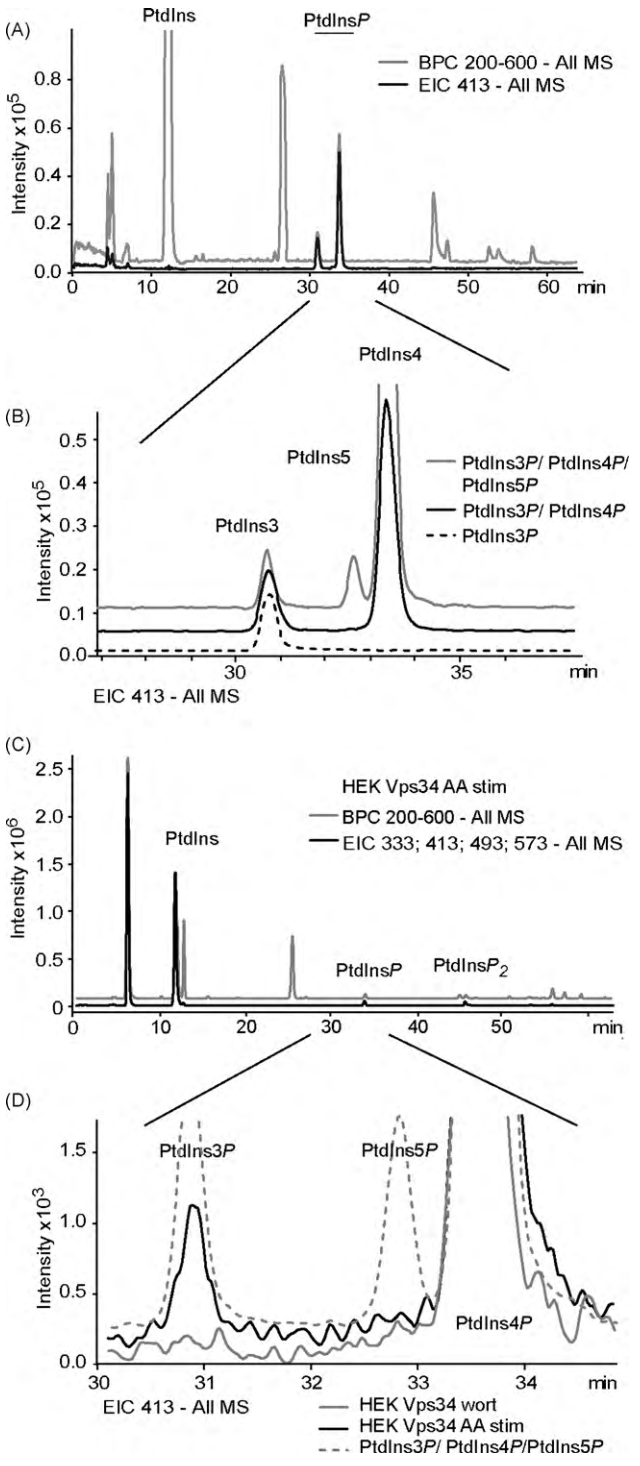

Fig. 5. (A and B) Extracted ion chromatogram (EIC) and base peak chromatogram (BPC) of mixed standards of phosphoinositide monophosphates separated according to method 3. Separation of PtdIns3*P*, PtdIns4*P* and PtdIns5*P* was achieved. (C) BPC and EIC of a HEK Vps34 cell sample. (D) EIC of HEK Vps34 cell samples that were amino acid stimulated and incubated with wortmannin 15 min prior to and during amino acid stimulation. The increase in PtdIns3*P* following amino acid starvation and subsequent stimulation was blocked by addition of wortmannin. Column: Phenomenex Aqua C18 (250 mm × 4.6 mm, 5 μm). A: H_2O (+5 mM DMHA), B: methanol (+5 mM DMHA). Gradient: 15% B to 50% B in 60 min.

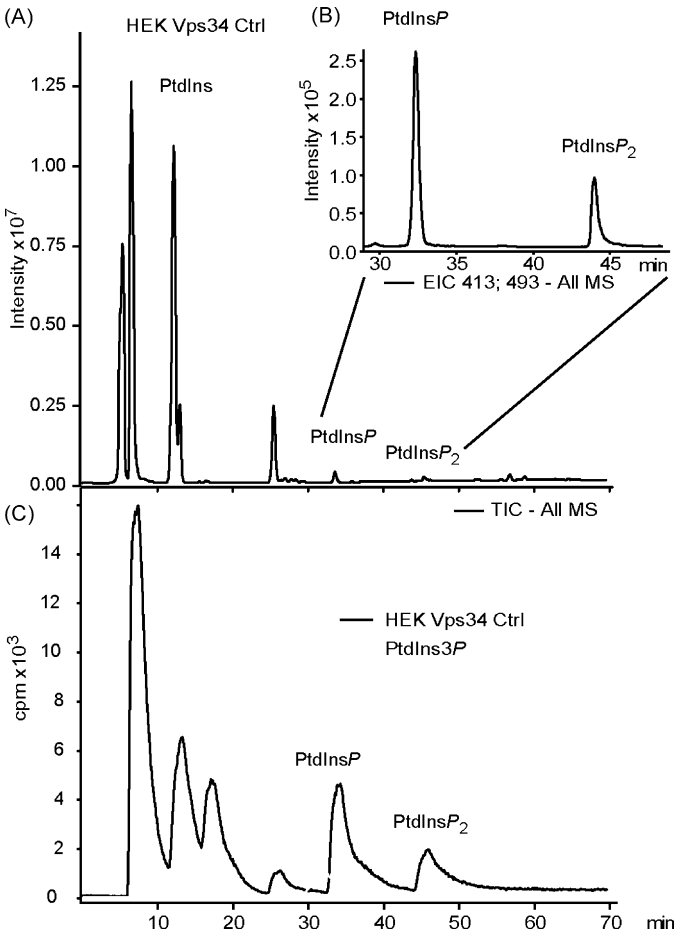

Fig. 6. (A and B) Total ion chromatogram (TIC) and extracted ion chromatogram (EIC) of a HEK Vps34 control cell sample separated according to method 3. (C) Chromatogram of parallel online flow scintillation analysis of the same HEK Vps34 cell sample and a standard of PtdIns3*P*. Column: Phenomenex Aqua C18 (250 mm × 4.6 mm, 5 μm). A: Methanol (+5 mM DMHA), B: acetonitrile (+5 mM DMHA). Gradient: 15% B to 50% B in 60 min.

Küenzi, unpublished data). Thus, a semi-quantitative analysis that compares peak intensities of highly variable (e.g. PtdIns(3,4,5)P_3) and basically unvaried (e.g. PtdIns(4,5)P_2) headgroups is currently the most suitable approach.

The direct parallel analysis with online flow scintillation and mass spectrometry showed the comparability of the two methods. The LC–MS assay presented here offers a superior approach for analysis of intracellular PI levels including differentiation of the biologically relevant PtdIns*P* and PtdInsP_2 isomers.

Further development of the method can be envisaged by a translation to UPLC, thereby taking advantage of shorter analyses and equal or superior chromatographic resolution. There is a general need for further improvement of sample workup in PI analysis, as isolation and deacylation of the PtdIns is time-consuming and difficult. Also, the issue of possible discriminatory extraction of certain PtdIns needs further investigation. Nevertheless, the LC–MS methods presented here enable simultaneous analysis of all currently known deacylated PtdIns and thus are a useful tool for cell signalling studies.

References

[1] L.C. Skwarek, G.L. Boulianne, Great expectations for PIP: phosphoinositides as regulators of signaling during development and disease, Dev. Cell 16 (2009) 12–20.
[2] M.P. Wymann, R. Schneiter, Lipid signalling in disease, Nat. Rev. Mol. Cell Biol. 9 (2008) 162–176.

[3] B. Payrastre, K. Missy, S. Giuriato, S. Bodin, M. Plantavid, M. Gratacap, Phosphoinositides: key players in cell signalling, in time and space, Cell. Signal. 13 (2001) 377–387.
[4] I.H. Batty, J. van der Kaay, A. Gray, J.F. Telfer, M.J. Dixon, C.P. Downes, The control of phosphatidylinositol 3,4-bisphosphate concentrations by activation of the Src homology 2 domain containing inositol polyphosphate 5-phosphatase 2, SHIP2, Biochem. J. 407 (2007) 255–266.
[5] M.J. Clague, S. Urbe, J. de Lartigue, Phosphoinositides and the endocytic pathway, Exp. Cell Res. 315 (2008) 1627–1631.
[6] D. Manna, A. Albanese, W.S. Park, W. Cho, Mechanistic basis of differential cellular responses of phosphatidylinositol 3,4-bisphosphate and phosphatidylinositol 3,4,5-trisphosphate-binding pleckstrin homology domains, J. Biol. Chem. 282 (2007) 32093–32105.
[7] R.H. Michell, V.L. Heath, M.A. Lemmon, S.K. Dove, Phosphatidylinositol 3,5-bisphosphate: metabolism and cellular functions, Trends Biochem. Sci. 31 (2006) 52–63.
[8] G. Di Paolo, P. De Camilli, Phosphoinositides in cell regulation and membrane dynamics, Nature 443 (2006) 651–657.
[9] J.B. Morris, K.A. Hinchliffe, A. Ciruela, A.J. Letcher, R.F. Irvine, Thrombin stimulation of platelets causes an increase in phosphatidylinositol 5-phosphate revealed by mass assay, FEBS Lett. 475 (2000) 57–60.
[10] C. Pendaries, H. Tronchere, C. Racaud-Sultan, F. Gaits-Iacovoni, S. Coronas, S. Manenti, M.P. Gratacap, M. Plantavid, B. Payrastre, Emerging roles of phosphatidylinositol monophosphates in cellular signaling and trafficking, Adv. Enzyme Regul. 45 (2005) 201–214.
[11] D. Sbrissa, O.C. Ikonomov, R. Deeb, A. Shisheva, Phosphatidylinositol 5-phosphate biosynthesis is linked to PIKfyve and is involved in osmotic response pathway in mammalian cells, J. Biol. Chem. 277 (2002) 47276–47284.
[12] A.E. Wurmser, J.D. Gary, S.D. Emr, Phosphoinositide 3-kinases and their FYVE domain-containing effectors as regulators of vacuolar/lysosomal membrane trafficking pathways, J. Biol. Chem. 274 (1999) 9129–9132.
[13] H. Guillou, L.R. Stephens, P.T. Hawkins, Quantitative measurement of phosphatidylinositol 3,4,5-trisphosphate, Methods Enzymol. 434 (2007) 117–130.
[14] P.T. Ivanova, S.B. Milne, M.O. Byrne, Y. Xiang, H.A. Brown, Glycerophospholipid identification and quantitation by electrospray ionization mass spectrometry, Methods Enzymol. 432 (2007) 21–57.
[15] K.R. Auger, L.A. Serunian, S.P. Soltoff, P. Libby, L.C. Cantley, PDGF-dependent tyrosine phosphorylation stimulates production of novel polyphosphoinositides in intact cells, Cell 57 (1989) 167–175.
[16] H. Hama, J. Torabinejad, G.D. Prestwich, D.B. DeWald, Measurement and immunofluorescence of cellular phosphoinositides, Methods Mol. Biol. 284 (2004) 243–258.
[17] T.E. Rusten, H. Stenmark, Analyzing phosphoinositides and their interacting proteins, Nat. Methods 3 (2006) 251–258.
[18] S.B. Milne, P.T. Ivanova, D. DeCamp, R.C. Hsueh, H.A. Brown, A targeted mass spectrometric analysis of phosphatidylinositol phosphate species, J. Lipid Res. 46 (2005) 1796–1802.
[19] M. Pulfer, R.C. Murphy, Electrospray mass spectrometry of phospholipids, Mass Spectrom. Rev. 22 (2003) 332–364.
[20] M.R. Wenk, L. Lucast, G. Di Paolo, A.J. Romanelli, S.F. Suchy, R.L. Nussbaum, G.W. Cline, G.I. Shulman, W. McMurray, P. De Camilli, Phosphoinositide profiling in complex lipid mixtures using electrospray ionization mass spectrometry, Nat. Biotechnol. 21 (2003) 813–817.
[21] A.D. Postle, D.C. Wilton, A.N. Hunt, G.S. Attard, Probing phospholipid dynamics by electrospray ionisation mass spectrometry, Prog. Lipid Res. 46 (2007) 200–224.
[22] S.K. Dove, F.T. Cooke, M.R. Douglas, L.G. Sayers, P.J. Parker, R.H. Michell, Osmotic stress activates phosphatidylinositol-3,5-bisphosphate synthesis, Nature 390 (1997) 187–192.
[23] M. Laffargue, J.M. Ragab-Thomas, A. Ragab, J. Tuech, K. Missy, L. Monnereau, U. Blank, M. Plantavid, B. Payrastre, P. Raynal, H. Chap, Phosphoinositide 3-kinase and integrin signalling are involved in activation of bruton tyrosine kinase in thrombin-stimulated platelets, FEBS Lett. 443 (1999) 66–70.
[24] R.D. Byrne, M. Garnier-Lhomme, K. Han, M. Dowicki, N. Michael, N. Totty, V. Zhendre, A. Cho, T.R. Pettitt, M.J. Wakelam, D.L. Poccia, B. Larijani, PLCgamma is enriched on poly-phosphoinositide-rich vesicles to control nuclear envelope assembly, Cell Signal. 19 (2007) 913–922.
[25] M. Garnier-Lhomme, R.D. Byrne, T.M.C. Hobday, S. Gschmeissner, R. Woscholski, D.L. Poccia, E.J. Dufourc, B. Larijani, Nuclear envelope remnants: fluid membanes enriched in STEROLS and ploy phosphoinositides, PLOS One 4 (2009) 1–11.
[26] T.R. Pettitt, S.K. Dove, A. Lubben, S.D. Calaminus, M.J. Wakelam, Analysis of intact phosphoinositides in biological samples, J. Lipid Res. 47 (2006) 1588–1596.
[27] H. Ogiso, R. Taguchi, Reversed-phase LC/MS method for polyphosphoinositide analyses: changes in molecular species levels during epidermal growth factor activation in A431 cells, Anal. Chem. 80 (2008) 9226–9232.
[28] C. Nasuhoglu, S. Feng, J. Mao, M. Yamamoto, H.L. Yin, S. Earnest, B. Barylko, J.P. Albanesi, D.W. Hilgemann, Nonradioactive analysis of phosphatidylinositides and other anionic phospholipids by anion-exchange high-performance liquid chromatography with suppressed conductivity detection, Anal. Biochem. 301 (2002) 243–254.
[29] T. Gunnarsson, L. Ekblad, A. Karlsson, P. Michelsen, G. Odham, B. Jergil, Separation of polyphosphoinositides using normal-phase high-performance liquid chromatography and evaporative light scattering detection or electrospray mass spectrometry, Anal. Biochem. 254 (1997) 293–296.
[30] M. Laffargue, R. Calvez, P. Finan, A. Trifilieff, M. Barbier, F. Altruda, E. Hirsch, M.P. Wymann, Phosphoinositide 3-kinase gamma is an essential amplifier of mast cell function, Immunity 16 (2002) 441–451.
[31] B. Dewald, M. Baggiolini, Platelet-activating factor as a stimulus of exocytosis in human neutrophils, Biochim. Biophys. Acta 888 (1986) 42–48.
[32] E.G. Bligh, W.J. Dyer, A rapid method of total lipid extraction and purification, Can. J. Biochem. Physiol. 37 (1959) 911–917.
[33] N.G. Clarke, R.M. Dawson, Alkaline O leads to N-transacylation. A new method for the quantitative deacylation of phospholipids, Biochem. J. 195 (1981) 301–306.
[34] M.P. Gratacap, S. Severin, G. Chicanne, M. Plantavid, B. Payrastre, Different roles of SHIP1 according to the cell context: the example of blood platelets, Adv. Enzyme Regul. 48 (2008) 240–252.
[35] A. Sorisky, W.G. King, S.E. Rittenhouse, Accumulation of PtdIns(3,4)P2 and PtdIns(3,4,5)P3 in thrombin-stimulated platelets. Different sensitivities to $Ca2^{+}$ or functional integrin, Biochem. J. 286 (Pt 2) (1992) 581–584.
[36] P. Gulati, G. Thomas, Nutrient sensing in the mTOR/S6K1 signalling pathway, Biochem. Soc. Trans. 35 (2007) 236–238.
[37] T. Nobukuni, M. Joaquin, M. Roccio, S.G. Dann, S.Y. Kim, P. Gulati, M.P. Byfield, J.M. Backer, F. Natt, J.L. Bos, F.J. Zwartkruis, G. Thomas, Amino acids mediate mTOR/raptor signaling through activation of class 3 phosphatidylinositol 3OH-kinase, Proc. Natl. Acad. Sci. U.S.A. 102 (2005) 14238–14243.
[38] M.P. Byfield, J.T. Murray, J.M. Backer, hVps34 is a nutrient-regulated lipid kinase required for activation of p70 S6 kinase, J. Biol. Chem. 280 (2005) 33076–33082.

7.3 Plasmid maps

pRK5_Myc-S6K1__p237

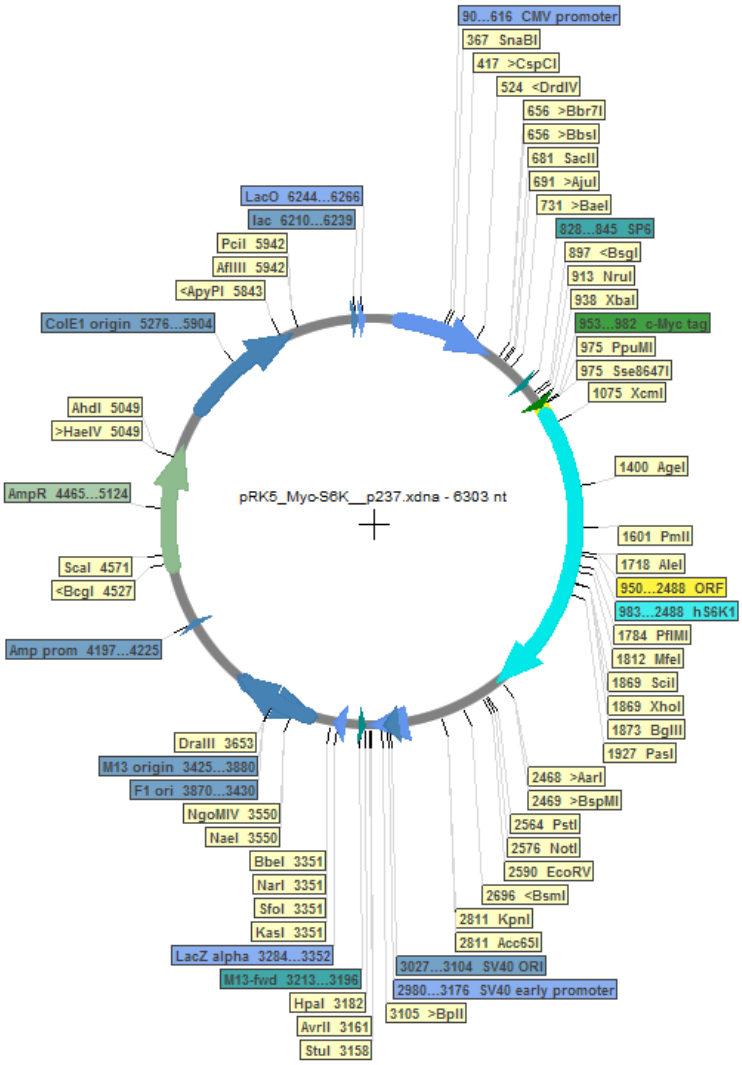

ORF: 950-2488
Myc-tag starts at 953
Human S6K1 with AGVF at 983, and ends with RMNL at 2488.
Unique sites are depicted in light yellow.
Kind gift of G. Thomas (University of Cincinnati, USA).

pcDNA3_tkGST-hVps34__p256

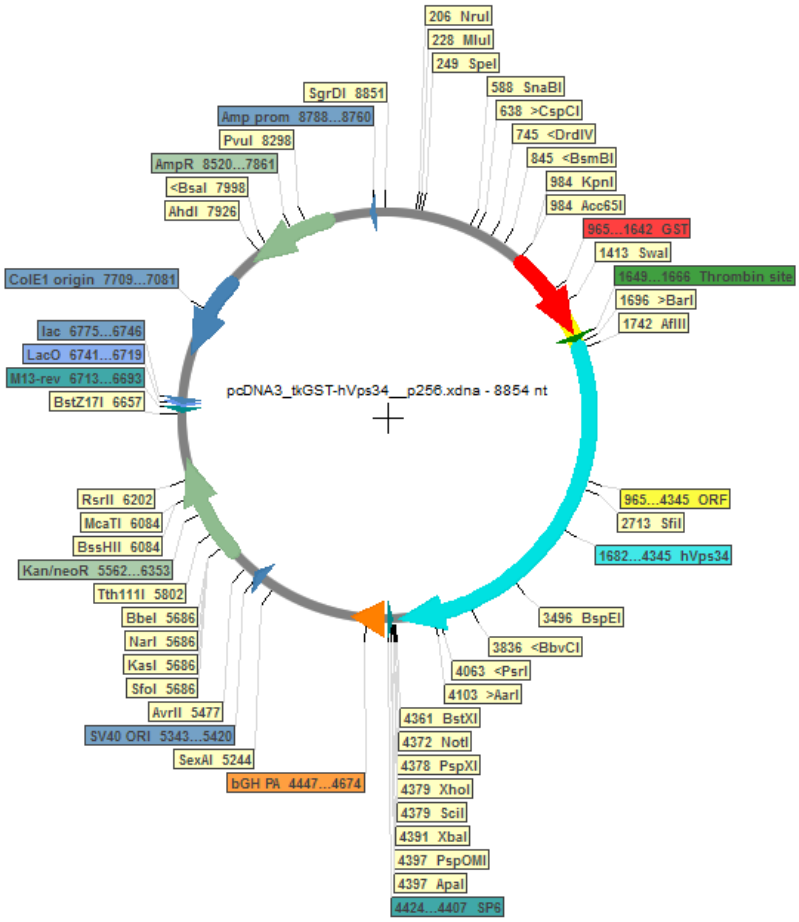

ORF: 965-4345
GST-tag starts at 965
hVps34 with MGEA at 1682, and ends with QYWRK at 4345.
Unique sites are depicted in light yellow.
Laboratory plasmid collection.

pEGFP-N1_PH-Btk__p530

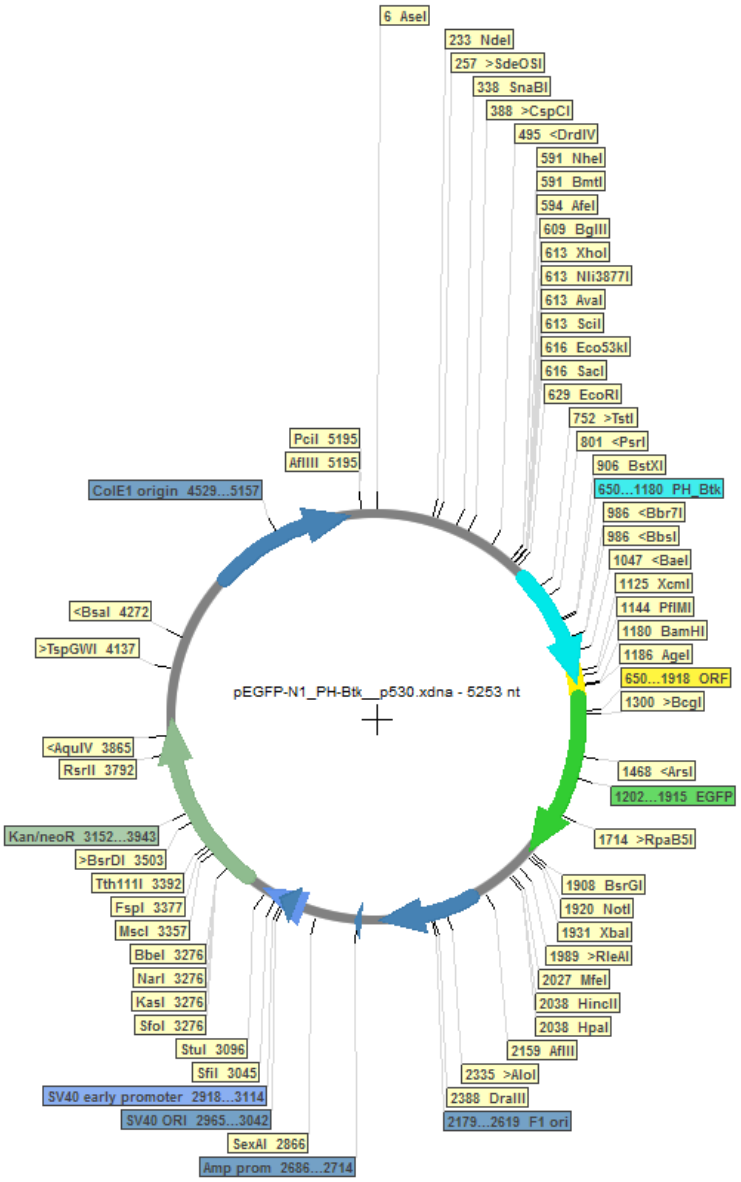

ORF: 650-1918
EGFP at 1202-1915
PH domain of Btk starts at 650 and ends at 1180.
Unique sites are depicted in light yellow.
Plasmid was a kind gift of T. Balla (NICHD, Maryland, USA).

pcDNA3_p110g wt-CAAX^{KRas}__p594

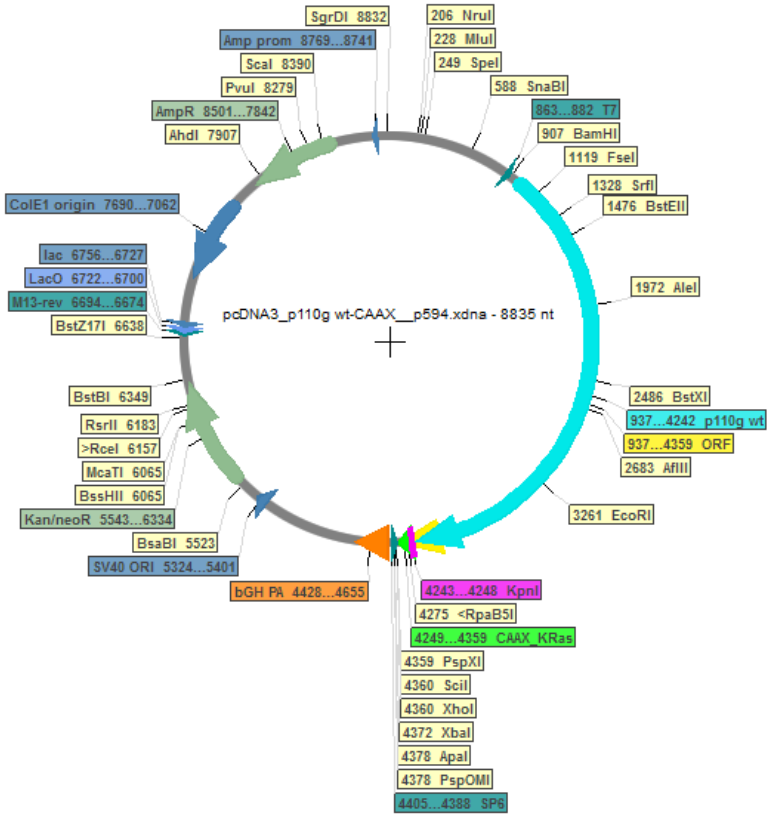

ORF: 937-4359
p110g wt at 937-4242 followed by GT (KpnI site, depicted in violet) and CAAX box of K-Ras with STOP codon at 4359.
Unique sites are depicted in light yellow.
Laboratory plasmid collection.

pEGFP-C2_2xFYVE HRS__p607

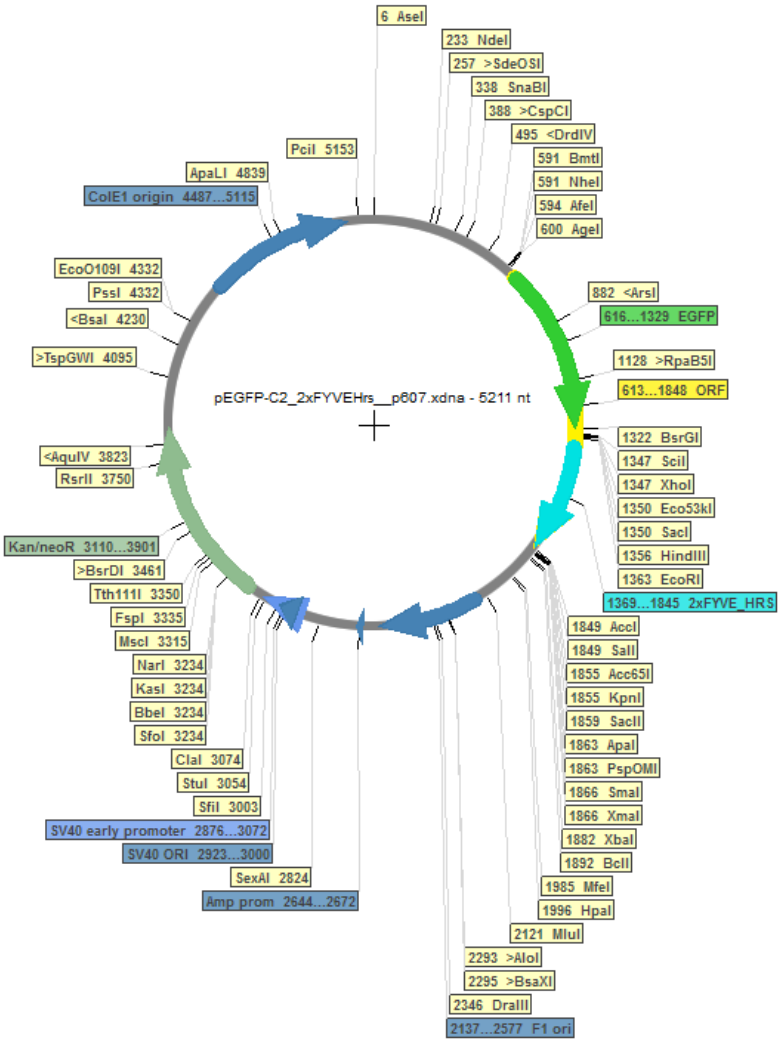

ORF: 613-1848
EGFP at 616-1329
2xFYVE^{HRS} (tandem FYVE domain of HRS) starts at 1369 and ends at 1848.
Unique sites are depicted in light yellow.
Laboratory plasmid collection.

pEGFP-C1_PH-TAPP1__p705

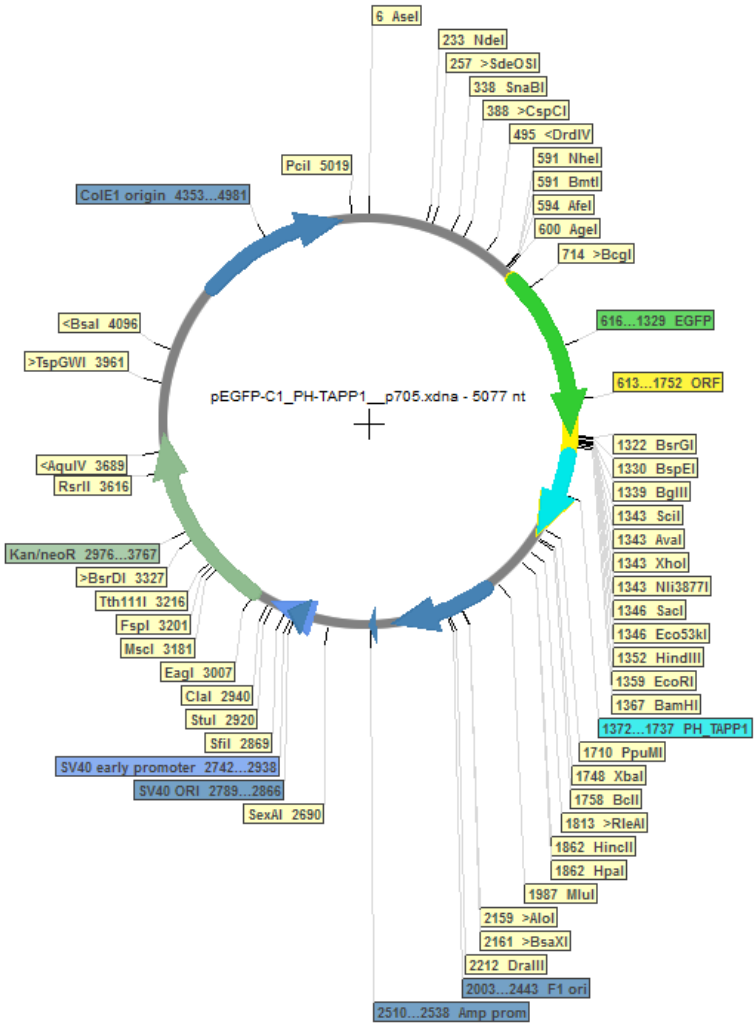

ORF: 613-1752
EGFP at 616-1329
PH domain of TAPP1 starts at 1372 and ends at 1737.
Unique sites are depicted in light yellow.
Laboratory plasmid collection.

pcDNA3_tkHA-hVps34__p1033

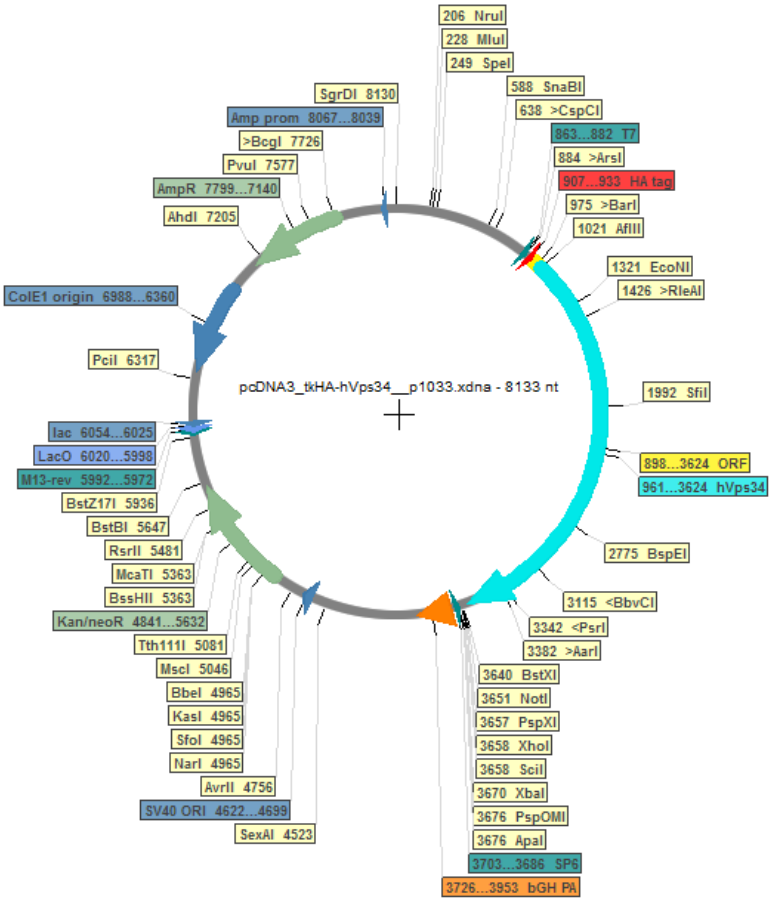

ORF: 898-3624,
HA-tag starts at 907
hVps34 starts with MGEA at 961 and ends with QYWRK at 3624.
Unique sites are depicted in light yellow.
Anna Melone (this thesis).

pcDNA3_tkGST-hVps34 K636R__p1122

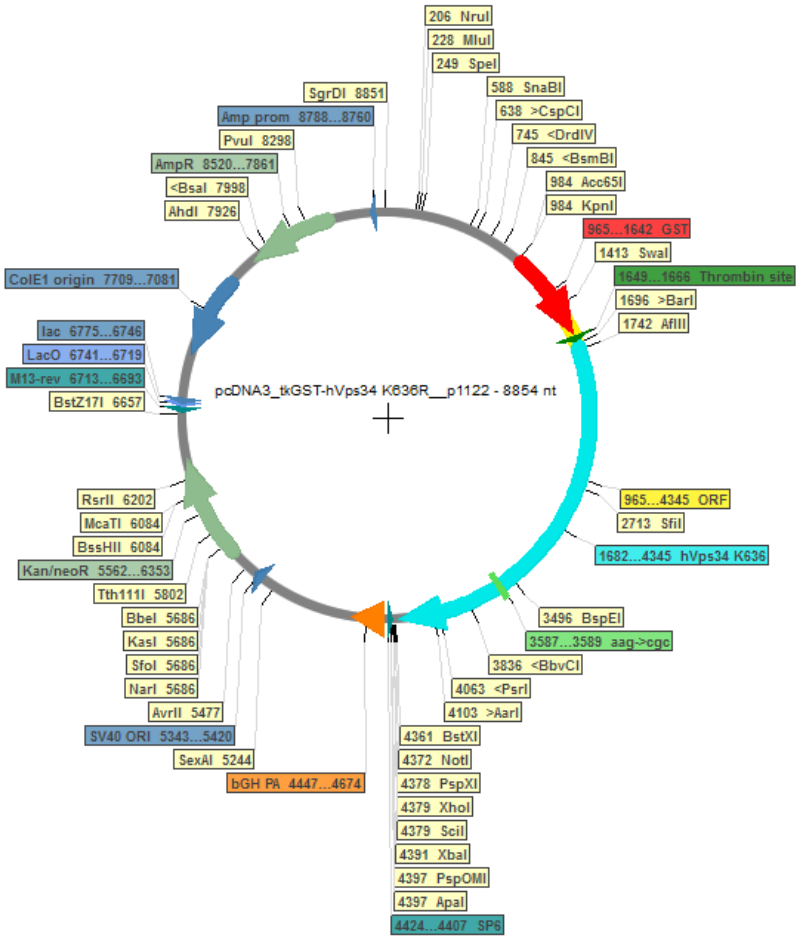

ORF: 965-4345
GST-tag starts at 965
hVps34 with MGEA at 1682, and ends with QYWRK at 4345.
K->R mutation introduced through 3 point mutations at 3587-3589 (aag -> cgc; depicted in green).
Unique sites are depicted in light yellow.
Anna Melone (this thesis).

pcDNA3_tkHA-hVps34 K636R__p1130

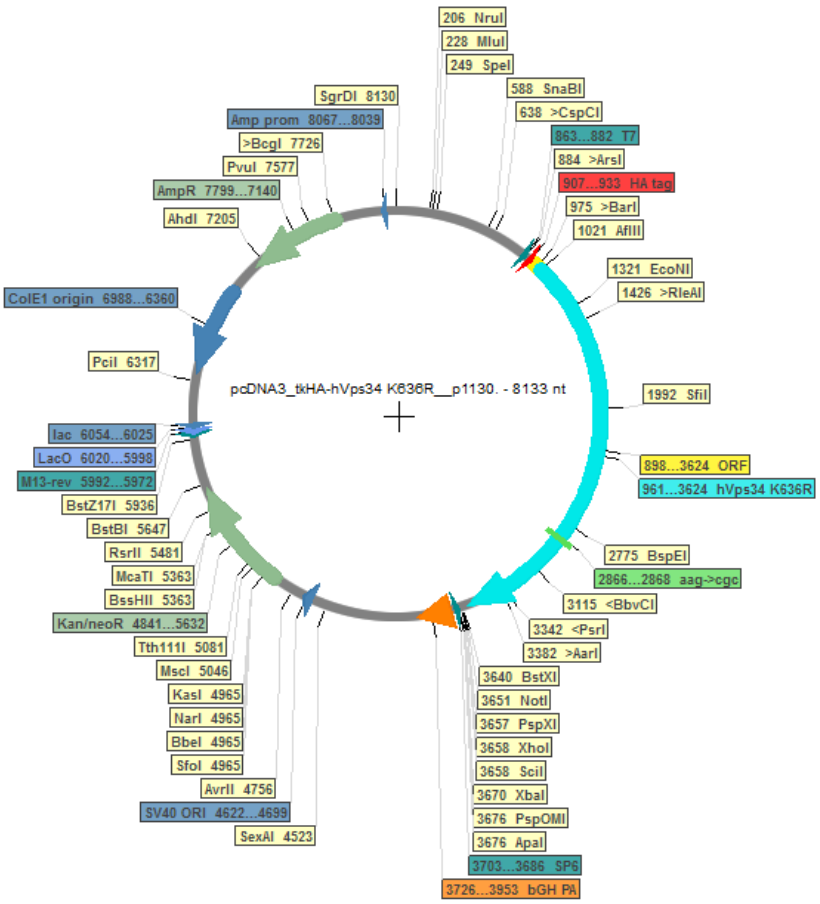

ORF: 898-3624,
HA-tag starts at 907
hVps34 starts with MGEA at 961 and ends with QYWRK at 3624.
K->R mutation introduced through 3 point mutations at 2866-2868 (aag -> cgc; depicted in green).
Unique sites are depicted in light yellow.
Anna Melone (this thesis).

pRK5_HA-mTOR__p1274

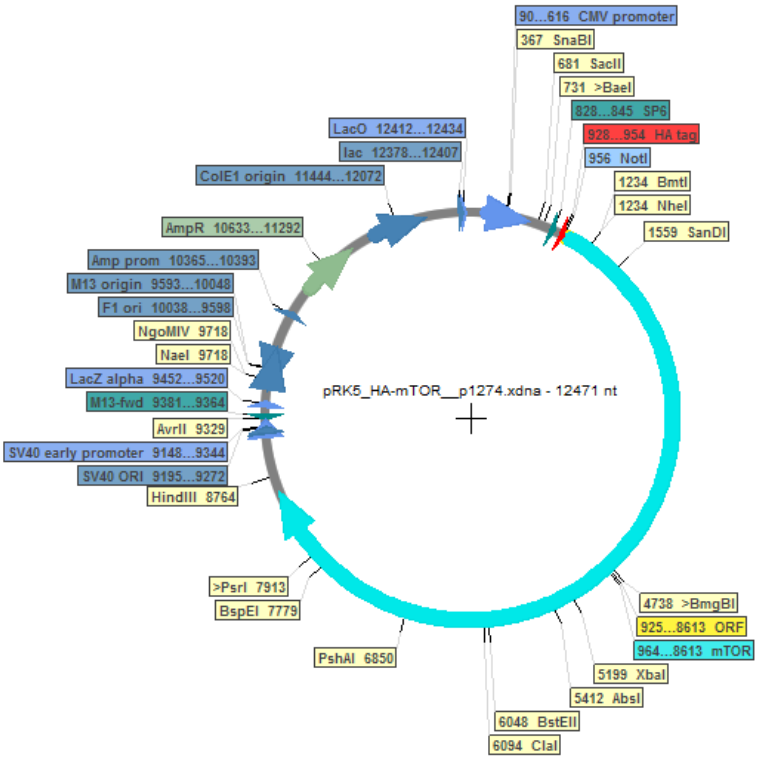

ORF: 925-8613
HA-tag starts at 924
mTOR starts at 964 with MLGTG and ends with WCPFW at 8613.
Unique sites are depicted in light yellow.
Plasmid was a kind gift of M. Hall (University of Basel, Switzerland).

pRK5_HA-Raptor 3'UTR__p1275

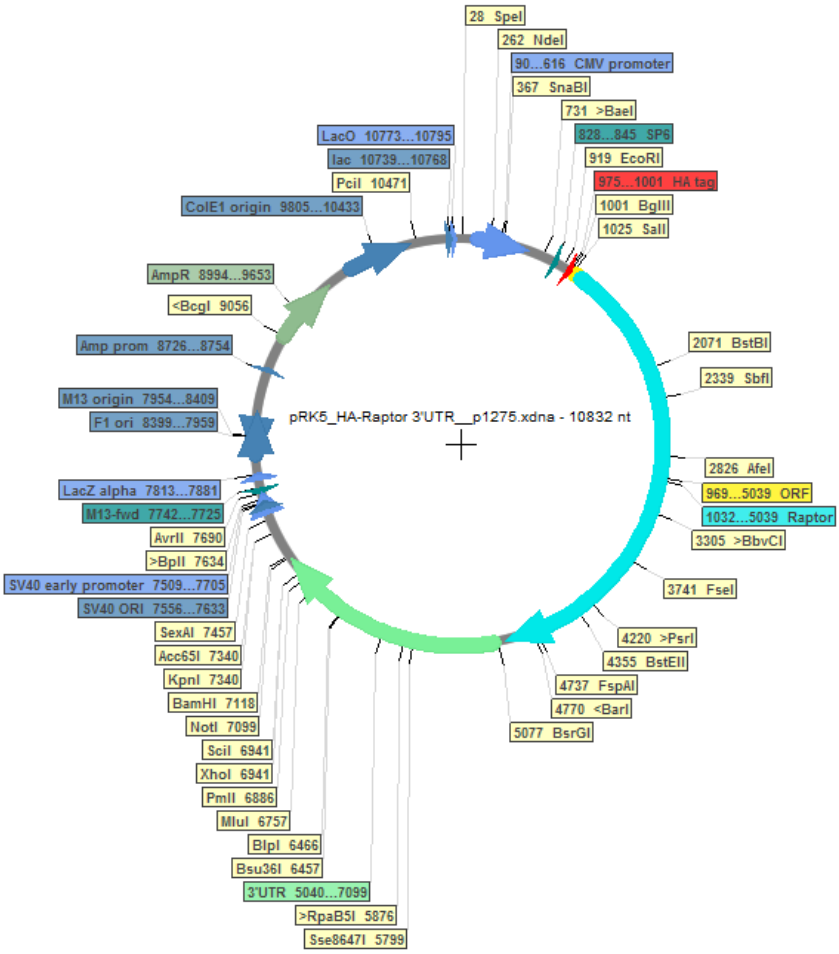

ORF: 969-5039
HA-tag starts at 975
Raptor starts at 1032 with MESEML and ends with VEKRVR at 5039.
3'-UTR of Raptor: 5040-7099 (depicted in green)
Unique sites are depicted in light yellow.
Plasmid was a kind gift of M. Hall (University of Basel, Switzerland).

pEGFP-C1_Rheb__p1277

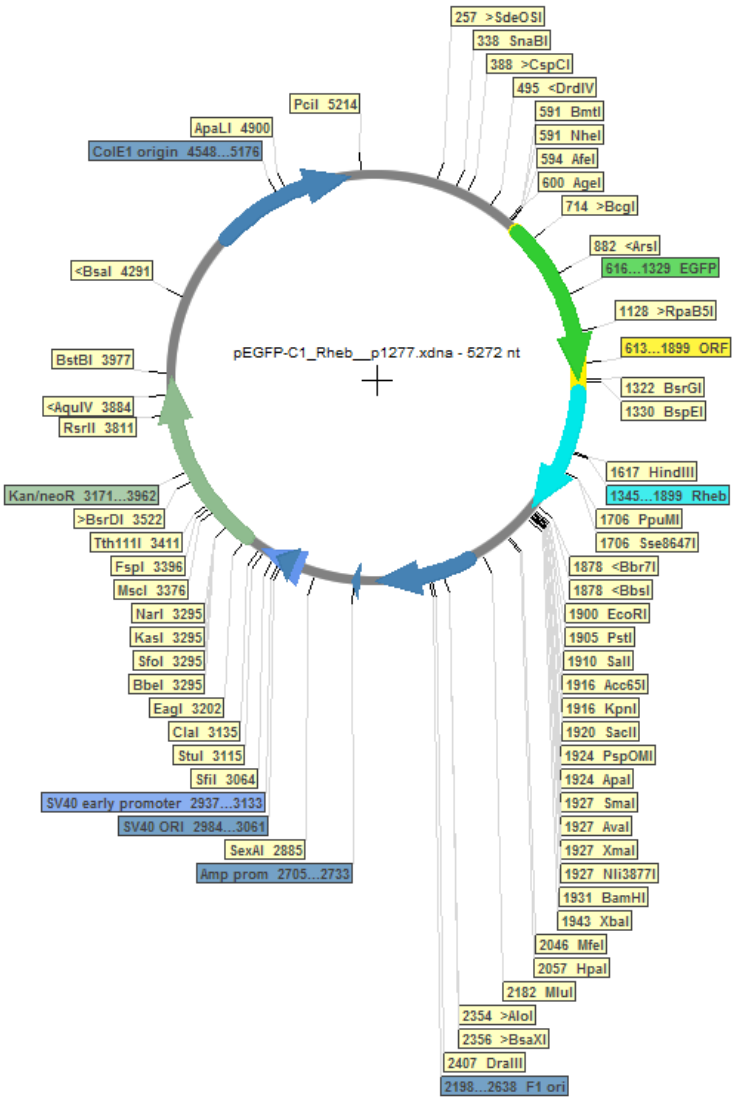

ORF: 613-1899
EGFP at 616-1329
Rat Rheb starts at 1345 with MPQSKS and ends at 1899.
Unique sites are depicted in light yellow.
Plasmid was a kind gift of M. Hall (University of Basel, Switzerland).

pcDNA3.1+_Rab5a__p1287

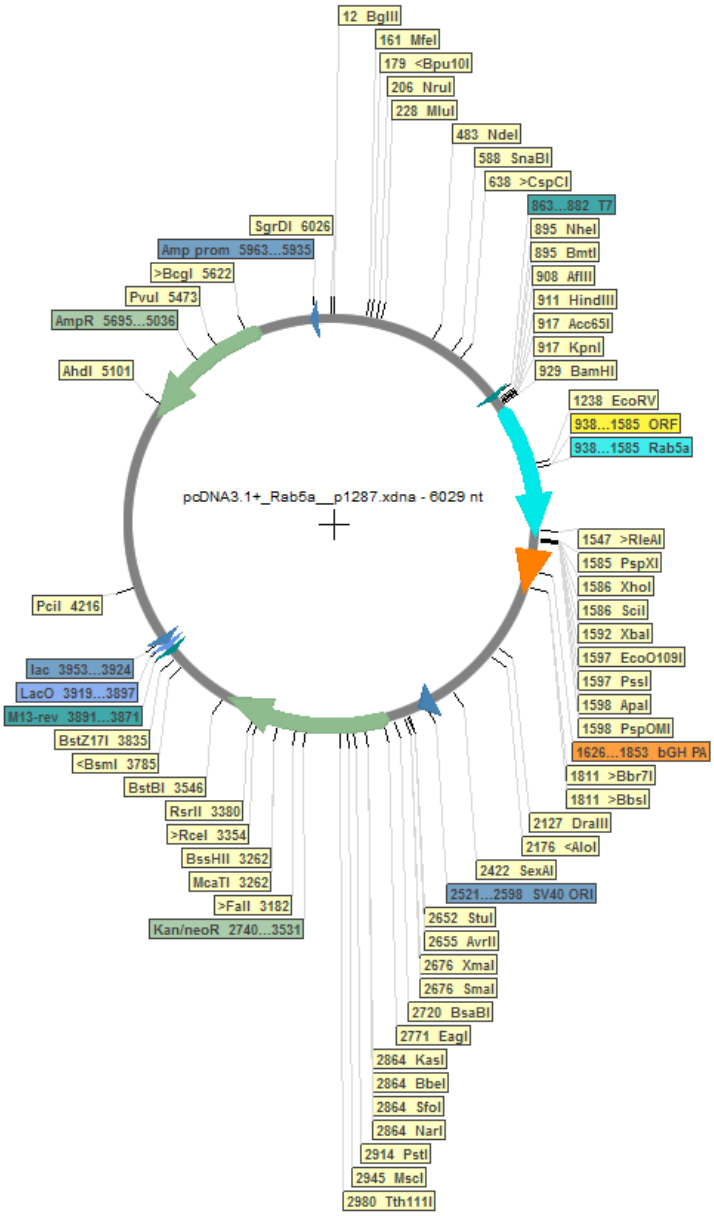

ORF: 938-1585
Rab5a starts at 938 and ends at 1585
Unique sites are depicted in light yellow.
Plasmid obtained from Missouri S&T cDNA Resource Center, www.cdna.org

pcDNA3.1+_Rab7__p1289

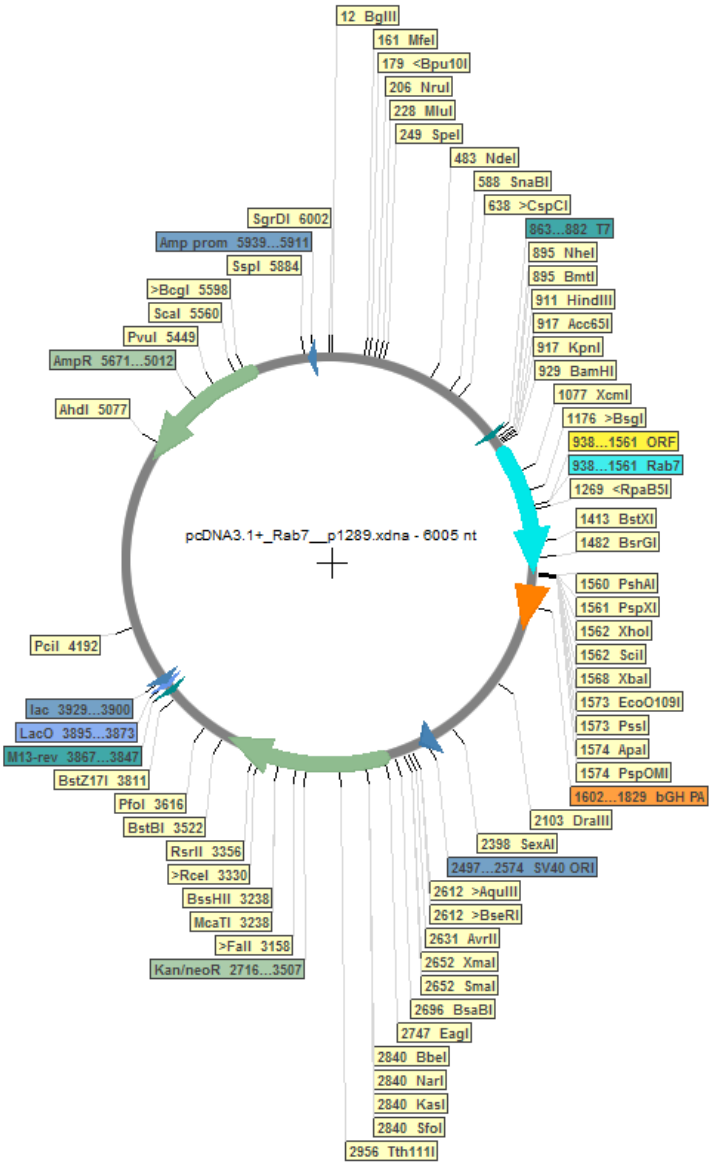

ORF: 938-1561
Rab7 starts at 938 and ends at 1561
Unique sites are depicted in light yellow.
Plasmid obtained from Missouri S&T cDNA Resource Center, www.cdna.org

pEGFP-C1_Rab5a__p1313

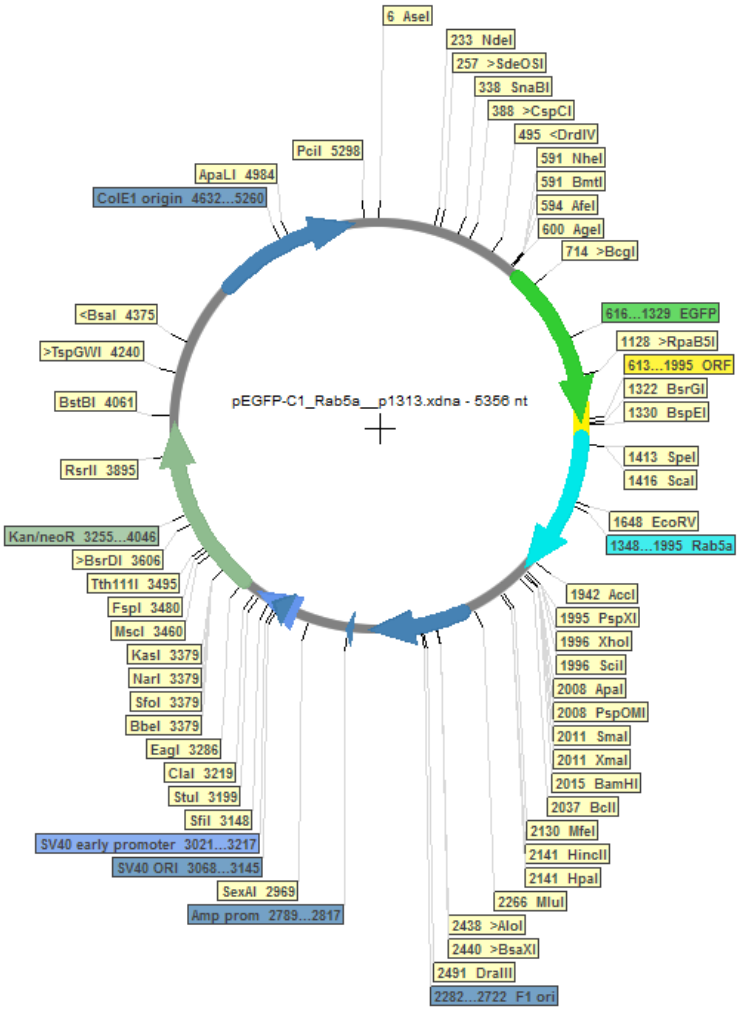

ORF: 613-1995
EGFP at 616-1329
Rab5a starts at 1348 and ends at 1995.
Unique sites are depicted in light yellow.
Anna Melone (this thesis).

pEGFP-C1_Rab7__p1315

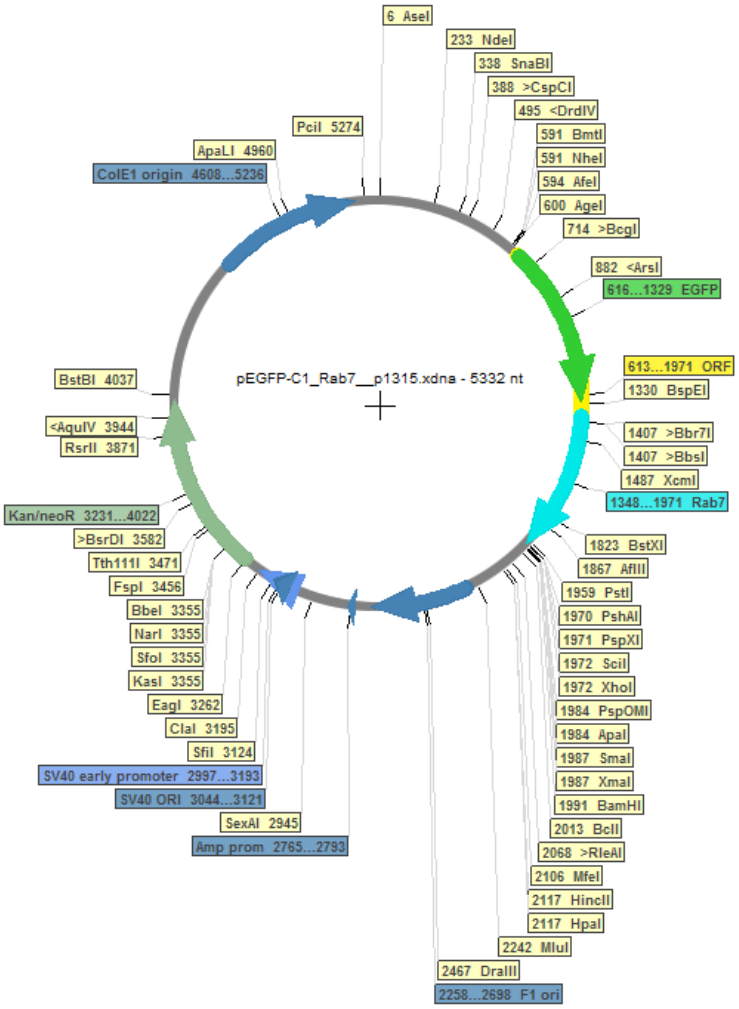

ORF: 613-1971
EGFP at 616-1329
Rab7 starts at 1348 and ends at 1971.
Unique sites are depicted in light yellow.
Anna Melone (this thesis).

pRK5_HA-Raptor-CAAX KRas__p1320

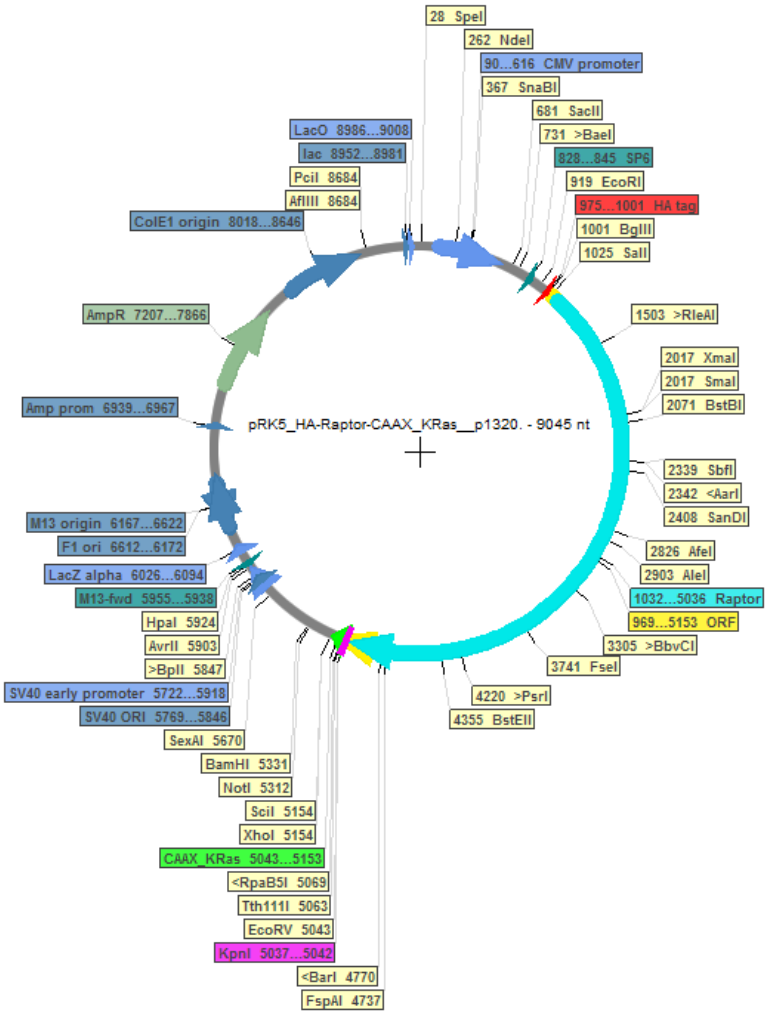

ORF: 969-5153
HA-tag starts at 975
Raptor starts at 1032 with MESEML and ends with VEKRVR at 5036 followed by GT (KpnI site; depicted in violet) and CAAX box of K-Ras with STOP at 5153.
Unique sites are depicted in light yellow.
Anna Melone (this thesis).

pRK5_HA-Raptor-Rheb15__p1321

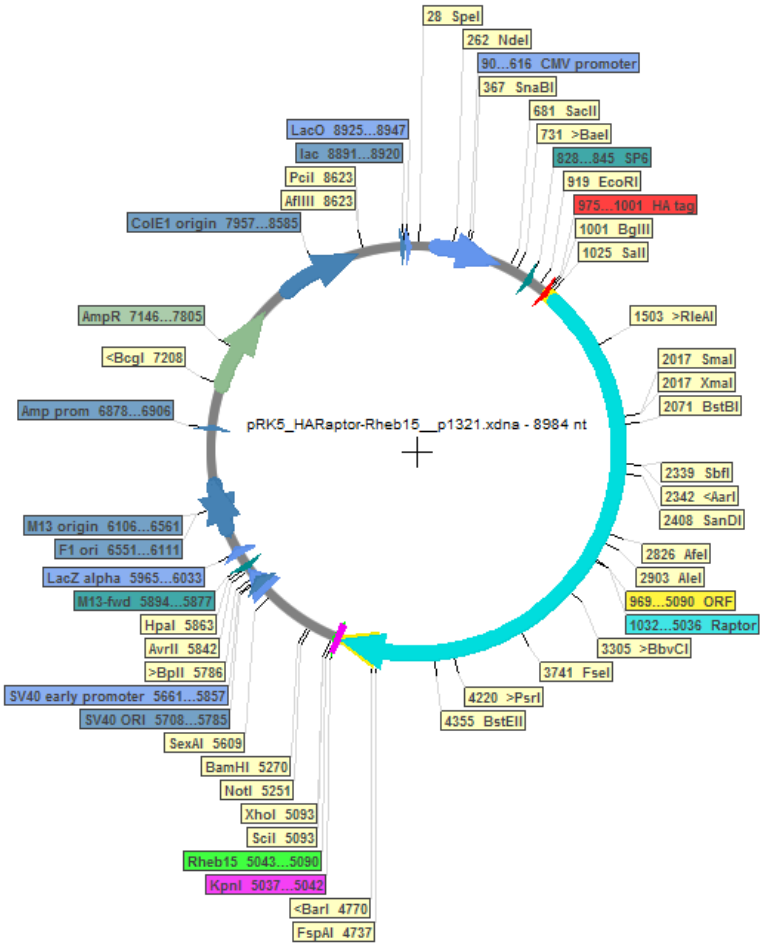

ORF: 969-5090
HA-tag starts at 975
Raptor starts at 1032 with MESEML and ends with VEKRVR at 5036 followed by GT (KpnI site; depicted violet) and last 15 amino acids of Rheb (IDGAASQGKSSCSVM; taken from p1277) with STOP at 5090.
Unique sites are depicted in light yellow.
Anna Melone (this thesis).

pEGFP-C2_2xFYVE HRS C215S__p1332

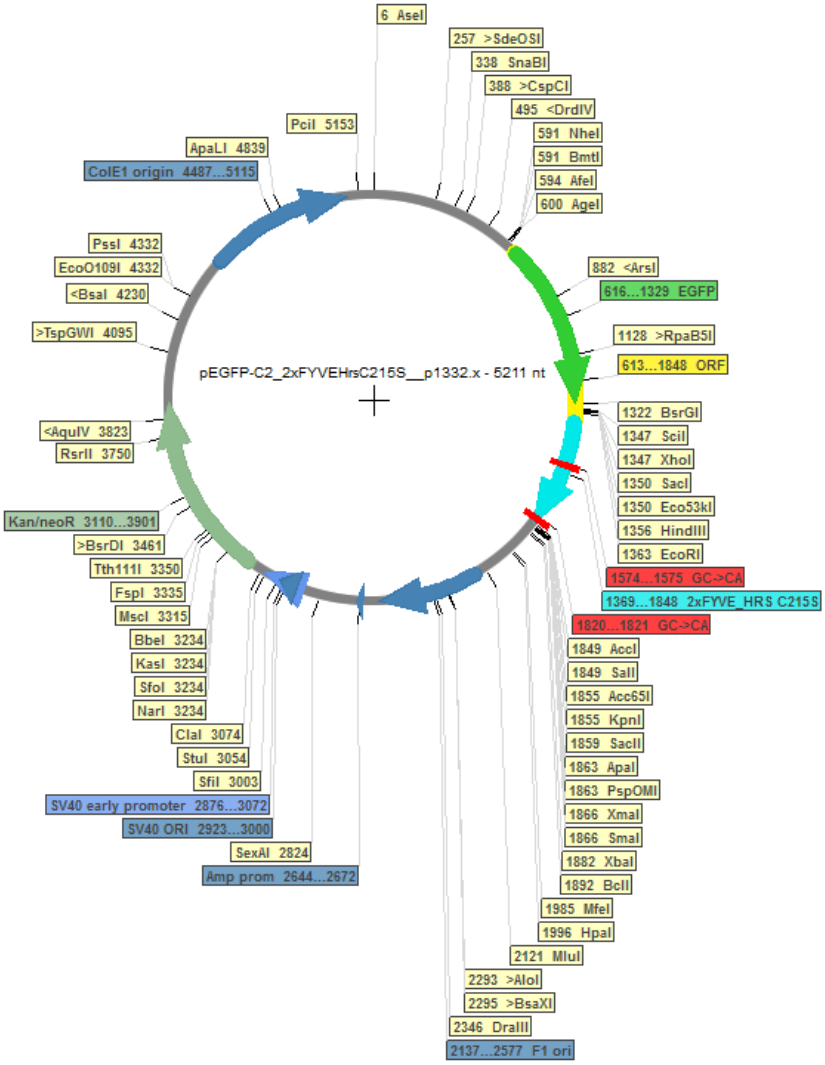

ORF: 613-1848
EGFP at 613-1329
2xFYVE HRS C215S starts at 1369 and ends at 848.
2x C->S mutations introduced through 4 point mutations (depicted in red): G1574C, C1575A, G1820C and C1821A
Unique sites are depicted in light yellow.
Plasmid was a kind gift of H. Stenmark (University of Oslo, Norway).

7.4 Abbreviations

A375	human malignant melanoma cell line
AA	amino acids
Akt	product of the retrovirus AKT8
AMP	adenosine monophosphate
AMPK	adenosine monophosphate-activated protein kinase
APS	ammonium persulfate
Arg	arginine
ATP	adenosine trisphosphate
base pair	bp
BSA	bovine serum albumin
Btk	Bruton's tyrosine kinase
Ca^{2+}	calcium ions
cm	centimeter
DEPTOR	DEP domain-containing mTOR-interacting protein
DMEM	Dulbecco's modified Eagle's medium
DMSO	dimethylsulfoxide
DNA	deoxyribonucleic acid
dNTP	deoxynucleoside triphosphate
DTT	dithiothreitol
4E-BP1	eukaryotic initiation factor 4E-binding protein
E. coli	escherichia coli
EAA	essential amino acids
EEA1	early endosomal antigen 1
EGFP	enhanced green fluorescent protein
ERK	extracellular-signal related kinase
ETDA	ethylenediamine tetraacetate
EtOH	ethanol
FCS	fetal calf serum
FRB	FKBP12-rapamycin binding domain
FYVE	Zinc finger domain as present in Fab1, YOTB, Vac1, and EEA1
g	gram
GAP	GTPase activating protein
GDP	guanosine diphosphate
GEF	guanine exchange factor
Gln	L-glutamine
Grb2	Growth factor receptor-bound protein 2
GTP	guanosine triphosphate
GTPase	guanosinetriphosphatase
h	hour(s)
HA	hemagglutinin
HEK293	human embryonic kidney 293 cell line
HeLa	human cervical adenocarcinoma cell line
HER911	human embryonic retinoblast cell line
HOPS	homotypic fusion and vacuole protein sorting
HRP	Horseradish peroxidase
HRS	hepatocyte growth factor-regulated tyrosine kinase substrate
IGF	insulin growth factor
IRS	insulin receptor substrate
kDA	kilo Dalton
l	liter
LB	luria broth

LKB1	liver kinase B1
M	mol/l
MAPK	mitogen-activated protein kinase
MEF	mouse embryonic fibroblast
MEK	MAPK/ERK kinase
min	minute(s)
ml	milliliter
mLST8	mammalian lethal with sec thirteen
mRNA	messenger RNA
mSin1	mammalian stress-activated map kinase-interacting protein 1
mTOR	mammalian target of rapamycin
mTORC	mTOR complex
n	nano
μ	micro
μg	microgram
μl	microliter
OD	optical density
O/N	over night
PA	phosphatidic acid
PAGE	Polyacrylamide gel electrophoresis
PAT	proton-assisted amino acid transporter
PBS	phosphate buffered saline
PCR	polymerase chain reaction
PDK	phosphoinositide-dependent kinase
PEST	penicillin-streptomycin
PFA	paraformaldehyde
PH	pleckstrin homology
pH	potential hydrogenii
PI	phosphoinositide
PI3K	phosphatidylinositol 3-kinase
PIKfyve	PtdIns(3)P 5-kinase
PIKK	PI3K-related protein kinase
PKB	protein kinase B
PLD	phospholipase D
PMSF	phenylmethylsulfonylfluoride
PRAS40	proline-rich Akt substrate of 40 kDa
Protor	protein observed with rictor
PtdIns	phosphatidylinositol
PtdIns(3)P	phosphatidylinositol 3-phosphate
PtdIns(3,4)P_2	phosphatidylinositol 3,4-bisphosphate
PtdIns(3,4,5)P_3	phosphatidylinositol 3,4,5-triphosphate
PtdIns(3,5)P_2	phosphatidylinositol 3,5-bisphosphate
PtdIns(4,5)P_2	phosphatidylinositol 4,5-bisphosphate
PVDF	polyvinylidene fluoride
PX	phox homology domain
Rab	GTPase
Rag	GTPase
Ragulator	Rag and mTORC1 regulator
Raptor	regulatory-associated protein of mTOR
Ras	GTPase
Rheb	Ras homologue enriched in brain
Rictor	rapamycin-insensitive companion of mTOR
RNA	ribonucleic acid
RNAi	RNA interference

rpm	revolutions per minute
RPMI	Roswell Park Memorial Institute (medium)
RSK	p90 ribosomal S6 kinase
RT	room temperature
RTK	receptor tyrosine kinase
S6K	p70 ribosomal S6 kinase
SB	sample buffer
SDS	sodium dodecylsulfate
SEM	standard error of the mean
Ser	serine
shRNA	short hairpin RNA
siRNA	small interference RNA
Sos	son of sevenless
TAE	Tris-acetate-EDTA
TAPP1	tandem PH domain containing protein 1
TBS	Tris buffered saline
TBST	Tris buffered saline with Tween
TE	Tris-EDTA
TEMED	N, N, N', N'-tetraethylmethlylendiamide
Thr	threonine
TLC	thin layer chromatography
TOS	TOR signaling motif
Tris	Tris(hydroxymethyl)aminomethane
TSC	tuberous sclerosis complex
TSC1	also named hamartin
TSC2	also named tuberin
U	Unit
UV	ultraviolet
V	Volt
Vps	vacuolar protein sorting
V-ATPase	vacuolar H^+-adenosine triphosphatase ATPase
v/v	volume/volume
w/o	without
w/v	weight/volume
WT	wild-type

Curriculum Vitae

Personal data

Name: Anna Melone
Date of birth: 29.04.1977
Place of origin: Möhlin AG
Nationality: Swiss, Italian

Professional experience

2005 – present	PhD thesis at the Institute of Biochemistry and Genetics, Department of Biomedicine, University of Basel, Switzerland Supervisor Prof. Dr. Matthias P. Wymann Project: "Endosomal docking of mTOR modulates mTORC1 activity"
2004	Scientific research (7 months) in Infection Biology, Biozentrum, University of Basel, Switzerland Supervisor: Prof. Dr. Jean Pieters Project: "*In vivo* analysis of trafficking of *Mycobacterium Bovis* BCG in the phagosome-lysosome pathway"
2002 – 2004	Diploma thesis in Infection Biology, Biozentrum, University of Basel, Switzerland Supervisor: Prof. Dr. Jean Pieters Project: "Establishment of an experimental system for the *in vivo* analysis of lysosomal trafficking"

Education

March 2005 – present	PhD studies in the Institute of Biochemistry and Genetics, Department of Biomedicine, University of Basel, Switzerland
2002 – 2004	Diploma thesis in Biochemistry/Infection Biology, Biozentrum, University of Basel, Switzerland
1999 – 2004	Studies in Biologie II equivalent to M Sc Mol Biol, University of Basel, Switzerland
1995 – 1999	Matura with focus on languages, Gymnasium Muttenz BL

Languages

German	mother tongue
Italian	mother tongue
English	written and spoken fluently
French	Matura level

Courses

27.02.06 - 03.03.06 Animal experimentation course, Module 1, Institute für Labortierkunde (Universität Zürich)

Meetings and Presentations

TOR, PI3K and Akt – 20 Years on" Symposium, Basel, 11-13 September 2011, attendance

Anna Melone, Ann C.Mertz, Carsten Schultz, Matthias P. Wymann (2010), "PI3*P*-dependent signaling of the nutrient sensor mTOR", Biochemical Society Conferences, mTOR signaling in health and disease, London, 11-12 November, **oral and poster presentation**

Targeting the kinome, Basel, 4-6 December 2006, attendance

Research Seminar at the Infection Biology Department, Biozentrum, University of Basel, October 2004, "*In vivo* analysis of trafficking of *Mycobacterium Bovis* BCG in the phagosome-lysosome pathway", **oral presentation**

Anna Melone, Jean Pieters (2004), "*In vivo* analysis of trafficking of *Mycobacterium Bovis* BCG in the phagosome-lysosome pathway". Biozentrum symposium 2004, St Chrischona, Switzerland, **poster presentation**

Research seminar at the Biochemistry Department, Biozentrum, University Basel, May 2003, "Establishment of an experimental system for the *in vivo* analysis of lysosomal trafficking", **oral presentation**

Publications

Sabine Kiefer, Johannes Rogger, **Anna Melone**, Ann C. Mertz, Anna Koryakina, Matthias Hamburger, Peter Küenzi (2010). Separation and detection of all phosphoinositide isomers by ESI-MS. J Pharm Biomed Anal 53(3): 552-558

Anna Melone, Romina Marone, Devaraj Subramanian, Carsten Schultz, Matthias P. Wymann. mTORC1 regulated by PtdIns(3)P and PtdIns(3,5)P_2. Manuscript in preparation.

Acknowledgements

First of all I would like to thank Matthias Wymann for giving me the opportunity to perform my PhD thesis in his laboratory on a very complex, not always easy to understand but interesting and challenging project. I learned a lot in these years. I am also grateful for his support and scientific discussions.

I would like to express my gratitude to Christoph Moroni who accepted to be my co-referee and evaluated my work.

I am also grateful to Jean Pieters who agreed to be my chairperson during my examination.

I would like to thank Carsten Schultz for providing the synthetic PtdIns(3)P/AM.

My gratitude goes also to my present and former lab colleagues, for the time we spent together in the lab. Especially I would like to thank:
- Romina Marone for critical reading of my thesis, for sharing you expertise with me and for your helping hands.
- Mirjam Zimmermann and Ruben Cal for drawing the chemical structures.

Further I would like to thank:
- Nicole Scherr for listening to my complaints and worries and for having always words of comforts.
- Yvonne Arnold for our lunch times. It was a diversion to my laboratory days.

Special thanks go to my brothers for always being interested in what I am doing.

Finally, my greatest thank goes to my parents, without their support I would not have been able to conclude my PhD thesis.
Ai miei genitori, per essermi sempre accanto. Senza il vostro sostegno non avrei mai finito la tesi. Grazie.